Journal of the Serbian Chemical Society

*e*rsion
*e*lectronic

Available on line at

СХД
1897

www.shd.org.rs/JSCS/

CONTENTS

Available online at www.shd.org.rs/JSCS/

Stereoselective cyclo-addition reactions of azomethine ylides catalysed by *in situ* generated Ag(I)/bisphosphine complexes

RONALD GRIGG[1]*, SUREN HUSINEC[2#] and VLADIMIR SAVIĆ[1,3*#]

[1]Molecular Innovation, Diversity and Automated Synthesis (MIDAS) Centre, Department of Chemistry, Leeds University, Woodhouse Lane, Leeds LS2 9JT, UK, [2]Institute of Chemistry, Technology and Metallurgy, Centre for Chemistry, P.O. Box 815, Njegoševa 12, 11000 Belgrade, and [3]Department of Organic Chemistry, Faculty of Pharmacy, University of Belgrade, Vojvode Stepe 450, 11000 Belgrade, Serbia

Abstract: Stereoselective cyclo-addition reactions of azomethine ylides promoted by *in situ* generated Ag(I)/bisphosphine complexes were studied. Under the optimised conditions, the pyrrolidine products were isolated in up to 84 % yield and with up to 71 % *e.e.* The effects of various reaction variables on the stereoselectivity were also investigated.

Keywords: azomethine ylides; stereoselectivity; chiral phosphine; Ag(I).

INTRODUCTION

1,3-Dipolar cyclo-addition reactions of metallo-azomethine ylides to electron deficient alkenes constitute a powerful tool for the preparation of substituted pyrrolidine derivatives.[1] If the metallo-ylide is generated in the presence of a chiral ligand, the pyrrolidine product can be obtained in a stereoselective manner, Scheme 1.
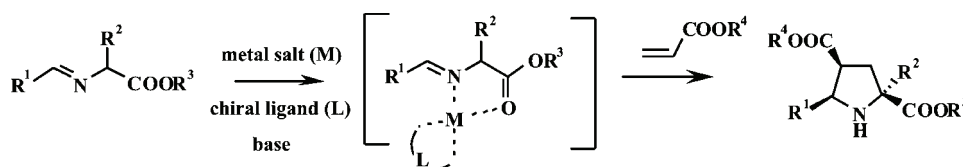
Scheme 1. Metal catalysed cycloaddition reactions of azomethine ylides.

Pioneering studies of stereoselective cyclo-additions of these ylides employed the stoichiometric amount of chiral cobalt complexes[2a] or a chiral auxilia-

---

*Corresponding authors. E-mails: r.grigg@leeds.ac.uk; vladimir.savic@pharmacy.bg.ac.rs
Serbian Chemical Society member.

ry.[1a,b,d,2b–j] Recently, more efficient metal[3a–p] and organo-catalytic[3q,r] variations of this transformation have been developed. Various metal salts have been employed, such as Co (II),[2a] Mn(II),[2a] Ag(I),[3a–e] Cu(I/II),[3g–l] Au(I),[3m] Zn(II),[3n] Ca(II),[3o] Ni(II)[3p] in conjunction with a range of chiral ligands.

Of particular interest are the Ag(I)-based methods, which afford pyrrolidines with a high level of enantioselectivity and in good yield, invariably *via* an *endo* transition state. Under the standard conditions (Scheme 1), the use of base is necessary in order to generate the azomethine ylide, but this may be avoided by employing AgOAc as a Lewis acid.[4] In addition, the selection of a ligand in conjunction with an Ag(I) salt provides access to both enantiomeric pyrrolidine products.[5] In recent years, the development of Cu(I)/Cu(II) methods provided additional valuable synthetic methods, which is reflected in the high level of enantioselectivity[3g–l] and the potential to rationally control *exo/endo* selectivity.[3h]

RESULTS AND DISCUSSION

In this paper, initial results obtained in Ag(I)-promoted, stereoselective cyclo-addition reactions of metallo-azomethine ylides employing the bisphosphine ligand **1**:
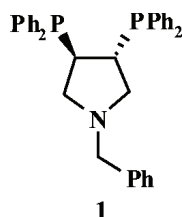
easily accessible from tartaric acid,[6] are discussed.

The cyclo-addition reactions of azomethine ylides generated from imines were performed using equimolar amounts of imine, dipolarophile, AgOTf and the ligand **1** in CH_2Cl_2 as the solvent in the presence of NEt_3 as a base, Scheme 2 and Table I. The products were isolated by flash chromatography and the *e.e.* was determined by ^{1}H-NMR spectroscopy using the chiral shift reagent, (+)-tris[(3--heptafluoropropylhydroxymethylene)camphorato]europium(III).[7]
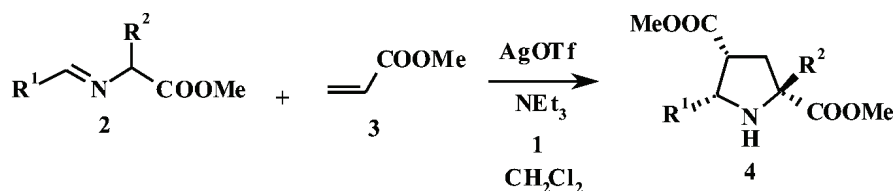
Scheme 2. Ag(I)/**1** catalysed cyclo-addition reactions of azomethyne ylides.

Most of the reactions afforded the products in good yields (Table I), with reaction times of 3–4 h, suggesting that presence of the ligand did not significantly affect either the yield or the reaction time. The reaction employing the *S*-methylcysteine-derived imine, Table I, entry e, surprisingly, resulted in the recovery of the starting materials only. This may be the result of Ag(I) coordination by the thioether moiety, forming a complex which excluded either N or O coordination of the metal centre.[8] Chelate formation involving the iminoester functionality (see Scheme 1) is essential for lowering the pK_a of the α-C–H bond and the generation of the ylide,[1a] a process potentially disrupted by a competitive coordination of Ag(I) by an additional donor atom. Interestingly, when the thioether containing imine **2f** was used, the expected product was isolated in good yield. This may suggest that the aromatic thioether is a weaker coordinating agent than the aliphatic one, allowing equilibrium between different species, including those leading to the ylide.

TABLE I. Stereoselective Ag(I) catalysed 1,3-dipolar cycloaddition reactions

Entry	R (imine **2**)	R (product **4**)	*e.e.*, %[a]	Yield, %[b]
a	**2a**: R^1 = 2-naphthyl R^2 = H	**4a**: R^1 = 2-naphthyl R^2 = H	49	69
b	**2b**: R^1 = 2-naphthyl R^2 = CH$_3$	**4b**: R^1 = 2-naphthyl R^2 = CH$_3$	66	80
c	**2c**: R^1 = 2-naphthyl R^2 = benzyl	**4c**: R^1 = 2-naphthyl R^2 = benzyl	64	72
d	**2d**: R^1 = 2-naphthyl R^2 = 3-indolylmethyl	**4d**: R^1 = 2-naphthyl R^2 = 3-indolylmethyl	67	84
e	**2e**: R^1 = 2-naphthyl R^2 = methylthiomethyl	**4e**: R^1 = 2-naphthyl R^2 = methylthiomethyl	–	–
f	**2f**: R^1 = 2-(methylthio)phenyl R^2 = CH$_3$	**4f** : R^1 = 2-(methylthio)phenyl R^2 = CH$_3$	61	74

[a]Assigned by ^{1}H-NMR using chiral shift reagent; [b]isolated yield

The observed enantioselectivity ranged from 49 to 67 %. Although the enantioselectivity was lower for the glycine imine **2a** compared to the other substituted imines, **2b**, **2c**, **2d** and **2f**, there was no significant difference in the *e.e.* between the later ones. This puzzling result could be due to the Thorpe–Ingold effect which decreases the =N–C–CO angle and increases the steric congestion in the transition state.[9]

The absolute stereochemistry of product **4a** (2*R*, 4*R*, 5*S*) was established by comparison of its optical rotation ($[\alpha]_D$ –11.3°) with the optical rotation of (2*R*, 4*R*, 5*S*)-dimethyl 5-(2-naphthyl)pyrrolidine-2,4-dicarboxylate ($[\alpha]_D$ –19.5°) synthesized by a different method.[10] Based on all these results, a transition state was proposed, Fig. 1. It was assumed that the Ag(I) complex has a 4-coordinate square planar geometry. The donor atoms comprise the two phosphorus atoms from the

Available online at www.shd.org.rs/JSCS/

ligand and the nitrogen and the oxygen atoms from the imine. The approach of the dipolarophile to the *re* face of the imine *via* an *endo* transition state is less favoured due to steric interactions between the pseudo-axial phenyl group on the phosphorus and the ester group of the dipolarophile. The *si* face of the imine is less shielded due to pseudo-equatorial orientation of the phenyl substituent and, therefore, the approach of the dipolarophile from this side leads to the observed product.
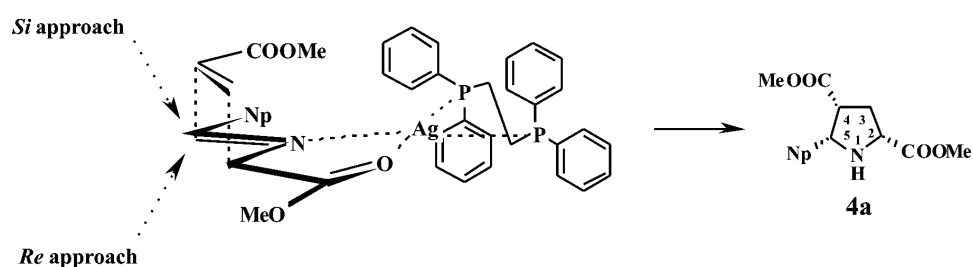
Fig. 1. Proposed transition state for the Ag(I)/**1** catalysed cycloaddition reactions (the pyrrolidine ring of the ligand omitted for clarity).

After these initial results, the effects of various reaction parameters on the enantioselectivity were investigated. Performing the reaction of imine **2b** and acrylate **3** at a lower temperature, Table II, entry a, slightly improved the *e.e.* without influencing the reaction yield. At –78 °C, Table II, entry b, the reaction was very slow and it is likely that the major part of the reaction occurred as the reaction mixture was gradually warmed up.

TABLE II. The effect of temperature on enantioselectivity

Entry	Imine	Product	t / °C	*e.e.*, %[a]	Yield, %[b]
a	**2b**	**4b**	–20	71	78
b	**2b**	**4b**	–78 to r.t.	71	78

[a]Assigned by ^{1}H-NMR using chiral shift reagent; [b]isolated yield

Variation of the base gave some unexpected results, Table III. When (*R*)- or (*S*)-*N,N,α*-trimethylbenzylamine or pyridine (Table III, entries d and e) were used instead of triethylamine, no cyclo-adduct was obtained. The ^{1}H-NMR spectrum of the crude reaction mixture indicated the presence of starting materials only. This may suggest that the formation of Ag(I) complexes containing these bases as ligands prevented the coordination of the imine and subsequent formation of the ylide. Ag(I)/pyridine complexes are known and their stability depends on the coordination number.[11] On the other hand, the benzylamine derivatives may act as bidentate ligands. The 1:1 complexes of Ag(I) with 2-allylpyridine and vinyldiphenylphosphine, as well as related complexes, have been reported in the literature.[12] When stronger bases than triethylamine were used, such as DBU,

sparteine and tetramethyl-*t*-butylguanidine, Table III, entries a–c, the reaction times were shorter but, unfortunately, the *e.e.* slightly decreased. This might indicate that apart from the phosphine/Ag(I) complex catalysed reaction, a reaction promoted by the base/Ag(I) complex occurred as well. Although steric factors play an important role in the stability of amine/Ag(I) complexes, increased amine bulk may stabilise the complex and, therefore, promote the competitive non-stereoselective process.[11c,13]

TABLE III. The effect of base on enantioselectivity

Entry	Imine	Product	Base	e.e., %[a]	Yield, %[b]
a	**2b**	**4b**	DBU	57	87
b	**2b**	**4b**	Sparteine	57	80
c	**2b**	**4b**	$Me_2N\overset{N\,^tBu}{\underset{}{\diagup\diagdown}}NMe_2$	49	88
d	**2b**	**4b**	$Ph\overset{}{\underset{}{\diagup\diagdown}}NH_2$ [c]	–	–
e	**2b**	**4b**	Pyridine	–	–

[a]Assigned by ^{1}H-NMR using chiral shift reagent; [b]isolated yield; [c]both (*R*)- and (*S*)- enantiomers were surveyed

The proposed transition state model, Fig. 1, suggests that the approach of the dipolarophile to the dipole is controlled by steric interactions involving the phenyl substituent on the phosphorus and the ester group on the dipolarophile. This prompted evaluation of bulkier ester functionalities of both the dipole and the dipolarophile, Scheme 3, Table IV. When imine *t*-butyl ester **5** was used (Table IV, entry a), the *e.e*. was similar to that observed for imine methyl ester **2a** (Scheme 2, Table I, entry a). This may indicate that the imine ester group does not play a crucial role in inducing the stereoselectivity, which would be expected based on the proposed transition state. On the other hand, *t*-butyl acrylate **6b** (Table IV, entry b) was shown to be ineffective in this reaction, affording the product in only 28 % yield after 4 days. The use of benzyl ester **6a** resulted in a slightly lower *e.e*. (Table IV, entry c).

2 **b.** R^1 = Me R^2 = Me
5 R^1 = *t*-Bu, R^2 = H

3 R^3 = Me
6 **a.** R^3 = PhCH$_2$
  b. R^3 = *t*-Bu

AgOTf
NEt$_3$
1
CH$_2$Cl$_2$

7 **a.** R^1 = *t*-Bu, R^2 = H, R^3 = Me
  b. R^1 = Me, R^2 = Me, R^3 = *t*-Bu
  c. R^1 = Me, R^2 = Me, R^3 = CH$_2$Ph
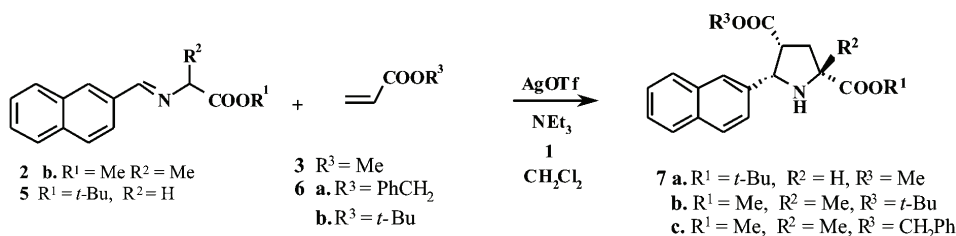
Scheme 3. Ag(I)/**1** catalysed cycloaddition reactions of azomethine ylides.

In conclusion, the effect of chiral bisphosphine **1** in stereoselective cyclo-addition reactions of metallo-azomethine ylides generated in the presence of AgOTf was studied. Under the optimized conditions, pyrrolidine products were obtained in good yields with up to 71 % *e.e.*

TABLE IV. Effect of steric factors on the *e.e.*

Entry	Imine	Acrylate	Product	*e.e.*, %[a]	Yield, %[b]
a	**5**	**3**	**7a**	48	91
b	**2b**	**6b**	**7b**	–	28[c]
c	**2b**	**6a**	**7c**	57	67

[a]Assigned by ^{1}H-NMR using chiral shift reagent; [b]isolated yield; [c]reaction time: 4 days

EXPERIMENTAL

Melting points were determined on a Kofler hot-stage apparatus and are uncorrected. Microanalyses were obtained using a Carlo Erba Elemental Analyser MOD 1106. Mass spectral data were recorded using a VG-AutiSpec spectrometer operating at 70 eV. Nuclear magnetic resonance spectra were recorded at 300 MHz using a General Electric QE300 instrument and at 400 MHz using a Bruker WP400 instrument. Chemical shift are given in parts per million (δ) downfield from tetramethylsilane as the internal standard. Unless otherwise specified, deuterochloroform was used as the solvent. Silica gel 60 (230–400mesh) was employed for flash chromatography.

Of the prepared compounds, the imines **2a**,[14a] **2b**,[14b] **2c**[14c] and **2d**[14c] and pyrrolidines **4a**–**d**[14c] are reported in the literature. Some analytical and spectral data of the newly synthesised compounds are given below.

All *e.e.* values reported in this study were established by ^{1}H-NMR spectroscopy using the chiral shift reagent tris[(3-heptafluoropropylhydroxymethylene)-(+)-camphorato]europium(III). The reagent was added in small portions (2–3 mg) to the $CDCl_3$ solution (NMR tube) of the product until a good baseline separation of the enantiomeric signals for the methyl
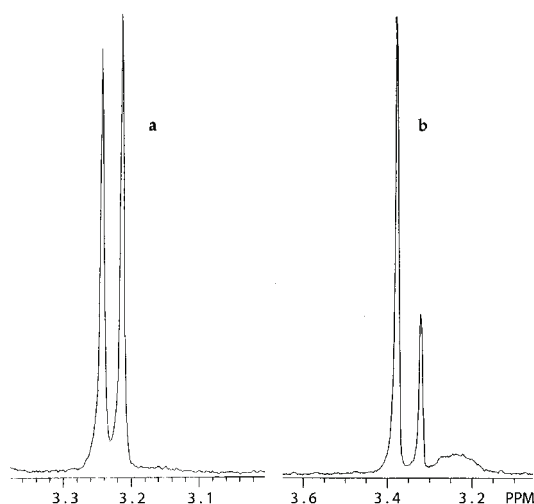

Fig. 2. Separation of the enantiomeric signals.

protons of the ester was observed. The experiment was performed using the products discussed above and the corresponding racemic mixtures. A typical example, Fig. 2, shows the separation of the COOMe signals for the racemic **4a** (Fig. 2a) and the same product obtained with 49 % *e.e*. (Fig. 2b).

General procedure for the preparation of imines

A mixture of aldehyde (0.010 mol), amino ester hydrochloride (0.012 mol), triethylamine (0.018 mol) and anhydrous MgSO$_4$ (3–4 g) in dichloromethane (30 mL) was stirred for 12 h. The obtained solid was separated by filtration and the filtrate washed with water (2×20 mL). The organic layer was then dried (MgSO$_4$) and the solvent evaporated under reduced pressure. When possible, the imines were further purified by distillation or crystallisation. The imines **2f** and **5**, obtained as colourless oils, were used without further purification.

Methyl N-*[2-(methylthio)benzylidene]alaninate (2f)*. ^{1}H-NMR (CDCl$_3$, δ / ppm): 1.58 (3H, *d*, *J* = 7.9 Hz, CCH$_3$), 2.47 (3H, *s*, SCH$_3$), 3.77 (3H, *s*, COOCH$_3$), 4.22 (1H, *q*, *J* = 7.8 Hz, CH), 7.20–7.42 (3H, *m*, ArH), 7.98 (1H, *d*, ArH), 8.82 (1H, *s*, N=CH). MS (EI) (*m/z* (%)): 236, M$^+$–1 (1), 205 (8), 182 (26), 167 (33), 141 (11), 128 (22), 119 (28), 98 (59), 85 (63), 72 (33), 55 (79), 43 (100).

t-*Butyl* N-*(2-naphthalenylmethylene)glycinate (5)*. ^{1}H-NMR (CDCl$_3$, δ / ppm): 1.52 (9H, *s*, *t*-Bu), 4.38 (2H, *s*, CH$_2$), 7.51 (2H, *m*, ArH), 7.83 (3H, *m*, ArH), 8.25 (2H, *m*, ArH) 8.40 (1H, *s*, N=CH). MS (EI) (*m/z* (%)): 269, M$^+$ (8), 212 (28), 168 (100), 154 (21), 141 (83), 127 (22), 115 (19), 84 (6), 57 (71), 41 (56).

General procedure for the cyclo-addition reactions in the presence of AgOTf/phosphine 1

AgOTf (0.10 mmol) was added to a stirred solution of phosphine **1** (0.10 mmol) and imine (0.10 mmol) in dry CH$_2$Cl$_2$ (5.0 mL). The reaction mixture was stirred at room temperature for 20 min. Methyl acrylate (0.2–0.3 mmol) was then added followed by base (0.15–0.2 mmol) and the mixture was stirred at room temperature until thin layer chromatography indicated the absence of the starting material. The reaction mixture was then filtered through celite, the filtrate washed with water (2×), dried (MgSO$_4$) and the solvent evaporated under reduced pressure. The residue was purified by flash chromatography (SiO$_2$, petroleum ether/ /diethyl ether) to afford the product. The enantiomeric excess was determined by ^{1}H-NMR spectroscopy using tris[3-(heptafluoropropylhydroxymethylene)-(+)-camphorato]europium (III) as the chiral shift reagent.

Dimethyl 2-methyl-5-[2-(methylthio)phenyl]pyrrolidine-2,4-dicarboxylate (4f). Flash chromatography (SiO$_2$, 1:1 v/v petroleum ether–diethyl ether) afforded the product in 74 % yield as a pale yellow oil, which solidified upon standing; m.p. 76–80 °C. Anal. Calcd. for C$_{16}$H$_{21}$NO$_4$S: C, 59.45; H, 6.50; N, 4.35 %. Found: C, 59.65; H, 6.60; N, 4.2 %. ^{1}H-NMR (CDCl$_3$, δ / ppm): 1.58 (3H, *s*, SCH$_3$), 2.10 (1H, *dd*, *J* = 13.8 and 7.5 Hz, 3-H), 2.49 (3H, *s*, CH$_3$C), 2.77 (1H, *dd*, *J* = 13.7 and 3.0 Hz, 3-H), 3.12 (3H, *s*, COOCH$_3$), 3.51 (1H, *m*, 4-H), 3.83 (3H, *s*, COOCH$_3$), 5.01 (1H, *d*, *J* = 7.8 Hz, 5-H), 7.20 (3H, *m*, ArH), 7.41 (1H, *d*, *J* = 7.6 Hz, ArH). MS (EI) (*m/z* (%)): 323, M$^+$ (5), 264 (100), 237 (24), 223 (18), 204 (22), 188 (11), 162 (53), 150 (15), 121 (10), 91 (7), 77 (8).

t-*Butyl 4-methoxycarbonyl-5-(2-naphthyl)pyrrolidine-2-carboxylate (7a)*. Flash chromatography (SiO$_2$, 1:1 v/v petroleum ether–diethyl ether) afforded the product in 91 % yield as a colourless oil which solidified upon standing; m.p. 67–69 °C. Anal. Calcd. for C$_{21}$H$_{25}$NO$_4$: C, 70.95; H, 7.05; N, 3.95 %. Found: C, 70.65; H, 7.15; N, 3.70 %. ^{1}H-NMR (CDCl$_3$, δ / ppm): 1.77 (9H, *s*, *t*-Bu), 2.45 (2H, *m*, 3-H), 2.67 (1H, *br s*, NH), 3.15 (3H, *s*, COOCH$_3$), 3.42 (1H, *q*, *J* = 7.5 Hz, 4-H), 3.93 (1H, *t*, *J* = 7.6 Hz, 2-H), 4.67 (1H, *d*, *J* = 7.6 Hz, 5-H), 7.45 (3H, *m*,

ArH), 7.82 (4H, *m*, ArH). MS (EI) (*m/z* (%)): 269, M$^+$ (8), 212 (28), 168 (100), 154 (21), 141 (83), 127 (22), 115 (19), 84 (6), 57 (71) 41 (56).

Benzyl 2-methoxycarbonyl-2-methyl-5-(2-naphthyl)pyrrolidine-4-carboxylate (7c). Flash chromatography (SiO$_2$, 3:7 v/v petroleum ether-ether) afforded the product in 74 % yield as a colourless oil which solidified upon standing; m.p. 85.5–87 °C. Anal. Calcd. for C$_{25}$H$_{25}$NO$_4$: C, 74.45; H, 6.20; N, 3.45 %. Found: C, 74.35; H, 6.1; N, 3.25 %. ^{1}H-NMR (CDCl$_3$, δ / ppm): 1.56 (3H, *s*, CCH$_3$), 2.17 and 2.83 (2×1H, 2×*m*, 3-H), 3.35 (1H, *br s*, NH), 3.48 (1H, *br m*, 4-H), 3.83 (3H, *s*, COOCH$_3$), 4.39 and 4.61 (2×1H, 2×*d*, *J* = 12.0 Hz, C**H**$_2$Ph), 4.82 (1H, *d*, *J* = 6.6 Hz, 5-H), 6.65 (2H, *d*, ArH), 7.00 (2H, *t*, ArH), 7.15 (1H, *m*, ArH), 7.41 (1H, *d*, ArH), 7.47 (2H, *m*, ArH), 7.76 (4H, *m*, ArH). MS (EI) (*m/z* (%)): 404, M$^+$+1 (4), 344 (100), 298 (11), 241 (65), 208 (36), 181 (70), 155 (11), 140 (20), 91 (97), 65 (12), 42 (20).

ИЗВОД

СТЕРЕОСЕЛЕКТИВНЕ ЦИКЛОАДИЦИОНЕ РЕАКЦИЈЕ АЗОМЕТИНСКИХ ИЛИДА КАТАЛИЗОВАНЕ *IN SITU* ГЕНЕРИСАНИМ Ag(I)/БИСФОСФИНСКИМ КОМПЛЕКСИМА

RONALD GRIGG[1], СУРЕН ХУСИНЕЦ[2] и ВЛАДИМИР САВИЋ[1,3]

[1]Molecular Innovation, Diversity and Automated Synthesis (MIDAS) Centre, Department of Chemistry, Leeds University, Woodhouse Lane, Leeds LS29JT, UK, [2]Институт за хемију, технологију и металургију, Центар за хемију, п. пр. 815, Његошева 12, 11000 Београд и [3]Институт за органску хемију, Фармацеутски факултет, Универзитет у Београду, Војводе Степе 450, 11000 Београд

Проучаване су стереоселективне циклоадиционе реакције азометинских илида катализоване комплексима сребра и бисфосфинског лиганда генерисаних *in situ*. Пиролидински деривати изоловани су у добрим приносима и са енантиоселективношћу до 71 %. Проучавани су такође и ефекти реакционих услова на стереоселективност ових реакција.

REFERENCES

1. a) R. Grigg, V. Sridharan, *Adv. Cycloadditions* **3** (1993) 161; b) S. Kanemasa, *Synlett* (2002) 1371; c) S. Husinec, V. Savic, *Tetrahedron: Asymmetry* **16** (2005) 2047; d) G. Pandey, P. Banerjee, S. Gadre, *Chem. Rev.* **106** (2006) 4484
2. a) P. Allway, R. Grigg, *Tetrahedron Lett.* **32** (1991) 5817; b) R. Grigg, *Tetrahedron Asymmetry* **6** (1995) 2475; c) G. Pandey, J. K. Laha, G. Lakshmaiah, *Tetrahedron* **58** (2002) 3525; d) S. Carlsson, H. Hoegberg, *J. Chem. Soc. Perkin Trans. 1* (2002) 1076; e) G. Cravotto, G. B. Giovenzana, T. Pilati, M. Sisti, G. Palmisano, *J. Org. Chem.* **66** (2001) 8447; f) S. Karlsson, H.-E. Hogberg, *Tetrahedron Asymmetry* **12** (2001) 1975; g) P. Garner, O. Dogan, J. W. Youngs, V. O. Kennedy, J. Protasiewicz, R. Zaniewski, *Tetrahedron* **57** (2001) 71; h) D. Alker, G. Hamblett, L. M. Harwood, S. M. Robertson, D. J. Watkin, C. E. Williams, *Tetrahedron* **54** (1998) 6089; i) H. Waldmann, E. Blaeser, M. Jansen, H. P. Letschert, *Chem. Eur. J.* **1** (1995) 150; j) R. M. Williams, W. Zhai, D. J. Aldous, S. C. Aldous, *J. Org. Chem.* **57** (1992) 6527; k) S. Kanemasa, H. Yamamoto, E. Wada, T. Sakurai, K. Urushido, *Bull. Chem. Soc. Jpn.* **63** (1990) 2857; l) D. M. Cooper, R. Grigg, S. Hargreaves, P. Kennewell, J. Redpath, *Tetrahedron* **51** (1995) 7791

Available online at www.shd.org.rs/JSCS/

3. a) J. M. Longmire, B. Wang, X. Zhang, *J. Am. Chem. Soc.* **124** (2002) 13400; b) C. Chen, X. Li, S. Schreiber, *J. Am. Chem. Soc.* **125** (2003) 1017; c) C. Alemparte, G. Blay, K. A. Jorgensen, *Org. Lett.* **7** (2005) 4569; d) W. Zeng, Y. G. Zhou, *Tetrahedron Lett.* **48** (2007) 4619; e) C. Najera, M. de Gracia Retamosa, J. M. Sansano, *Org. Lett.* **9** (2007) 4025; f) Y. Oderaotoshi, W. Cheng, S. Fujitomi, Y. Kasano, S. Minakata, M. Komatsu, *Org. Lett.* **5** (2003) 5043; g) S. Cabrera, R. G. Arrayas, J. C. Carretero, *J. Am. Chem. Soc.* **127** (2005) 16394; h) W. Gao, X. Zhang, M. Raghunath, *Org. Lett.* **7** (2005) 4241; i) X. Yan, Q. Peng, Y. Zhang, K. Zhang, W. Hong, X. Hou, Y. Wu, *Angew. Chem., Int. Ed.* **45** (2006) 1979; j) T. Llamas, R. G. Arrayas, J. C. Carretero, *Org. Lett.* **8** (2006) 1795; k) S. Cabrera, R. G. Arrayas, B. Martin-Matute, F. P. Cosio, J. C. Carretero, *Tetrahedron* **63** (2007) 6587; l) S. Fukuzawa, H. Oki, *Org. Lett.* **10** (2008) 1747; m) A. D. Melhado, M. Luparia, F. D. Toste, *J. Am. Chem. Soc.* **129** (2007) 12638; n) A. S. Gothelf, K. V. Gothelf, R. G. Hazell, K. A. Jorgensen, *Angew. Chem. Int., Ed.* **41** (2002) 4236; o) S. Saito, T. Tsubogu, K. Seki, Y. Yamashita, S. Kobayashi, *J. Am. Chem. Soc.* **130** (2008) 13321; p) J. Shi, M. Zhao, Z. Lei, M. Shi, *J. Org. Chem.* **73** (2008) 305; q) L. J. Vicario, S. Reboredo, D. Badia, L. Carrillo, *Angew. Chem., Int. Ed.* **46** (2007) 5168; r) M. Xue, X. M. Zhang, L. Z. Gong, *Synlett* (2008) 691
4. W. Zeng, Y. Zhou, *Org. Lett.* **7** (2005) 5055
5. W. Zeng, G. Chen, Y. Zhou, Y. Li, *J. Am. Chem. Soc.* **129** (2007) 750
6. U. Nagel, E. Kinzel, J. Andrade, G. Prescher, *Chem. Ber.* **119** (1986) 3326
7. R. R. Fraser in *Asymmetric Synthesis,* vol. 1, J. D. Morrison, Ed., Academic Press, New York, 1983, p. 173
8. a) L. D. Petit, K. F. Siddiqui, H. Kozlowski, T. Kowalik, *Inorg. Chim. Acta* **55** (1981) 87; b) C. A. McAuliffe, *Inorg. Chem.* **12** (1973) 1699; c) D. F. S. Natusch, L. J. Porter, *J. Chem. Soc. A* (1971) 1527
9. M. E. Jung, G. Piizzi, *Chem. Rev.* **105** (2005) 1735
10. P. Allway, R. Grigg, *Tetrahedron Lett.* **32** (1991) 5817, and references cited therein
11. a) G. Popa, C. Luca, V. Magearu, *J. Chim. Phys.* **62** (1965) 449; b) J. E. House, *Ill. State Acad. Sci.* **60** (1967) 312; c) R. J. Lancashire in *Comprehensive Coordination Chemistry,* Vol. 5, G. Wilkinson, Ed., Pergamon Press, Oxford, 1987, p. 775
12. R. E. Yingst, B. E. Douglas, *Inorg. Chem.* **3** (1964) 1177
13. R. D. Hanckok, *J. Chem. Soc. Dalton Trans.* (1980) 416
14. a) D. A. Barr, R. Grigg, N. H. Q. Gunaratne, J. Kemp, P. McMeekin, V. Sridharan, *Tetrahedron* **44** (1988) 557; b) K. Amornraksa, D. Barr, G. Donegan, R. Grigg, P. Ratananukul, V. Sridharan, *Tetrahedron* **45** (1989) 4649; c) R. Grigg, D. M. Cooper, S. Holloway, S. McDonald, E. Millington, M. A. B. Sarker, *Tetrahedron* **61** (2005) 8677.

Substituted pyridopyrimidinones. Part IV.
2-Chloro-4*H*-pyrido[1,2-*a*]pyrimidin-4-one as
a synthone of some new heterotricycles

MOHAMED ABASS*, MOSTAFA M. ISMAIL, WAFAA R. ABDEL-MONEM
and AISHA S. MAYAS

*Department of Chemistry, Faculty of Education, Ain Shams University,
Roxy, Cairo 11757, Egypt*

Abstract: 2-Chloro-4*H*-pyrido[1,2-*a*]pyrimidin-4-one (**1**) was utilized as a synthone precursor to prepare novel heterotricyclic systems. 2-Azido and 2-hydrazino derivatives (**2** and **3**) were obtained by nucleophilic replacement evolving compound **1**. The hydrazine derivative **3** was transformed into the azido derivative **2** by nitrosation. Treatment of compound **3** with [bis(methylthio)methylene]malononitrile afforded 2-pyrazolylpyridopyrimidine **4**. When compound **1** was reacted with 5-amino-3-(methylthio)-1*H*-pyrazole-4-carbonitrile, the same compound **4** was obtained with no evidence for the production of (pyrazolylamino)pyridopyrimidine **5** or pyrazolodipyridopyrimidine **6**. Poly-functionalized dipyridopyrimidine **8** was obtained by reaction of compound **1** with 2-[(methylthio)-(phenylamino)methylene]propanedinitrile. Cyanoguanidine was reacted with compound **1** to afford *N*-pyridopyrimidinylguanidine **9**, which was subjected to cyclization reaction, in presence of piperidinium acetate, to give pyridopyrimidopyrimidine **10**.

Keywords: pyridopyrimidine; dipyridopyrimidine; pyridopyrimidopyrimidine.

INTRODUCTION

Recently, a convenient new synthesis of 2-chloro-4*H*-pyrido[1,2-*a*]pyrimidin-4-one (**1**) was described.[1] It is well-known that this type of *α*-haloheterocyclic compounds are susceptible to synthetically important nucleophilic substitutions.[2–5] Many hetero-fused pyrimidines exhibit attractive cancer chemotherapy properties as antitumor agents.[6] Risperidone, SSR6907, and ramastine are derivatives of pyrido[1,2-*a*]pyrimidin-4-one, which show antipsychotic activity.[7–9] Dominguez *et al.*[10] reported that some hetero-fused tricyclic systems exhibited significant antimalarial activity. It was cited that the biological reac-

---

11

tivity of this category of compounds is essentially due to presence of the pyrido[1,2-*a*]pyrimidinone moiety in their molecular structure.[11] In this study, it was planned to utilize the readily available chloro derivative to obtain novel polycyclic compounds, which could be expected to possess antimalarial activity.

RESULTS AND DISCUSSION

Analytical and spectral characterization of the prepared compounds

*2-Azido-4*H-*pyrido[1,2-*a]*pyrimidin-4-one (2)*. Anal. Calcd. for $C_8H_5N_5O$ (FW 187.16): C, 51.34; H, 2.69; N, 37.42 %; Found: C, 50.96; H, 2.54; N, 37.40 %. IR (KBr, cm^{-1}): 3073, 3042, 2129 (N_3), 1718 (C=O), 1634 (C=N), 1565, 1517, 1455, 1412, 1110, 930, 839, 782, 760. ^{1}H-NMR (200 MHz, DMSO-d_6, δ / ppm): 5.85 (1H, *s*, C_3–H), 7.55 (1H, *dd*, *J* = 7.5, 3.6 Hz, C_7–H), 7.63 (1H, *d*, *J* = 7.4 Hz, C_9–H), 8.08 (1H, *dd*, *J* = 7.4, 3.4 Hz, C_8–H), 8.99 (1H, *d*, *J* = 7.5 Hz, C_6–H). MS (*m/z* (*I* / %)): M$^+$ 187 (34).

*2-Hydrazino-4*H-*pyrido[1,2-*a]*pyrimidin-4-one (3)*. Anal. Calcd. for $C_8H_8N_4O$ (FW 176.18): C, 54.54; H, 4.58; N, 31.80 %; Found: C, 54.42; H, 4.42; N, 31.77 %. IR (KBr, cm^{-1}): 3428, 3340, 3328, 3270 (NHNH$_2$), 3072, 1690 (C=O), 1636 (C=N), 1610, 1570, 1518, 1445, 1352, 1080, 776. ^{1}H-NMR (200 MHz, DMSO-d_6, δ / ppm): 4.30 (2H, *b*, NH$_2$), 5.62 (1H, *s*, C_3–H), 7.31 (*dd*, 1H, *J* = 7.4, 3.6 Hz, C_7–H), 7.56 (1H, *d*, *J* = 7.2 Hz, C_9–H), 7.95 (1H, *dd*, *J* = 7.2, 3.5 Hz, C_8–H), 8.12 (1H, *b*, NH), 8.93 (1H, *d*, *J* = 7.4 Hz, C_6–H). MS (*m/z* (*I* / %)): M$^+$ 176 (80).

*5-Amino-3-(methylthio)-1-(4-oxo-4*H-*pyrido[1,2-*a]*pyrimidin-2-yl)-1*H-*pyrazole-4-carbonitrile (4)*. Anal. Calcd. for $C_{13}H_{10}N_6OS$ (FW 298.33): C, 52.34; H, 3.38; N, 28.17; S, 10.75 %; Found: C, 52.33; H, 3.38; N, 28.10; S, 10.50 %. IR (KBr, cm^{-1}): 3360, 3265 (NH), 3115, 3071, 3043, 2924, 2210 (CN), 1676 (C=O), 1614 (C=N), 1549, 1501, 1457, 819, 762. ^{1}H-NMR (200 MHz, DMSO-d_6, δ / ppm): 2.56 (3H, *s*, SCH$_3$), 6.59 (1H, *s*, C_3–H), 7.43 (1H, *m*, C_7–H), 8.08 (2H, *m*, C_9–H + C_8–H), 8.38 (2H, *s*, NH$_2$), 8.99 (1H, *d*, *J* = 7.4 Hz, C_6–H). ^{13}C-NMR (70 MHz, DMSO-d_6, δ / ppm): 38.5, 93.7, 100.1, 116.4, 118.0, 121.3, 124.2, 130.6, 133.8, 148.7, 149.7, 154.4, 158.9.

*4-Imino-2-(methylthio)-5-oxo-1-phenyl-1,5-dihydro-4*H-*dipyrido-[1,2-*a:2',3'-d]-*pyrimidine-3-carbonitrile (8)*. Anal. Calcd. for $C_{19}H_{13}N_5OS$ (FW 359.41): C, 63.50; H, 3.65; N, 19.49; S, 8.92 %; Found: C, 6.40; H, 3.30; N, 19.20; S, 8.60 %. IR (KBr, cm^{-1}): 3292 (NH), 3065, 3039, 3001, 2928, 2202 (CN), 1671 (C=O), 1621 (C=N), 1596, 1524, 1492, 1261, 759; ^{1}H-NMR (200 MHz, DMSO-d_6, δ / ppm): 2.08 (3H, *s*, SCH$_3$), 7.05–8.29 (8H, *m*, 5H$_{arom.}$+ C_7–H + C_9–H + C_8–H), 8.85 (1H, *d*, *J* = 7.5 Hz, C_6–H), 10.19 (1H, *s*, NH). ^{13}C-NMR (70 MHz, DMSO-d_6, δ / ppm): 35.5, 89.3, 96.4, 115.3, 117.7, 122.4, 112.9, 125.2, 129.7, 136.2, 139.0, 140.5, 142.1, 151.2, 156.0, 160.3, 165.9.

N-*Cyano-*N'-*(4-oxo-4*H-*pyrido[1,2-*a]*pyrimidin-2-yl)guanidine (9)*. Anal. Calcd. for $C_{10}H_8N_6O$ (FW 228.21): C, 52.63; H, 3.53; N, 36.83 %; Found: C,

52.31; H, 3.40; N, 36.72 %; IR (KBr, cm^{-1}): 3429, 3383 (NH), 3334, 3249, 3194 (NH), 3151, 2920, 2207 (CN), 1669 (C=O), 1639 (C=N), 1571, 1506, 1434, 1357, 777, 721, 669. ^{1}H-NMR (200 MHz, DMSO-d_6, δ / ppm): 5.40 (1H, s, NH, disappeared with D$_2$O), 6.0 (1H, s, NH, disappeared with D$_2$O), 6.55 (1H, s, C$_3$––H), 7.40 (1H, dd, J = 7.5, 3.6 Hz, C$_7$–H), 7.49 (1H, d, J = 7.5 Hz, C$_9$–H), 7.82 (1H, dd, J = 7.5, 3.6 Hz, C$_8$–H), 7.95–8.08 (1H, bs, NH, disappeared with D$_2$O), 8.80 (1H, d, J = 7.5 Hz, C$_6$–H). ^{13}C-NMR (70 MHz, DMSO-d_6, δ / ppm): 94.3, 115.5, 119.2, 122.6, 124.9, 138.0, 151.2, 157.3, 164.8, 165.8; MS (m/z (I / %)): M$^+$ 228 (28).

*2,4-Diamino-5*H-*pyrido[1,2-*a]*pyrimido[4,5-*d]*pyrimidin-5-one* (**10**). Anal. Calcd. for C$_{10}$H$_8$N$_6$O (FW 228.21): C, 52.63; H, 3.53; N, 36.83 %; Found: C, 52.50; H, 3.20; N, 36.50 %. IR (KBr, cm^{-1}): 3435, 3328 (NH$_2$), 3221, 3172 (NH), 3075, 2936, 1668 (C=O), 1620 (C=N), 1585, 1535, 1440, 1330, 778, 725. ^{1}H-NMR (200 MHz, DMSO-d_6, δ / ppm): 6.59 (2H, s, NH$_2$ disappeared with D$_2$O), 6.68 (2H, s, NH$_2$ disappeared with D$_2$O), 7.44 (1H, dd, J = 7.6, 3.7 Hz, C$_7$–H), 7.52 (1H, d, J = 7.5 Hz, C$_9$–H), 7.89 (1H, dd, J = 7.5, 3.6 Hz, C$_8$–H), 8.94 (1H, d, J = 7.6 Hz, C$_6$–H). ^{13}C-NMR (70 MHz, DMSO-d_6, δ / ppm): 98.5, 114.9, 125.4, 128.0, 136.2, 146.2, 154.6, 158.9, 165.5, 169.8; MS (m/z (I / %)): M$^+$ 228 (100).

Chemistry

Reaction of the chloro-compound **1** with sodium azide was performed in DMF, leading to 2-azidopyridopyrimidinone (**2**).[12,13] The IR spectrum of the product showed a sharp medium peak at v_{max} 2129 cm^{-1}, which is characteristic for the azide function. The same compound was afforded when 2-hydrazinopyridopyrimidinone (**3**) was treated with *in situ* freshly obtained nitrous acid. This hydrazine–azido conversion was previously described by Kovačič *et al.*,[12] albeit they did not give any characterization for the structure of the azido product but the same melting point was obtained. The hydrazine **3** was preliminary obtained *via* refluxing the chloro compound **1** with hydrazine hydrate, according to the method described by Oakes and Rydon,[14] who did not give spectral characterization of the structure of the product. The IR and ^{1}H-NMR spectra of the hydrazine **3** are given herein to fortify the proposed structure (Scheme 1).

Reaction of the chloro-compound **1** with 5-amino-3-(methylthio)-1*H*-pyrazole-4-carbonitrile,[15] in boiling DMF, did not lead to the expected 5-(pyridopyrimidinylamino)-1*H*-pyrazole-4-carbonitrile (**5**) or its targeted cyclized isomer pyrazolo[3',4':1,6]pyrido-[2,3-*d*]pyrido[1,2-*a*]pyrimidinone (**6**). IR spectroscopy revealed the occurrence of the cyano function at v_{max} 2210 cm^{-1}. The ^{1}H-NMR spectrum showed the existence of NH$_2$ at δ 8.38 ppm, which disappeared on addition of D$_2$O, besides δ 6.59 ppm, which is specific for position 3 of pyridopyrimidinone and the four proton set of the pyridine ring. These results suggested

that the obtained compound is 1-(pyridopyrimidin-2-yl)pyrazole (**4**). The production of the pyrazole **4** can be attributed to the greater nucleophilicity character of the ring nitrogen compared with the α-amino group, which backs to the mesomeric effect. However, a clear-cut establishment of the structure was achieved from the cyclization of the hydrazine **3** with [bis(methylthio)methylene]-malononitrile.[16,17] This reaction was reported for the formation of 1-substituted 5-amino-3-(methylthio)-1*H*-pyrazole-4-carbonitriles starting from hydrazines[18] (Scheme 1).
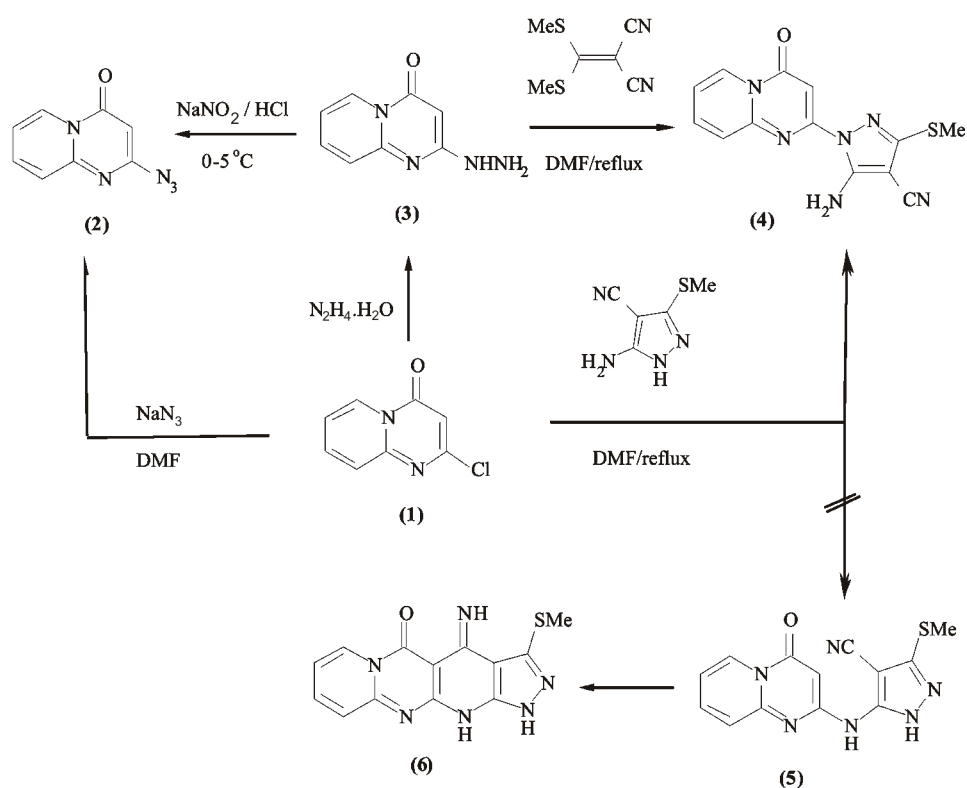
Scheme 1.

2-[(Methylthio)(phenylamino)methylene]propanedinitrile was subjected to reaction with the chloro compound **1** in refluxing DMF. Surprisingly, the intended 2-{(methylthio)[phenyl(4-oxo-4*H*-pyrido[1,2-a]pyrimidin-2-yl)amino]}propanedinitrile (**7**) was not isolated. The spectra of the product showed the occurrence of an imino function and at the same time the disappearance of the characteristic signal due to C–H at position 3. This suggested that the obtained product was cyclized in a cascade nucleophilic reaction to yield dipyrido[1,2-*a*:2',3'-*d*]pyrimidine **8** (Scheme 2).

Scheme 2.
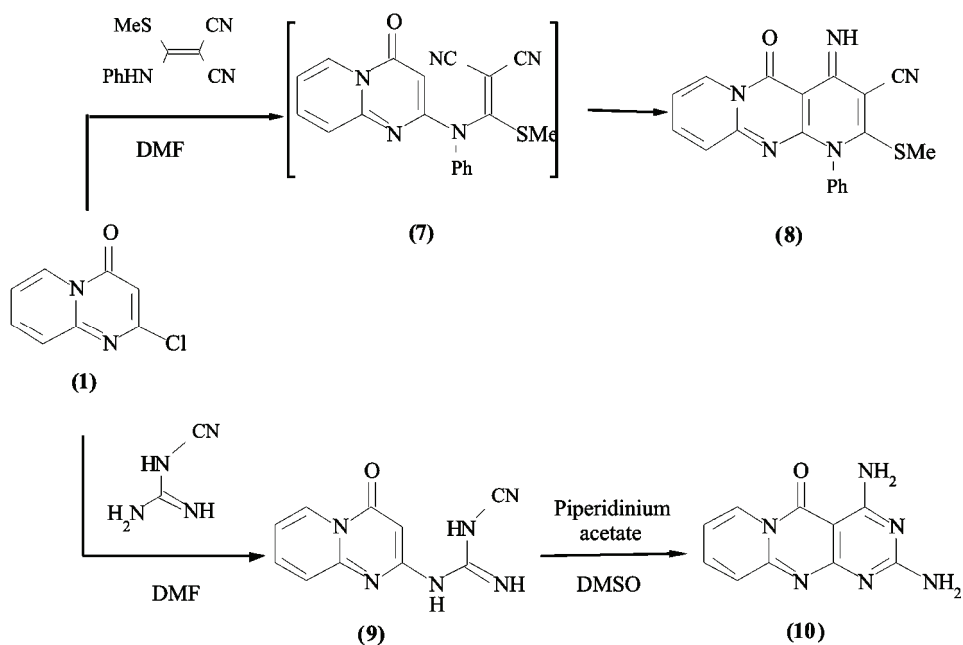
Reaction of the chloro compound **1** with cyanoguanidine in boiling DMF gave the claimed *N*-cyano-*N'*-(pyridopyrimidinyl)guanidine **9**. The IR spectrum exhibited a sharp absorbance peak at v_{max} 2207 cm^{-1} due to the CN function. Trials for cyclization of this guanidine derivative met success by the action of piperidinium acetate in boiling DMSO. It is thought that the relatively high boiling temperature of DMSO is conditional for such a reaction because attempts to perform the same reaction in THF, dioxane, and DMF were not successful. The structure of the product was confirmed from its spectral data which suggested that the product is pyrido[1,2-*a*]pyrimido[4,5-*d*]pyrimidinone **10** (Scheme 2).[10]

EXPERIMENTAL

Melting points were determined in an open capillary tube on a digital Gallen-Kamp MFB-595 apparatus. The IR spectra were taken on a Perkin-Elmer FT-IR 1650, using samples in KBr disks. The ^{1}H-NMR (200 MHz) and ^{13}C-NMR (70 MHz) spectra were recorded on Varian Gemini-200 spectrometer, using DMSO-d_6 as the solvent and TMS as the internal reference. The mass spectrum was determined on a HP-MS 5988 mass spectrometer by direct inlet, operating at 70 eV. Elemental microanalysis was performed on a Perkin Elmer CHN--2400 Analyzer.

*2-Azido-4*H-*pyrido[1,2-*a]*pyrimidin-4-one (**2**)*

Method A. To a solution of the chloro-derivative **1** (10 mmol) in DMF (20 mL), sodium azide (15 mmol) was added and the reaction mixture was heated on a boiling water bath for 2

h. Then the reaction mixture was diluted with ice-water (20 mL) and left to stand for 1 h. The product was filtered and crystallized from DMF/H$_2$O (1:1). Yield 80 %, m.p. 160–161 °C.

Method B. To a stirred cold (0–5 °C) solution of the hydrazino derivative **3** (10 mmol), in 2 M hydrochloric acid (10 mL), an aqueous 1 M sodium nitrite solution (10 mL,) was added dropwise. Then, stirring was continued at room temperature for 1 h and the obtained precipitate was filtered and crystallized from DMF/H$_2$O (1:1) to give the azido derivative **2**. Yield: 72 %, m.p. 160–161 °C (m.p. 160–163 °C[12]).

*2-Hydrazino-4*H-*pyrido[1,2-*a*]pyrimidin-4-one (3)*

A mixture of the chloro-compound **1** (10 mmol) and hydrazine hydrate (15 mmol) in DMF (10 mL) was refluxed for 1 h. Then the reaction mixture was poured onto crushed ice and the solid deposits were filtered and crystallized from ethanol to give the hydrazine compound **3**. Yield: 69 %, m.p. 240–242 °C (m.p. 245 °C[14]).

*5-Amino-3-(methylthio)-1-(4-oxo-4*H-*pyrido[1,2-a]pyrimidin-2-yl)-1*H-*pyrazole-4-carbonitrile (4)*

Method A. To a solution of the hydrazino compound **3** (5 mmol) in DMF (20 mL), [bis-(methylthio)methylene]malononitrile (5 mmol) was added and the reaction mixture was refluxed for 2 h. The solid product, which separated after cooling, was filtered using a suction pump, washed thoroughly with ethanol and crystallized from DMF. Yield: 89 %, m.p. > 300 °C.

Method B. A mixture of the chloro-compound **1** (5 mmol) and 5-amino-(3-methylthio)- -1*H*-pyrazole-4-carbonitrile[15] (5 mmol) in DMF (20 mL) was boiled under reflux for 2 h. Afterwards, the reaction mixture was left to cool to room temperature. The so-obtained crystalline deposit was filtered and recrystallized from DMF to give pyridopyrimidylpyrazole **4**. Yield: 77 %.

*4-Imino-2-(methylthio)-5-oxo-1-phenyl-1,5-dihydro-4*H-*dipyrido-[1,2-*a*:2',3'-*d*]pyrimidine-3- -carbonitrile (8)*

A mixture of the chloro-compound **1** (10 mmol) and 2-[(methylthio)(phenylamino)-methylene]propanedinitrile (10 mmol) in DMF (25 mL) was heated under reflux for 4 h. Subsequently, the reaction mixture was left to cool to room temperature. The obtained yellow crystalline material was filtered off and recrystallized from DMF to give compound **8**. Yield: 73 %, m.p. 257–258 °C.

N-*Cyano*-N'-*(4-oxo-4*H-*pyrido[1,2-*a*]pyrimidin-2-yl)guanidine (9)*

A mixture of the chloro compound **1** (5 mmol) and cyanoguanidine (5 mmol) in DMF (20mL) was heated under reflux for 4 h. After cooling to room temperature, the mixture was diluted with cold water and the solid that deposited was collected by filtration and crystallized from acetone to give the guanidine derivative **9**. Yield: 80 %, m.p. 178–180 °C.

*2,4-Diamino-5*H-*pyrido[1,2-*a*]pyrimido[4,5-*d*]pyrimidin-5-one (10)*

A solution of the guanidine derivative **9** (5 mmol) and piperidinium acetate (from 0.15 g piperidine and 0.1 g acetic acid, 1.5 mmol) in DMSO (25 mL) was heated under reflux for 4 h. The reaction mixture was left to cool to room temperature. The so-formed precipitate was filtered off and washed several times with absolute ethanol. The product was crystallized from DMF to give the yellowish orange diamine **10**. Yield 85 %, m.p.> 300 °C (Lit.[10] data is not available).

И З В О Д

СУПСТИТУИСАНИ ПИРИДОПИРИМИДИНОНИ. ДЕО IV.
2-ХЛОРО-4Н-ПИРИДО[1,2-*a*]ПИРИМИДИН-4-ОН КАО СИНТОН
НЕКИХ НОВИХ ХЕТЕРОЦИКЛИЧНИХ ЈЕДИЊЕЊА

MOHAMED ABASS, MOSTAFA M. ISMAIL, WAFAA R. ABDEL-MONEM и AISHA S. MAYAS

Department of Chemistry, Faculty of Education, Ain Shams University, Roxy, Cairo 11757, Egypt

2-Хлоро-4*H*-пиридо[1,2-*a*]пиримидин-4-он (**1**) је коришћен као синтон-прекурсор за синтезу нових хетеротрицикличних система. 2-Азидо- и 2-хидразино-деривати (**2** и **3**) добијени су нуклеофилном супституцијом из једињења **1**. Хидразино-дериват **3** трансформисан је нитрозовањем у азидо-дериват **2**. Третирањем једињења **3** са [бис(метилтио)метилен]малононитрилом добијен је 2-пиразолилпиридопиримидин (**4**). Реакцијом једињења **1** са 5-амино--3-(метилтио)-1*H*-пиразол-4-карбонитрилом добијено је исто једињење **4** без грађења пиразолиламино)пиридопиримидино **5** или пиразолодипиридопиримидина **6**. Поли-функционализован дипиридопиримидин **8** добивен је реакцијом једињења **1** са 2-[(метилтио)-фениламино)метилен]пропандинитрилом. Цијаногванидин је третиран са једињењем **1** градећи *N*-ридопиримидинилгванидин **9**, који реакцијом циклизације у присуству пиперидинијум-ацетата, даје пиридопиримидопиримидин **10**.

(Примљено 27. новембра 2008, ревидирано 9. јуна 2009)

REFERENCES

1. M. Abass, A. S. Mayas, *Heteroatom Chem.* **18** (2007) 19
2. H. R. Snyder, M. M. Robison, *J. Am. Chem. Soc*. **74** (1952) 4910
3. A. R. Katritzky, A. J. Waring, *J. Chem. Soc.* (**1962**) 1544
4. M. di Braccio, G. Roma, M. Mazzei, A. Balbi, P. Schiantarelli, S. Cadel, S. Bongrani, *Farmaco* **43** (1988) 705
5. C. Plug, W. Frank, C. Wentrup, *J. Chem. Soc., Perkin Trans 2* (**1999**) 1087
6. S. Wang, A. Folkes, I. Chuckowree, X. Cockcroft, S. Sohal, W. Miller, J. Milton, S. P. Wren, N. Vicker, P. Depledge, J. Scott, L. Smith, H. Jones, P. Mistry, R. Faint, D. Thompson, S. Cocks, *J. Med. Chem.* **47** (2004) 1329
7. O. Bruno, C. Brullo, S. Schenone, F. Bondavalli, A. Ranise, M. Tognolini, M. Impicciatore, V. Ballabeni, E. Barocelli, *Bioorg. Med. Chem.* **14** (2006) 121
8. K. L. E. Josephine, P. S. M. Aloysius, B. F. Paul, *PCT Int. Appl. WO* 2000020422 A1 20000413, 2000; Chem. Abstr. *CA* 265 188t
9. K. L. E. Josephine, V. D. Keybus, F. M. Alfons, M. J. Carolus, *PCT Int. Appl. WO* 2000020421 A2 20000413, 2000; Chem. Abstr. *CA* 265187c
10. J. Dominguez, J. Charris, L. Iarrusso, S. Lopez, G. Lobo, F. Riggione, *Farmaco* **51** (1996) 781
11. A. R. Katritzky, J. W. Rogers, R. M. Witek, S. K. Nair, *Arkivoc* **8** (2004) 52
12. M. Kovačič, S. Polanc, B. Stanovnik, M. Tišler, *J. Heterocycl. Chem.* **11** (1974) 949
13. S. Polanc, B. Stanovnik, M. Tišler, *J. Org. Chem.* **41** (1976) 3152
14. V. Oakes, H. N. Rydon*, J. Chem. Soc.* (1958) 209
15. J. S. Larsen, M. A. Zahran, E. B. Pedersen, C. Nielsen, *Monatsh. Chem.* **130** (1999) 1167
16. M. Abass, *Phosphorus, Sulfur Silicon Relat. Elem.* **170** (2003) 1413
17. K. A. Jensen, L. Hendriksen, *Acta Chem. Scand.* **22** (1968) 1107
18. Y. Tominaga, Y. Honkawa, M. Hara, A. Hosomi, *J. Heterocycl. Chem.* **27** (1990) 775.

Stability evaluation of house dust mite vaccines for sublingual immunotherapy

LIDIJA BURAZER[1]*, KATARINA MILOVANOVIĆ[1], TANJA
ĆIRKOVIĆ-VELIČKOVIĆ[2#] and MARIJA GAVROVIĆ-JANKULOVIĆ[2#]

[1]*Institute of Virology, Vaccines and Sera – Torlak, Vojvode Stepe 458, Belgrade and*
[2]*Faculty of Chemistry, Department of Biochemistry, Studentski trg 16, Belgrade, Serbia*

Abstract: Allergen-specific immunotherapy with house dust mite (HDM) allergen extracts can effectively alleviate the symptoms of allergic rhinitis and asthma. The efficacy of the immunotherapeutic treatment is highly dependent on the quality of house dust mite vaccines. This study was performed to assess the stability of house dust mite allergen vaccines prepared for sublingual immunotherapy. Lyophilized *Dermatophagoides pteronyssinus* (Dpt) mite bodies were the starting material for the production of sublingual vaccines in four therapeutic concentrations. The stability of the extract for vaccine production, which was stored below 4 °C for one month, showed consistence in the protein profile in SDS PAGE. ELISA-inhibition showed that the potencies of Dpt vaccines during a 12 month period were to 65–80 % preserved at all analyzed therapeutic concentrations. This study showed that glycerinated Dpt vaccines stored at 4 °C preserved their IgE-binding potential during a 12 month period, implying their suitability for sublingual immunotherapeutic treatment of HDM allergy.

Keywords: *Dermatophagoides pteronyssinus*; allergen extract; vaccines; ELISA inhibition; stability.

INTRODUCTION

The protein allergens of house dust mite *Dermatophagoides pteronyssinus* can cause severe allergic disease in susceptible individuals.[1] Allergen extract prepared from cultured dust mites has been used for diagnosis as well as for sublingual-swallow immunotherapy. The beneficial effect of immunotherapy (IT) with crude extract or partly purified allergen had been demonstrated in certain IgE-mediated disorders, such as seasonal allergic rhinitis and asthma.[2,3]

Allergen stability, *i.e.*, persistence of adequate quantities of relevant antigens in an allergen vaccine from the time of initial assay to the time of clinical use, is

19

enhanced by addition of glycerol to the vaccine solution.[4,5] Mite extracts contain at least 20 well-characterized allergens. Several of these proteins appear to be highly immunoreactive in humans with evidence of specific IgE to the individual allergens in up to 80 % of individuals allergic to mites.[5] Four of these allergen groups (1, 3, 6 and 9) are proteolytic enzymes and, due to their biological activity, may compromise the stability of extracts. Several investigators evaluated the stability of mite allergens in commercially available vaccine preparations.[4,6–9] Due to the presence of proteolytic enzymes, glycerol has been considered as a stabilizing agent in house dust mite allergen extracts,[10] since protease inhibitors did not contribute to the stability of a mite extract.[11] However, in addition to optimization of the procedure for the preparation of a potent allergen vaccine, evaluation of its stability from the time of preparation to the intended clinical use is of major importance for reliable and effective immunotherapeutic treatment.

The aim of this work was to investigate the relative potency of a mite sublingual-swallow immunotherapeutic vaccine stabilized with 50 % glycerol, stored at 4 °C (producer recommendation) over a 12-month period. The stability of a pure mite extract was also examined over a 1-month storage period at the same temperature as used for the preparation of vaccines.

EXPERIMENTAL

Allergen extract preparation

The house dust mite extract was prepared from dried house dust mite bodies of *Dermatophagoides pteronyssinus*. The certificate of analysis for the starting material declared 95 % purity and 5 % medium particles. The extraction procedure was realized according to the manufacturer's recommendation.[12] In brief, the extraction was performed overnight at 4–8 °C using a 1 % solution in 0.15 M phosphate-buffered saline (PBS) pH 7.6. The extract was clarified by centrifugation at 2000 rpm for 30 min and subsequently filtered through a 0.22 µm membrane disc filter (Pall Europe Limited, Portsmouth, UK). The protein content was quantified according to the Kjeldal method.[13]

Allergen vaccines preparation

The *D. pteronyssinus* protein extract was used for the preparation of sublingual-swallow vaccines in PBS with 50 % glycerol. The vaccine marked as "3", with a concentration of 1000 PNU (protein nitrogen units), was used for the preparation of three serial dilutions designated as "2", "1", and "0", containing 125, 16 and 2 PNU, respectively. All vaccines were stored at 4 °C during the investigation period.

Human sera

The sera from 10 patients allergic to house dust mites with a documented clinical history of HDM allergy and without a record on immunotherapy to this allergen were used for the serological analysis.

SDS PAGE and Western blot

SDS PAGE was performed according to Laemmli.[14] The gel was either stained with Coomassie Brilliant Blue R-250 (CBB) to visualize the separated proteins or the resolved components were blotted by a semi-dry electrotransfer onto a nitrocellulose membrane (0.45

μm, Serva, Heidelberg, Germany). The membrane was blocked in 20 mM Tris-buffered saline (TBS) containing 1 % BSA and 0.1 % Tween 20 for 1 h and dried until development.

IgE detection

IgE-reactive proteins were detected in Western blots with 5-fold diluted individual patient's sera in TBS-buffer with 0.1 % BSA. Alkaline phosphatase labeled monoclonal anti-human IgE (1:1000, Sigma Chemical Co., St Louis MO, USA) was used as the secondary antibody. The binding patterns were visualized with a substrate solution of 1.5 mg BCIP (5-bromo-4-chloro-3-indolyl phosphate, Serva, Heidelberg, Germany) and 3 mg NBT (nitro blue tetrazolium, Serva, Heidelberg, Germany) in 10 mL of 100 mM Tris buffer, containing 150 mM NaCl and 5 mM $MgCl_2$, pH 9.6, according to Harlow & Lane.[15]

Evaluation of vaccine potency by ELISA-inhibition

The potency of each of the four vaccines was investigated by ELISA-inhibition with a pool of the sera from the allergic persons. Vaccine sampling has been performed after zero, three and 12 months of storage, and the potency was titrated in 6 dilutions. Microtiter plates (Nunc-Immuno Plate, Maxisorp, Inter med, Denmark) were coated with 100 μl/well (10 μg/mL protein concentration) of *D. pteronyssinus* extract in 0.06 M carbonate buffer, pH 9.6, overnight at 4 °C. The plate was washed with PBS containing 0.05% Tween 20 (PBS-T) and blocked with 0.1% bovine serum albumin dissolved in PBS-T (PBS-T-B) for 1 h at room temperature. The subsequent steps were performed using PBS-T-B as diluent, and washings in PBS-T were realized between the following steps: the plate was incubated with 100 μl of the pool of patients' sera (CAP class 1 to 6; diluted 1:5 in PBS-T-B) previously incubated with decreasing concentrations of the vaccine (diluted 1, 5, 10, 100, 500, 1000 and 5000 times) at 37 °C for 2 h. Subsequently, the plate was incubated with 100 μl of anti-human IgE (Sigma) for 2 h at room temperature. The assay was developed by adding 100 μl of the enzyme substrate (pNPP 1 mg/mL in 0.1 M diethanolamine buffer, pH 9.6), and the absorbance was measured at 405 nm using a plate reader (Multiskan) after 60 min of incubation. A serum from a non-allergic person was used as the negative control.

RESULTS AND DISCUSSION

SDS PAGE

Coommasie Brilliant Blue staining of a one-dimensional SDS PAA gel revealed a complex protein pattern for the Dpt extract in the range of about 12–116 kD (Fig. 1). The dominant protein bands were at about 116 kD, 25–30 kD, and 12–18 kD. SDS-PAGE analysis of pure non-glycerinated Dpt extract was employed for the evaluation of the extract quality, expressed through the protein bands detected after one month of storage. Under the employed experimental conditions, storage of the Dpt extract at 4 °C was suitable as the starting material for vaccine production. A longer period of storage (two months) revealed deterioration of the protein extract, suggesting one-month period at 4 °C as the maximum for an extract intended for vaccine preparation.

IgE binding profile of separated mite components

Immunoblots were performed using the sera of allergic patients with specific IgE class 6, and class 3 (Fig. 2). These immunoblots showed that patients' sera

Available online at www.shd.org.rs/JSCS/

class 6 recognized most of the proteins present in the extract while patients' sera class 3 recognized proteins of about 14 and 25 kD (major allergens) and some of higher molecular mass.
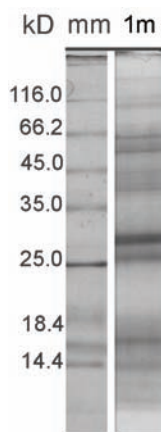
Fig. 1. Separation of house dust mite whole-body extracts by SDS gel electrophoresis on a 12 % PA gel: mm – molecular mass markers, 1m – 1st month.
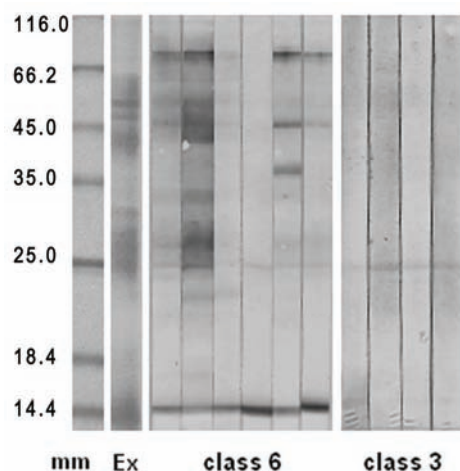
Fig. 2. IgE reactivity of the HDM extract with patients' sera class 6 and class 3, mm – molecular mass markers, Ex – extract.

ELISA-inhibition

Dpt vaccine "0" and "1" showed 100 % inhibition in full concentration after zero and after three months; however, the potency was reduced to 66 %, and 75 %, respectively after 12 months (Figs. 3 and 4). A remarkable decrease in potency of both vaccines was noticed within the first dilution and continued throughout the investigated period. The decrease could be ascribed not only to dilution of the glycerol as the stabilizing agent of the allergen proteins, but also to protein instability in diluted concentrations (2, and 16 PNU). Vaccines "2" and "3" showed 100 % inhibition after zero and after three months period. The high IgE inhibition

potential of these vaccines (> 80 %) was preserved after 12 months (Figs. 5 and 6). Vaccine "3", with the highest allergen concentration, retained high IgE inhibition potential at almost all dilutions after 12 months storage.
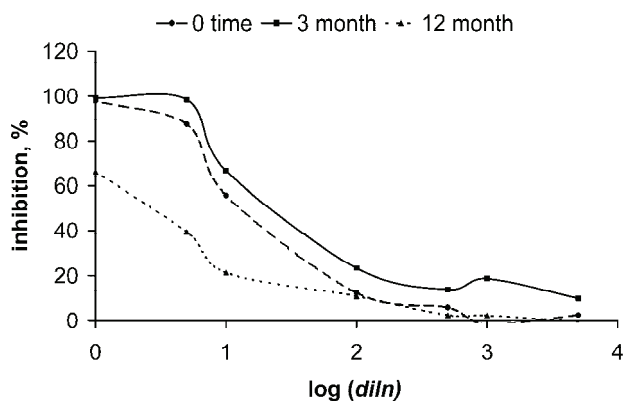
Fig. 3. IgE ELISA-inhibition of vaccine SLIT "0" during 12 months: percentage of inhibition *vs.* logarithm of dilution, (diln – volumetric ratio of solution and diluent).
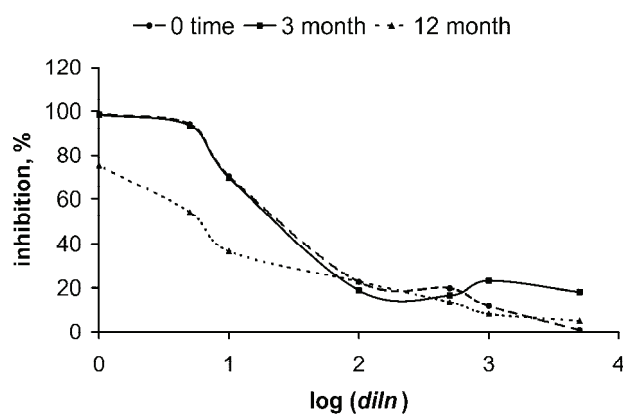
Fig. 4. IgE ELISA-inhibition of vaccine SLIT "1" during 12 months: percentage of inhibition *vs.* logarithm of dilution, (diln – volumetric ratio of solution and diluent).
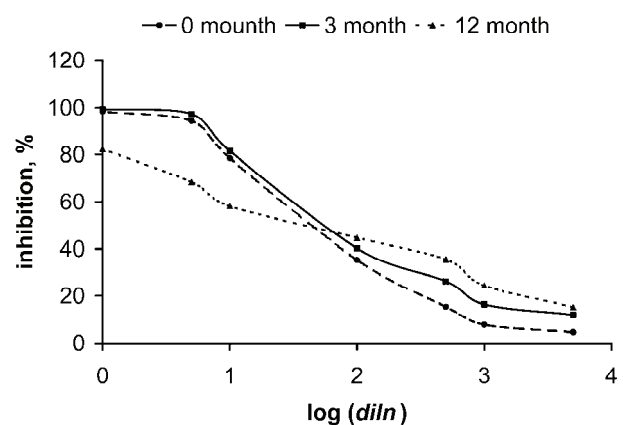
Fig. 5. IgE ELISA-inhibition of vaccine SLIT "2" during 12 months: percentage of inhibition *vs.* logarithm of dilution, (diln – volumetric ratio of solution and diluent).
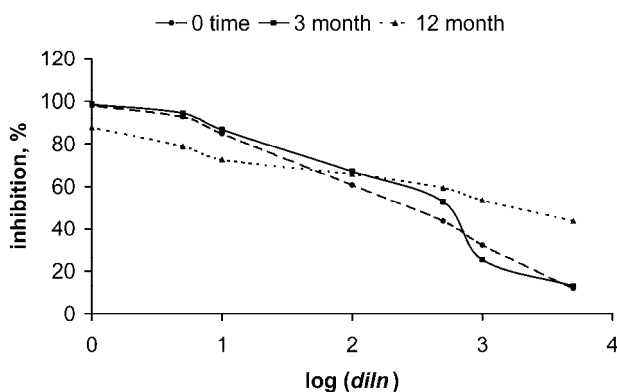
Fig. 6. IgE ELISA-inhibition of vaccine SLIT "3" during 12 months: percentage of inhibition *vs.* logarithm of dilution, (diln – volumetric ratio of solution and diluent).

The stability of allergen extracts expressed as IgE inhibition potential depends on many factors, including the starting material, the method of manufacture, dilution, stored temperature, *etc*. It was already noticed that the loss of potency was higher in diluted allergen extracts and at higher storage temperatures.[16] Nelson *et al.* explained the loss of potency in dilute extracts by adsorption of protein onto the surface of the vial, which could be decreased by the addition of extra protein, such as human serum albumin, to the extract.[17] Thereafter, the presence of proteases in some allergen extracts, which could break down allergenic proteins, was recognized as an additional cause for the loss of potency. The presence of proteases was confirmed in allergen extracts of fungi,[18] cockroaches and house dust mite.[19,20]

Allergen manufacturers usually recommend storage of commercial allergen vaccines at 4 °C for a 12-month period.[12] Guided by this recommendation, the stability of Dpt allergen vaccine intended for application in sublingual-swallow immunotherapy was investigated. Four therapeutic concentrations were analyzed: solution "3", with the highest concentration (1000 PNU), was used for the preparation of serial vaccine dilutions in the proportion 1:7. Solution "3" showed the highest stability maintained over 12 months, expressed as more than 80 % preserved inhibition potential. The other solutions also retained a high % of inhibition (more than 65 %) during the investigated period. Glycerol used in the vaccine preparation seems to be a good stabilizer for *D. pteronyssinus* allergens. A protective effect was reported for 25 % glycerol, while 50 % glycerol, which was also found to be effective in the present study, was described as being able to inhibit enzyme activity.[16]

CONCLUSIONS

This study showed that allergen vaccines intended for sublingual HDM immunotherapy fulfill the requirement for the estimated potency, derived from an assay of total allergenic activity to be not less than 50 % of the stated potency,[21]

by retaining more than 65 % of inhibition after 12 months storage at 4 °C. All relevant Dpt allergens were presented in the primary house dust mite extract which was used for the preparation of the vaccines. However, the rapid advancement in recombinant DNA technology, peptide synthesis and protein analysis will offer new opportunities for the design and improvements in the standardization of allergen vaccines in the near future.

И З В О Д

ИСПИТИВАЊЕ СТАБИЛНОСТИ ВАКЦИНЕ КУЋНЕ ПРАШИНЕ
ЗА СУБЛИНГВАЛНУ ИМУНОТЕРАПИЈУ

ЛИДИЈА БУРАЗЕР[1], КАТАРИНА МИЛОВАНОВИЋ[1], ТАЊА ЋИРКОВИЋ-ВЕЛИЧКОВИЋ[2]
и МАРИЈА ГАВРОВИЋ-ЈАНКУЛОВИЋ[2]

[1]Инсȃиȃуȃ за вирусолоīију, вакцине и серуме Торлак, Беоīрад и
[2]Хемијски факулȃеȃ, Универзиȃеȃ у Беоīраду, Беоīрад

Алерген-специфична имунотерапија представља поступак који може да промени ток болести код алергијског ринитиса и астме. Квалитет вакцине припремљене од кућних гриња значајно утиче на ефикасност имунотерапеутског третмана. Испитивање је имало за циљ процену стабилности вакцине кућних гриња намењене за сублингвалну имунотерапију. Тело лиофилозованих *Dermatophagoides pteronyssinus* гриња (Dpt-гриња) употребљено је као полазни материјал за производњу сублингвалне вакцине у 4 различита терапеутска разблажења. Потентност Dpt вакцина праћена ELISA-инхибицијом у 4 терапеутска разблажења, након 12 месеци задржан је у свим разблажењима у опсегу 65–80 %. Испитивање је показало да глицеролом стабилизоване Dpt вакцине за сублигвалну имунотерапију, уз чување на 4 °C задржавају алергени потенцијал (> 65 %) након 12 месеци од њихове припреме, и као такве могу се користити за третман алергије на кућне гриње.

(Примљено 30. априла, ревидирано 7. јула 2009)

REFERENCES

1. T. A. E. Plats-Mills, J. A. Woodfolk, in *Allergy and allergic diseases*, A. B. Kay, Ed., Blackwell Science, Oxford, 1997, p. 888
2. E. Femandez-Caldas, L. Puerta, R. F. Lockey, in *Allergens and allergen immunotherapy*, R. F. Lockey, S. C. Bukantz, Eds., Marcel Dekker, New York, 1999, p. 181
3. J. Bousquet, I. J. Ansotqui, R. van Ree, P. G. Burney, T. Zuberbier, P. van Cauwenberg, *Allergy* **59** (2004) 1
4. J. Bousquet, F. Djoukadar, B. Hewitt, F. B. Michel, *Clin. Allergy* **15** (1985) 29
5. A. Nacrdal, J. S. Vilsvik, *Clin. Allergy* **13** (1983) 149
6. W. R. Thomas, W. Smith, B. J. Hales, M. D. Carter, B. J. Bennet, H. D. Shen, E. R. Tovey, K. Y. Chua, *Arb. Paul Ehrlich Inst. Bundesamt Sera Impfstoffe Frankfurt am Main* **91** (1997) 87
7. J. Ackland, G. A Stewart, *J. Allergy Clin. Immunol.* **74** (1984) 848
8. H. S. Nelson, D. Ilke, A. Buchmeier, *J. Allergy Clin. Immunol.* **98** (1996) 382

 9. N. R. Niemeijer, H. F. Kaufman, W. van Hove, A. E. Dubois, J. G. de Monchy, *Ann. Allergy Asthma Immunol.* **76** (1996) 535
10. T. Liu, Y. Lin, *Ann. Allergy Asthma Immunol.* **80** (1998) 177
11. L. N. Soldatova, E. J. Paupore, S. H. Burk, R. Pastor, J. E. Slater, *J. Allergy Clin. Immunol.* **105** (2000) 482
12. *Processing Instruction*, Institute Torlak, Belgrade, 2008
13. D. M. Bollag, M. D. Rozycki, S. J. Edelstein, *Protein Methods*, 2nd ed., Wiley-Liss Inc., New York, 1996, p. 68
14. U. K. Laemmli, *Nature*, **227** (1970) 680
15. E. Harlow, D. Lane, *Cold Spring Harb. Protoc.*, 2006, doi:10.1101/pdb.prot4300
16. H. S. Nelson, *J. Allergy Clin. Immunol.* **67** (1981) 64
17. H. S. Nelson, *J. Allergy Clin. Immunol.* **63** (1979) 417
18. R. E. Esch, in *Regulatory control and standardization of allegenic extracts*, R. Klein, Ed., Gustav Fischer Verlag, Stuttgart, 1990, p. 171
19. S. Wongtim, S. R. Lehrer, J. F. Salvaggio, W. E. Horner, *Allergy Proc.* **14** (1993) 263
20. C. King, S. Brennan, P. J. Thompson, G. A. Stewart. *J. Immunol.* **161** (1998) 645
21. *Specific Requirements for the Production and Control of Allergen Products*, Directive 81/852/EEC, 1994.

Essential oils of *Thymus pulegioides* and *Thymus glabrescens* from Romania: chemical composition and antimicrobial activity

MARIANA PAVEL[1*], MIHAILO RISTIĆ[2] and TATJANA STEVIĆ[2]

[1]University of Medicine and Pharmacy, Faculty of Pharmacy, Bucharest, Romania and [2]Institute for Medicinal Plant Research "Dr. Josif Pančić", Belgrade, Serbia

Abstract: The aim of this work was to analyse the chemical composition and antimicrobial properties of essential oils isolated from two wild-growing species of thyme (*Thymus pulegioides* L. and *T. glabrescens* Willd.) originating from different locations in Romania. The yield of essential oil was determined according to European Pharmacopoeia standards. Qualitative and quantitative analysis of the oils was performed using GC and GC/MS. The antimicrobial activity was tested by the microdilution technique against Gram-negative and Gram-positive bacteria (*Escherichia coli*, *Salmonella typhimurium*, *S. enteritisdis*, *Enterobacter cloacae*, *Pseudomonas aeruginosa*, *Proteus mirabilis*, *Staphylococcus aureus*, *S. epidermidis*, *Streptococcus faecalis*, *Bacillus subtilis*, *Micrococcus luteus*, *M. flavus* and *Listeria monocytogenes*) and human pathogen yeast *Candida albicans*. The essential oil of *Thymus pulegioides* was obtained in a yield of 0.7–1 % (v/d.w. herbal drug) and the main components were carvacrol (50.5–62.6 %), γ-terpinene (9.8–9.9 %) and *p*-cymene (5.8–7.1 %). The essential oil of *T. glabrescens* was obtained in a yield of 0.7 (v/d.w. herbal drug) and the main components were geraniol (55.5 %), neryl acetate (11.1 %) and *β*-bisabolene (6.7 %). The essential oils inhibited microbial growth at concentrations of 10.8–27 μl/ml.

Keywords: *Thymus pulegioides*; *Thymus glabrescens*; essential oil; antimicrobial; composition.

INTRODUCTION

Thymus species (Lamiaceae) are important aromatic plants that synthesize remarkable amount of volatile compounds referred to as essential oil.[1–4]

The essential oils of more than one hundred species of the genus *Thymus* have been chemically investigated, revealing about 360 different volatile components in total. Among these, the monoterpenes were the most prominent group while sesquiterpenes represent a lower percentage of the volatiles. Generally,

---

plants of the genus *Thymus* are considered the most common source of the mono-terpenoid phenols, thymol and carvacrol.[1–3,5]

Essential oils derived from plants of *Thymus* genus have been found to possess significant antifungal, insecticidal, and antimicrobial activities. These properties depend greatly on their chemical compositions and are mainly attributed to their contents of carvacrol (antifungal properties) and thymol (antiseptic).[5–10] These terpenoid phenols bind to the amine groups of the proteins of the bacterial membrane, which alters their permeability and results in the death of the bacteria. In addition, thymol and carvacrol were shown to induce a decrease in the intracellular adenosine triphosphate (ATP) pool of *E. coli* and an increase of the extracellular ATP. Antibacterial activity was also observed for the aliphatic alcohols, especially geraniol, and ester components.[5]

Previous studies reported that Gram-positive bacteria (*Staphylpcoccus aureus*, *Listeria monocytogenes* and *Bacillus cereus*) are more susceptible to essential oils than Gram-negative bacteria (*Escherichia coli* and *Salmonella enteritidis*).[5,6]

The aim of the present study was to elucidate the chemical composition of the essential oils of two of the species of *Thymus* growing wild in Romania, as well as to establish their antimicrobial and antifungal properties. The two analyzed species were *Thymus pulegioides* L. and *T. glabrescens* Willd. The essential oil of *T. pulegioides* L. has been studied extensively in the world and several chemotypes were recorded (carvacrol-type, thymol-type, linalool-type or geraniol-type).[5,8,11–15] According to different studies, *T. pulegioides* essential oil is a broad-spectrum agent that inhibits the growth of moulds and yeasts (*Candida*, *Aspergillus*) and bacteria.[5,8] *T. glabrescens* essential oil has been scantily investigated.[16–18]

EXPERIMENTAL

Plant material

Aerial parts of *Thymus pulegioides* were collected at the flowering stage from two areas of the Bucegi Mountains, Buşteni (sample A) and Sinaia area (sample B), at different altitudes (1000 and 1800 m above sea level). Aerial parts of *T. glabrescens* (sample C), were gathered at flowering stage from the district of Gorj. The plant material was dried under laboratory conditions (24–25 °C) for three weeks and stored. Dr. V. Ciocarlan from the University of Agronomy of Bucharest identified the plants and voucher specimens were stored in the herbarium of the Faculty of Pharmacy, University of Medicine and Pharmacy of Bucharest.

Isolation of the essential oils

Thirty grams of air-dried plant material (two replicates for all chemotypes) were submitted, to hydrodistillation for 3 h using a Clevenger-type apparatus, according to the standard procedure reported in the European Pharmacopoeia.[19]

Gas chromatography

Qualitative and quantitative analyses of the oils were performed using GC and GC/MS. The GC analysis was realised on a GC HP-5890 II instrument equipped with a split-splitless

injector attached to an HP-5 column (25 m×0.32 mm, 0.52 μm film thickness) and a flame-ionisation-detector (FID). The carrier gas flow rate (H_2) was 1 ml/min, the split ratio 1:30, the injector temperature 250 °C and the detector temperature was 300 °C, while the column temperature was linearly programmed from 40–260 °C (at a rate of 4 °/min) and then kept at 260 °C for an additional 20 min. The same analytical conditions were employed for the GC/MS analysis, where an HP G 1800C Series II GCD system was used together with an HP-5MS capillary column (30 m×0.25 mm, 0.25 μm film thickness). The transfer line was heated at 260 °C. The mass spectra were acquired in the EI mode (70 eV), in the *m/z* range 40–400. The carrier gas was helium (0.9 ml/min). Identification of the individual oil components was accomplished by comparison of the retention times of the peaks with those of standard substances and by matching the mass spectral data with those from MS libraries (Wiley 275L, NIST/NBS) using a computer search and the literature.[20] For the purpose of quantitative analysis, the area percentages obtained registered by the FID were used as the base.

Micro-organisms

The antimicrobial activity of the essential oils was evaluated against the Gram-negative bacteria: *Escherichia coli* (ATCC 25922), *Salmonella typhimurium* (ATCC 14028), *S. enteritidis* (ATCC 13176), *Enterobacter cloacae* (ATCC 13883), *Pseudomonas aeruginosa* (ATCC 27853) and *Proteus mirabilis* (ATCC 14273), the Gram-positive bacteria: *Staphylococcus aureus* (ATCC 25923), *S. epidermidis* (ATCC 12228), *Streptococcus faecalis* (ATCC 12952), *Bacillus subtilis* (ATCC 6051), *Micrococcus luteus* (ATCC 10240), *M. flavus* (ATCC 14452), and *Listeria monocytogenes* (NCTC 7973), and the human pathogen yeast *Candida albicans* (ATCC 10231). The micro-organisms were obtained from the Mycological Laboratory, Department of Plant Physiology, Institute for Biological Research "Siniša Stanković", Belgrade, Serbia.

Antimicrobial assay

The minimal inhibitory concentrations (*MIC*) were determined by the microdilution broth method according to references of the National Committee for Clinical Laboratory Standards.[21,22]

The essential oil was diluted in dimethyl sulphoxide (DMSO) in the relation 1:1. Serial dilutions (ranging from 5 to 30 μl/ml) of the stock solutions of essential oil were tested in a microtiter plate (96 wells). The standard antibiotics streptomycin and nystatin (1 mg/ml in DMSO) were used to control the sensitivity of the tested bacteria and fungi. Two growth controls, the medium (Muller–Hinton or Sabouraud broth) and the medium with 2.0 % (v/v) DMSO, were tested for each strain.

The microplates were incubated for 24 h or 48 h at 35–37 °C. The *MIC* values were determined as the lowest concentration of oil inhibiting the visible growth of each micro-organism in the microwells.

The experiments, performed in duplicate, were repeated independently two times and essentially the same results were obtained.

RESULTS AND DISCUSSION

The essential oil was obtained from air-dried plant material in a yield of 0.99–1 % v/w for sample A – *Thymus pulegioides* from Busteni, 0.7 % v/w for sample B – *T. pulegioides* from Sinaia and 0.73 % v/w for sample C – *T. glabrescens*. These results are in conformity with the European Pharmacopoeia standard for Serpylli herba (a yield of at least 0.3 %).[19]

The chemical compositions of the examined essential oils are given in Table I.

TABLE I. The chemical composition of the tested essential oils in mass % (GC/FID (Area, %)) of *Thymus pulegioides* (samples A and B) and *T. glabrescens* (sample C) collected from different regions of Romania (*RI* = retention index; n.i = not identified)

Constituent	*RI*	*T. pulegioides* (sample A)	*T. pulegioides* (sample B)	*T. glabrescens* (sample C)
α-Thujene	922	1.0	0.7	0.1
α-Pinene	927	0.5	0.7	0.1
Camphene	942	0.2	0.2	0.1
1-Octen-3-ol	978	0.7	1.9	0.2
β-Myrcene	987	1.2	1.6	0.1
3-Octanol	996	0.2	0.7	n.i.
α-Phellandrene	1000	0.2	0.2	n.i.
α-Terpinene	1012	1.3	1.5	0.1
p-Cymene	1020	7.1	5.8	1.6
Limonene	1023	0.8	n.i.	n.i.
β-Phellandrene	1024	n.i.	0.4	n.i.
1,8-Cineole	1026	n.i.	0.4	0.3
cis-β-Ocimene	1035	0.2	0.9	n.i.
γ-Terpinene	1054	9.8	9.9	0.2
cis-Sabinene hydrate	1064	0.2	n.i.	n.i.
Linalool	1099	0.4	0.3	0.7
Borneol	1162	0.6	0.2	0.2
Terpinen-4-ol	1174	0.5	0.4	0.1
p-Cymen-8-ol	1186	0.1	n.i.	n.i.
cis-Dihydrocarvone	1197	0.1	0.1	n.i.
trans-Dihydrocarvone	1203	0.1	n.i.	n.i.
trans-Piperitol	1205	n.i.	n.i.	0.1
Nerol	1228	n.i.	n.i.	2.2
Thymol methyl ether	1230	0.5	n.i.	0.5
Carvacrol methyl ether	1240	3.4	0.2	1.4
Geraniol	1257	n.i.	n.i.	55.5
Geranial	1269	n.i.	n.i.	0.5
Thymol	1293	6.6	1.6	1.5
Carvacrol	1304	50.5	62.6	4.7
α-Cubebene	1345	n.i.	n.i.	0.1
α-Terpinyl acetate	1346	0.4	n.i.	n.i.
Neryl acetate	1362	n.i.	n.i.	11.1
Carvacrol acetate	1371	n.i.	0.1	n.i.
β-Bourbonene	1378	0.1	n.i.	1.2
trans-β-Caryophyllene	1413	5.8	5.1	3.6
β-Copaene	1422	0.1	n.i.	0.2
Aromadendrene	1434	0.1	0.1	0.1
α-Humulene	1447	0.2	0.1	0.3
allo-Aromadendrene	1453	n.i.	n.i.	0.1
cis-Muurola-4(14),5-diene	1459	n.i.	n.i.	0.1
γ-Muurolene	1470	0.2	n.i.	0.2

TABLE I. Continued

Constituent	RI	T. pulegioides (sample A)	T. pulegioides (sample B)	T. glabrescens (sample C)
Germacrene D	1475	0.1	0.1	4.0
β-Bisabolene	1503	5.2	1.9	6.7
δ-Cadinene	1517	0.4	0.2	0.5
Caryophyllene oxide	1576	0.3	0.5	0.5

The chemical composition of *T. pulegioides* essential oil did not vary depending on the harvest location. In sample A (*T. pulegioides* from Sinaia), the main components were monoterpenoid phenols (57.1 %), of which carvacrol was the most abundant (50.5 %). Monoterpenoid hydrocarbons were also important constituents of this sample, reaching up to 15.5 %, as were sesquiterpenoid hydrocarbons with 12.4 %. Monoterpenoid alcohols were present in only small percentages of 1.5 %, whilst the sesquiterpenoid ones were not identified. Other identified components were phenol methyl ethers of thymol and carvacrol (3.9 %). High percentages of phenol precursors were identified: 9.8 % γ-terpinene and 7.1 % *p*-cymene.

In sample B (*T. pulegioides* from Busteni), phenols were also the main components (64.2 %), and carvacrol was again the most important one (62.6 %), together with only 1.6 % thymol. Monoterpenoid hydrocarbons represented 22.1 % of the total peak area and sesquiterpenoid ones represented 7.7 %. Monoterpenoid alcohols and sesquiterpenoid alcohols were present in a small percentage of 1.5 %. The phenol precursors were present in almost the same quantities as in sample A: 9.9 % γ-terpinene and 5.8 % *p*-cymene.

The chemical composition of sample C (*T. glabrescens* essential oil) was essentially different from those of samples A and B. Monoterpenoid hydrocarbons were present in a very small percentage (2.17 %), whereby *p*-cymene was the only compound in this group present in a percent of over 1 % (1.6 %). The most important constituents were monoterpenoid alcohols (58.9 %), of which geraniol was the most abundant (55.5 %), while its isomer, nerol was present in concentration of 2.2 %. Sesquiterpenoid hydrocarbons were rather abundant (17.4 %), especially β-bisabolene (6.7 %), germacrene D (4.0 %) and *trans*-β-caryophyllene (3.6 %). The only ester that was identified, nerol acetate, had a significant percentage of 11.1 %. The monoterpenoid phenols were present in very small quantities: thymol, 1.5 % and carvacrol, 4.7 %.

The present results are in concordance with previous studies; the most abundant components of tested essential oils were monoterpenes.[5] Samples A and B, representing *T. pulegioides* essential oil could be classified into phenolic group of *Thymus* essential oils, while sample C (*T. glabrescens* essential oil) is of a non-phenolic type.

Evaluation of the *MIC* values showed that the oils were active against the majority of the tested strains in concentrations of 10.8 – 27 µl/ml (Table II).

TABLE II. Antimicrobial activity of *T. pulegioides* and *T. glabrescens* essential oils and standards (*MIC* / µl ml^{-1}) for Gram-negative bacteria, Gram-positive bacteria and *Candida albicans* (h.c. = higher concentrations needed than the ones tested; n.t. = not tested)

Strain	*T. pulegioides* Sinaia	*T. pulegioides* Busteni	*T. glabrescens*	Streptomycin	Nystatin
Escherichia coli	10.8	27.0	13.5	5.2	n.t.
Salmonella typhi	27.0	21.6	10.8	38	n.t.
Salmonella enteritidis	16.2	10.8	27.0	38	n.t.
Enterobacter cloacae	10.8	10.8	13.5	38	n.t.
Pseudomonas aeruginosa	27.0	10.8	10.8	16	n.t.
Proteus mirabilis	10.8	h.c.	10.8	5.2	n.t.
Staphylococcus aureus	h.c.	10.8	h.c.	5.2	n.t.
Staphylococcus epidermidis	h.c.	h.c.	h.c.	5.2	n.t.
Streptococcus faecalis	h.c.	16.2	10.8	27	n.t.
Bacillus subtilis	10.8	h.c.	16.2	5.2	n.t.
Micrococcus luteus	h.c.	h.c.	h.c.	16	n.t.
Micrococcus flavus	10.8	27.0	10.8	5.2	n.t.
Listeria monocytogenes	27.0	27.0	16.2	16	n.t.
Candida albicans	10.8	10.8	10.8	n.t.	5.2

Escherichia coli, *Enterobacter cloacae*, *Proteus mirabilis*, *Bacillus subtilis* and *Micrococcus flavus* were the strains most susceptible to sample A, *T. pulegioides* essential oil (*MIC* = 10.8 µl/ml). Higher concentrations of sample B, same type of essential oil, were required to inhibit the growth of *E. coli* or *M. flavus* (*MIC* = 27.0 µl/ml). *T. pulegioides* essential oil (sample B) inhibited the growth of *Staphylococcus aureus* (*MIC* = 10.8 µl/ml) and *Streptococcus faecalis* (*MIC* = 16.2 µl/ml). The antimicrobial activity of *T. pulegioides* essential oil was expected considering its chemical composition (the main components being phenols, which are known antimicrobial agents).

Sample C (*T. glabrescens* essential oil) inhibited the growth of *Salmonella typhimurium*, *Pseudomonas aeruginosa* and *P. mirabilis* (*MIC* = 10.8 µl/ml). The growth of Gram-positive bacteria was inhibited by this sample at concentrations of 10.8–16.2 µl/ml. According to the literature, this activity could be related to the presence of monoterpenoid alcohols in this sample, especially of geraniol (55.5 %), which manifests an antiseptic activity comparable to that of thymol, often against *Pseudomonas*.[3]

All the tested samples showed antifungal effects by inhibiting the growth of *Candida albicans* at an *MIC* of 10.8 µl/ml. Previous studies showed antifungal

activity at *MIC* values of 0.32–0.64 μl/ml for certain Portugal varieties of *T. pulegioides* essential oil, which contained thymol (26.0 %) and carvacrol (21.0 %).[8]

Other species of the genus *Thymus*, such as *T. longicaulis*, *T. magnus* or *T. quinquecostatus*, with high amounts of monoterpenoid phenols or alcohols also exhibited a broad spectrum of activity against a variety of pathogenic bacteria and yeasts.[6,7,10]

This study confirmed once again that species of the genus *Thymus* are common sources of essential oil containing phenols or other constituents that manifest antimicrobial activity.

CONCLUSIONS

Thymus pulegioides and *T. glabrescens* from Romania are important sources of essential oils, the yield of essential oil being 0.7–1.0 % (v/d.w. herbal drug). The main constituents of the essential oil are monoterpenoid phenols (especially carvacrol) in *T. pulegioides*, and monoterpenoid alcohols (especially geraniol) in *T. glabrescens*.

The tested essential oils have antimicrobial and antifungal activity; they inhibit in small concentrations (10.8–27 μl/ml) the growth of Gram-positive and Gram-negative bacteria, and *Candida albicans*.

И З В О Д

ЕТАРСКА УЉА *Thymus pulegioides* И *Thymus glabrescens* ИЗ РУМУНИЈЕ:
ХЕМИЈСКИ САСТАВ И АНТИМИКРОБНО ДЕЛОВАЊЕ

MARIANA PAVEL[1], МИХАИЛО РИСТИЋ[2] и ТАТЈАНА СТЕВИЋ[2]

[1]University of Medicine and Pharmacy, Faculty of Pharmacy, Bucharest, Romania и
[2]Институт за проучавање лековитог биља "Др. Јосиф Панчић", Београд

Циљ рада је био испитивање хемијског састава и антимикробне активности етарских уља изолованих из две самоникле врсте тимијана (*Thymus pulegioides* L. и *T. glabrescens* Willd.) пореклом са различитих локалитета у Румунији. Садржај етарског уља одређен је према актуелној Европској фармакопеји. Квалитативна и квантитативна анализа уља урађене су гаснохроматографски (GC/FID и GC/MS), док је антимикробна активност испитана микродилуционом техником на Грам-негативне и Грам-позитивне бактерије (*Escherichia coli*, *Salmonella typhimurium*, *S. enteritidis*, *Enterobacter cloacae*, *Pseudomonas aeruginosa*, *Proteus mirabilis*, *Staphylococcus aureus*, *S. epidermidis*, *Streptococcus faecalis*, *Bacillus subtilis*, *Micrococcus luteus*, *M. flavus* и *Listeria monocytogenes*) и хумани патогени квасац *Candida albicans*. Сува биљна дрога *T. pulegioides* је садржавала 0,7–1 % (v/m) етарског уља чије су главне компоненте биле карвакрол (50,5–62,5 %), γ-терпинен (9,8—9,9 %) и *p*-цимен (5,7–7,1 %). *T. glabrescens* је садржавао око 0,7 % (v/m) етарског уља у сувој херби, а главни састојци тога уља били су гераниол (55,5 %), нерил-ацетат (11,1 %) и *β*-бисаболен (6,7 %). Оба испитивана етарска уља инхибирала су развој тест-организама са којима је рађено већ при концентрацијама од 10,8–27 μl/ml.

REFERENCES

1. J. Bruneton, *Pharmacognosy, Phytochemistry, Medicinal Plants*, Lavoisier Publishing, Paris, 1995, p. 287
2. M. Wichtl, R. Anton, *Plantes Therapeutiques*, Editions Tec & Doc, Paris, 1999, p. 530
3. V. Istudor, *Farmacognozie Fitochimie Fitoterapie*, Ed. II, Medicală, Bucharest, 2001, p. 60 (in Romanian)
4. K. Ložienė, P. R. Venskutonis, A. Šipailienė, J. Labokas, *Food Chem.* **103** (2007) 546
5. E. Stahl-Biskup, F. Saez, *Thyme, The Genus Thymus*, Taylor & Francis, London, New York, 2002, p. 268
6. N. Chorianopoulos, E. Kalpoutzakis, N. Aligiannis, S. Mitaku, G. J. Nychas, S. A. Haroutounian, *J. Agric. Food Chem.* **52** (2004) 8261
7. I. Rasooli, S. A. Mirmostafa, *Fitoterapia* **73** (2002) 244
8. E. Pinto, C. Pina-Vaz, L. Salgueiro, M. J. Gonçalves, S. Costa-de-Oliveira, C. Cavaleiro, A. Palmeira, A. Rodrigues, J. Martinez-de-Oliveira, *J. Med. Microbiol.* **55** (2006) 1367
9. M. L. Faleiro, M. G. Miguel, F. Ladeiro, F. Venâncio, R. Tavares, J. C. Brito, A. C. Figueiredo, J. G. Barroso, L. G. Pedro, *Lett. Appl. Microbiol.* **36** (2003) 35
10. S. Seungwon, J.-H. Kim, *Planta Med.* **70** (2004) 1087
11. E. Stahl-Biskup, *Planta Med.* **3** (1986) 163
12. P. Martonfi, A. Greijtovski, M. Repcak, *Biochem. Syst. Ecol.* **22** (1994) 819
13. J. Mastelic, K. Grzunov, A. Kravar, *Riv. Ital. EPPOS* **3** (1992) 19
14. P. Martonfi, *J. Essent. Oil Res*. **4** (1992) 173
15. D. Motskute, G. Bernotene, *Rastit. Resur.* **34** (1998) 131
16. I. Gered Csegedi, I. Gergely, Z. Csath, *Rev. Med. (Tg. Mures)* **16** (1970) 85
17. I. Gered Csegedi, *Farmacia* **8** (1970) 485
18. Z. Kisgyorgy, K. Csedo, H. Horster, J. Gergely, G. Racz, *Rev. Med.* (Tg. Mureş) **29** (1983) 124
19. *European Pharmacopoeia,* 6th ed., Strasbourg, Council of Europe, 2008, pp. 251, 3219
20. R. P. Adams, *Identification of Essential Oil Components by Gas Chromatography/Mass Spectrometry*, 4th ed., Allured Publishing Corporation, Carol Stream, IL, 2007
21. NCCLS – National Committee for Clinical Laboratory Standards, *Reference method for broth dilution antifungal susceptibility testing of yeasts*, Approved Standard M27-A, Villanova, PA, 1997
22. NCCLS – National Committee for Clinical Laboratory Standards, *Development of* in vitro *susceptibility testing criteria and quality control parameters*, Tentative guideline M23-T3, Villanova, PA, 1998.

Composition and antimicrobial activity of the essential oil of the leaves of black currant (*Ribes nigrum* L.) cultivar Čačanska crna

TATJANA STEVIĆ[1], KATARINA ŠAVIKIN[1], MIHAILO RISTIĆ[1], GORDANA ZDUNIĆ[1], TEODORA JANKOVIĆ[1]*, DRAGANA KRIVOKUĆA-ĐOKIĆ[1] and TODOR VULIĆ[2]

[1]Institute for Medicinal Plants Research „Dr. Josif Pančić", Tadeuša Košćuška 1, 11000 Belgrade and [2]Faculty of Agronomy, University of Belgrade, Nemanjina 6, 11080 Zemun, Serbia

Abstract: The essential oil from the leaves of the Serbian black currant cultivar Čačanska crna, obtained by hydrodistillation, was analyzed by gas chromatography-flame ionization detection and GC–mass spectrometry. The most abundant volatile compounds were Δ^3-carene (18.7 %), β-caryophyllene (17.7 %), sabinene (11.6 %), *cis*-β-ocimene (10.6 %) and α-terpinolene (10.6 %). The antimicrobial activity of the oil was evaluated against 14 micro-organisms, including two clinical isolated strains, using the broth microdilution method. The most susceptible micro-organisms were *Escherichia coli, Streptococcus faecalis*, *Staphylococcus aureus, Candida albicans* and *Trichophyton mentagrophytes* isolates. Furthermore, the flavonol aglycones in the leaves after acid hydrolysis were qualitatively and quantitatively analysed by HPLC, and quercetin was found to be the dominant compound (84 mg/g dw).

Keywords: black currant leaves; Čačanska crna; essential oil; antimicrobial activity.

INTRODUCTION

Black currant, *Ribes nigrum* L. (Grossulariaceae), is a woody shrub spontaneously growing in central and eastern Europe, while in temperate regions it is mostly cultivated.[1] In the flora of Serbia, only four species of the genus *Ribes* are native, namely *Ribes grossularia* L., *R. alpinum* L., *R. petraeum* Wulfen and *R. multiflorum* Kit. *R. nigrum* is one of a few species from this genus that has been introduced in the country. Black currant cultivar Čačanska crna from Serbia was obtained in 1980 by open pollination of the cultivar Malling Jet, and was selected in 1984. It has now started to be grown experimentally in an area certified for organic production.

Available online at www.shd.org.rs/JSCS/

The most important product of black currant is berries, due to their high levels of anthocyanins, flavonols, ellagitannins, and vitamin C. The leaves and buds are also important raw materials for the food and cosmetics industries.[2–4] Black urrant leaves are used in European folk medicine to treat rheumatism, arthritis and respiratory problems.[1] The chemical constituents of leaves are flavonoids, especially derivatives of kaempferol and quercetin, myricetin and isorhamnetin glycosides, and proanthocyanidins. The essential oil of black currant leaves was studied previously and differences in the monoterpene hydrocarbon profile between different cultivars were reported.[5,6]

As the black currant cultivar Čačanska crna has not hitherto been investigated, the aim of the present study was to analyze the composition of the essential leaf oil by the gas chromatography–mass spectrometry (GC/MS) method and to define its chemotype according to the percentages of the main constituents. Furthermore, the antimicrobial activity of the oil was assayed using the broth microdilution method. In order to obtain a more detailed chemical profile of this cultivar, the flavonol aglycones in the leaves after acid hydrolysis were analyzed qualitatively and quantitatively using high performance liquid chromatography (HPLC).

<div align="center">EXPERIMENTAL</div>

Plant material

Leaves of black currant cultivar Čačanska crna were collected in June 2008 from the experimental field certified for organic production on the mountain Kopaonik (locality Lukovska Banja, 1000 m). The leaves were air-dried for five days and used for chemical analyses.

Essential oil isolation

The volatile oil of the *Ribes nigrum* leaves was obtained by hydrodistillation for four hours of 100 g of air-dried sample using a Clevenger-type apparatus.[7] The yield (%) of the oils was calculated based on the moisture-free mass. The oil was subjected to qualitative and quantitative analysis by GC and the antimicrobial activity of the oil was tested.

GC and GC/MS analysis

The analysis was realized by gas chromatography with flame ionization detection (GC/FID) and mass spectrometric detection (GC/MS). In the first instance, a model HP-5890 Series II gas chromatograph equipped with a split-splitless injector, an HP-5 capillary column (25 m× ×0.32 mm, film thickness 0.52 μm) and a flame ionization detector (FID) was employed. Hydrogen was used as the carrier gas (1 mL/min). The injector was heated at 250 °C, the detector at 300 °C, while the column temperature was linearly programmed from 40–260 °C (4 °/min). The GC/MS analysis was performed under almost the same analytical conditions, using an HP G 1800C Series II GCD analytical system, equipped with an HP-5MS column (30 m×0.25 mm×0.25 μm). Helium was used as carrier gas (0.9 mL/min). The transfer line (MSD) was heated at 260 °C. The EI mass spectra (70 eV) were acquired in the scan mode in the *m*/*z* range 40–400. In each case, 1 μL of sample solution in ethanol (20 μL/2 mL) was injected in the split mode (1:30). Identification of constituents was realized by matching their mass spectra and retention indices with those obtained from authentic samples and/or NIST/ /Wiley spectra libraries, using different types of search (PBM/NIST/AMDIS) and available li-

terature data.[8,9] The percentage compositions were obtained from electronic integration measurements using flame ionization detection.

Determination of antimicrobial activity

Microbial strains. The antimicrobial activity was tested against Gram-negative bacteria: *Escherichia coli* (ATCC 25922), *Salmonella typhimurium* (ATCC 14028), *Enterobacter cloacae* (ATCC 13883), *Pseudomonas aeruginosa* (ATCC 27853), *P. tolaasii* (NCTC 387), *Proteus mirabilis* (ATCC 14273), Gram-positive bacteria: *Staphylococcus aureus* (ATCC 25923), *S. epidermidis* (ATCC 12228), *Streptococcus faecalis* (ATCC 12952), *Bacillus subtilis* (ATCC 6051), *Micrococcus luteus* (ATCC 10240), *M. flavus* (ATCC 14452) and *Listeria monocytogenes* (ATCC 15313), the human pathogen yeast *Candida albicans*, as well as clinical isolated dermatomycetes *Trichophyton mentagrophytes* and *Epidermophyton floccosum*. The organisms were obtained from the Mycological Laboratory, Department of Plant Physiology, Institute for Biological Research, Belgrade, Serbia.

Broth microdilution method. In vitro antimicrobial studies were performed according to the broth microdilution method. For antimicrobial testing, the oil was diluted 1:1 in DMSO. For each experiment, a control disk with pure solvent was used as the blind control. The minimum inhibitory concentrations (*MIC*) values of the essential oil were determined using the broth microdilution method in 96-hole plates.[10] Serial dilutions of stock solutions of the oil in broth medium (Muller–Hinton broth for bacteria and Sabouraud broth for yeast) were prepared in a microtiter plate (96 wells). The microbial suspensions were adjusted with sterile saline to a concentration of 1.0×10^5 CFU/ml. The microplates were incubated at 48 °C for 24 h. The *MIC* values were determined as the lowest concentration of the oil that visibly inhibited the growth of each organism in the microwells. The standard antibiotic streptomycin (1 mg/mL DMSO) was used to control the sensitivity of the tested bacteria, whereas nystatin (1 mg/mL DMSO) was used as the control against the yeasts.

The mycelial growth test with malt agar (MA) was used to investigate the antifungal activity of the essential oil. The essential oil was added into MA and poured into Petri dishes. The microplates were incubated for 72 h at 28 °C. Commercial fungicides, miconazole for *T. mentagrophytes* and bifonazole for *E. floccosum*, were used as positive controls. Each assay was repeated three times, independently.

Determination of total phenolics and tannin contents

The total phenolics were estimated by the Folin–Ciocalteu method with slight modifications.[11] Two hundred microliters of extract (20 mg/10 mL MeOH) were added to 1 mL of 1:10 diluted Folin–Ciocalteu reagent. After 4 min, 800 μl of sodium carbonate (75 g/L) were added. After 2 h incubation at room temperature, the absorbance at 765 nm was measured. Gallic acid (0–100 mg/L) was used for the plotting of a standard curve. The results are expressed as milligrams of gallic acid equivalents per gram of dry weight of plant extract (mg GAE/g dw). The measurements were realized in triplicate and the mean values were calculated.

The tannin content in the extract was determined quantitatively by its adsorption on standard hide powder.[12] This method is an indirect determination. The tannin content is equivalent to the difference between the total polyphenol content and the polyphenol content that remained after the tannins had been adsorbed by the hide powder.

HPLC analysis of flavonoid aglycones

Three flavonol aglycones (quercetin, myricetin and kaempferol) were analyzed after extraction and acid hydrolysis of the flavonol glycosides. Leaf samples (2 g) were extracted with methanol (20 mL) and 5 % sulphuric acid (20 mL) on a boiling water bath for 2 h. The extract

Available online at www.shd.org.rs/JSCS/

was filtered, neutralized with 10 % NaHCO$_3$ to pH 7 and evaporated under vacuum to 1/3 volume. After re-extraction with diethyl ether (3×50 mL), the ether extract was evaporated and dissolved in methanol (5 mL).

The HPLC analyses were performed using an Agilent series 1200 RR instrument with a DAD detector, on a reverse phase Lichrospher RP-18 analytical column, 250×4 mm i.d., particle size 5 μm (Agilent). Mobile phase A (H$_2$O containing 1 vol % 0.03 M H$_3$PO$_4$) and mobile phase B (MeCN); the elution was performed according to the following scheme: 90 % A 0–5 min, 90–80 % A 5–10 min, 80 % A 10–20 min, 80–40 % A 20–30 min, 40–0% A 30––35 min. Detection was performed at 260 and 340 nm. Standards quercetin, myricetin and kaempferol were obtained from Fluka, Germany. The amounts of the compounds were calculated using calibration curves. All experiments were repeated three times. The results are presented as milligrams per gram of dry weight.

RESULTS AND DISCUSSION

Chemical composition of essential oil

The light yellow oil was obtained in 0.12 % yield from the leaves of black currant cultivar Čačanska crna. The results of GC and GC/MS analysis are summarized in Table I. Of the 62 detected compounds, 59 were identified, representing 99.6 % of the total oil composition. According to literature data, black currant buds and leaves essential oils mainly consist of aliphatic and oxygenated mono- and sesquiterpenes.[3,5,6] Hydrocarbon terpenes were the most abundant components in the Čačanska crna cultivar oil (93 %), while oxygenated terpenes constituted 4.7 % to the total oil. A similar ratio of these two main fractions was reported previously in steam distillates of black currant buds.[13] The major constituents in the oil in the present study were Δ^3-carene (18.7 %), β-caryophyllene (17.7 %), sabinene (11.6 %), *cis*-β-ocimene (10.6 %) and α-terpinolene (10.6 %). Previous chemotaxonomic studies defined Δ^3-carene, sabinene and terpinolene as distinguishing components in black currant cultivars.[3,14] All of these hydrocarbon monoterpenes were also present in high amounts in Čačanska crna, as reported in Ben Lomond cultivar leaf oil.[5] In the other earlier studied cultivars, such as Ben Alder, Ben Connan, Ben Tirran and Wellington, the level of sabinene was considerably lower than the amounts of Δ^3-carene and terpinolene. Therefore, these cultivars might represent another chemotype, according to the main essential oil components.[5,6]

TABLE I. Constituents of black currant leaf essential oil from the cultivar Čačanska crna (KIE: RRI experimentally determined (calibrated AMDIS); KIL: RRI, literature values[8])

Constituents	KIE	KIL	Content, mass %
trans-2-Hexenal	859	846	0.10
p-Xylene	870	864	0.06
α-Thujene	920	924	0.20
α-Pinene	926	932	0.98
α-Fenchene	939	945	0.08
Camphene	940	946	0.12

Available online at www.shd.org.rs/JSCS/

TABLE I. Continued

Constituents	KIE	KIL	Content, mass %
Sabinene	969	969	11.63
1-Octen-3-ol	977	974	0.67
β-Myrcene	987	988	1.83
$Δ^2$-Carene	995	1001	0.21
α-Phellandrene	999	1002	0.24
$Δ^3$-Carene	1007	1008	18.67
α-Terpinene	1111	1014	0.51
p-Cymene	1017	1020	0.06
o-Cymene	1019	1022	0.26
β-Phellandrene	1023	1025	2.06
cis-β-Ocimene	1036	1032	10.64
trans-β-Ocimene	1046	1044	6.94
γ-Terpinene	1054	1054	0.34
cis-Sabinene hydrate	1064	1065	0.05
α-Terpinolene	1084	1086	10.58
Undecane	1095	1100	0.05
allo-Ocimene	1125	1128	0.09
trans,trans-2,6-dimethyl-1,3,5,7-Octatetraene	1131	1134	0.05
trans-epoxy-Ocimene	1142	1137	0.09
Terpinen-4-ol	1173	1174	0.17
α-Terpineol	1188	1186	0.05
Methyl salicylate	1190	1190	0.07
Nerol	1227	1227	0.07
Geraniol	1253	1249	0.46
Bornyl acetate	1281	1287	0.19
δ-Elemene	1332	1335	0.04
α-Terpenyl acetate	1346	1346	0.07
Citronellyl acetate	1351	1350	0.12
β-Bourbonene	1379	1387	0.05
β-Elemene	1387	1389	0.50
β-Caryophyllene	1418	1417	17.67
γ-Elemene	1429	1434	0.18
α-Humulene	1449	1452	2.43
Alloaromadendrene	1455	1458	0.07
γ-Muurolene	1472	1478	0.14
Germacrene D	1477	1484	4.28
β-Selinene	1481	1489	0.07
Bicyclogermacrene	1491	1500	0.80
α-Muurolene	1499	1500	0.42
trans,trans- α-Farnesene	1504	1505	0.19
δ-Cadinene	1518	1522	0.42
Hedycaryol	1545	1546	0.05
Germacrene B	1550	1559	0.62
Germacrene D-4-ol	1570	1574	0.92
Caryophyllene oxide	1577	1582	1.23
Humulene epoxide II	1603	1608	0.20

Available online at www.shd.org.rs/JSCS/

TABLE I. Continued

Constituents	KIE	KIL	Content, mass %
Helifolen-12-al	1623	1338	0.06
τ-Cadinol	1635	1338	0.31
α-Cadinol	1649	1652	0.41
14-Hydroxy-*cis*-caryophyllene	1666	1666	0.13
Eudesma-4(15),7-dien-1β-ol	1680	1687	0.12
Amorpha-4,9-dien-2-ol	1712	1725	0.04
Phytol	2107	2112	0.53
Total			99.62

The sesquiterpene fraction constituted 31.3 % of the oil of Čačanska crna leaves. Some sesquiterpenes could be considered as black currant flavour contributors.[13] Among them, germacrene B and bicyclogermacrene have not been previously detected in the leaves of black currant.

Antimicrobial activity

In this study, the antimicrobial activity of the oil was evaluated *in vitro* against Gram-positive and Gram-negative bacterial strains, human pathogen yeast *Candida albicans*, as well as two clinical isolated micromycetes, using the broth microdilution method. The results of antimicrobial activity are given in Table II. The black currant leaf oil showed antimicrobial activity with *MIC* values ranging from 1.0–27.0 µL/mL. The most sensitive was the *Trichophyton mentagrophytes* isolate (*MIC* = 1.0 µL/mL), followed by the bacteria *Escherichia coli*, *Streptococcus faecalis* and *Staphylococcus aureus* and the yeast *C. albicans* (*MIC* = 2.7 µL/mL). *Listeria monocytogenes* showed high resistance to the tested oil.

TABLE II. Minimal inhibitory concentrations (*MIC* / µL mL^{-1}) of black currant cultivar Čačanska crna leaf essential oil

Tested microorganisms	Leaf oil	Control[a]
Escherichia coli	2.7	5.2
Salmonella typhimurium	13.5	38
Streptococcus faecalis	2.7	27
Staphylococcus aureus	2.7	5.2
Pseudomonas aeruginosa	13.5	16
Pseudomonas tolaasii	16.2	27
Proteus mirabilis	13.5	5.2
Bacillus subtilis	5.4	5.2
Micrococcus luteus	13.5	16
Micrococcus flavus	16.2	5.2
Listeria monocytogenes	27.0	16
Candida albicans	2.7	5.2[b]
Trichophyton mentagrophytes	1.0	1.0[c]
Epidermophyton floccosum	3.0	3.0[d]

[a]Streptomycin; [b]nystatin; [c]miconazole; [d]bifonazole

As suggested in a previous investigation, the activity of the oils is related to the respective composition of the essential oils.[15] The obtained inhibitory effect of the essential oil in the present study might have been due to the activity of its main constituents against particular bacteria or yeasts. Previous studies indicated that Δ^3-carene showed high activities against *E. coli, Micrococcus luteus*, *S. aureus*, *Pseudomonas aeruginosa* and *Bacillus subtilis*, while β-caryophyllene exerted a strong activity against *P. aeruginosa* and a moderate activity against *E. coli*.[15,16] In addition, it was possible that components present in lower amounts in the oil might be involved in some type of synergism with the other active compounds.[17] The mechanism of the antimicrobial action of terpenes is not fully understood but it is speculated to involve membrane disruption by the lipophilic compounds.[15]

Analysis of the phenolic compounds

The amounts of total phenolics and tannins were 40.1±2.1 mg GAE/g dw and 2.1 %, respectively. The flavonoid compounds were analysed in a methanol extract of black currant cultivar Čačanska crna leaves after acid hydrolysis using HPLC (Fig. 1). Myricetin, quercetin and kaempferol were detected, of which quercetin was the most abundant (84±2.4 mg/g dw), followed by kaempferol (43.6±1.6 mg/g dw) and myricetin (9.5±0.4 mg/g dw). These flavonols were previously reported to be dominant in buds and leaves of other black currant cultivars, such as Goliath and Noir de Bourgogne, and the ratios between these aglycones were different in the various tested cultivars.[18] The significant amounts of flavonol agly-
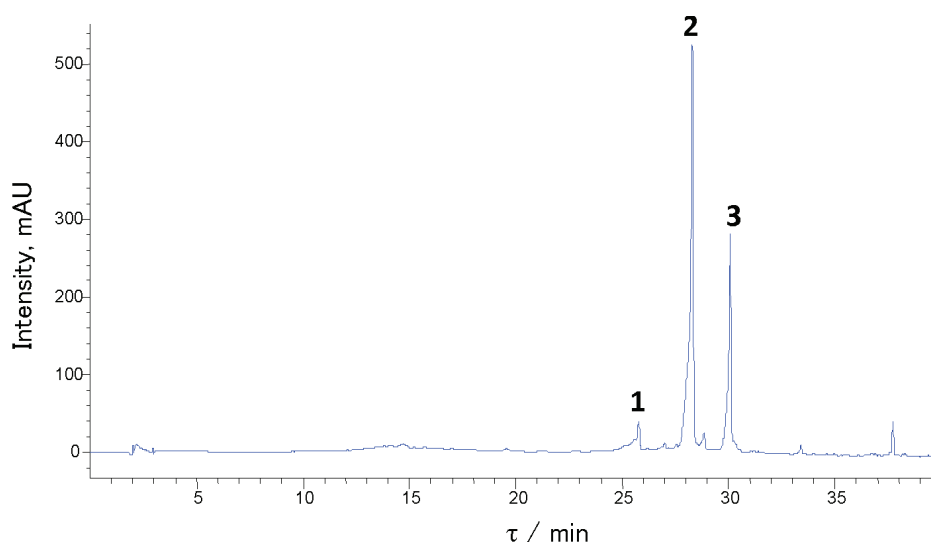

Fig. 1. HPLC chromatogram of the methanol extract of black currant cultivar Čačanska crna leaves; **1** – myricetin; **2** – quercetin; **3** – kaempferol.

Available online at www.shd.org.rs/JSCS/

cones, known to possess the anti-oxidative activity, confirms the usage of leaves of black currant in traditional medicine. Recent studies have indicated that the incidence of rheumatoid arthritis is partially related to damage of the anti-oxidative system.[19,20]

CONCLUSIONS

The essential leaf oil from black currant cultivar Čačanska crna contains a very complex mixture of terpene compounds, with Δ^3-carene, β-caryophyllene, sabinene, *cis-β*-ocimene and α-terpinolene as the major compounds. According to these results, this black currant cultivar might belong to the same chemotype as the Ben Lomond cultivar. Since the leaf oil showed a wide range of antimicrobial effect, its use in the treatment of various bacterial and fungal infections could be beneficial. These inhibitory effects are also interesting in relation to the prevention of contamination in many food products caused by micro-organisms such as *Staphylococcus* spp., *Salmonella* spp., *Bacillus* spp., *Pseudomonas fluorescens* and *Clostridium botulinum*.[17]

The leaves of the black currant cultivar Čačanska crna are also a rich source of natural antioxidants such as polyphenols. The intake of flavonoids and other antioxidant compounds from food is associated with reduced risk of coronary heart disease, stroke and cancer. In view of this, black currant leaves extracts could be of interest for further investigations.

И З В О Д

ХЕМИЈСКИ САСТАВ И АНТИМИКРОБНА АКТИВНОСТ ЕТАРСКОГ УЉА ЛИСТА ЦРНЕ РИБИЗЛЕ (*Ribes nigrum* L.), СОРТА ЧАЧАНСКА ЦРНА

ТАТЈАНА СТЕВИЋ[1], КАТАРИНА ШАВИКИН[1], МИХАИЛО РИСТИЋ[1], ГОРДАНА ЗДУНИЋ[1], ТЕОДОРА ЈАНКОВИЋ[1], ДРАГАНА КРИВОКУЋА-ЂОКИЋ[1] и ТОДОР ВУЛИЋ[2]

[1]Институт за проучавање лековитог биља "Јосиф Панчић", Тадеуша Кошћушка 1, 11000 Београд и [2]Пољопривредни факултет, Немањина 6, 11080 Земун

Применом GC/MS методе анализирано је етарско уље изоловано хидродестилацијом из листа црне рибизле, сорта чачанска црна. Међу идентификованим компонентама, најзаступљеније су биле Δ^3-карен (18,7 %), β-кариофилен (17,7 %), сабинен (11,6 %), *cis-β*-оцимен (10,6 %) и α-терпинолен (10,6 %). Антимикробна активност уља је одређена микродилуционом методом на 14 сојева микроорганизама од којих су 2 клинички изолати. Најосетљивији микроорганизми били су *Escherichia coli*, *Streptococcus faecalis*, *Staphylococcus aureus*, *Candida albicans*, и изолат *Trichophyton mentagrophytes*. Урађена је и квалитативна и квантитативна HPLC анализа хидролизованог екстракта листа којом је утврђено да је флавонол кверцетин доминантна компонента.

(Примљено 9. априла, ревидирано 1. јуна 2009)

REFERENCES

1. M. Wichtl, *Teedrogen*, Wissenschaftliche Verlagsgesellschaft, Stuttgart, 1994, p. 421
2. M. Anttonen, R. Karjalainen, *J. Agric. Food Chem.* **54** (2006) 7530
3. A. Dvaranauskaite, P. Venskutonis, C. Raynaud, T. Talou, P. Viškelis, E. Dambrauskiene, *J. Agric. Food Chem.* **56** (2008) 3279
4. J. Piry, A. Pribela, J. Durčanska, P. Farkaš, *Food Chem.* **54** (1995) 73
5. R. Mariott, in *Flavors and Fragrances, a World Perspective*, B. M. Lawrence, B. D. Mookherjee, B. J. Willis, Eds., Elsevier, Amsterdam, 1988, p. 387
6. D. W. Griffiths, G. W. Robertson, A. N. E. Birch, R. M. Brennan, *Phytochem. Anal.* **10** (1999) 328
7. *Yugoslavian Pharmacopoeia Ph. Yug. IV*, National Institute for Health Protection, Belgrade, Serbia, 1984, p. 126
8. R. P. Adams, *Identification of Essential Oils Components by Gas Chromatography/Quadrupole Mass Spectroscopy*, 4th ed., Allured Publishing Corporation, Card Stream, IL, 2007
9. H. Detlev, *Mass Finder 4: GC/MS Visualisation, Interpretation, and Library Adminis-tration Mass Spectral Library: Terpenoids and Related Constituents of Essential Oils*, Hamburg, 2008–2009
10. National Committee for Clinical Laboratory Standards (NCCLS), *Methods for dilution antimicrobial Susceptibility Tests for Bacteria That Grow Aerobically*, Approved Standard, 5th ed., NCCLS document, Wayne, PA, 2000, p. M7
11. P. G. Waterman, S. Mole, *Analysis of Phenolic Plant Metabolites*, Blackwell Scientific Publication, Oxford, 1994, p. 16
12. *European Pharmacopoeia 5.0*, Council of Europe, Strasbourg Cedex, 2005, 221
13. J. L. Le Quere, A. Latrasse, *J. Agric. Food Chem.* **38** (1990) 3
14. M. Kerslake, A. Latrasse, J. L. Le Quere, *J. Sci. Food Agric.* **47** (1989) 43
15. H. J. D. Dorman, S. G. Deans, *J. Appl. Microbiol.* **88** (2000) 308
16. L. Jirowetz, S. Bail, G. Buchbauer, Z. Denkova, A. Slavchev, A. Stoyanova, E. Schmidt, M. Geissler, *Sci. Pharm.* **74** (2006) 189
17. M. Marino, C. Bersani, G. Comi, *Int. J. Food Microbiol.* **67** (2001) 187
18. J. Tabart, C. Kevers, J. Pincemail, J. O. Defraigne, J. Dommes, *J Agric. Food Chem.* **54** (2006) 6271
19. A. Seven, S. Guezel, M. Aslan, V. Hamuryudan, *Clin. Biochem.* **41** (2008) 538
20. K. M. Surapneni, V. S. C. Gopan, *Ind. J. Clin. Biochem.* **23** (2008) 41.

Determination of the polyphenol contents in Macedonian grapes and wines by standardized spectrophotometric methods

VIOLETA IVANOVA[1,2*], MARINA STEFOVA[1] and FABIO CHINNICI[3]

[1]*Institute of Chemistry, Faculty of Natural Sciences and Mathematics, Sts. Cyril and Methodius University, Arhimedova 5, 1000 Skopje,* [2]*Department for Enology, Institute of Agriculture, Sts. Cyril and Methodius University, Aleksandar Makedonski bb, Skopje, FYR Macedonia and* [3]*Department of Food Science, University of Bologna, Viale Fanin 40, 40127 Bologna, Italy*

Abstract: Wines and grapes contain a large array of phenolic compounds belonging to non-flavonoids and flavonoids. This study evaluates the polyphenolic contents of six commercial red and white Macedonian wines and four grape varieties. Spectrophotometric methods were applied for the determination of the total phenolics, the total flavonoids, the total anthocyanins and the total catechins. The efficiency of acetone/water (80/20) and methanol/water (80/20) solutions for the extraction of polyphenols from grape pulp, seeds and skins were compared. The best extraction efficiency was achieved using acetone/water. The obtained results showed that Macedonian grapes are rich in polyphenols, whereby the highest concentration of total phenolics was found for Vranec grapes. The analyzed wines contained high contents of polyphenol; the highest contents were found for Disan wine produced from the Vranec variety of grapes (1515 mg/L total phenolics, 1103 mg/L total flavonoids, 237 mg/L total anthocyanins and 845 mg/L total catechins). Principal component analysis was employed to check possible groupings of the studied red and white wine samples. A clear separation of white wines from red ones was observed.

Keywords: wine; grape; polyphenols; spectrophotometry; berry extraction.

INTRODUCTION

Wines and grapes contain a number of polyphenolic constituents classified as flavonoids and non-flavonoids that play a major role in enology. They contribute to the sensory characteristics of wine, especially colour, flavour and astringency and, therefore, to the differences between red and white wines.[1] The family of wine flavonoids includes flavonols, flavanols and anthocyanins, whereby

---

45

the non-flavonoids include phenolic acids (hydroxybenzoic and hydroxycinnamic acids and their derivatives) and stilbenes. Red wines contain all the above phenolics, while white wines contain mainly phenolic acids and flavanols.

Grape anthocyanins are red pigments, located in the first external layers of the hypodermal tissue and mainly in the vacuoles,[2] as well as in special structures called anthocyanoplasts,[3] while the teinturier varieties contain anthocyanins also in the pulp cells. The most important grape anthocyanins are the 3-glucoside forms of cyanidin, peonidin, petunidin, delphinidin and malvidin.[4] Flavonols are located in the solid parts of grapes, particularly in the skin and herbaceous parts and are mainly present as the 3-glycosides and 3-glucuronides of quercetin and myricetin, the 3-glucosides of kaempferol and isorhamnetin, and laricitrin and syringetin, predominantly found as 3-glucosides.[5,6] Catechins are located mainly in the seeds and skins.[7–10] The major monomers are (+)-catechin, (–)-epicatechin and (–)-epicatechin-3-*O*-gallate.

Many authors have studied the phenolic compounds in grapes and wines using HPLC as the most suitable analytical technique.[4,11–18] However, this technique is not available in wineries for routine analyses, whereas spectrophotometric methods, as more affordable techniques with lower expenses, lower reagent consumption and rapid measurements, can be used for wine and grape analyses to follow the changes in the polyphenol contents during grape ripening and their changes during the wine-making process. The most commonly used are methods for the determination of the total phenolics,[19–21] anthocyanins,[22–24] flavan-3-ols[21,25,26] and flavonoids.[27–30]

The FYR Macedonia is characterized by a distinctive habitat, a sub-Mediterranean climate and a very long tradition of grape growing and high quality wine making. Due to the deficiency of data for Macedonian wines and grapes, the purpose of this study was to establish a preliminary database for the polyphenolic contents of selected Macedonian wines and grapes from the Tikveš vineyard area by measuring the content of total phenolics, total anthocyanins, total flavonoids and total catechins, as well as the colour intensity and tint of the red wines.

<div align="center">EXPERIMENTAL</div>

Grape samples

The content of phenolic compounds was determined for the following grape varieties: Vranec, Cabernet Sauvignon, Muscat Hamburg and Riesling (vintage 2006). Grape berries used for this study were grown at the vineyards of the Institute of Agriculture in Skopje. Samples from the cultivars were harvested in their technological ripening stage (22.5, 20.6, 21.1 and 18.5 °Brix, for Vranec, Cabernet Sauvignon, Muscat Hamburg and Riesling, respectively). The sampling was randomly made by picking berries from the top, central, and bottom parts of the clusters. The Vranec samples were collected from an 8-year-old vineyard (13.4 ha); the M. Hamburg and Riesling samples were collected from 18-year-old vineyards (3.1 and 2.5 ha, respectively) and the Cabernet Sauvignon samples from a 7-year-old vineyard (0.1 ha). The distance between the rows was 2.8 m and distance between the vines was 1.2 m. The

samples (10 kg from 30–40 plants were sampled and then reduced to 1 kg for each variety) were kept frozen before analysis. All the determinations were performed in triplicate.

Wine samples

Four red (vintage 2003) and four white wines (vintage 2003) from the Bovin Winery, located in the Tikveš vineyard area, were analyzed. The wines were obtained from the most widespread red cultivars (Vranec, Merlot and Cabernet Sauvignon) and white grape cultivars (Riesling, Smederevka, Sauvignon Blanc and Temjanika).

Instrumentation and reagents

Analysis of the polyphenols was performed with an HP 8452 Agilent UV–Vis spectrophotometer. The reagent *p*-(dimethylamino)cinnamaldehyde (*p*-DMACA), gallic acid and (+)- -catechin were purchased from Fluka (Switzerland), and the Folin–Ciocalteu reagent was from Merck (Germany). All the other employed reagents were of analytical grade purity.

Preparation of the grape skins, seeds and pulps for analyses

The pedicels were removed and the berries were manually skinned. The seeds were separated from the pulp, washed with distilled water and then blotted on paper. Skins were blotted on paper towels to remove any residual pulp. The skins and seeds were ground and the pulp was blended. The skins (1 g), seeds (1 g) and pulp (1 g) were extracted twice for 15 min with 10 mL acetone/water (80/20, v/v) containing HCl (0.1/10, v/v) to prevent oxidation of the polyphenols in an ultrasonic bath at room temperature and then stirred for 30 min on a magnetic agitator. After centrifugation (3000 rpm for 10 min), the supernatants from both extractions were combined and made up to a final volume of 25 mL with distilled H_2O. The extracts were filtered through 0.45 µm membrane filters (Iso-Disc Filter, PTFE, Supelco) before spectrophotometric determination of the total phenolics, total anthocyanins, total flavonoids and total catechins.

Total phenolics assay

The Folin–Ciocalteu method[20] was used for the determination of the total phenolics. In brief, an aliquot (1 mL) of the appropriate diluted extracts was added to a 10 mL volumetric flask, containing 5 mL of distilled water. Then, 0.5 mL of Folin-Ciocalteu reagent was added and the contents mixed. After 3 min, 1.5 mL Na_2CO_3 solution of concentration 5 g/L was added and made up to a total volume of 10 mL distilled water. After keeping the samples at 50 °C (water bath) for 16 min in sealed flasks and subsequent cooling, their absorbances were read at 765 nm against distilled water as the blank. A calibration curve was constructed using gallic acid standard solutions (0–100 mg/L). The concentration of total phenolics is expressed as the gallic acid equivalent (GAE) per 1 g of fresh sample. All samples were prepared in triplicate.

Total flavonoids assay

Total flavonoid content was evaluated according to a colorimetric assay with aluminium chloride.[27] A 1 mL aliquot of wine sample or grape extract (appropriately diluted) was added to a 10 mL volumetric flask containing 4 mL of distilled water, followed by the addition of 0.3 mL of solution of $NaNO_2$ (0.5 g/L). After 5 min, 0.3 mL of a 1 g/L solution of $AlCl_3$ was added and 6 min later, 2 mL of NaOH (1 mol/L) was added to the mixture. The total volume was made up to 10 mL with distilled water, the solution was mixed and the absorbance was measured at 510 nm against a water blank. Catechin was used as the standard for the construction of a calibration curve and the concentrations are expressed as catechin equivalents (mg/g CE).

Total anthocyanins assay

The determination of the total anthocyanins was realised by the method proposed by Di Stefano *et al.*[21] The samples were diluted with a solution consisting of 70/30/1 (v/v/v)ethanol/water/HCl (concentrated) and the absorbance was measured at 540 nm. Due to the lack of a malvidin-3-glucoside standard, the total anthocyanic contents are expressed as malvidin-3-glucoside equivalents and calculated using the following equation purposed by Di Stefano, *et al.*:[21]

$$TA_{540\ nm}\ (\text{mg/L}) = A_{540\ nm}16.7d$$

where $A_{540\ nm}$ is the absorbance at 540 nm and d is the dilution.

Total catechins assay

The concentration of total catechins was measured using the *p*-(dimethylamino)cinamaldehyde (*p*-DMACA) method.[22] The contents of catechins in the wines are expressed as catechin equivalents (CE mg/L). An aliquot (1 mL) of an appropriately diluted sample was added to a 10 mL volumetric flask followed by the addition of 3 drops of glycerol and 5 mL *p*-DMACA reagent. The total volume was made up to 10 mL with methanol and after 7 min, the absorbance was read at 640 nm against a methanol blank. The DMACA reagent was prepared immediately before use, and contained 1 % (w/v) DMACA in a cold mixture of methanol and HCl (4:1).

Colour intensity, hue, colour composition and brilliance of the wines

The colour intensity is determined by the content and structure of the anthocyanins present in a wine and is defined as the sum of the absorbances at 420, 520 and 620 nm.[30] The absorbance of a wine was directly measured at 420, 520 and 620 nm using a 2 mm optical path and the colour intensity (*CI*), hue or tint (*T*), proportion of red colour (% *Rd*), proportion of blue colour (% *Bl*), proportion of yellow colour (% *Ye*) and the brilliance of the wine (*dA*) were calculated.[30] The tint of a wine is defined as the ratio A_{420}/A_{520}, and gives a measure of the "tint" or redness of the wine.[30] The colour composition of the wines, expressed as percentage, was calculated according to the following equations:

$$\%\ Ye\ \text{or}\ \%\ Rd\ \text{or}\ \%\ Bl = 100(A_{\lambda}/CI)$$

where: % *Ye* is the percentage of yellow colour ($\lambda = 420$ nm) in the overall colour, % *Rd* is the percentage of red colour ($\lambda = 620$ nm) and % *Bl* is the percentage of blue colour ($\lambda = 520$ nm) in the overall wine colour. The brilliance of a wine was calculated by the expression:

$$dA\ (\%) = (1 - (A_{420} + A_{620}/2A_{520}))\times100$$

Statistical analysis

Statistical treatment, including means, standard deviations and Principal Component Analyses, was performed using the PC software package TANAGRA 1.4.28 (Lyon, France). The test of Student–Newman–Keul of multiple comparisons of the mean values was applied to the results of the concentrations of the different phenolics to ascertain possible significant differences between the studied wines and grape varieties.

Available online at www.shd.org.rs/JSCS/

RESULTS AND DISCUSSION

Calibration and accuracy tests for total phenolics, total flavonoids and total catechins methods

The common spectrophotometric method for the determination of the total phenolics content using the Folin–Ciocalteu reagent has been widely used in the area of enology and viticulture. This method is based on oxidation–reduction reactions in which phenolics are oxidised and show maximum absorbance in the wavelength region between 725 and 765 nm. In this study, a procedure based on the reported method[20] was used with some modifications based on testing the effects of temperature and time of the reaction between Folin–Ciocalteu reagent and standard solutions of gallic acid.

The results obtained from the test, for two concentration levels, at ambient temperature and at 50 °C, are presented in Table I as standard deviation (*SD*) and relative error (in %) with respect to the theoretical concentration.

TABLE I. Standard deviations (*SD*) and relative errors (e_r) for different time of reaction at ambient temperature and 50 °C

Time, h (ambient temp.)	Gallic acid (100 mg/L)		Gallic acid (150 mg/L)	
	Concentration found[a], mg/L	e_r / %	Concentration found[a], mg/L	e_r / %
1	98.2 ± 0.64	–1.80	143 ± 0.80	–4.66
1.5	101 ± 1.31	1.00	151 ± 0.98	0.66
2	119 ± 1.32	19.0	161 ± 0.90	7.33
2.5	134 ± 0.69	34.0	166 ± 1.06	10.66
3	147 ± 1.17	47.0	182 ± 0.84	21.33
Time, min (50 °C)	Concentration found[a], mg/L	e_r / %	Concentration found[a], mg/L	e_r / %
10	90.5 ± 0.81	–9.50	137 ± 0.90	–8.66
15	96.4 ± 1.00	–3.60	139 ± 0.96	–7.33
16	101 ± 1.04	1.00	153 ± 1.57	2.00
17	102 ± 0.91	2.00	155 ± 1.41	3.33
18	105 ± 1.07	5.00	161 ± 1.59	7.33
20	105 ± 1.30	5.00	166 ± 1.17	11.0

[a]Values are the average from 3 replicates ± *SD*

As can be seen from Table I, the optimal results, *i.e.*, the lowest relative errors of 1.00 and 0.66 % for both analyzed concentration levels, were obtained when the solutions were allowed to stand for one hour and thirty minutes at ambient temperature. Shorter and longer reaction times caused higher relative errors. A significant reduction of the analysis time, with a very low relative error, was achieved when the prepared solutions were allowed to stand at 50 °C. The best results with lowest relative errors (1.00 and 2.00 %), were obtained when the solution was kept at 50 °C for 16 min, hence this procedure was used for the calibration and for the analysis of the wine and grape skin, seed and pulp samples. The calculated linear dependence of absorbance (*A*) on the mass concen-

Available online at www.shd.org.rs/JSCS/

tration (γ) of gallic acid in a series of standard solutions, with correlation coefficient 0.9997, was the following:

$$A(G) = 0.005385\,\gamma(G) \text{ [mg/L]} - 0.007261$$

The accuracy of the procedure was checked using the standard additions method on an actual red wine sample and satisfactory results (Recovery = 102 – – 106 %, Table II) confirmed that the method is accurate and convenient for quantitative analysis.

TABLE II. Accuracy of the standardized methods for the determination of the total phenolics, total flavonoids and total catechins in wine

Standard addition γ / mg L^{-1}	Calculated γ / mg L^{-1}	Experimentally found[a] γ / mg L^{-1}	SD	Recovery, %
Total phenolics				
–	–	1118	24.14	–
250	1368	1454	62.08	106
625	1743	1782	36.53	102
1000	2118	2215	44.3	104
Total Flavonoids				
–	–	697	21.95	–
100	797	836	21.98	105
250	945	945	28.82	99.8
400	1097	1037	65.74	94.5
Total Catechins				
–	–	8.3	0.47	–
4	12.3	11.8	0.83	96.3
10	18.3	18.6	1.16	102
16	24.3	23.8	1.26	98.0

[a]Values are the average from 3 replicates

For the determination of the total flavonoids, a chlorometric method using AlCl$_3$ was applied for the analysis of the wines and grape extracts. This method is based on the formation of stable complexes with the C-4 keto group and either the C-3 or C-5 hydroxyl group of flavones and flavonols, which exhibit maximum absorbance at 510 nm. On the other hand, the determination of catechins by the *p*-DMACA assay is based on the formation of coloured products in reaction of this aldehyde reagent with tannins.[25] The absorbances of the resulting products of this reaction involving monomeric flavan-3-ols ((+)-catechin and (-)-epicatechin) are read at 640 nm. For the determination of the total flavonoids and catechins in the analysed wine and grape extracts, calibration diagrams with five concentration points of catechin as the standard were constructed. The obtained linear dependences of the absorption of catechin, *A*(C) and the mass concentration of catechin, γ(C) in pure solutions, with correlation coefficients 0.9979 for flavonoids (1) and 0.9993 for catechins (2), were the following:

$$A(C) = 0.002889\chi(C)\ [mg/L] - 0.03774 \qquad (1)$$
$$A(C) = 0.025183\chi(C)\ [mg/L] + 0.000627 \qquad (2)$$

The accuracy of these spectrophotometric methods was also checked by the standard additions method in red wine (Recovery = 94.5 – 105 % for flavonoids and Recovery = 96.3 – 102 % for catechins) (Table II).

Grape extraction procedures

Most of the procedures for determination of polyphenols in grapes use aqueous methanol or acetone for extraction. Marinova *et al.*[31] used 80 % aqueous methanol for extraction on an ultrasonic bath. Kennedy *et al.*[32] extracted the phenolics from skins with 66 % aqueous acetone during 24 h at 20 °C and evaporated the solvent after filtration of the extract. Montealegre *et al.*[33] used methanol, water and formic acid for extraction of the phenolic compounds from lyophilized skins and seeds. In this work, methanol and acetone (80 % aqueous solutions, v/v with 0.1 % HCl) were tested for the extraction of the phenolic components and the obtained results were compared. The efficiency of extraction was checked by re-extraction of the residue using the same procedure. It was noticed that one extraction step was not enough for the total removal of the analyzed components from the skins, seeds and pulp. Second and third extractions of the residue were performed, whereby no detectable amounts of polyphenols were determined in the third extract. Therefore, the first two extracts were combined and then analyzed. The standard deviations and the sum of concentrations for the total phenolics, total flavonoids, total anthocyanins and total catechins obtained with two extraction steps with methanol/water (80/20) and acetone/water (80/20) are shown in Table III. The measurements were averaged and the results are given as the mean with the standard deviation. It was found that an overall slightly better extraction efficiency of the phenolics from the skins and seeds was achieved using acetone. This was mainly evident for the extraction of catechins from skins and the extraction of flavonoids from the seeds, which can probably be attributed

TABLE III. Polyphenolic contents determined in the methanol and acetone skins and seeds extracts and percent difference between both extracts (*TP*: total phenolics, *TF*: total flavonoids, *TA*: total anthocyanins, *TC*: total catechins)

Vranec grapes	Methanol extracts[a], mg/g	Acetone extracts[a], mg/g	Difference, %
Skins/*TP*	48.1 ± 1.13	48.4 ± 1.13	0.62
Skins/*TF*	6.90 ± 0.42	7.01 ± 0.29	1.59
Skins/*TA*	11.5 ± 0.68	11.9 ± 0.65	3.48
Skins/*TC*	2.24 ± 0.18	2.71 ± 0.28	20.98
Seeds/*TP*	162 ± 5.65	166 ± 5.66	2.47
Seeds/*TF*	15.3 ± 0.75	18.9 ± 0.60	23.53
Seeds/*TC*	24.6 ± 1.15	25.3 ± 1.69	2.85

[a]Values are the average from 3 replicates

Available online at www.shd.org.rs/JSCS/

to the more efficient dissolution of the external lipidic layer of the seeds by ace-tone, which is less polar and thus a better solvent for lipids than methanol, yield-ing the largest amounts of polyphenols.[34]

Composition of grape phenolic

The developed spectrophotometric methods for the determination of the total phenolics, total anthocyanins, total flavonoids and total catechins in grape ex-tracts of skin, seed and pulp were applied. The results obtained for Vranec, Ca-bernet Sauvignon, Muscat Hamburg and Riesling grapes varieties are presented in Table IV.

TABLE IV. Phenolic composition (mg/g, fresh weight) of grapes varieties Vranec, Cabernet Sauvignon, Muscat Hamburg and Riesling (*TP*: total phenolics, *TF*: total flavonoids, *TA*: total anthocyanins, *TC*: total catechins)

Grape variety		TP^a / mg L^{-1}	TF^a / mg L^{-1}	TA^a / mg L^{-1}	TC^a / mg L^{-1}
Vranec	Pulp	2.58 ± 0.14	0.77a ± 0.11	0.15 ± 0.01	0.15 ± 0.02
	Seed	166 ± 1.61	18.9 ± 0.68	–	25.3d ± 0.96
	Skin	48.4 ± 1.94	7.01 ± 0.36	11.9 ± 0.83	2.71e ± 0.33
Cabernet	Pulp	1.65 ± 0.11	0.65ab ± 0.06	0.02a ± 0.003	0.08ab ± 0.12
Sauvignon	Seed	113 ± 0.70	7.35 ± 0.43	–	17.2 ± 0.44
	Skin	31.5 ± 1.41	23.3 ± 0.97	5.67 ± 0.17	2.62e ± 0.13
Muscat	Pulp	1.14a ± 0.16	0.39bc ± 0.05	0.03a ± 0.003	0.05ac ± 0.01
Hamburg	Seed	135 ± 2.33	9.4 ± 0.71	–	24.2d ± 0.52
	Skin	37.6 ± 1.30	2.94d ± 0.22	2.74 ± 0.09	4.08 ± 0.31
Riesling	Pulp	1.06a ± 0.12	0.50c ± 0.05	–	0.05bc ± 0.01
	Seed	126 ± 1.55	15.8 ± 0.22	–	22.1 ± 0.34
	Skin	10.2 ± 0.84	3.65d ± 0.23	–	1.55 ± 0.07

[a]Values with the same letter(s) within a column are not significantly different at $p < 0.05$ by the Student––Newman–Keul's test

The polyphenolic compounds were mainly located in the grape seeds and skins, whereas the pulp contained a very low concentration of these components. From the data obtained in this study, it was observed that the seeds contained the highest contents of total phenolics (*TP*), total flavonoids (*TF*) and total catechins (*TC*), whereas anthocyanins (*TA*) were mainly located in the skins. It was found that the seeds from the Vranec variety contained the highest amounts of total phenolics, total flavonoids and total catechins among the analysed varieties, which was in concordance with previously published data for this variety from other regions of the Balkan Peninsula.[35] As expected, the highest concentration of total anthocyanins was also found in the skin extracts of the Vranec variety. It should be emphasized here that the Vranec variety dominates in the Macedonian vine-yards; it is the autochthonous variety for Montenegro and a regionally well--known variety grown in Serbia and Croatia, traditionally used for the production of high quality wines, such as the analysed Vranec and Disan (discussed below),

which are characterized by an intense dark red colour. Hamburg grapes, a traditional table grape variety, also contained a high level of polyphenolic components and are thus recommended for regular human consumption.

Wine phenolic composition and colour variables of the wines

The results for *TP*, *TF*, *TA* and *TC* for the analyzed red and white wines are presented in Table V. The highest concentrations of phenolic compounds, flavonoids and catechins were found in the Disan wine and the values for the total anthocyanins were very close to those obtained for the Vranec wine. Disan and Vranec wines contain 1515 and 1382 mg/L total phenolics, respectively, which are in agreement with some previous results (1470–1684 mg/L total phenols) for several types of dessert wines made from Vranec cultivars.[36] Both wines were produced from the Vranec grape variety grown in a distinctive region rich with minerals and micronutrients. Disan is traditionally made from later harvested more senescent Vranec grapes, after reduction of the crop before blooming. According to Magarino and San-José,[37] the phenolic content increases throughout the ripening of the grape and it is expected that wines made from later harvested grapes would contain higher contents of phenolics, as was observed from the obtained results for the Disan wine. However, the concentrations of the phenolic families in wines depend not only on the grape variety, but also on additional factors, such as the edaphoclimatic conditions, the enological practices, the storage conditions, *etc*.[13,38–40] During bottle aging of wine, modifications in the polyphenolic composition occur as a result of different transformations, such as oxidation processes, condensation and polymerization reactions including direct reactions between anthocyanins and flavanols or reactions between anthocyanins and flavanols through ethyl bridges,[41–43] whereby stable pigments are formed

TABLE V. Concentration (average from 3 replicates) of total phenolics, total flavonoids, total anthocyanins and total catechins in the analysed red and white wines (*TP*: total phenolics, *TF*: total flavonoids, *TA*: total anthocyanins, *TC*: total catechins)

Wine	Colour	Vintage year	TP^a / mg L^{-1}	TF^a / mg L^{-1}	TA^a / mg L^{-1}	TC^a / mg L^{-1}
Vranec	Red	2003	1382 ± 38.2	922a ± 12.0	239ab ± 14.8	834a ± 28.3
Disan (Vranec)	Red	2003	1515 ± 27.6	1104 ± 70.7	237ac± 9.89	846a ± 27.5
Cabernet Sauvignon	Red	2003	1185 ± 50.2	910a ± 22.6	258d ± 13.4	755 ± 25.4
Merlot	Red	2003	1119 ± 28.9	686 ± 17.7	267bcd ± 16.9	566 ± 27.5
Riesling	White	2003	205ab ± 11.3	70.8b ± 1.27	–	11.9b ± 1.09
Smederevka	White	2003	230c ± 12.0	69.7b ± 1.13	–	20.7 ± 0.85
Sauvignon Blanc	White	2003	218ac ± 16.3	52.4 ± 2.97	–	11.1b ± 0.30
Temjanika (Muscat de Frontignan)	White	2003	185b ± 9.89	61.3 ± 2.68	–	9.37 ± 0.87

[a]Values with the same letter(s) within a column are not significantly different at $p < 0.05$ by the Student––Newman–Keul's test

which stabilize the wine colour. All these reactions are related to changes in the colour and sensorial characteristics, such as the flavour, bitterness and astringency of the final wine. White wines contain lower contents of polyphenols compared to red wines. Among the analysed white wines, the highest phenolic content was measured for the Smederevka wine, the most widely cultivated white grape variety in Macedonia, and the lowest value was observed for the Temjanika wine.

The data for the total flavonoid contents showed that all the analyzed red wines had high flavonoid levels, comparable to the published results for other world wines.[21] The highest flavonoid content was found in the Disan wine made from the Vranec grape variety. The total flavonoid values for the analysed Smederevka and Riesling wines were similar and not statistically different.

The values of total anthocyanins in the analysed wines were very similar and were in concordance with published results for 10 red wines most spread in the region of former Yugoslavia, whereas the Vranec and Cabernet Sauvignon were found to have the highest amounts of anthocyanins.[35] All the analyzed red wines contained high levels of catechins with the Disan and Vranec wines containing, as expected, the highest contents. These results are in agreement with published data for these types of wines from other regions.[44]

The contents of catechins in the white wines were lower compared to the red wines, with the highest concentrations being observed for the Smederevka wine.

Katalinić *et al.*[45] measured the phenolic content of ten wines and obtained results in ranges 2402–3183 and 292–308 mg/L for the total phenolics in red and white wines, respectively. The analyzed wines contained 69.7–398 mg/L total anthocyanins, the flavonoid content, expressed as mg/L gallic acid, ranged from 1941–2893 mg/L, and the content of catechins was 0.25–12.7 mg/L. The anthocyanic content measured for Cabernet Sauvignon wines made from grapes treated with different irradiation were 320–402 mg/L.[46] The obtained results for the analysed Macedonian wines were also in agreement with the data published by Savova *et al.*[47] for 21 Bulgarian wines and the found total phenolics and total anthocyanic contents were 921–1821 and 22–274 mg/L, respectively.

Red and white wines have a different phenolic composition, which is characteristic for each variety. The polyphenolic content of the final wine depends not only on the grape variety, but also on the different winemaking procedures applied for production. Red wine production includes the procedure of maceration, which is not applied for white wine production, *i.e.*, white wines are produced without grape mash, having no contact with the grape skins. Therefore, white wines (Table V) contained lower amounts of polyphenols.

The results for the colour variables of the analyzed samples are presented in Table VI, from which it can be seen that the values of the colour intensity were between 0.98 for Vranec to 1.45 for Cabernet Sauvignon and it varied from one

variety to another. With regard to tint, low values (0.5–0.7) are characteristic for young red wines, which increase throughout aging. In this study, the tint values for the wines were relatively high, ranging from 0.71 (for Vranec and Disan) to 0.85 (for Merlot). The values for the brilliance of the wine, *dA*%, were below 40 %, which showed that the colour of the red wine was dark and atypical.[30] It can be seen that the lowest value for this parameter was found for the Merlot wine (46.6 %), which had the highest yellow proportion (41.5 %). The Vranec and Disan had *dA* % values greater than 50 %, which shows that the red colour was dominant in these wines. The obtained results for the analysed wines were in agreement with previously published data.[21,38,47]

TABLE VI. Colour composition of the analyzed red wines (the values are average from 3 replicates); *CI*: colour intensity, *T*: tint, *Ye* %: percentage of yellow colour contribution, *Rd* %: percentage of red colour contribution, *Bl* %: percentage of blue colour contribution in the overall colour, *dA* %: brilliance of the wine

Wine	Vintage year	*CI*	*T*	*Ye* %	*Rd* %	*Bl* %	*dA* %
Vranec	2003	0.98	0.71	37.0	51.9	11.0	53.8
Disan (Vranec)	2003	1.24	0.71	36.9	52.2	10.9	54.2
Cabernet Sauvignon	2003	1.45	0.81	39.7	48.7	11.6	47.3
Merlot	2003	1.14	0.85	41.5	48.4	10.2	46.6

The obtained results suggest that the analysed Macedonian red and white wines and grapes did not significantly differ in terms of phenolic contents from other varieties in the world. The Vranec wines, compared to the analysed Merlot and Cabernet Sauvignon wines, possessed the highest phenolic potential, as shown by the highest results for the concentrations of the compounds from different phenolic groups.

Principal component analysis

Principal component analysis (PCA) was applied in order to investigate the possible grouping of red and white wines samples according to the content of total phenolics, total flavonoids, and total catechins. From Table VII and the correlation score plot in Fig. 1, it can be seen that the first principal component (PC1), had the dominant influence, accounting for 99.61 % of the variability and the second principal component (PC2) accounted for 0.23 % of the variability, *i.e.*, together, PC1 and PC2 account for 99.84 % of the total variance.

A clear separation was noticed between the red and white wines: the white wines were located in the second principal component and red wines in the first principal component. A further distinction was made in the white wine group according to PC2: the Temjanika and Riesling were located in the positive part of PC2 and separated from Smederevka and Sauvignon Blanc, which were located in the negative part of PC2. The red wines were also further divided, whereby the Vranec and Disan were grouped and located in the negative part of PC1, while

the Merlot was located very low in the negative part of PC1 and Cabernet Sauvignon, very high in the positive part of PC1.

TABLE VII. Individual influence of the principal components (PC1: first principal component, PC2: second principal component, PC3: third principal component)

Influence	PC1	PC2	PC3
Eigen value	2.9884	0.0068	0.0048
Explained (%)	99.61	0.23	0.16
Cumulated (%)	99.61	99.84	100
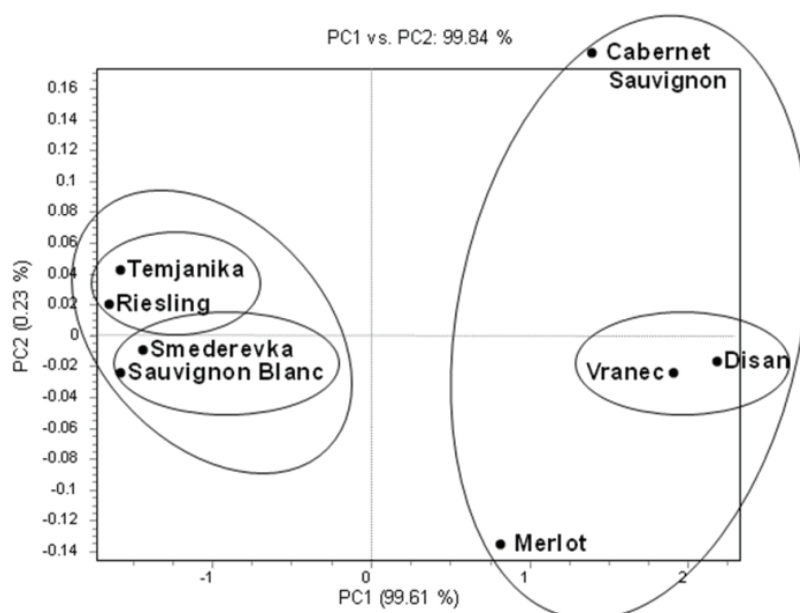
Fig. 1. Principal Component score plot (PC1 and PC2) of the studied white and red wines, based of spectrophotometric data for the total phenols, total flavonoids and total catechins.

CONCLUSIONS

The obtained results showed that the phenolic compositions of local Macedonian wines and grapes are similar to the cultivars from other countries in quantity and quality. The Vranec variety possesses the highest phenolic potential with a high content of total phenolics, total flavonoids, total anthocyanins and total catechins and the wine had a high value of the colour intensity. The accuracy of the commonly used spectrophotometric methods was checked by the standard addition method and the Folin-Ciocalteu assay was slightly modified in order to shorten the analysis time. Extraction of polyphenolic compounds from grape skin, seed and pulp was performed with acetone/water (80/20) and its efficiency checked.

Available online at www.shd.org.rs/JSCS/

Applying appropriate winemaking technologies, the Vranec grape variety can be a raw material for making high quality and premium Macedonian wines. This was supported by the results for the wines Vranec and Disan, for which the highest concentrations of total phenolics, flavonoids, anthocyanins and catechins were evidenced in this study.

И З В О Д

ОДРЕЂИВАЊЕ САДРЖАЈА ПОЛИФЕНОЛА У МАКЕДОНСКОМ ГРОЖЂУ И ВИНУ СТАНДАРДНИМ СПЕКТРОФОТОМЕТРИЈСКИМ МЕТОДАМА

VIOLETA IVANOVA[1,2], MARINA STEFOVA[1] и FABIO CHINNICI[3]

[1]*Institute of Chemistry, Faculty of Natural Sciences and Mathematics, Sts. Cyril and Methodius University, Arhimedova 5, 1000 Skopje, FYR Macedonia,* [2]*Department for Enology, Institute of Agriculture, Sts. Cyril and Methodius University, Aleksandar Makedonski bb Skopje, FYR of Macedonia u* [3]*Department of Food Science, University of Bologna, Viale Fanin 40, 40127 Bologna, Italy*

Вино и грожђе садрже велики број флавоноида и нефлавоноидних фенолних једињења. У овој студији је одређиван полифенолни састав шест комерцијалних црвених и белих македонских вина и четири врсте грожђа. Спектрофотометријске методе су коришћене за одређивање укупних фенола, флавоноида, антоцијана и катехина. Упоређивана је ефикасност раствора ацетон/вода (80/20) и метанол/вода (80/20) у екстракцији полифенола из пулпе, коштица и љуске зрна грожђа. Ефикаснија екстракција је постигнута смешом ацетон/вода. Добијени резултати су показали да је македонско грожђе богато полифенолима, а највећа концентрација укупних фенола је нађена у грожђу врсте Вранец. Анализирана вина, такође, садрже доста полифенола, посебно вино Дисан од грожђа Вранец (1515 mg/L укупних фенола, 1103 mg/L укупних флавоноида, 237 mg/L укупних антоцијана и 845 mg/L укупних катехина). Анализа основних компоненти је примењена на испитиване узорке и нађена је јасна разлика између врста белих вина и црвених вина.

REFERENCES

1. P. Ribéreau-Gayon, Y. Glories, A. Maujean, D. Dubourdieu, *Handbook of enology, Vol. 2: The chemistry of wine and stabilization and treatments,* John Wiley & Sons Ltd., Chichester, 2000, p. 141
2. A. Ros Barceló, A. A. Calderón, J. M. Zapata, R. Muñoz, *Scientia Horticulturae* **57** (1994) 265
3. R. C. Pecket, C. J. Small, *Phytochemistry* **19** (1980) 2571
4. L. W. Wulf, C. W. Nagel, *Am. J. Enol. Vitic.* **29** (1978) 42
5. F. Mattivi, R. Guzzon, U. Vrhovsek, M. Stefanini, R. Velasco, *J. Agric. Food Chem.* **54** (2006) 7692
6. N. Castillo-Muñoz, S. Gómez-Alonso, E. García-Romero, I. Hermosín-Gutiérrez, *J. Agric. Food Chem.* **55** (2007) 992
7. Z. Czochanska, L. Y. Foo, R. H. Newman, L. J. Porter, W. A. Thomas, W. T. Jones, *J. Chem. Soc., Chem. Commun.* **8** (1979) 375
8. L. J. Porter, L. N. Hirtstich, B. G. Chang, *Phytochemistry* **25** (1986) 223
9. R. J. M. Da Silva, J. Rigaud, V. Cheynier, A. Cheminat, M. Moutounet, *Phytochemistry* **30** (1991) 1259

Available online at www.shd.org.rs/JSCS/

10. J.-M. Souquet, V. Cheynier, F. Brossaud, M. Moutounet, *Phytochemistry* **43** (1996) 509
11. I. McMurrough, J. McDowell, *Anal. Biochem.* **91** (1978) 92
12. M. L. González-Sanjosé, L. J. R. Barrón, C. Díez, *J. Sci. Food Agric.* **51** (1990) 337
13. G. Mazza, L. Fukumoto, P. Delaquis, B. Girard, B. Ewert, *J. Agric. Food Chem.* **47** (1999) 4009
14. P. Viñas, C. López-Erroz, J. J. Marín-Hernández, M. Hernández-Córdoba, *J. Chromatogr. A* **871** (2000) 85
15. B. Sun, I. Spranger, F. Roque-do-Vale, C. Leandro, P. Belchior, *J. Agric. Food Chem.* **49** (2001) 5809
16. E. Boselli, R. B. Boultnon, J. H. Throngate, N. G. Frega, *J. Agric. Food Chem.* **52** (2004) 3843
17. P. Avar, M. S. P. Nikfardjam, S. Kunsági-Máté, G. Montskó, Z. Szabó, K. Böddi, R. Ohmacht, L. Márk, *Int. J. Mol. Sci.* **8** (2007) 1028
18. R.-B. A. de Quirós, J. López-Hernández, P. Ferraces-Sasais, M. A. Lage-Yusty, *J. Sep. Sci.* **30** (2007) 1262
19. L. Singleton, J. R. Rossi, *Am. J. Enol. Vitic.* **16** (1965) 144
20. K. Slinkard, V. L. Singleton, *Am. J. Enol. Vitic.* **28** (1977) 9
21. R. Di Stefano, M. C. Cravero, *L'enotecnico Ottobre* (1989) 81
22. R. Di Stefano, M. C. Cravero, N. Gentilini, *L'Enotecnico I Maggio* (1989) 83
23. J. Burns, P. T. Gardner, J. O'Neil, S. Crawford, I. Morecroft, D. B. McPhail, C. Lister, D. Matthews, M. R. MacLean, M. E. J. Lean, A. Crozier, *J. Agric. Food Chem.* **48** (2000) 220
24. P. Ho, M. Da Conceição, M. Silva, T. A. Hogg, *J. Sci. Food Agric.* **81** (2003) 1269
25. D. Treutter, C. Santos-Buelga, M. Gutmann, H. Kolodziej, *J. Chromatogr. A* **667** (1994) 290
26. A. Arnous, D. P. Makris, P. Kefalas, *J. Agric. Food Chem.* **49** (2001) 5736
27. J. Zhishen, T. Mengeheng, W. Jianming, *Food Chem.* **64** (1999) 555
28. G. Mazza, L. Fukumoto, P. Delaquis, B. Girard, B. Ewert, *J. Agric. Food Chem.* **47** (1999) 4009
29. D. Kim, O. K. Chun, Y. J. Kim, H. Moon, C. Y. Lee *J. Agric. Food Chem.* **51** (2003) 6509
30. Y. Glories, *Vigne Vin* **18** (1984) 253
31. D. Marinova, F. Ribarova, M. Atanassova, *J. Univ. Chem. Tech. Metall.* **40** (2005) 255
32. J. A. Kennedy, M. A. Matthews, A. L. Waterhouse, *Am. J. Enol. Vitic.* **53** (2002) 268
33. R. R. Montealegre, R. R. Peces, J. L. C. Vozmediano, J. M. Gascueña, E. G. Romer, *J. Food Compos. Anal.* **19** (2006) 687
34. S. Kallithraka, C. Garcia-Viguera, P. Bridle, J. Bakker, *Phytochem. Anal.* **6** (1995) 265
35. V. Kovać, in *Proceedings of the Vojvodina Chamber of Commerce XXII*, Novi Sad, Yugoslavia, 1980, p. 263 (in Serbian)
36. K. Boškov, Z. Božinović, M. Petkov, B. Vojnoski, in *Symposium Proceedings of II Balkan Symposium of Viticulture and Enology*, Pleven, 2004, p. 242
37. S. P. Magariño, M. J. G. San-Jośe, *Food Chem.* **96** (2006) 197
38. M. L. González-Sanjosé, L. J. R. Barrón, C. Díez, *J. Sci. Food Agric.* **51** (1990a) 337
39. A. G. Reynolds, R. M. Pool, L. R. Mattick, *Vitis* **25** (1986) 85
40. M. S. Andreas, M. L. González-Sanjosé*, Zubía monográfico* (1995) 79
41. J. Bakker, C. F. Timberlake, *J. Agric. Food Chem.* **45** (1997) 35

42. H. Fulcrand, C. Benabdeljalil, J. Rigaud, V. Cheynier, M. Mountounet, *Phytochemistry* **47** (1998) 1401
43. M. Schwarz, G. Hofmann, P. Winterhalter, *J. Agric. Food Chem.* **52** (2004) 498
44. M. D. Goldenberg, A. Karumanchiri, E. Tsang, G. J. Soeleas, *Am. J. Enol. Vitic.* **49** (1998) 23
45. V. Katalinić, M. Milos, D. Modum, I. Musić, M. Boban, *Food Chem*. **86** (2004) 593
46. J. A. Kennedy, M. A. Matthews., A. L. Waterhouse, *Am. J. Enol. Vitic.* **53** (2002) 268
47. S. T. Savova, S. Dimov, F. Ribarova, *J. Food Comp. Anal.* **15** (2002) 647.

Available online at www.shd.org.rs/JSCS/

Synthesis, characterization and DNA cleavage activity of nickel(II) adducts with aromatic heterocyclic bases

M. S. SURENDRA BABU[1], PITCHIKA G. KRISHNA[2],
K. HUSSAIN REDDY[1]* and G. H. PHILIP[2]

*[1]Department of Chemistry, Sri Krishnadevaraya University, Anantapur-515003 and
[2]Department of Zoology, Sri Krishnadevaraya University, Anantapur-515003, India*

Abstract: Mixed ligand complexes of nickel(II) with 2,4-dihydroxyacetophenone oxime (DAPO) and 2,4-dihydroxybenzophenone oxime (DBPO) as primary ligands, and pyridine (Py) and imidazole (Im) as secondary ligands were synthesized and characterized by molar conductivity, magnetic moments measurements, as well as by electronic, IR, and ^{1}H-NMR spectroscopy. Electrochemical studies were performed by cyclic voltammetry. The active signals are assignable to the Ni$^{III/II}$ and Ni$^{II/I}$ redox couples. The binding interactions between the metal complexes and calf thymus DNA were investigated by absorption and thermal denaturation. The cleavage activity of the complexes was determined using double-stranded pBR322 circular plasmid DNA by gel electrophoresis. All complexes showed increased nuclease activity in the presence of the oxidant H_2O_2. The nuclease activities of mixed ligand complexes were compared with those of the parent copper(II) complexes.

Keywords: Ni(II) complexes; oximes; mixed ligands; DNA interaction; cleavage activity.

INTRODUCTION

Studies on the chemical modification of nucleic acids by transition metal complexes are of paramount importance for designing chemotherapeutic drugs, regulating gene expression and designing tools for molecular biology.[1–6] Many coordination compounds of transition metal ions accomplish nucleolytic cleavage. Nickel is a remarkably versatile metal in biological chemistry. It is a necessary component of certain metallo-proteins but simultaneously an environmental carcinogen causing DNA damage and protein–DNA crosslinks. Nickel compounds have two characteristics in common with leading antitumour drugs: direct metal binding to N7 of guanine is possible and nickel complexes are able

---

61

to catalyze oxidative damage to nucleic acids.[7–9] It was found that high-valent nickel species may also mediate through sequence-specific oxidative cleavage of DNA by designed metallo-proteins.[10] A number of authors have concluded that Ni^{2+} binds covalently to the N7 atom of guanine and adenine.[11–13] Nickel-induced carcinogenesis involves the oxidation of Ni^{2+} to Ni^{3+} by intracellular oxidants, such as H_2O_2.[14] This oxidation of nickel, presumably through Fenton-type reactions, results in the formation of reactive oxygen species, which can then cause oxidative damage to DNA. Recent reports on the nucleolytic activity of oxime complexes[15,16] prompted us to investigate the structural peculiarities and nuclease activity of Ni(II) oxime complexes and aromatic base(pyridine/imidazole) adducts.

EXPERIMENTAL

Apparatus and reagents

2,4-Dihydroxyacetophenone and 2,4-dihydroxybenzophenone were purchased from Merck and the metals used in the preparation of the complexes were of reagent grade. The solvents used in the synthesis of the ligands and metal complexes were distilled before use. All other chemicals were of AR grade and were used without further purification. Agarose, used in gel electrophoresis, was purchased from Sigma-Aldrich. Calf thymus DNA (CT DNA) and plasmid pBR322 were purchased from Genie Biolabs, Bangalore, India. The elemental analyses were performed using a Perkin-Elmer 2400 CHNS elemental analyzer. The magnetic moments were determined in the polycrystalline state using a PAR model-155 vibrating sample magnetometer operating at a field strength of 2–8 kG. Nickel of high purity (saturation moment 55 e.m.u./g) was used as the standard. The molar conductance of the complexes in DMF (10^{-3} M) solution was measured at 28 ± 2 °C with a Systronic model 303 direct-reading conductivity bridge. The electronic spectra were recorded in DMF employing a Shimadzu UV-160A spectrophotometer. The FTIR spectra were recorded in the range 4000–50 cm^{-1} with a Bruker IFS 66V in KBr discs and polyethylene medium. The ^{1}H-NMR spectra of parent complexes in DMSO-d_6 solvent were recorded on JEOL GSX 400NB multinuclear FT-NMR spectroscope at SAIF, IIT, Madras. The voltammetric measurements were performed using a Bio-Analytical System (BAS) CV-27 assembly in conjunction with an *x–y* recorder. The measurements were made on degassed (N_2 bubbling for 5 min) solutions in DMF (10^{-3} M) containing 0.10 M tetraethylammonium perchlorate as the supporting electrolyte. The three-electrode system consisted of a glassy carbon (working), platinum (auxiliary) and Ag//AgCl (reference) electrodes.

Synthesis of complexes

Ni(DAPO)$_2$ (**1**) was prepared by mixing NiCl$_2$ (4.3 g, 0.025 mol) and 2,4-dihydroxyacetophenone (8.3 g, 0.050 mol) in a 1:2 ratio in 50 % aqueous ethanolic medium. The reaction mixture was maintained at pH 8 using 1.0 M sodium acetate solution and stirred for 30 min. The obtained green precipitate was filtered, washed with hot water and cold methanol. The complex was dried at 110 °C.

Ni(DBPO)$_2$ (**2**) was prepared as described above, but using 2,4-dihydroxybenzophenone to afford a thick green precipitate.

[Ni(DAPO)$_2$Py$_2$] (**3**) was synthesised by dissolving the nickel(II) complex of DAPO (3.0 g, 0.018 mol) in pyridine (3.0 ml) in a Schlenk tube. The solution was stirred magnetically for

30 min and *n*-hexane (25 ml) was added. After standing at room temperature for 3–4 days, a dark green product formed which was filtered, washed with water and *n*-hexane and dried under reduced pressure over CaCl$_2$.

[Ni(DBPO)$_2$Py$_2$] (**4**) was prepared by dissolving the nickel(II) complex of DBPO (0.60 g, 0.026 mol) in pyridine (10 ml) in a schlenk tube. The solution was stirred magnetically for 30 min and *n*-hexane (25 ml) was added. After standing at room temperature for 7 days, a dark green product formed which was filtered, washed with water and *n*-hexane and dried under reduced pressure over CaCl$_2$.

[Ni(DAPO)$_2$Im$_2$] (**5**) was prepared by placing the nickel(II) complex of DAPO (1.67 g, 0.0100 mol) in a 250 ml round bottom flask. Imidazole (3.4 g, 0.050 mol) dissolved in 30 ml of CH$_2$Cl$_2$ was added to the contents of the flask. The reaction mixture was refluxed on a water bath for 2 h. On cooling, a dark green precipitate formed which was filtered, washed with cold *n*-hexane and dried under vacuo over CaCl$_2$.

[Ni(DBPO)$_2$Im$_2$] (**6**) was synthesised by placing the nickel(II) complex of DBPO (0.010 mol) in a 250 ml round bottom flask. Imidazole (0.050 mol) dissolved in 30 ml of CH$_2$Cl$_2$ was added to the contents of the flask. The reaction mixture was refluxed on a water bath for 2 h. On cooling, a dark green precipitate formed which was filtered, washed with cold *n*-hexane and dried under vacuum over anhydrous CaCl$_2$.

DNA binding and cleavage experiments

All measurements with CT DNA were performed in buffer Tris–HCl 5 mM (pH 7.2), 50 mM NaCl. The UV absorbance ratio $\lambda_{260}/\lambda_{280}$ was 1.8–1.9, indicating the DNA was sufficiently free of protein.[13] The concentration of CT DNA per nucleotide was determined from the absorption intensity at 260 nm with the known ε value of 6600 M^{-1} cm^{-1}.[17] The absorption titrations were performed by adding increasing amounts of CT DNA to a solution of the complex at a fixed concentration contained in a quartz cell and recording the UV–Vis spectrum after each addition. The absorption of CT DNA was subtracted by adding the same amounts of DNA to a blank. The data were then fitted to Eq. (1) to obtain the intrinsic binding constant, K_b.[18]

$$[DNA] / (\varepsilon_a - \varepsilon_f) = [DNA] / (\varepsilon_b - \varepsilon_f) + 1/K_b(\varepsilon_b - \varepsilon_f) \qquad (1)$$

where ε_a, ε_f and ε_b are the apparent, free and bound metal complex extinction coefficients, respectively. A plot of $[DNA] / (\varepsilon_a - \varepsilon_f)$ *vs*. [DNA] gave a slope of $1/(\varepsilon_b - \varepsilon_f)$ and a *y*-intercept equal to $1/K_b(\varepsilon_b - \varepsilon_f)$. Thus, K_b is the ratio of the slope to the *y*-intercept.

DNA melting experiments were performed using a spectrophotometer connected to a thermostat. The absorbance of DNA (75 µM) at 25–80 °C in both the absence and presence of 7.5 µM of the complex was recorded at 260 nm. The melting temperature (T_m) was calculated by plotting the temperature *vs*. the relative absorption intensity (A/A_0).

A DMF solution containing the metal complexes (10 µM) in a clean Eppendorf tube was treated with pBR322 plasmid DNA (3.3 µl of 150 µg/ml) in Tris-HCl buffer (0.10 M, pH 8.0) containing NaCl (50 mM) in presence and absence of additives. The contents were incubated for 1 h at 37 °C and loaded onto a 1 % agarose gel after mixing 5 µl of loading buffer (0.25 % bromophenol blue + 25 % xylene cyanol + 30 % glycerol, sterilized distilled). The electrophoresis was performed at a constant voltage (80 V) until the bromophenol blue had travelled through 75 % of the gel. Subsequently, the gel was stained for 10 min by immersion in ethidium bromide solution. The gel was then destained for 10 min by keeping it in sterile distilled water. The plasmid bands were visualized by viewing the gel under a transilluminator and photographed.

RESULTS AND DISCUSSION

Nickel complexes were prepared using oxime ligands with nickel chloride, and further with pyridine and imidazole to form mixed ligand complexes. All the complexes were freely soluble in DMF and DMSO, slightly soluble in methanol and ethanol, and insoluble in water.

The evaluated analytic and spectroscopic characteristics of the prepared complexes are given below

Ni(DAPO)$_2$ (1). Yield: 81 %; m.p.: 198–202 °C. Anal. Calcd. for C$_{16}$H$_{16}$N$_2$O$_6$Ni: C, 49.16; H, 4.12; N, 7.12 %; found: C, 49.36; H, 4.10; N, 7.11 %. FTIR (KBr, cm^{-1}): 1605 (C=N), 458 (N–Ni), 523 (O–Ni). ^{1}H-NMR (CDCl$_3$, δ / ppm): 2.0 (3H, *s*, CH$_3$), 6.2–6.4 (2H, *dd*, Ar, *J* = 3.4 Hz), 7.2 (1H, *d*, Ar *J* = = 6.2 Hz), 9.6 (1H, *s*, OH), 11.8 (1H, *s*, oxime OH).

Ni(DBPO)$_2$ (2). Yield: 63 %; m.p.: 256–260 °C. Anal. Calcd. for C$_{26}$H$_{18}$N$_2$O$_6$Ni: C, 60.42; H, 3.91; N, 5.41 %; found: C, 60.25; H, 3.92; N, 5.32 %. FTIR (KBr, cm^{-1}): 1614 (C=N), 455 (N–Ni), 576 (O–Ni). ^{1}H-NMR (δ / ppm): 6.2–6.4 (3H, *m*, Ar), 7.2 (5H, *m*, Ar), 10.6 (1H, *br s*, phenolic OH),12.4 (1H, *s*, oxime OH).

[Ni(DAPO)$_2$Py$_2$] (3). Yield: 42 %; m.p: 170–172 °C. Anal. Calcd. for C$_{26}$H$_{26}$N$_4$O$_6$Ni: C, 56.82; H, 4.77; N, 10.2 %; found: C, 56.91; H, 4.78; N, 10.6 %. FTIR (KBr, cm^{-1}): 1600 (C=N), 472 (N–Ni), 690 (N–Ni of Py), 548 (O–Ni).

[Ni(DBPO)$_2$Py$_2$] (4). Yield: 38 %; m.p.: 212–214 °C. Anal. Calcd. for C$_{36}$H$_{30}$N$_4$O$_6$Ni: C, 64.21; H, 4.49; N, 8.73 %; found: C, 64.25; H, 4.46; N, 8.71 %. FTIR (KBr, cm^{-1}): 1613 (C=N), 460 (N–Ni), 699 (N–Ni of Py), 565 (O–Ni).

[Ni(DAPO)$_2$Im$_2$] (5). Yield: 65 %; m.p.: 118–190 °C. Anal. Calcd. for C$_{22}$H$_{24}$N$_6$O$_6$Ni: C, 50.18; H, 4.59; N, 15.9 %; found: C, 50.18; H, 4.52; N, 15.72 %. FTIR (KBr, cm^{-1}): 1590 (C=N), 472 (N–Ni), 710 (N–Ni of Im), 562 (O–Ni).

[Ni(DBPO)$_2$Im$_2$] (6). Yield: 49 %; m.p.: 198–202 °C. Anal. Calcd. for C$_{32}$H$_{28}$N$_6$O$_6$Ni: C, 59.01; H, 4.33; N, 12.9 %; found: C, 58.72; H, 4.32; N,12.8 %. FTIR (KBr, cm^{-1}): 1595 (C=N), 475 (N–Ni), 715 (N–Ni of Im), 560 (O–Ni).

The elemental analysis supported the 1:2 compositions of the metal and ligands. The molar conductance data of these nickel complexes suggested their non-electrolytic nature (Table I). The magnetic moment values of the parent complexes suggested that they are diamagnetic, while the corresponding pyridine and imidazole complexes, having a magnetic momentum in range 3.0–3.6 μ_B, were paramagnetic and favoured octahedral geometry with a $^3A_{2g}$ ground state.

The electronic spectra of the studied Ni(II) complexes are given in Fig. 1. The electronic spectra of all complexes consisted of three bands: one at ≈10000 cm^{-1} due to $^3A_{2g} \rightarrow {}^3T_{2g}$ (v_1), ≈17000 cm^{-1} due to $^3A_{2g} \rightarrow {}^3T_{1g}$ (v_2) and ≈29000 cm^{-1} due to $^3A_{2g} \rightarrow {}^3T_{2g}$ (v_3), which clearly indicates octahedral stereochemistry. The spectral data were utilized to compute important ligand field parameters (10 *Dq* and *B*) using the ligand field of spin allowed transitions in the d^8

configuration. The values of 10 Dq and the Racah interelectronic repulsion parameter (B) were employed to calculate ν_2 and ν_3 and the results are given in Table II.

TABLE I. Magnetic moment and molar conductivity data of Ni(II) complexes and adducts **1–4**

Compound	Complex	Molar conductance, S cm² mol⁻¹	Magnetic moment μ_{eff} / μ_B
1	[Ni(DAPO)$_2$][a]	15.4	Diamagnetic
2	[Ni(DAPO)$_2$Py$_2$][b]	13.4	3.16
3	[Ni(DAPO)$_2$Im$_2$][c,d]	12.2	3.18
4	[Ni(DBPO)$_2$][e]	8.8	Diamagnetic
5	[Ni(DBPO)$_2$Py$_2$]	7.4	2.89
6	[Ni(DBPO)$_2$Im$_2$][d]	7.2	2.93

[a]DAPO = 2,4-dihydroxyacetophenone oxime; [b]Py = pyridine; [c]Im = imidazole; [d]decomposes on staying for more than 32 h in DMF solution; [e]DBPO = 2,4-dihydroxybenzophenone oxime
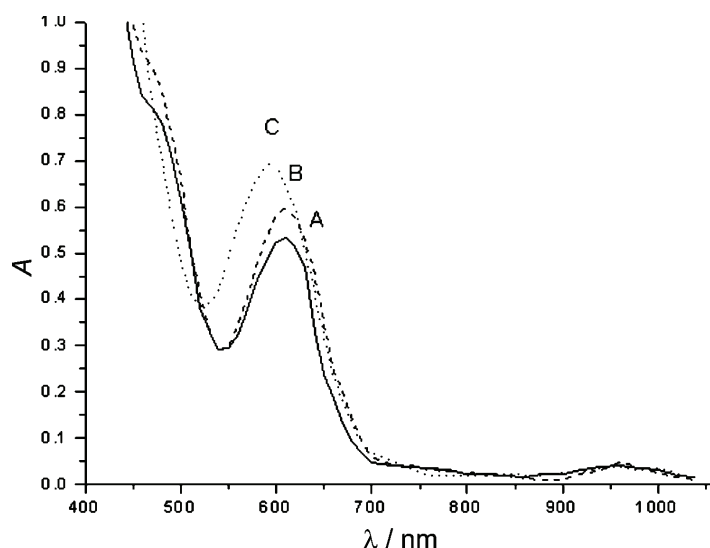
Fig. 1. Electronic spectra of the complexes, a) [Ni(DAPO)$_2$],
b) [Ni(DAPO)$_2$Py$_2$] and c) [Ni(DAPO)$_2$Im$_2$].

Comparison of the 10Dq and B values indicates that the ligands formed reasonably strong covalent bonds within the complexes. The high values of 10Dq and B are also consistent with coordination of the oxime nitrogen. The ratios of ν_1 and ν_2 lie between 1.56–1.68, as expected for octahedral nickel(II) complexes.[19] The Racah interelectronic repulsion parameters (B) and the covalent factor (B_{35}) are used for establishing the position of the present ligands in a nephelauxetic series. The data for these complexes gave h_x values from 0.90 to 1.19, suggesting that the present ligands may be placed between water and ammonia. As the *LSFE* values of the complexes were nearly the same, they reflected almost identical coordination around the central metal ion.

TABLE II. Electronic spectral data (cm^{-1}) and ligand field parameters of the studied Ni(II) complexes

Complex	Method of evaluations	v_1	v_2	v_3	β	Δ	B_{35}	$10\ Dq$	v_2-v_1	v_2/v_1	LFSE	h_x
[Ni(DAPO^a)$_2$]	Observed	10760	16660	28980	890.6	649	0.89	10760	5900	1.54	30.74	1.07
	Calculated	10Dq	17301	28331					6541	1.60		
[Ni(DAPO)$_2$Py$_2$]	Observed	10790	16950	28980	904	432	0.87	10790	6160	1.57	30.80	1.09
	Calculated	10Dq	17381	28548					6591	1.61		
[Ni(DAPO)$_2$Im$_2$]	Observed	10820	17120	28750	934.2	562	0.82	10820	6308	1.64	29.25	1.05
	Calculated	10Dq	17840	29650					6060	1.61		
[Ni(DBPO^b)$_2$]	Observed	10790	16780	29185	902.1	601	0.88	10790	5990	1.54	30.82	1.10
	Calculated	10Dq	17376	28524					6586	1.61		
[Ni(DBPO)$_2$Py$_2$^{c}]	Observed	10810	16890	29225	912.3	542	0.89	10810	6080	1.56	30.89	1.11
	Calculated	10Dq	17433	28683					6623	1.61		
[Ni(DBPO)$_2$Im$_2$^{d}]	Observed	10820	17240	29250	933.6	561	0.82	10820	6420	1.60	30.54	1.10
	Calculated	10Dq	17840	29650					7020	1.64		

^{a}2,4-dihydroxyacetophenone oxime; ^{b}2,4-dihydroxybenzophenone oxime, ^{c} pyridine, ^{d}imidazole

Important IR spectral band data of the nickel(II) complexes are present in Table III. The ν_{OH} stretching vibrations of phenolic groups observed at 3200––3000 cm^{-1} in the spectra of the ligands are absent in the spectra of the complexes, suggesting that the phenolic oxygen is coordinated to the metal. The $\nu_{C=N}$ band observed at 1620–1630 cm^{-1} in the spectra of the ligands is shifted to lower frequency in those of the complexes and adducts. This indicates that the metal coordinates to the nitrogen of the oxime group. The band at 1550–1530 cm^{-1} is assigned to $\nu_{C=N}$ stretching in pyridine and imidazole. An absorption band appearing around 3400 cm^{-1} in the complexes of DAPO and DBPO is assigned to the free phenolic –OH group present in the *para* position of the aromatic ring. A broad and nearly flat band present in the region 3000–2900 cm^{-1} indicates that the oxime OH proton is not released during the formation of the metal chelates. The shape of this band in the metal chelates can be attributed to intramolecular hydrogen bonding, which lies in a plane, suggesting the formation of very stable five--membered rings. The non-ligand absorptions in the regions 470–450 cm^{-1} and 570–520 cm^{-1} are tentatively assigned to ν_{M-N} and ν_{M-O}, respectively. The strong absorption band at 260–220 cm^{-1} is absent in the spectra of the metal complexes but appeared in the adducts; a weak band also appeared in region 650–730 cm^{-1}. These bands are assigned to the ν_{M-N} (pyridine/imidazole) vibrational mode, indicating the presence of pyridine/imidazole in coordination with nickel in the adducts.

TABLE III. Selected IR bands (cm^{-1}) of the studied Ni(II) complexes with tentative assignment (*vs* = very strong, *s* = strong, *m* = medium, *w* = weak)

Complex	ν_{OH} (oxime)	$\nu_{C=N}$	$\nu_{C=N}$ (Py/Im)	ν_{M-N}	ν_{M-N} (Py/Im)	ν_{M-O}
[Ni(DAPO)$_2$]	3290 *s*	1605 *vs*	–	468 *w*	–	592 *w*
[Ni(DAPO)$_2$(Py)$_2$]	3350 *s*	1600 *s*	1555 *w*	472 *w*	690 *m*	562 *w*
[Ni(DAPO)$_2$(Im)$_2$]	3330 *s*	1590 *s*	1560 *w*	476 *w*	710 *m*	548 *w*
[Ni(DBPO)$_2$]	3300 *s*	1614 *vs*	–	455 *w*	–	576 *w*
[Ni(DBPO)$_2$(Py)$_2$]	3320 *s*	1613 *s*	1545 *w*	460 *w*	699 *m*	–
[Ni(DBPO)$_2$(Im)$_2$]	3310 *s*	1612 *s*	1560 *w*	455 *w*	705 *m*	568 *w*

The ^{1}H-NMR spectra of parent complexes were taken in DMSO-d_6. The phenolic proton peaks present in the spectra of the ligands are absent in the ^{1}H-NMR spectra of all complexes, suggesting coordination of the phenolic oxygen to the metal.

Based on the elemental analysis, magnetic moments, electronic, IR and ^{1}H--NMR data, tentative structures of the complexes and adducts are given in Fig. 2a and 2b, respectively.
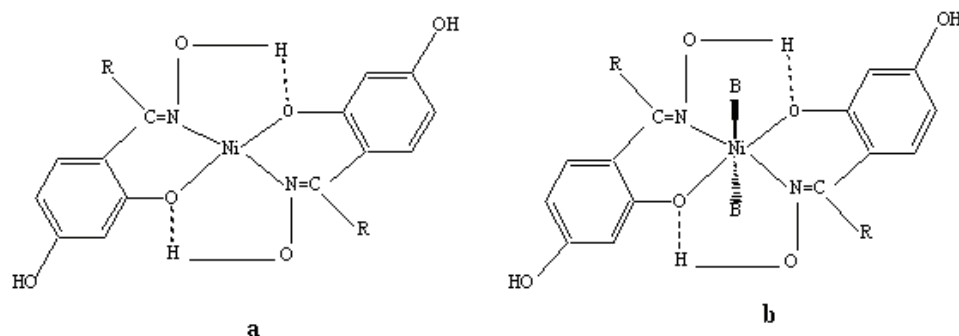
Available online at www.shd.org.rs/JSCS/

Fig. 2. a) Structure of the nickel(II) complexes, where R = CH$_3$ – 2,4-dihydroxyacetophenone oxime (DAPO) or R = C$_6$H$_5$ – 2,4-dihydroxybenzophenone oxime (DBPO) and b) structure of the nickel(II) adducts, where R = CH$_3$ – 2,4-dihydroxyacetophenone oxime (DAPO) or C$_6$H$_5$ – 2,4-dihydroxybenzophenone oxime (DBPO) and B = pyridine or imidazole.

Cyclic voltammetry

The oxidation–reduction potentials of the nickel ion in the complexes were studied by cyclic voltammetry. The cyclic voltammograms of the nickel(II) complexes were recorded in DMF containing tetraethylammonium perchlorate (0.10 M) as the supporting electrolyte. The cyclic voltammetric profiles of representtative complexes are given in Fig. 3. The electrochemical data of all complexes obtained at the glassy carbon electrode in DMF are given in Table IV. The redox behaviour of the nickel(II) complexes showed two active responses by cyclic voltammetry. The $E_{1/2}$ values of the nickel complexes were observed in the potential range –1.75 to –1.45 *vs*. Ag/AgCl, assigned to the Ni$^{III/II}$ couple and in the potential range –1.50 to –0.95 V *vs*. Ag/AgCl, assigned to Ni$^{II/I}$. Repeated scans as well as various scan rates showed that dissociation did not occur in these complexes. The large non-equivalence of the current intensity of the cathodic and anodic peaks indicates the quasi-reversible behaviour of these complexes. The ΔE_p values were greater than the Nernstian values ($\Delta E_p \approx 59$ mV) for a one--electron redox system. This indicates a considerable reorganization of the coordination sphere during electron transfer, as was observed for a number of other nickel (II) complexes. As can be seen from Table IV, the pyridine and imidazole adducts had higher $E_{1/2}$ values than the parent complexes, showing that the addition of the second ligand slightly destabilized the Ni(II) oxidation state. The $\Delta G^{\ominus}$ values of the mixed ligand complexes were lower than those of the parent complexes, showing that the adducts were less stable than the parent complexes.
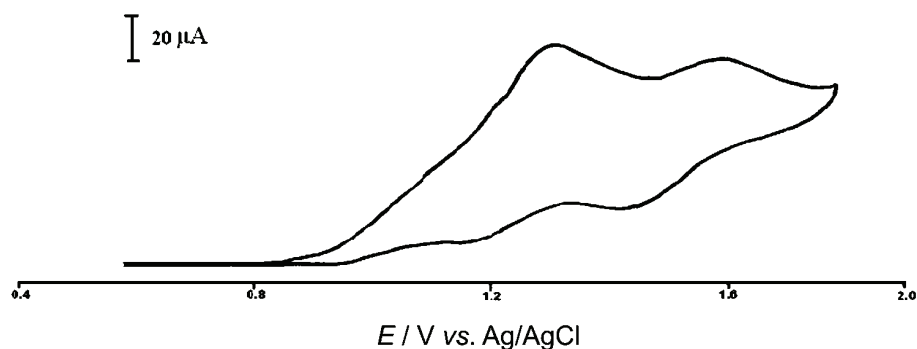
Fig. 3. Cyclic voltammogram of [Ni(DAPO)$_2$Im$_2$] at a scan rate of 50 mV s^{-1}.

A comparison of the $E_{1/2}$ values of this redox couple of the present complexes with other analogous nitrogen donor macrocycles revealed that the oxime complexes undergo a more facile redox change, which seems to be a requirement for DNA cleavage.[20]

TABLE IV. Cyclic voltammetric data of the Ni(II) DAPO and DBPO complexes with or without pyridine/imidazole ligands (recorded in DMF at room temperature with Et$_4$NClO$_4$ as the supporting electrolyte; glassy carbon as the working electrode, Pt wire as the auxiliary electrode and Ag/AgCl as the reference electrode; scan rate: 50 mV s^{-1})

Complex	Redox couple	$E_{p,c}$ / V	$E_{p,a}$ / V	ΔE_p / mV	$E_{1/2}$ / V	log K_c[a]	$-\Delta G^{\ominus}$[b] / kJ mol^{-1}
[Ni(DAPO)$_2$]	III/II	−1.52	−1.45	70	−1.48	–	–
	II/I	−1.25	−0.97	280	−1.11	9.31	54
[Ni(DAPO)$_2$(Py)$_2$]	III/II	−1.48	−1.45	30	−1.47	–	–
	II/I	−1.19	−0.89	300	−1.04	9.97	58
[Ni(DAPO)$_2$(Im)$_2$]	III/II	−1.54	−1.41	130	−1.47	4.32	25
	II/I	−1.20	−0.94	260	−1.07	8.64	50
[Ni(DBPO)$_2$]	III/II	−1.64	−1.53	110	−1.58	3.66	22
	II/I	−1.37	−1.12	250	−1.25	8.31	48
[Ni(DBPO)$_2$(Py)$_2$]	III/II	−1.72	−1.58	140	−1.65	4.65	27
	II/I	−1.33	−1.09	240	−1.21	7.98	46
[Ni(DBPO)$_2$(Im)$_2$]	III/II	−1.74	−1.58	160	−1.66	4.68	28
	II/I	−1.34	−1.10	240	−1.22	7.98	46

[a]log $K_c = 0.434 nF/RT\Delta E_p$; [b]$\Delta G^{\ominus} = -2.303 RT$log K_c

Binding of the nickel(II) complexes with CT DNA

The interaction of the nickel(II) complexes with CT DNA was monitored by UV–Vis spectroscopy in the 265–280 nm and 300–315 nm regions. In the presence of increasing amounts of CT DNA, the spectra of all the complexes showed a decrease in the intensity of the bands in the case of parent complexes and increase in the intensity for the mixed ligand complexes (Fig. 4). However, the bands are shifted towards lower wavelengths (blue shift). The change in absorbance va-

lues with increasing amount of CT DNA were used to evaluate the intrinsic binding constant K_b for the complexes.
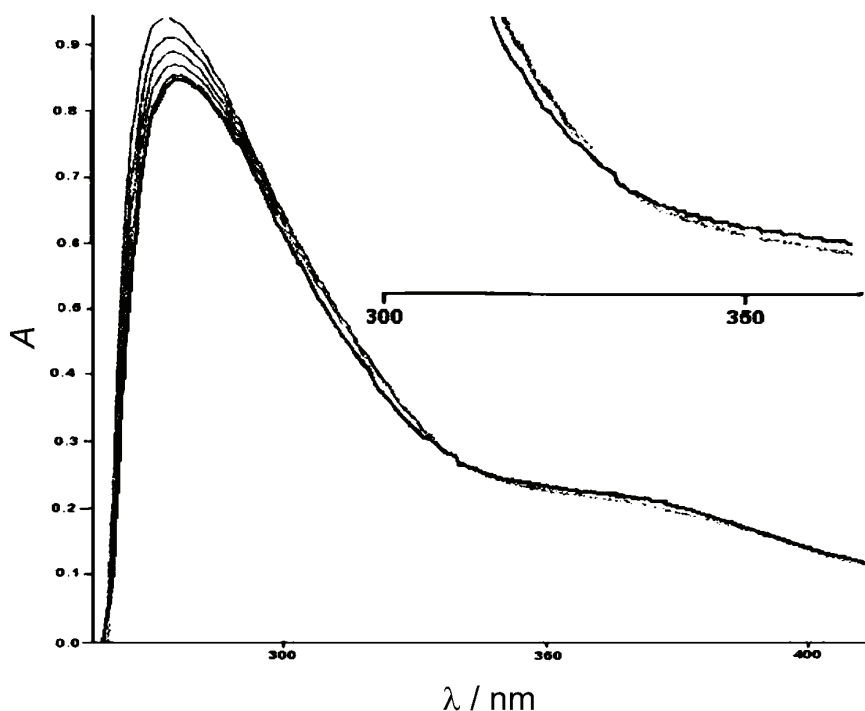
Fig. 4. UV–Vis spectra of [Ni(DAPO)$_2$Im$_2$] (37±0.5 μM) in the absence (dotted line) and presence of increasing amounts of CT DNA. Portion of the graph showing an isosbestic point at 337 nm is given in the inset.

In the presence of increasing amounts of CT DNA, the UV–Vis absorption of Ni(DAPO)$_2$ and Ni(DBPO)$_2$ showed hypsochromic shifts ($\Delta\lambda_{max}$: 0.5 to 5.0 nm) and hypochromism [hypochromicity: –7.4 % for Ni(DAPO)$_2$ and –12.4 % for Ni(DBPO)$_2$]. Ni(DBPO)$_2$ exhibited the highest percentage hypochromic shift and binding constant of all the parent complexes. In contrast, the mixed ligand complexes showed hyperchromic shifts with increasing amounts of calf thymus DNA. The pyridine adducts of Ni(DAPO)$_2$ and Ni(DBPO)$_2$ showed hyperchromicity of 6.5 and 11.8, respectively, while for the imidazole adducts, these values were 5.8 and 5.6. The change in hypochromic shifts to hyperchromic shifts when going from the parent complexes to the mixed ligand complexes suggest a change in the mode of DNA binding. This may be attributed to the change in the structure from square planar (parent complexes) to octahedral (mixed ligand complexes). The order of the binding of the complexes with DNA is as follows:

$Ni(DBPO)_2Im_2$ (2.6×10^6) > $Ni(DAPO)_2Im_2$ (2.4×10^6) > $Ni(DBPO)_2Py_2$ (1.8×10^6) > $Ni(DAPO)_2Py_2$ (1.6×10^6) > $Ni(DBPO)_2$ (3.4×10^5) > $Ni(DAPO)_2$ (2.9×10^5).

The strong DNA binding nature of the octahedral mixed ligand nickel complexes may be due to the additional π–π interactions through the aromatic ring of the nitrogen bases. The binding constants of the square planar parent complexes are also sufficiently high, possibly due to an intercalation mode of binding.[21]

Thermal denaturation

The binding of small molecules into the DNA double helix is known to increase the melting temperature of the helix, which is the temperature at which the double helix is denatured into single stranded DNA.[22] The value of extinction coefficient of the DNA bases at 260 nm in the double helical form is lower than in the single stranded form. Hence, melting of the helix leads to an increase in the absorption at this wavelength. Thus, the transition temperature from helix to coil can be determined by monitoring the absorbance of the DNA bases at 260 nm.

The thermal melting studies were performed at [DNA]/[complex] = 25. The T_m values were determined by monitoring the absorbance of DNA at 260 nm as a function of temperature. The melting point of free CT-DNA was 60 ± 1 °C under the employed experimental conditions. Under the same set of conditions, addition of $Ni(DAPO)_2$, $Ni(DAPO)_2Py_2$ and $Ni(DAPO)_2Im_2$ increased T_m (± 1 °C) by 3, 5 and 6 °C, respectively, while $Ni(DBPO)_2$, $Ni(DBPO)_2Py_2$ and $Ni(DBPO)_2Im_2$ increased T_m (± 1 °C) by 4, 5 and 7 °C, respectively. These increases of the T_m values of CT-DNA in the presence of the complexes indicated that these compounds stabilized the double helix of DNA.[23]

Cleavage activity of pBR322 plasmid DNA

Gel electrophoresis experiments using pBR322 circular plasmid DNA were performed with the ligands and complexes in the presence and absence of H_2O_2 as an oxidant. At micromolar concentrations for a 2 h incubation period, the ligands exhibited no significant cleavage activity in the absence and in presence of the oxidant (H_2O_2). The nuclease activity was greatly enhanced by the incorporation of the nickel ion into the respective ligands.

The cleavage activities of the nickel complexes on pBR322 are shown in Fig. 5. In Fig. 5, lanes 1 and 2 are controls while the other lanes contain nickel complexes in presence (odd lanes) and absence (even lanes) of oxidant (H_2O_2). The nickel complexes of DAPO and DBPO were run in lanes 3 and 4, and 9 and 10, respectively. It is clear that the parent complexes did not show a significant cleavage activity even in presence of the oxidant. Lanes 5 and 6, and 11 and 12 contained the pyridine adducts of $Ni(DAPO)_2$ and $Ni(DBPO)_2$, respectively, in the presence and absence of oxidant. Both adducts converted form I (super coiled) into form II (nicked). The cleavage activity of the nickel adducts was signifi-

cantly increased in the presence of the oxidant (H_2O_2). Similarly, the imidazole adducts also showed higher cleavage activity in the presence of oxidant. In lanes 13 and 14, containing $Ni(DBPO)_2Im_2$, significant cleavage activity was observed, while both form I and II were converted into smears in the presence of oxidant.
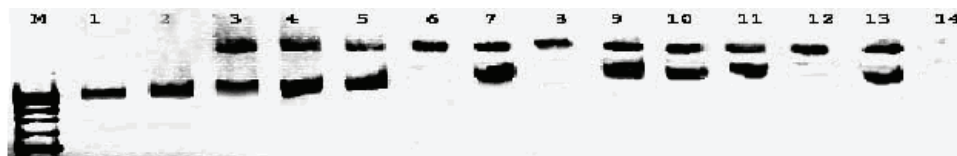

Fig. 5. Agarose gel (1 %) showing the results of electrophoresis of 3.3 μl of (150 μg ml^{-1}) pBR322 plasmid DNA, 2 μl of 0.1 M Tris-HCl (pH 8.0) buffer: 1 μl (1 mM) complex in DMF; 10 μl of sterilized water and 2 μl of 9.0 mM H_2O_2 were added, respectively, incubation at 37 °C (60 min); lane M : Marker, lane 1: DNA (control); lane 2: DNA + H_2O_2 (control); lane 3: $[Ni(DAPO)_2]$; lane 4: $[Ni(DAPO)_2]$ + H_2O_2; lane 5: $[Ni(DAPO)_2Py_2]$; lane 6: $[Ni(DAPO)_2Py_2]$ + H_2O_2; lane 7: $[Ni(DAPO)_2Im_2]$; lane 8: $[Ni(DAPO)_2Im_2]$ + H_2O_2; lane 9: $[Ni(DBPO)_2]$; lane 10: $[Ni(DBPO)_2]$ + H_2O_2; lane 11: $[Ni(DBPO)_2Py_2]$; lane 12: $[Ni(DBPO)_2Py_2]$ + H_2O_2; lane 13: $[Ni(DBPO)_2Im_2]$; lane 14: $[Ni(DBPO)_2Im_2]$ + H_2O_2.

From Fig. 5, it is evident that the $Ni(DBPO)_2Im_2$ complex showed significant cleavage activity in the presence of the oxidant. This may be attributed to the formation of hydroxyl free radicals, which oxidized Ni(II) to Ni(III), presumably through Fenton-type reactions, resulting in the formation of reactive oxygen species, which could then cause oxidative damage to DNA.[24]

CONCLUSIONS

Mixed ligand complexes having the formulae $Ni(L)_2L^1_2$ (where L = DAPO or DBPO and L^1 = pyridine (Py) or imidazole (Im)) were synthesized and characterized by magnetic susceptibility and elemental analysis, as well as by UV–Vis, IR and ^1H-NMR spectroscopy. The electronic spectral data suggested a square planar structure for the parent complexes and an octahedral structure for the adducts. The electrochemical data of these complexes, realised by cyclic voltammetry, showed the redox couple Ni^{III}/Ni^{II}. Absorption titrations were performed on CT DNA to study the binding nature. The values of the binding constant were sufficiently high (10^6) and comparable to other mixed ligands.[25] Both the binding constant and thermal denaturation studies suggested that these complexes bind to CT DNA by an intercalative mechanism.[26] The DNA cleavage activity of the nickel complexes determined on double-stranded pBR322 circular plasmid DNA showed that these complexes cleave DNA by an oxidation mechanism, mainly through a Fenton reaction.

ИЗВОД

СИНТЕЗА, КАРАКТЕРИЗАЦИЈА И АКТИВНОСТ НИКАЛ(II) АДУКАТА СА АРОМАТИЧНИМ ХЕТЕРОЦИКЛИЧНИМ БАЗАМА ПРЕМА РАСКИДАЊУ DNA

M. S.SURENDRA BABU[1], PITCHIKA. G. KRISHNA[2], K. HUSSAIN REDDY[1] и G. H. PHILIP[2]

[1]*Department of Chemistry, Sri Krishnadevaraya University Anantapur-515003*
[2]*Department of Zoology, Sri Krishnadevaraya University Anantapur-515003, India*

Синтетисани су мешовито лигандни комплекси никла(II) са 2,4-дихидроксиацетофенон-оксимом (DAPO), 2,4-дихидроксибензофенон-оксимом (DBPO) као примарним лигандима и пиридином (Py), имидазолом (Im) као секундарним лигандима и окарактерисани моларном проводљивошћу, магнетним моментима, електронским, IR и ^{1}H-NMR спектрима. Електрохемијска испитивања извршена су цикличном волтаметријом. Активни сигнали су приписани редокс паровима Ni$^{III/II}$ и Ni$^{II/I}$. Интеракције везивања између металних комплекса и CT DNA изучаване су апсорпцијом и термичком денатурацијом. Активност комплекса према раскидању извршена је на двоструко спиралном pBR322 циркуларном плазмиду DNA коришћењем гел електрофорезе. Сви комплекси показали су повећану нуклеазну активност у присуству оксиданса (H$_2$O$_2$). Нуклеазне активности мешовито лигандних комплекса упоређене су са полазним бакар(II) комплексима.

(Примљено 21. јануара, ревидирано 7. октобра 2009)

REFERENCES

1. A. Yan, M. L. Tong, L. N. Ji, Z. W. Mao, *Dalton Trans.* (2006) 2066
2. Y. Z. Cheng, Z. Jing, B. W. Yan, X. Y. Cai, Y. Pin, *J. Inorg. Biochem.* **101** (2007) 10
3. J. K. B. Leigh, M. Z. Jeffrey, *Curr. Opin. Chem. Biol.* **9** (2005) 135
4. D. Shanta, A. N. R. Pattubala, A. R. Chakravarty, *Dalton Trans.* (2004) 697
5. A. Raja, V. Rajendiran, M. P. Uma, R. Balamurugan, C. A. Kilner, M. A. Halcrow, M. Palanaiandavar, *J. Inorg. Biochem.* **99** (2005) 1717
6. L. Lei, N. N. Murthy, T. Joshua, L. Zakharov, P. A. Y. Glenn, L. R. Arnold, D. K. Kenneth, S. E. Rokita, *Inorg. Chem.* **45** (2006) 7144
7. M. A. Halcrow, G. Christou, *Chem. Rev.* **94** (1994) 2421
8. P. Stavropoulos, M. C. Muetterties, M. Carrie, R. H. Holm, *J. Am. Chem. Soc.* **113** (1991) 8485
9. G. C. Tucci, R. H. Holm, *J. Am. Chem. Soc.* **117** (1995) 6489
10. I. Tommasi, M. Aresta, P. Giannoccaro, E. Quaranta, C. Fragale, *Inorg. Chim. Acta* **112** (1998) 38
11. U. Ermler, W. Grabarse, S. Shima, M. Goubeaud, R. K. Thauer, *Curr. Opin. Struct. Biol.* **8** (1998) 749
12. F. Dole, M. Medina, C. More, R. Cammack, P. Bertrand, B. Guigliarelli, *Biochemistry* **35** (1996) 16399
13. R. K. Andrews, R. L. Blakeley, B. Zerner, *The Bioinorganic Chemistry of Nickel*, J. R. Lancaster, Ed., VCH Publishers, New York, 1988, p. 141
14. F. Haq, M. C. R. Peter, *J. Inorg. Biochem.* **78** (2000) 217
15. N. Saglam, A. Colak, K. Serbest, S. Dulger, S. Guner, S. Karabocek, A. O. Belduz, *Biometals* **15** (2002) 357
16. M. S. Surendra Babu, K. Hussain Reddy, P. G. Krishna, *Polyhedron* **26** (2007) 572
17. M. E. Reichmann, S. A. Rice, C. A. Thomas, P. Doty, *J. Am. Chem. Soc.* **76** (1954) 3047

18. A. Wolfe, G. H. Shimer, T. Meehan, *Biochemistry* **26** (1987) 6392
19. E. Konig, *The nephelauxetic effect structure and bonding*, Springer, New York, 1971, p. 175
20. C. C. Cheng, S. E. Rokita, C. J. Burrows, *Angew. Chem.* **32** (1993) 273
21. L. A. Lipscomb, F. X. Zhou, S. R. Presnell, R. J. Woo, M. E. Peek, R. R. Plaskon, L. D. Williams, *Biochemistry* **35** (1983) 2818
22. J. Santa Lucia Jr., *Proc. Natl. Acad. Sci. USA* **95** (1998) 1460
23. S. Satyanaryana, J. C. Dabrowiak, J. B. Chaires, *Biochemistry* **32** (1993) 2573
24. R. B. Nair, E. S. Teng, S. L. Kirkland, C. J. Murphy, *Inorg. Chem.* **37** (1998) 139
25. J. Liu, H. Zhang, C. Chen, H. Deng, T. Lu, L. Ji, *Dalton Trans.* (2003) 114
26. Y. M. Song, Q. Wu, P. J. Yang, N. N. Luan, L. F. Wang, Y. M. Liu, *J. Inorg. Biochem.* **100** (2006) 1685.

A study of the formation constants of ternary and quaternary complexes of some bivalent transition metals

SANGITA SHARMA*, DIPIKA DALWADI and MADHURJYA NEOG

Department of Chemistry, Hemchandracharya North Gujarat University, Patan-384 265, Gujarat, India

Abstract: The formation of hetero-ligand 1:1:1, M(II)-Opda-Sal/Gly ternary and 1:1:1:1, M(II)-Opda-Sal-Gly quaternary complexes, where M(II) = Ni, Cu, Zn and Cd; Opda = *o*-phenylenediamine, Sal = salicylic acid, Gly = glycine, was studied pH-metrically in aqueous medium. The formation constants for the resulting ternary and quaternary complexes were evaluated at a constant ionic strength, $\mu = 0.20$ mol dm^{-3} and temperature, 30±0.1 °C. The order of the formation constants in terms of the metal ion for both type of complexes was found to be Cu(II) > Ni(II) > Zn(II) > Cd(II). This order was explained based on the increasing number of fused rings, the coordination number of the metal ions, the Irving – William order and the stability of various species. The expected species formed in solution were pruned with the Fortran IV program SPEPLOT and the stability of the ternary and quaternary complexes is explained.

Keywords: formation constants; transition metals; salicylic acid; quaternary complexes.

INTRODUCTION

Solution studies on binary and ternary complexes using divalent and trivalent metal ions has been extensively studied.[1–4] Although the formation of ternary complexes has been very well studied,[5–7] the formation of quaternary species with transition and inner transition metal ions has been limited to a few papers.[8–12] Only a few references have reported on quaternary complexes in which the metal ions not only form stable complexes, but also expand their coordination number. The increasing importance of ternary complexes, especially those involving ligands containing functional groups identical to those present in enzymes, *viz*. –COOH, –NH$_2$, *etc*., is obvious from the application of such complexes in many analytical and biological reactions.[13–14] Diamines, hydroxy acids and amino acids as complexing agent have been widely studied in binary systems[15–17]

75

but hitherto the literature does not corroborate where these ligands are used in combination for either ternary and quaternary systems. In addition, there is no comparative study which was performed on the formation constants of binary (monoligated), ternary (biligated) and quaternary (triligated) complexes of transition metals.

Herein, a comparative solution state electrometric study is reported on ternary (MLL′, ML′L″, MLL″) and triligated (quaternary) (MLL′L″) complexes, where M = Cu(II), Ni(II), Zn(II) and Cd(II) metal ions, and L = o-phenylenediamine, L′ = salicylic acid and L″ = glycine as ligands using the pH-metric technique in aqueous medium at a constant ionic strength $\mu = 0.20$ mol dm^{-3} and temperature 30±0.1 °C. The aim was to compare the stabilities of the various species in the solution state. The active forms of the species found in a computer-augmented modeling study were ML, ML$_2$, ML′, ML″, ML$_2$, ML″$_2$, ML$_2$H, MLL′, MLL″, ML′L″ and MLL′L″.

EXPERIMENTAL

Employed chemicals

All the chemicals used were of analytical reagent grade. o-Phenylenediamine, salicylic acid, glycine and the metal chlorides (Aldrich-USA) were used without further purification. The metal chloride solutions were acidified with accurately known amounts of HClO$_4$ to prevent hydrolysis. The exact concentrations of the solutions of the lanthanide nitrates were determined by complexometric titration with the disodium salt of EDTA.[18] All solutions were prepared in doubly distilled CO$_2$-free water. The carbonate-free NaOH solution was standardized by a reported method.[19] Perchloric acid was standardized with a standard NaOH solution and the constant ionic strength was maintained with the inert electrolyte sodium perchlorate (NaClO$_4$) (Reidel).

Apparatus

Potentiometric titrations were performed using a Systronics μ pH meter 361, having a combined glass electrode and a temperature probe with a readability ±0.1 °C. The temperature was maintained using a High Precision Water Bath Cat. No. MSW-274 with a readability ±0.1 °C. The titrations were realized in a specially designed glass cell with a magnetic stirrer under a nitrogen atmosphere to avoid any side reactions. The experimental procedure involved the potentiometric titration of the following sets of solutions:

1. acid titration: perchloric acid (0.20 M, 5.0 ml);
2. first ligand titration (L): perchloric acid (0.20 M, 5.0 ml) + Opda (0.020 M, 5.0 ml);
3. second ligand titration (L′): perchloric acid (0.20 M, 5.0 ml) + Sal (0.020 M, 5.0 ml);
4. third ligand titration (L″): perchloric acid (0.20 M, 5.0 ml) + Gly (0.020 M, 5.0 ml);
5. metal + first ligand titration (ML): perchloric acid (0.20 M, 5.0 ml) + metal (0.020 M, 5.0 ml) + Opda (0.020 M, 5.0 ml);
6. metal + second ligand titration (ML′): perchloric acid (0.20 M, 5.0 ml) + metal (0.020 M, 5.0 ml) + Sal (0.020 M, 5.0 ml);
7. metal + third ligand titration (ML″): perchloric acid (0.20 M, 5.0 ml) + metal (0.020 M, 5.0 ml) + Gly (0.020 M, 5.0 ml);
8. metal + first + second ligand titration (MLL′): perchloric acid (0.20 M, 5.0 ml) + metal (0.020 M, 5.0 ml) + Opda (0.020 M, 5.0 ml) + Sal (0.020 M, 5.0 ml);

9. metal + first + third ligand titration (MLL″): perchloric acid (0.20 M, 5.0 ml) + metal (0.020 M, 5.0 ml) + Opda (0.020 M, 5.0 ml) + Gly (0.020 M, 5.0 ml);

10. metal + second + third ligand titration (ML′L″): perchloric acid (0.20 M, 5.0 ml) + metal (0.020 M, 5.0 ml) + Sal (0.020 M, 5.0 ml) + Gly (0.020 M, 5.0 ml);

11. metal + first + second + third ligand titration (MLL′L″): perchloric acid (0.20 M, 5.0 ml) + metal (0.020 M, 5.0 ml) + Opda (0.020 M, 5.0 ml) + Sal (0.020 M, 5.0 ml) + Gly (0.020 M, 5.0 ml).

The total volume used in each cell was 50 ml and the ionic strength was maintained at 0.20 M (NaClO$_4$) at the temperature 30±0.1 °C in all sets. The titrations performed with carbonate-free standardized 0.20 M NaOH solution. The carbonate content was checked with a Gran Plot[20] and the required correction was made in the input file before using the computer programs.

Calculations

Ligand formation constants. The dissociation constants of o-phenylenediamine (pK_1 = = 4.61, pK_2 = 2.81), salicylic acid (pK_1' = 9.32, pK_2' = 2.31) and glycine (pK_1'' = 12.03, pK_2'' = = 2.93) were calculated by the method of Irving and Rosotti.[21] The formation constants were calculated using the BEST computer program; the results were comparable with literature values.[22]

Binary formation constants. The binary formation constant were calculated using the BEST program and results were comparable with literature values.[23]

Ternary formation constants. The ternary formation constants were calculated using a modified form of the Irving and Rossotti titration technique and equations reported earlier.[24]

Quaternary formation constants. The formation constants (log $K_{MLL'L''}$) of the quaternary complexes formed by the simultaneous coordination of all the ligands to the metal ion were calculated by the method of Ramamoorthy and Santappa[25] from the following expression:

$$K_{MLL'L''} = \frac{T_M - (1/3)AX}{(1/3)^4 A^4 X}$$

$$A = \frac{5T_M - T_{OH^-} - [H^+]}{3a + 6b}$$

where $a = [H^+]/(K_2 + K_2' + K_2'')$; $b = [H^+]/(K_1 K_2 + K_1' K_2' + K_1'' K_2'')$; $X = 1 + 3a + 3b$, and K_1, K_1' and K_1'' are the first dissociation constants and K_2, K_2' and K_2'' are the second dissociation constants of the selected ligands L, L′ and L″, respectively.

RESULTS AND DISCUSSION

The diamine has two protonable –NH$_2$ groups, salicylic acid two dissociable groups –OH and –COOH, while glycine has one protonable and one dissociable group. Using the Irving and Rossotti method, the pK_a values for diamine, glycine and salicylic acid were calculated and compared with literature values.[21,22] The nature of the curves was similar for all four metal ions selected in the present study. For the sake of brevity and comparison, only the curves for the binary, ternary and triligated (quaternary) complexes of Cu(II) with the Opda, Sal and Gly systems are discussed in detail and the titration results are presented in graphical form in Fig. 1.
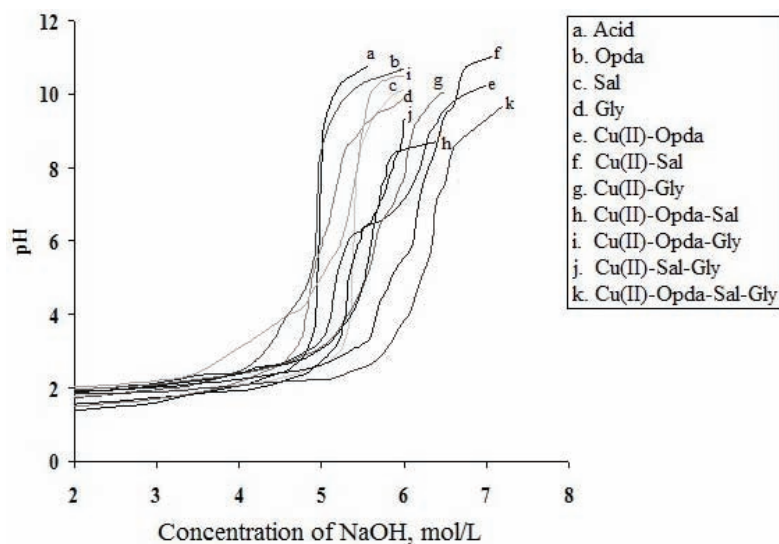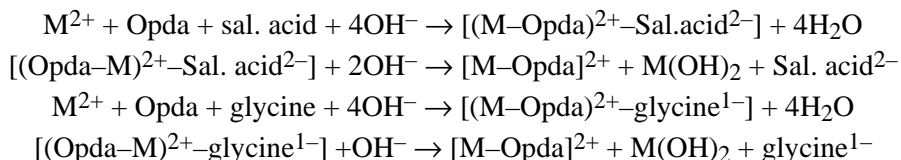
Fig. 1. Representative titration curves for triligated Cu(II)-Opda-Sal-Gly complexes
at 30±0.1 °C, $\mu = 0.20$ M (NaClO$_4$).

A well-defined inflection on curve b at pH ≈2.6 is due to protonation of ligand L, similarly types of inflection points at pH ≈3.4 and 5.7 are seen for curves c and d, which are the first dissociation constants for ligand L′ and L″, respecttively.

Binary systems. Curve e shows an inflection at pH ≈3, which may be attributed to the 1:1 Cu(II)-Opda binary complex. Another inflection at pH ≈7 can be attributed to 1:2 Cu(II)-Opda binary complexes. Similar types of inflection curves were obtained for Cu(II)-Gly at pH ≈2.7 and ≈6.5, and for Cu(II)-Sal at pH ≈2.5 and ≈6.8, respectively.

Ternary systems. Curve h, representing the titration of 1:1:1 Cu(II)-Opda-Sal species, gives an inflection at pH ≈3.0, showing the formation of the 1:1:1 ternary complex in the lower pH range. Curve i depicts the titration of Cu(II)-Opda-Gly system. The inflection at pH ≈3.5 indicates complexation of the metal ion with both ligands and the formation of ternary complexes. A precipitate appeared at pH ≈7.0. The reactions for the formation of 1:1:1 ternary complexes are presented below:

$$M^{2+} + Opda + sal.\ acid + 4OH^- \rightarrow [(M–Opda)^{2+}–Sal.acid^{2-}] + 4H_2O$$
$$[(Opda–M)^{2+}–Sal.\ acid^{2-}] + 2OH^- \rightarrow [M–Opda]^{2+} + M(OH)_2 + Sal.\ acid^{2-}$$
$$M^{2+} + Opda + glycine + 4OH^- \rightarrow [(M–Opda)^{2+}–glycine^{1-}] + 4H_2O$$
$$[(Opda–M)^{2+}–glycine^{1-}] + OH^- \rightarrow [M–Opda]^{2+} + M(OH)_2 + glycine^{1-}$$

A well-defined separation of curve j from curve f indicates the formation of 1:1:1 Cu(II)–Gly–Sal. Another inflection at pH 5.5 on curve (j) indicates disproportionation of the initially formed ternary complex at higher pH values.

Quaternary systems. Curve k represents the titration of the 1:1:1:1 Cu(II)--Opda-Sal-Gly quaternary system. An initial lowering of the pH value as compared to the binary and ternary systems and the separation at pH ≈2.2 represents the simultaneous addition of three ligands to the metal ion whereby 1:1:1:1 mixed ligand complexes are formed. The calculated values of the formation constants for the ternary and quaternary complexes and the corresponding free energies of formation are presented in Table I. The relative stabilities of the resulting quaternary species log $K_{LL'L''}$ in terms of the metal ions have the following order: Cu(II) > Ni(II) > Zn(II) > Cd(II), which is the same as in earlier observations.[26] This order can be explained based on the decreasing size and increasing ionic potential (charge/ratio) of the transition metals. The higher stabilities of the quaternary complexes compared to the ternary ones can be attributed to the increased number of fused rings and extra-stabilization caused by ligand–ligand interactions in the quaternary complexes.

TABLE I. Formation constants and free energies of formation of ternary (1:1:1) and triligated (1:1:1:1) complexes of M(II) ions at 30±0.1 °C and ionic strength, $\mu = 0.20$ M (NaClO$_4$)

Metal ions	1:1:1, M(II)-Opda-Sal/Gly				1:1:1:1 M(II)-Opda-Sal-Gly	
	Sal		Gly			
	log $K_{MLL'}$	ΔG / kcal mol^{-1}	ΔG / kcal mol^{-1}	log $K_{MLL'}$	log $K_{MLL'}$	ΔG / kcal mol^{-1}
Cu(II)	9.27	−1.34	−1.15	6.75	10.07	−1.39
Ni(II)	8.34	−1.26	−1.05	5.68	8.94	−1.32
Zn(II)	8.20	−1.27	−1.06	5.81	8.93	−1.31
Cd(II)	7.224	−1.19	−1.04	5.66	8.92	−1.32

The constancy of the calculated values of the stability constants observed in the region of the formation of the quaternary complex supports the formation of mixed ligand complexes. The almost negligible values of the percentage dissociation of the second proton of salicylic acid (0.99 %) and glycine (0.20 %) in the lower pH range (2.5–3.2), evaluated by the method of Serjent,[27] indicate that salicylic acid and glycine behave as monobasic acids and their second proton is liberated at pH > 5.

Species distribution diagrams

The various expected species of stoichiometric triligated systems are: LH, LH$_2$, L'H, L'H$_2$, L''H, L''H$_2$, MLH, ML, ML$_2$, ML'H, ML', ML'$_2$, ML''H, ML'', ML''$_2$, MLL', MLL'', ML'L'', MLL'L'' and these were assumed in different chemical models. The species distribution diagrams for all the systems under investigation were obtained for different metal to ligand ratios in solutions using the va-

lues of the calculated formation constants in the BEST fit chemical model, which supports the formation and stability of 1:1:1:1 MLL′L″ quaternary complexes.

In order to demonstrate these quantitative trends, the species distribution diagram obtained in a 1:1:1:1 solution of M(II), diamine (L), salicylic acid (L′) and glycine (L″) is shown in Fig. 2. The possibility of hydroxo and polynuclear species was also tested and detected by use of the SPEPLOT computer program.[28] The concentration of MLL′L″ species was 70 % for M(II)-Opda-Sal-Gly triligated systems. The negative values of the free energies of formation also supported the spontaneity of the reactions in the formation of the complexes.
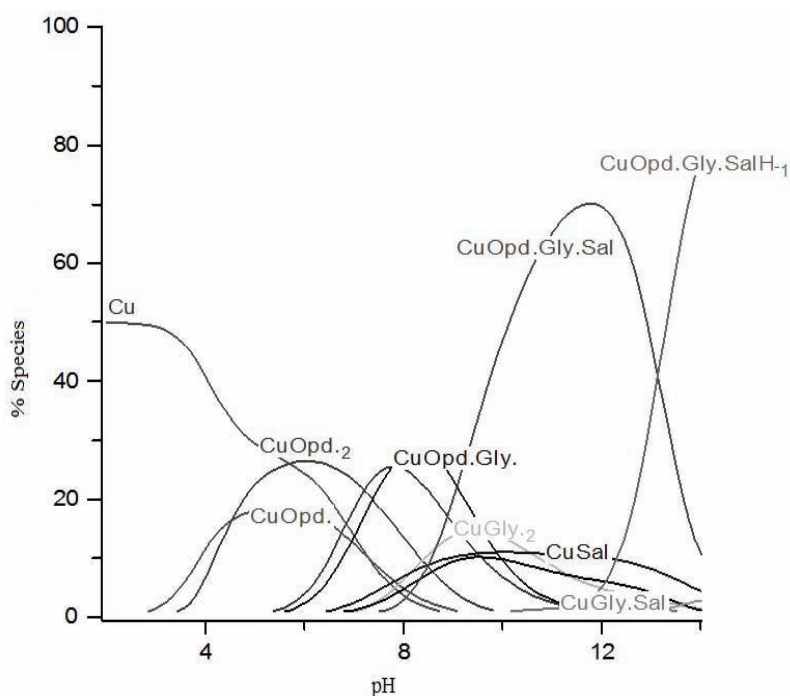
Fig. 2. Species distribution diagram for triligated Cu(II) Opda-Sal-Gly complexes at 30±0.1 °C, μ = 0.20 M (NaClO$_4$).

CONCLUSIONS

The stability of all the analogous complexes was in the order of Cu(II) > > Ni(II) > Zn(II) > Cd(II) as anticipated from the increasing charge density along the transition metal series. In term of complex species, the order was quaternary > > ternary, which can be explained based on the increased number of fused rings and the extra stabilisation caused by ligand-ligand interactions.

ИЗВОД

ПРОУЧАВАЊЕ КОНСТАНТИ НАСТАЈАЊА ТЕРНЕРНИХ И КВАРТЕРНЕРНИХ КОМПЛЕКСА НЕКИХ ДВОВАЛЕНТНИХ ПРЕЛАЗНИХ МЕТАЛА

SANGITA SHARMA, DIPIKA DALWADI и MADHURJYA NEOG

Department of Chemistry, Hemchandracharya North Gujarat University, Patan-384 265, Gujarat, India

Пехаматријски је изучавано настајање хетеролиганд 1:1:1 M(II)-Opda-Sal-Gly тернерних, односно 1:1:1:1 M(II)-Opda-Sal-Gly кватернерних комплекса у воденој средини, где је M(II) = Ni, Cu, Zn и Cd, а Opda = *o*-фенилендиамин, Sal = салицилна киселина, Gly = глицин. Константе настајања за добијене тернерне и кватернерне комплексе процењене су на константној јонској јачини $\mu = 0,20$ mol dm^{-3} и температури од 30±0,1 °C. Редослед константи настајања у односу на металне јоне за оба комплекса је био Cu(II) > Ni(II) > Zn(II) > Cd(II). Он је објашњен на основу Irving–William-овог редоследа заснованог на повећању броја кондензованих прстенова, координационог броја металних јона, редоследа и стабилности разних врста. Очекиване врсте настале у раствору су обрађене програмом SPEPLOT Fortran-a IV и објашњена је стабилност тернерних и кватернерних комплекса.

(Примљено 27. јануара, ревидирано 14. септембар 2009)

REFERENCES

1. S. Ramamoorthy, P. G. Manning, *J. Inorg. Nucl. Chem.* **34** (1972) 1977
2. P. D. Sherry, C. Yoshida, E. R. Birmbaun, D. W. Darnell, *J. Am. Chem. Soc.* **95** (1973) 3011
3. D. Agrawal, K. D. Gupta, K. K. Saxena, *Trans. SAEST* **38** (2003) 111
4. P. Deschamps, N. Zerrouk, I. Nicolis, T. Martens, E. Curis, M. Charlot, F. Girerd, J. J. Prange, T. Benazeth, S. Choumeil, J. C, A. Tomas, *Inorg. Chim. Acta* **353** (2003) 22
5. D. W. Darnell, E. R. Birmbaun, *J. Biol. Chem.* **245** (1970) 6484
6. K. Prasad, A. Koteswara Rao, M. S. Mohan, *J. Coord. Chem.* **16** (1987) 251
7. S. Belaid, S. Djebbar, O. Benali-Baitich, S. Ghalemm, M. A. Khan, G. Bouet, *Asian J. Chem.* **17** (2005) 811
8. S. S. Yadav, R. C. Sharma, *Trans. SAEST* **39** (2004) 39
9. M. P. Singh, S. C. Goyal, M. K. Rawat, *J. Ind. Council Chem.* **23** (2006) 84
10. S. Sinha, D. Bartaria, V. Krishna, *J. Indian Chem.* **83** (2006) 714
11. P. C. Dwivedi, S. P. Tripathi, R. C. Sharma, *J. Ind. Chem. Soc*. **61** (1984) 23
12. R. Kumar, G. K. Chaturvedi, R. C. Sharma, *J. Inog. Nucl. Chem.* **43** (1981) 2503
13. D. Banerjea, *Coordination Chemistry,* Tata McGraw Hill, New Delhi, India, 1994, p. 322
14. C. H. Evans, *Biochemistry of the Lanthanides,* Vol. 8, Plenum Press, London, UK, 1990, p. 19
15. P. I. Ting, G. H. Nahcollas, *Inorg. Chem.* **11** (1972) 2414
16. R. Dewitt, J. I. Watters, *J. Am. Chem. Soc.* **76** (1954) 3810
17. V. Amit, P. K. S. Chauhan, R. K. Paliwal, *Asian J. Chem.* **17** (2005) 855
18. H. A. Flaschka, *EDTA Titrations*, Pergamon, Oxford, UK, 1964
19. A. I. Vogel, *A Text Book of Quantitative Inorganic Analysis,* Longmans, London, 1978, p. 296
20. P. Grans, B. O. Sullivan, *Talanta* **51** (2000) 33
21. H. M. Irving, H. S. Rossotti, *J. Chem. Soc.* (1954) 2904
22. J. A. Dean*, Lange's handbook of chemistry.* 13th ed., McGraw-Hill Company, New York. USA, 1987

Available online at www.shd.org.rs/JSCS/

23. J. Inczedy, *Analytical Applications of Complex Equilibria,* John Wiley and Sons, New York, USA, 1976, p. 343
24. P. K. Bhattacharya, I. P. Mavani, C. R. Jajurkar, *Indian J. Chem.* **10** (1972) 742
25. S. Ramamoorthy, M. Santappa, *J. Indian Chem. Soc.* **9** (1971) 381
26. S. Chaberek, A. E. Martell, *J. Am. Chem. Soc.* **74** (1952) 6021
27. A. Albert, E. P. Serjeant, *J. Chem. Soc*. **89** (1967) 2859
28. L. Alderighi, P. Gans, A. Ienco, D. Peters, A. Sabatini, A. Vacca, *Coord. Chem. Rev.* **184** (1998–2000) 311.

Effect of a ring on the cyclic conjugation in another ring: applications to acenaphthylene-type polycyclic conjugated molecules

BORIS FURTULA, IVAN GUTMAN[*][#], SVETLANA JEREMIĆ
and SLAVKO RADENKOVIĆ

Faculty of Science, University of Kragujevac, P. O. Box 60, 34000 Kragujevac, Serbia

Abstract: In a recent work, a method was developed for assessing the influence $ief(G, Z_0 | Z_1)$ of a ring Z_1 on the energy effect of another ring Z_0 in a polycyclic conjugated molecule G. Herein, a report is given of detailed numerical investigations of $ief(G, Z_0 | Z_1)$ aimed at the elucidation of the influence of various six-membered rings on the intensity of cyclic conjugation in the five-membered ring of acenaphthylene-type molecules. The earlier discovered regularities for cyclic conjugation in acenaphthylene-type molecules (in particular, the PCP rule and the linear rule) could thus not only be rationalized, but also a number of hitherto concealed regularities could be envisaged.

Keywords: cyclic conjugation; energy effect of cyclic conjugation; acenaphthylene-type hydrocarbons; PCP-rule.

INTRODUCTION

In the theory of polycyclic conjugated molecules,[1–3] it is well known that the size and mutual arrangement of the rings have a profound influence on the behavior of the π-electrons and, therefore, on practically all physical and chemical properties of the respective compounds. A method for assessing the effect of individual rings on the total π-electron energy was already elaborated in the 1970s and since then found numerous chemical applications; for details see the review[4] and the recent papers.[5–12] The energy effect (*ef*) of a ring can be viewed as a measure of the intensity of cyclic conjugation in this ring.

Most of the investigations of the π-electron properties of polycyclic conjugated molecules were focused on benzenoid hydrocarbons.[3,4] Acenaphthylenes and fluoranthenes are structurally very similar to benzenoid systems, differing from them by the presence of a single five-membered ring. Yet, their systematic

---

* Corresponding author. E-mail: gutman@kg.ac.rs
# Serbian Chemical Society member.

83

study commenced only quite recently[13] and was eventually extended to species the odd-membered ring of which has a size greater than five.[12] A number of general properties of these benzenoid-like systems could be established,[8–12,14,15] of which the most interesting are those related to cyclic conjugation in the five--membered ring.[8–11]

In this paper, acenaphthylene-type conjugated molecules are considered. Their structure is evident from Fig. 1 and the subsequent figures; a more formal definition can be found elsewhere.[13]
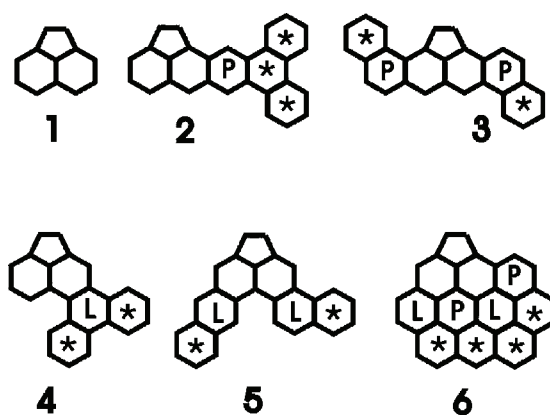
Fig. 1. Acenaphthylene (**1**) and some of its congeners (**2**–**6**). The six-membered rings attached to the parent hydrocarbon (**1**) that are in a PCP and a linear constellation are marked by P and L, respectively; the other rings are marked by asterisks. A six-membered ring is said to be in a PCP constellation if it is connected to the five-membered ring by a single carbon–carbon bond. A six-membered ring is said to be in a linear constellation if it is separated from the five-membered ring by two carbon–carbon bonds.[8,9,11]

According to their position with regard to the five-membered ring, three types of six-membered rings can be distinguished in acenaphthylenes: rings in a PCP constellation, rings in a linear constellation, and rings that neither are in a PCP nor in a linear constellation; for explanation and examples see Fig. 1.

Based on a large number of calculations, it has been established[8–11] that six--membered rings in a PCP constellation significantly increase the *ef*-value, *i.e.*, the magnitude of the cyclic conjugation, in the five-membered ring (the so-called PCP rule), whereas rings in a linear constellation slightly decrease it (the so-called linear rule). However, a theoretical explanation of these empirical regularities was not possible to find. Namely, by introducing a new six-membered ring into the acenaphthylene molecule, a large number of structural features (*e.g.*, the number of carbon and hydrogen atoms, the number of carbon–carbon bonds, *etc.*) are simultaneously changed and it is not easy to separate cyclic from non-cyclic effects. A way out of this problem was recently proposed.[16] Its essence is that

instead of comparing cyclic conjugation in two acenaphthylene species of different size and structure, one extracts the influence of a ring on the *ef*-value of another ring within the same molecule.

If, as usual,[4] the energy effect of a ring (or cycle) Z_0 of a polycyclic conjugated molecule the molecular graph of which is G is denoted by $ef(G, Z_0)$, then the influence of another ring (or cycle) Z_1 on the value of $ef(G, Z_0)$ will be denoted by $ief(G, Z_0 | Z_1)$. How this latter quantity is calculated is briefly described in the subsequent section.

THEORY

Let G be the molecular graph[13,17] of an acenaphthylene-type system, possessing n vertices. Let Z_0 be its (unique) five-membered ring and Z_1 another ring of G, which necessarily must be of size six. Denote by $\phi(G, x)$ the characteristic polynomial[17] of the graph G and let $\varphi(G - Z_0, x)$, $\varphi(G - Z_1, x)$, and $\varphi(G - Z_0 - Z_1, x)$ be, respectively, the characteristic polynomials of the subgraphs $G - Z_0$, $G - Z_1$, and $G - Z_0$. Let further i be the imaginary unit, $i = \sqrt{-1}$.

It was shown[16] that the influence of ring Z_1 on the energy effect of ring Z_0 can be expressed as:

$$ief(G, Z_0 | Z_1) = \frac{2}{\pi} \int_{-\infty}^{+\infty} \left[\frac{A_1(x) + iB_1(x)}{A(x) + iB(x)} - \frac{A_1(x) + iB_1(x) - 2iA_{01}(x)}{A(x) + iB(x) - 2iA_0(x)} \right] dx \quad (1)$$

where

$$\varphi(G, ix) = i^n \left[A(x) + iB(x) \right]$$

$$\varphi(G - Z_0, ix) = i^{n-5} \left[A_0(x) \right]$$

$$\varphi(G - Z_1, ix) = i^{n-6} \left[A_1(x) + iB_1(x) \right]$$

$$\varphi(G - Z_0 - Z_1, ix) = i^{n-11} \left[A_{01}(x) \right]$$

and where A, B, A_0, A_1, B_1 and A_{01} are polynomials (in the variable x) all coefficients of which are positive or zero; for more details see Ref. 16.

The calculation of the right-hand side of Eq. (1) is not easy. However, the true problem with Eq. (1) is that its structure-dependency is so complicated that no generally valid conclusion could be deduced from it. Using certain, pertinently chosen by not very accurate, approximations, the right-hand side of Eq. (1) could be simplified as:[16]

$$ief(G, Z_0 | Z_1) \approx \frac{8}{\pi} \int_0^\infty \frac{A_0(x) \left[A(x) A_{01}(x) - A_0(x) A_1(x) \right]}{A(x) \left[A(x)^2 + 4A_0(x)^2 \right]} dx \quad (2)$$

The advantage of formula (2) is that all terms in it, except the difference:

$$A(x) A_{01}(x) - A_0(x) A_1(x) \quad (3)$$

Available online at www.shd.org.rs/JSCS/

are necessarily positive-valued for all $x > 0$. Therefore, the sign of the right-hand side of Eq. (2), and thus also of *ief*, depends on the sign of Eq. (3).

It could be demonstrated[16] that if the ring Z_1 is in a PCP constellation to the five-membered ring Z_0, then Eq. (3) is a polynomial of degree $2n$–13 with a positive leading coefficient. Consequently, Eq. (3) gives positive values for, at least, sufficiently large x, implying that the right-hand side of Eq. (2) is also positive-valued, in good agreement with the PCP rule. If the ring Z_1 is in a linear constellation to the five-membered ring Z_0, then Eq. (3) is a polynomial of degree $2n$–15 with a negative leading coefficient, implying that the right-hand side of Eq. (2) is negative-valued, in harmony with the linear rule. If the ring Z_1 neither is in a PCP nor in a linear constellation to the five-membered ring Z_0, then Eq. (3) is a polynomial of degree $2n$–17 or lower, but the sign of its leading coefficient is not always the same. In other words, in this case the *ief* may assume both positive and negative values. The following numerical studies gave examples for both $ief > 0$ and $ief < 0$.

NUMERICAL WORK

In view of the fact that all the general regularities for $ief\,(G, Z_0 \,|\, Z_1)$, outlined in the preceding section,[16] were deduced employing the approximate expression (2), the first point that needs to be checked by numerical calculation is whether there is any agreement between the approximate and exact *ief*-values. That such an agreement does indeed exist is seen from Fig. 2.
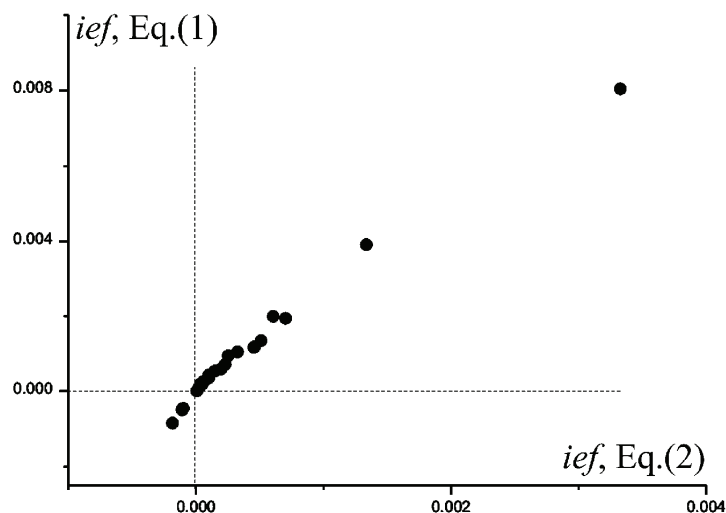
Fig. 2. Correlation between the exact (Eq. (1)) and approximate (Eq. (2)) values of $ief\,(G, Z_0 \,|\, Z_1)$ for acenaphthylene congeners, where Z_0 is the five-membered and Z_1 some six-membered ring, numerical values are available from the authors upon request. It should be noted that in no case do the approximate and exact *ief*-values differ in sign.

The data presented in Fig. 2 show that from a quantitative point of view, the approximation (2) is not particularly good: the *ief*-values computed by means of Eq. (2) are about two-times smaller than the exact *ief*-values. On the other hand, the correlation between the approximate and exact *ief*-values is remarkably good. For qualitative considerations, it is of greatest importance that whenever the right-hand side of Eq. (2) is positive (resp. negative), then the right-hand side of Eq. (1) is also found to be positive (resp. negative). This implies that the inferences made based on Eq. (2) and the sign of the polynomial (3), specified in the preceding section, remain valid also if the *ief* is calculated by means of Eq. (1). In particular, our earlier offered[16] proofs of the PCP rule and the linear rule are now seen to hold at the exact level of the theory.

In order to learn about the long-range influences on cyclic conjugation, the $ief(G, Z_0 \mid Z_k)$-values were examined for the six-membered rings Z_k, $k = 1, 2, \ldots, h$ of the acenaphthylene congeners $\mathbf{A}_h$ and $\mathbf{B}_h$ depicted in Fig. 3. The respective *ief*-values are plotted in Figs. 4 and 5.
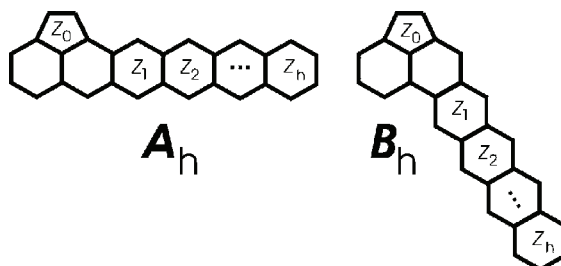
Fig. 3. The acenaphthylene congeners used for testing the influence of far-lying six-membered rings, Z_k, $k = 1, 2, \ldots, h$, on the cyclic conjugation in the five-membered ring Z_0, see Figs. 4 and 5.

The ring Z_1 in the system $\mathbf{A}_h$ is in a PCP constellation and, in harmony with the PCP rule, $ief(A_h, Z_0 \mid Z_1)$ is positive-valued. The rings Z_k, $k = 2, \ldots, h$, may be viewed as extending the PCP constellation. As seen from Fig. 4, the influence of these latter rings is also positive and monotonically decreases with increasing k, *i.e.*, with the increasing distance from the five-membered ring. It may be said that the *ief*-values of the rings Z_k, $k = 1, 2, \ldots, h$ in $\mathbf{A}_h$ have a regular behavior.

The case $h = 2$ is exceptional since in $\mathbf{A}_2$, the influence of the ring Z_2 is greater than that of Z_1. One should note that $\mathbf{A}_2$ is the same as the naphthaleno-acenaphthylene **7**, depicted in Fig. 6. Its *ief*-values will be discussed in more detail in connection with Fig. 6 and Table I.

The situation with the system $\boldsymbol{B}_h$ is somewhat more complex. The ring Z_1 in $\boldsymbol{B}_h$ is in a linear constellation and, in harmony with the linear rule, $ief(B_h, Z_0 \mid Z_1)$ is negative-valued. The rings Z_k, $k = 2, \ldots, h$, may be viewed as extending the linear constellation. However, their *ief*-values are positive or near-zero. As seen from Fig. 5, the influence of these latter rings increases with increasing distance

from the five-membered ring and slightly decreases only at very large distances. It is difficult to understand such an irregular behavior and its rationalization will remain a task for the future.
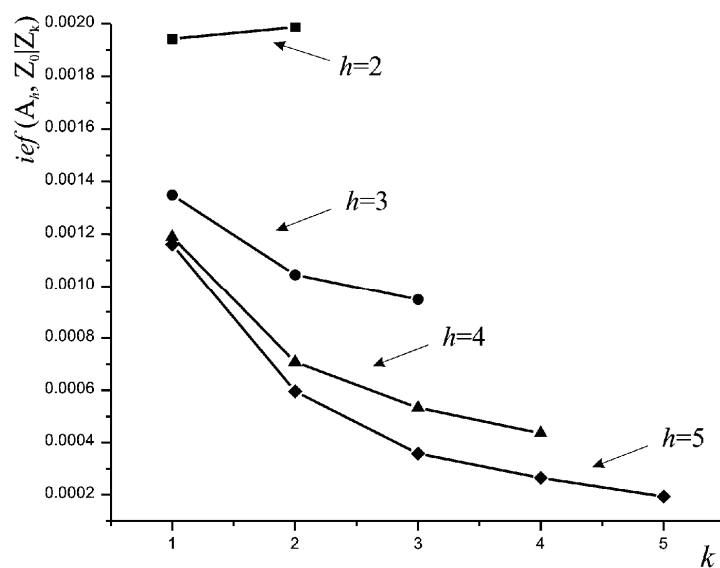

Fig. 4. Influence of the ring Z_k of the acenaphthylene congeners A_h on the magnitude of the cyclic conjugation in the five-membered ring Z_0, *cf*. Fig. 3.
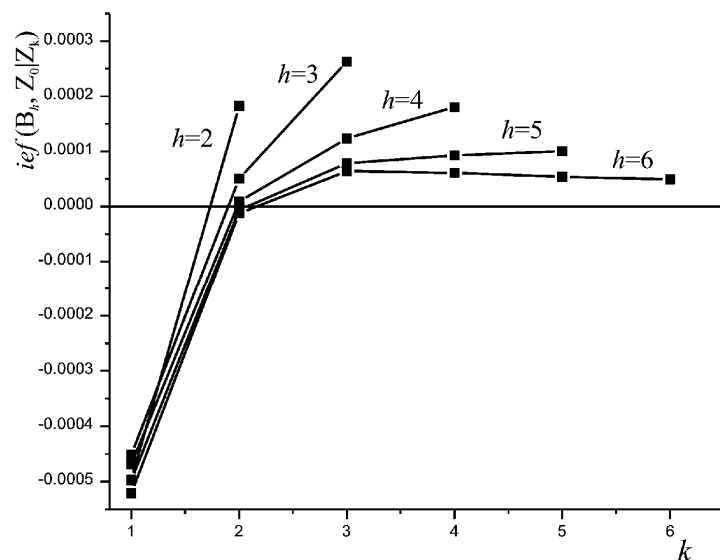

Fig. 5. Influence of the ring Z_k of the acenaphthylene congeners B_h on the magnitude of the cyclic conjugation in the five-membered ring Z_0, *cf*. Fig. 3.

Available online at www.shd.org.rs/JSCS/

Motivated by the above-described peculiarities of the *ief*-values of distant--lying rings, their detailed study was undertaken. From the numerous examples examined, in the following, only the results for the six naphthalenoacenaphthyl-enes, species **7**–**12** depicted in Fig. 6, will be presented. The respective *ief*-values are given in Table I. Note that A_2 and B_2 in Fig. 3 are the same as **7** and **10** in Fig. 6.
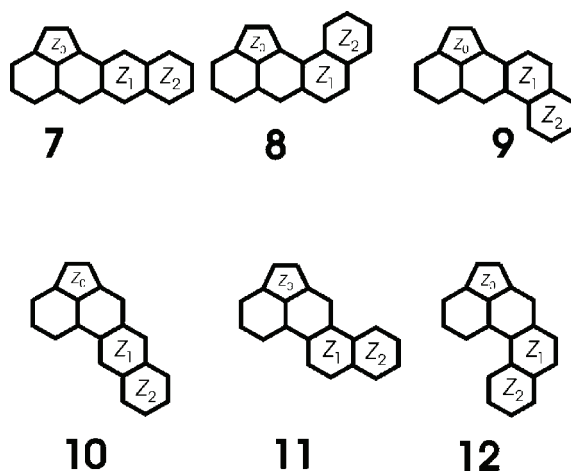
Fig. 6. The six possible naphthaleno-annelated acenaphthylenes; their $ief(G, Z_0 | Z_1)$ - and $ief(G, Z_0 | Z_2)$ -values are given in Table I.

TABLE I. Influence of the six-membered rings in the naphthalene fragment on the magnitude of the cyclic conjugation of the five-membered ring of the naphthalenoacenaphthylenes depicted in Fig. 6. The $ief(G, Z_0 | Z_1)$ -values clearly obey the PCP rule (in the case of **7**, **8** and **9**) and the linear rule (in the case of **10**, **11** and **12**). For a discussion on $ief(G, Z_0 | Z_2)$ see text

Compound	$ief(G, Z_0 | Z_1)$	$ief(G, Z_0 | Z_2)$
7	0.00194	0.00199
8	0.00158	–0.00154
9	0.00154	–0.00106
10	–0.00050	0.00018
11	–0.00053	0.00048
12	–0.00042	0.00015

As can be seen from Table I, the $ief(G, Z_0 | Z_1)$ -values behave just as expected based on the PCP rule and the linear rule. A general regularity for the $ief(G, Z_0 | Z_2)$ -values could not be envisaged. As already noted, in the case of molecule **7**, $ief(G, Z_0 | Z_2) > ief(G, Z_0 | Z_1)$ in spite of the fact that Z_2 is more distant from Z_0 than Z_1. For the systems **8** and **9**, $ief(G, Z_0 | Z_2)$ is negative, whereas for **7**, **10**, **11** and **12**, it is positive. Furthermore, although molecules **11** and **12** are known to have very similar π-electron properties, their $ief(G, Z_0 | Z_2)$ --values differ significantly.

Available online at www.shd.org.rs/JSCS/

In view of the above, it can be concluded that in the case of six-membered rings in the PCP and linear constellation, the simple and generally valid rules exist for their influence on the cyclic conjugation in the five-membered ring of acenaphthylene congeners. In contrast to this, rings at a greater distance from the five-membered ring (those marked by asterisks in Fig. 1) exhibit a quite irregular and "counterintuitive" behavior.

И З В О Д

УТИЦАЈ ПРСТЕНА НА ЦИКЛИЧНУ КОНЈУГАЦИЈУ У ДРУГОМ ПРСТЕНУ: ПРИМЕНА НА ПОЛИЦИКЛИЧНЕ МОЛЕКУЛЕ АЦЕНАФТИЛЕНСКОГ ТИПА

БОРИС ФУРТУЛА, ИВАН ГУТМАН, СВЕТЛАНА ЈЕРЕМИЋ и СЛАВКО РАДЕНКОВИЋ

Природно-математички факултет Универзитета у Крагујевцу

Недавно је развијена метода за процену утицаја $ief(G, Z_0 | Z_1)$ прстена Z_1 на енергетски ефекат неког другог прстена Z_0 у полицикличном конјугованом молекулу G. У овом раду саопштавамо резултате детаљних нумеричких истраживања $ief(G, Z_0 | Z_1)$, усмерених на проучавање утицаја разних шесточланих прстенова на интензитет цикличне конјугације у петочланом прстену молекула аценафтиленског типа. Овим су могле бити разјашњене раније откривене правилности за цикличну конјугацију у једињењима аценафтиленског типа (нарочито, ПЦП правило и линеарно правило), али су уочене и неке друге законитости.

(Примљено 2. јуна 2009)

REFERENCES

1. A. Graovac, I. Gutman, N. Trinajstić, *Topological Approach to the Chemistry of Conjugated Molecules*, Springer-Verlag, Berlin, 1977
2. J. R. Dias, Molecular *Orbital Calculations Using Chemical Graph Theory*, Springer-Verlag, Berlin, 1993
3. M. Randić, *Chem. Rev*. **103** (2003) 3449
4. I. Gutman, *Monatsh. Chem.* **136** (2005) 1055
5. I. Gutman, S. Stanković, J. Đurđević, B. Furtula, *J. Chem. Inf. Model.* **47** (2007) 776
6. I. Gutman, S. Stanković, *Monatsh. Chem.* **139** (2008) 1179
7. R. Ponec, S. Fias, S. Van Damme, P. Bultinck, I. Gutman, S. Stanković, *Coll. Czech. Chem. Commun.* **74** (2009) 147
8. I. Gutman, J. Đurđević, A. T. Balaban, *Polycyclic Arom. Comp*. **29** (2009) 3
9. J. Đurđević, I. Gutman, J. Terzić, A. T. Balaban, *Polycyclic Arom. Comp.* **29** (2009) 90
10. J. Đurđević, I. Gutman, R. Ponec, *J. Serb. Chem. Soc*. **74** (2009) 549
11. I. Gutman, J. Đurđević, *J. Serb. Chem. Soc.* **74** (2009) 765
12. I. Gutman, S. Jeremić, V. Petroviić, *Indian J. Chem*. **48A** (2009) 658
13. I. Gutman, J. Đurđević, *MATCH Commun. Math. Comput. Chem*. **60** (2008) 659
14. J. Đurđević, S. Radenković, I. Gutman, *J. Serb. Chem. Soc.* **73** (2008) 989
15. I. Gutman, J. Đurđević, S. Radenković, A. Burmudžija, *Indian J. Chem*. **37A** (2009) 194
16. S. Radenković, J. Đurđević, I. Gutman, *Chem. Phys. Lett.* **475** (2009) 289
17. I. Gutman, O. E. Polansky, *Mathematical Concepts in Organic Chemistry*, Springer-Verlag, Berlin, 1986.

The Fujita combinatorial enumeration for the non-rigid group of 2,4-dimethylbenzene

ALI MOGHANI[1]*, SOROOR NAGHDI SEDEH[1] and MOHAMMAD REZA SOROUHESH[2]

[1]*Department of Color Physics, Institute for Colorants, Paints and Coatings (ICPC), Tehran* and [2]*Department of Mathematics, Islamic Azad University, South Branch Tehran, Tehran, Iran*

Abstract: Using non-rigid group theory, it was previously shown that the full non-rigid group of 2,4-dimethylbenzene is an ummatured and isomorphic to the group $C_2 \times (C_3 wr C_2)$ of order 36, where C_n is the cyclic group of order *n*, the symbols $\times$ and wr stand for the direct and wreath products, respectively. Here-in, it is first shown that this group has 12 dominant classes. Then, the Marka-racter Table, the Table of all integer-valued characters and the unit subduced cycle index (*USCI*) Table of the full non-rigid group of 2,4-dimethylbenzene are successfully derived for the first time.

Keywords: Full non-rigid group; character; unit subduced cycle index; 2,4-di-methylbenzene.

INTRODUCTION

Shinsaku Fujita proposed the Markaracter Tables, which enabled characters and marks to be discussed on a common basis, then introduced Tables of integer--valued characters[1–3], which are obtained for finite groups.[1–17] Eventually, the Fujita theory was further developed and applied to a variety of problems concerning the enumeration of chemical species.[18–22]

A dominant class is defined as a disjoint union of conjugacy classes that corresponds to the same cyclic subgroup, which is selected as a representative of conjugate cyclic subgroups. Furthermore, the cyclic (dominant) subgroup G_i selected from a non-redundant set of cyclic subgroups of $\mathbf{G}$ is denoted by $\mathbf{SCS_G}$.[15–18,23,24] A rigid molecule is defined as one in which the barriers between its conformers are insuperable and there are no observable tunneling splittings. For non-rigid molecules, there are one or more contortional large amplitude vibration(s), such as inversion or internal rotation that give(s) rise to tunneling splittings. Due to this deformability, non-rigid molecules exhibit some interesting properties of in-

---

* Corresponding author. E-mail: moghani@icrc.ac.ir

91

tramolecular dynamics which can be studied more easily by resorting to group theory. Following the pioneering works of Longuet–Higgins,[25] the symmetry group of a non-rigid molecule group consists of all permutations and permutation–inversion operations which become feasible as the molecule tunnels through a number of potential energy maxima separated by multiple minima. The complete set of molecular conversion operations which commute with the nuclear motion operator contains overall rotation operations, which describe the rotation of the molecule as a whole, and the non-rigid tunneling motion operations, which describe molecular moieties moving with respect to the rest of the molecule. Such a set forms a group, which is called the full non-rigid group (f-NRG). Longuet–Higgins investigated the symmetry groups of non-rigid molecules in which changes from one conformation to another can occur easily. The method as described here is appropriate for molecules which consist of a number of CH_3 groups attached to a rigid framework.[26–35]

In the present study, the Fujita combinatorial enumeration tables of the f-NRG of 2,4-dimethybenzene (see Fig. 1) are investigated. The motivation for this study with the aid of GAP[36] is outlined and the reader is encouraged to consult these papers for background material as well as the basic computational techniques.[37–40]
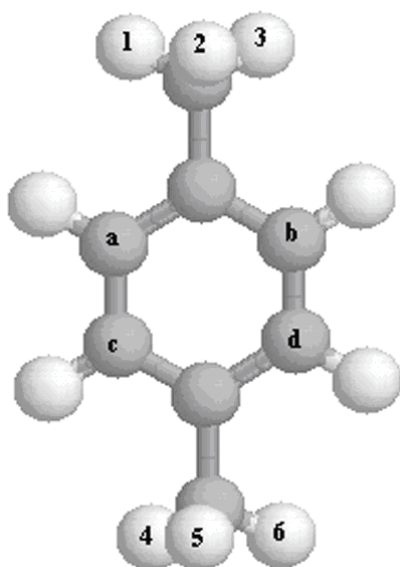
Fig. 1. The structure of 2,4-dimethylbenzene.

COMPUTATIONAL METHOD AND DISCUSSION

In this section, first some notations which will be kept throughout are described. Suppose X be a set, a permutation representation P of a finite group G is obtained when the group G acts on a finite set $X = \{x_1, x_2, \ldots, x_t\}$ from the right,

which means a mapping $\mathbf{P}: \mathbf{X} \times \mathbf{G} \to \mathbf{X}$ is given *via* $(x,g) \to xg$ such that the following holds: $(xg)g' = x(gg')$ and $x1 = x$, for each g, $g' \in \mathbf{G}$ and $x \in \mathbf{X}$. Now let it be assumed that one is given an action $\mathbf{P}$ of $\mathbf{G}$ on $\mathbf{X}$ and a subgroup $\mathbf{H}$ of $\mathbf{G}$. Let $\mathbf{G}_i$ and $\mathbf{G}_j$ be any subgroups of $\mathbf{G}$. A subduced representation is denoted by $\mathbf{G}(/\mathbf{G}_i)\downarrow\mathbf{G}_j$ as a subgroup of the coset representation $\mathbf{G}(/\mathbf{G}_i)$ that contains only elements associated with the elements of $\mathbf{G}_j$. A unit subduced cycle index (*USCI*)[3–6] is defined by:

$$Z(\mathbf{G}(/\mathbf{G}_i) \downarrow \mathbf{G}_j, s_{\mathrm{d}}) = \prod_{g \in \Omega} s_{d_g^{(ij)}}$$

where $s_{d_g^{(ij)}} = |\mathbf{G}_i|/|g^{-1}\mathbf{G}_i g \cap \mathbf{G}_j|$ and Ω is a transversal for the double coset decompositions concerning $\mathbf{G}_i$ and $\mathbf{G}_j$ for $i,j = 1,2,\dots,s$.

If $\mathbf{M}$ is a normal subgroup of $\mathbf{G}$ and $\mathbf{K}$ is another subgroup of $\mathbf{G}$ such that $M \cap K = \{e\}$ and $\mathbf{G} = MN = <\mathbf{M, N}>$, then $\mathbf{G}$ is called the semi direct product of $\mathbf{N}$ by $\mathbf{M}$, which is denoted by $\mathbf{N} : \mathbf{M}$. Let $\mathbf{K}$ and $\mathbf{H}$ be groups and suppose $\mathbf{H}$ acts on the set $\mathbf{\Gamma}$. Then the wreath product of $\mathbf{K}$ by $\mathbf{H}$, denoted by $\mathbf{K}$ wr $\mathbf{H}$ is defined to be the semi direct product $\mathbf{K}^{\mathbf{\Gamma}} : \mathbf{H}$ such that $\mathbf{K}^{\mathbf{\Gamma}} = \{f \mid f : \mathbf{\Gamma} \to \mathbf{K}\}$.[22–24]

The f-NRG of 2,4-dimethylbenzene is described by the direct product of the cyclic group of order two with $\mathbf{G}$, where $\mathbf{G}$ is the wreath product of the cyclic groups three and two, respectively, as follows[18]: if one sets $\alpha = (1,2,3)$, $\beta = (4,5,6)$ and $\gamma = (1,4)(2,5)(3,6)$, then $G = (<\alpha> \times <\beta>) : <\gamma>$, as a matter of fact, one has $\mathbf{G} \cong \mathbf{C}_3\mathrm{wr}\mathbf{C}_2$, see Fig. 1. Now the effect of the vertical operation is to interchange the carbon atoms $\{a,c\}$ with $\{b,d\}$. In this event, the methyl frameworks remain fixed and, hence, the f-NRG of the molecule is the direct product of $\mathbf{G}$ with a cyclic group of order two, namely $\mathbf{X} = \mathbf{C}_2 \times \mathbf{G}$. Now set $\mathbf{X} = \mathbf{C}_2 \times (\mathbf{C}_3\mathrm{wr}\mathbf{C}2)$ and run the following program at the GAP prompt to compute: the mark table, $M_{22 \times 22}$; the character table, $C_{18 \times 18}$ and the set, $SCS_{\mathbf{X}}$ of the f-NRG of 2,4-dimethylbenzene with symmetry $\mathbf{X} = \mathbf{C}_2 \times (\mathbf{C}_3\mathrm{wr}\mathbf{C}_2)$, as follows:

```
LogTo( "2,4-Dimethylbenzene.txt" );
c2:=CyclicGroup(IsPermGroup,(2));c3:=CyclicGroup(IsPermGroup,(3));
G:=WreathProduct(c3,c2);X:=DirectProduct(c2,G);
Order(X);IsPermGroup(X);
Char:=CharacterTable(X);s:=ConjugacyClassesSubgroups(X);
Sort("s");
V:=List(ConjugacyClassesSubgroups(X),x->Elements(x));
M:=TableOfMarks(X);Len:=Length(V);y:=[];
for i in [1,2..Len]do
if IsCyclic(V[i][1])then Add(y,i);
fi;od;Display(Char);Display(s);
Print("Char", "\n");Print("V", "\n");LogTo( );
Print("2,4-Dimethylbenzene.txt", "\n");
```

After running the program, it can be seen that the non-redundant set of sub-groups of X, consists the following elements: G_1 = Id, G_2 = <(1,2)>, G_3 = = <(3,6)(4,7)(5,8)>, G_4 = <(1,2)(3,6)(4,7)(5,8)>, G_5 = <(3,4,5)(6,7,8)>, G_6 = <(3,4,5)>, G_7 = <(3,5,4)(6,7,8)>, G_8 = <(1,2),(3,6)(4,7)(5,8)>, G_9 = <(1,2)(3,4,5)(6,7,8)>, G_{10} = <(1,2)(3,4,5)>, G_{11} = <(3,6)(4,7)(5,8)(3,5,4)(6,7,8)>, G_{12} = <(1,2)(3,5,4)(6,7,8)>, G_{13} = <(3,6)(4,7)(5,8)(3,4,5)(6,7,8)>, G_{14} = <(1,2)(3,6)(4,7)(5,8)(3,4,5)(6,7,8) >, G_{15} = <(1,2)(3,6)(4,7)(5,8)(3,5,4)(6,7,8)>, G_{16} = <(3,4,5)(6,7,8)>, G_{17} = = <(1,2)(3,6)(4,7)(5,8)(3,4,5)(6,7,8)>, G_{18} = <(1,2)(3,6)(4,7)(5,8)(3,4,5)(6,7,8)>, G_{19} = <(1,2)(3,4,5)(6,7,8)>, G_{20} = <(3,6)(4,7)(5,8)(6,7,8)>, G_{21} = <(1,2)(3,6)(4,7)(5,8)(6,7,8)> and G_{22} = X.

In addition, X has exactly 12 dominant classes as stored in Table I such that K_5, K_6, K_8, K_9, K_{10} and K_{12} are unmaturated (*i.e.*, the union of some conjugacy classes), see Table 1.

TABLE I. The dominant classes (K_i) and their corresponding cyclic subgroups (H_i) of f-NRG of 2,4-dimethylbenzene

i	$H_i \in SCG_X$	K_i
1	G_1	1a
2	G_2	2a
3	G_3	2b
4	G_4	2c
5	G_5	3a $\cup$ 3b
6	G_6	3c $\cup$ 3e
7	G_7	3d
8	G_9	6a $\cup$ 6b
9	G_{10}	6c $\cup$ 6d
10	G_{12}	6e $\cup$ 6g
11	G_{13}	6f
12	G_{14}	6h $\cup$ 6i

To compute the Markaracter Table of X, *i.e.*, M^C, first, the non-redundant set of cyclic subgroups of X (*i.e.*, H_j, j = 1,2,…12) stored in Table 1 is calculated using the above GAP program. Furthermore, the nomenclature for consecutive classes of elements of order n must be defined, thus, for example, if an element g has order n, then its class is denoted by nx, where x runs over the letters a, b, etc. To calculate the indices of all the unit subduced cycles of X, for instance $Z(G (/G_i)\downarrow G_{17}, s_d)$, in addition to the above program, the following GAP program must be applied:

G17= GroupWithGenerators (1,2),(3,6)(4,7)(5,8),(3,4,5)(6,7,8));
M17:=TableOfMarks(G17);
Inv:=(M17)^-1;
s17:=ConjugacyClassesSubgroups(G17);Sort(s17);

*A:=[[36,0,0,0,0,0,0,0,0,0],[18,18,0,0,0,0,0,0,0,0],[18,0,6,0,0,0,0,0,0,0],[18,0,0,6
,0,0,0,0,0,0],[12,0,0,0,12,0,0,0,0,0],[12,0,0,0,0,0,0,0,0,0],[12,0,0,0,0,0,0,0,0,0],
[9,9,3,3,0,3,0,0,0,0],[6,6,0,0,6,0,6,0,0,0],[6,6,0,0,0,0,0,0,0,0],[6,0,6,0,0,0,0,0,0,0
],[6,6,0,0,0,0,0,0,0,0],[6,0,2,0,6,0,0,2,0,0],[6,0,0,2,6,0,0,0,2,0],[6,0,0,6,0,0,0,0,0,
0],[4,0,0,0,4,0,0,0,0,0],[3,3,1,1,3,1,3,1,1,1],[3,3,3,3,0,3,0,0,0,0],[2,2,0,0,2,0,2,0,
0,0],[2,0,2,0,2,0,0,2,0,0],[2,0,0,2,2,0,0,0,2,0],[1,1,1,1,1,1,1,1,1,1]];*

    Column17:=A*(Inv);

Print("Column17","\n");

By using the above calculations, we are able to calculate the Fujita combi-
natorial enumeration tables (*i.e.*, the Markaracter Table, the Table of integer-va-
lued characters and the USCI Table) of the f-NRG of 2,4-dimethylbenzene stored
in Tables II–IV can be calculated, which would also be valuable in other appli-
cations, such as in the context of chemical applications of the graph theory and
aromatic compounds.[1,27–29]

TABLE II. The Markaracter Table for the f-NRG of 2,4-dimethylbenzene

M^C	H_1	H_2	H_3	H_4	H_5	H_6	H_7	H_8	H_9	H_{10}	H_{11}	H_{12}
$X(/H_1)$	36	0	0	0	0	0	0	0	0	0	0	0
$X(/H_2)$	18	18	0	0	0	0	0	0	0	0	0	0
$X(/H_3)$	18	0	6	0	0	0	0	0	0	0	0	0
$X(/H_4)$	18	0	0	6	0	0	0	0	0	0	0	0
$X(/H_5)$	12	0	0	0	12	0	0	0	0	0	0	0
$X(/H_6)$	12	0	0	0	0	6	0	0	0	0	0	0
$X(/H_7)$	12	0	0	0	0	0	12	0	0	0	0	0
$X(/H_8)$	6	6	0	0	6	0	0	6	0	0	0	0
$X(/H_9)$	6	6	0	0	0	3	0	0	3	0	0	0
$X(/H_{10})$	6	6	0	0	0	0	6	0	0	6	0	0
$X(/H_{11})$	6	0	2	0	6	0	0	0	0	0	2	0
$X(/H_{12})$	6	0	0	2	6	0	0	0	0	0	0	2

TABLE III. The Table of integer-valued characters for the f-NRG of 2,4-dimethylbenzene
(here, K_i and ϕ_i are the dominant class and Q-conjugacy character, respectively for $i = 1,2,…12$)

C^Q	K_1	K_2	K_3	K_4	K_5	K_6	K_7	K_8	K_9	K_{10}	K_{11}	K_{12}
ϕ_1	1	1	1	1	1	1	1	1	1	1	1	1
ϕ_2	1	1	–1	–1	1	1	1	1	–1	–1	–1	–1
ϕ_3	1	–1	1	–1	1	1	1	–1	1	1	1	–1
ϕ_4	1	–1	–1	1	1	1	1	–1	–1	–1	–1	1
ϕ_5	2	2	2	2	–1	–1	2	–1	–1	–1	2	–1
ϕ_6	2	2	–2	–2	–1	–1	2	–1	1	1	–2	1
ϕ_7	2	–2	2	–2	–1	–1	2	1	–1	–1	2	1
ϕ_8	2	–2	–2	2	–1	–1	2	1	1	1	–2	–1
ϕ_9	2	0	–2	0	–1	2	–1	0	1	–2	1	0
ϕ_{10}	2	0	2	0	–1	2	–1	0	–1	2	–1	0
ϕ_{11}	4	0	–4	0	1	–2	–2	0	–1	2	2	0
ϕ_{12}	4	0	4	0	1	–2	–2	0	1	–2	–2	0

TABLE IV. The unit subduced cycle indices for the f-NRG of 2,4-dimethylbenzene (*i.e.*, $Z(G(/G_i) \downarrow G_j, s_d)$ for $i,j = 1,2,\ldots22$)

USCI	$\downarrow G_1$	$\downarrow G_2$	$\downarrow G_3$	$\downarrow G_4$	$\downarrow G_5$	$\downarrow G_6$	$\downarrow G_7$	$\downarrow G_8$	$\downarrow G_9$	$\downarrow G_{10}$	$\downarrow G_{11}$
$G(/G_1)$	s_1^{36}	s_2^{18}	s_2^{18}	s_2^{18}	s_3^{12}	s_3^{12}	s_3^{12}	s_4^{9}	s_6^{6}	s_6^{6}	s_6^{6}
$G(/G_2)$	s_1^{18}	s_1^{18}	s_2^{9}	s_2^{9}	s_3^{6}	s_3^{6}	s_3^{6}	s_2^{9}	s_3^{6}	s_3^{6}	s_6^{3}
$G(/G_3)$	s_1^{18}	s_2^{9}	$s_2^{6}s_1^{6}$	s_2^{9}	s_3^{6}	s_3^{6}	s_3^{6}	$s_2^{3}s_4^{3}$	s_6^{3}	s_6^{3}	s_3^{6}
$G(/G_4)$	s_1^{18}	s_2^{9}	s_2^{9}	$s_2^{6}s_1^{6}$	s_3^{6}	s_3^{6}	s_3^{6}	$s_2^{3}s_4^{3}$	s_6^{3}	s_6^{3}	s_6^{3}
$G(/G_5)$	s_1^{12}	s_2^{6}	s_2^{6}	s_2^{6}	s_1^{12}	s_3^{4}	s_3^{4}	s_4^{3}	s_2^{6}	s_6^{2}	s_6^{2}
$G(/G_6)$	s_1^{12}	s_2^{6}	s_2^{6}	s_2^{6}	s_4^{3}	$s_3^{2}s_1^{6}$	s_4^{3}	s_4^{3}	s_6^{2}	$s_2^{3}s_6$	s_6^{2}
$G(/G_7)$	s_1^{12}	s_2^{6}	s_2^{6}	s_2^{6}	s_4^{3}	s_4^{3}	s_1^{12}	s_4^{3}	s_6^{2}	s_6^{2}	s_6^{2}
$G(/G_8)$	s_1^{9}	s_1^{9}	$s_2^{3}s_1^{3}$	$s_2^{3}s_1^{3}$	s_3^{3}	s_3^{3}	s_3^{3}	$s_2^{3}s_1^{3}$	s_3^{3}	s_3^{3}	s_3^{3}
$G(/G_9)$	s_1^{6}	s_1^{6}	s_2^{3}	s_2^{3}	s_1^{6}	s_3^{2}	s_3^{2}	s_3^{2}	s_1^{6}	s_3^{2}	s_6
$G(/G_{10})$	s_1^{6}	s_1^{6}	s_2^{3}	s_2^{3}	s_3^{2}	$s_1^{3}s_3$	s_3^{2}	s_2^{3}	s_3^{2}	$s_1^{3}s_3$	s_1^{6}
$G(/G_{11})$	s_1^{6}	s_2^{3}	s_1^{6}	s_2^{3}	s_3^{2}	s_3^{2}	s_6	s_2^{3}	s_6	s_6	s_1^{6}
$G(/G_{12})$	s_1^{6}	s_1^{6}	s_2^{3}	s_2^{3}	s_3^{2}	s_3^{2}	s_1^{6}	s_2^{3}	s_3^{2}	s_3^{2}	s_2^{3}
$G(/G_{13})$	s_1^{6}	s_2^{3}	$s_2^{2}s_1^{2}$	s_2^{3}	s_1^{6}	s_3^{2}	s_3^{2}	s_4s_2	s_2^{3}	s_6	s_3^{2}
$G(/G_{14})$	s_1^{6}	s_2^{3}	s_2^{3}	$s_2^{2}s_1^{2}$	s_1^{6}	s_3^{2}	s_3^{2}	s_4s_2	s_2^{3}	s_6	s_6
$G(/G_{15})$	s_1^{6}	s_2^{3}	s_2^{3}	s_1^{6}	s_3^{2}	s_3^{2}	s_1^{6}	s_2^{3}	s_6	s_6	s_2^{3}
$G(/G_{16})$	s_1^{4}	s_2^{2}	s_2^{2}	s_2^{2}	s_1^{4}	s_1^{4}	s_1^{4}	s_4	s_2^{2}	s_2^{2}	s_2^{2}
$G(/G_{17})$	s_1^{3}	s_1^{3}	s_1s_2	s_1s_2	s_1^{3}	s_3	s_3	s_1s_2	s_1^{3}	s_3	s_3
$G(/G_{18})$	s_1^{3}	s_1^{3}	s_1^{3}	s_1^{3}	s_3	s_3	s_1^{3}	s_1^{3}	s_3	s_3	s_1^{3}
$G(/G_{19})$	s_1^{2}	s_1^{2}	s_2	s_2	s_1^{2}	s_1^{2}	s_1^{2}	s_2	s_1^{2}	s_1^{2}	s_2
$G(/G_{20})$	s_1^{2}	s_1^{2}	s_1^{2}	s_2	s_1^{2}	s_1^{2}	s_1^{2}	s_2	s_2	s_2	s_1^{2}
$G(/G_{21})$	s_1^{2}	s_2	s_2	s_1^{2}	s_1^{2}	s_1^{2}	s_1^{2}	s_2	s_2	s_2	s_2
$G(/G_{22})$	s_1	s_1	s_1	s_1	s_1	s_1	s_1	s_1	s_1	s_1	s_1
$G(/G_1)$	s_6^{6}	s_6^{6}	s_6^{6}	s_6^{6}	s_9^{4}	s_{12}^{3}	s_{12}^{3}	s_{18}^{2}	s_{18}^{2}	s_{18}^{2}	s_{36}
$G(/G_2)$	s_6^{3}	s_6^{3}	s_6^{3}	s_6^{3}	s_9^{2}	s_6^{3}	s_6^{3}	s_9^{2}	s_{18}	s_{18}	s_{18}
$G(/G_3)$	s_6^{3}	$s_6^{2}s_3^{2}$	s_6^{3}	s_6^{3}	s_9^{2}	$s_{12}s_6$	s_6^{3}	s_{18}	s_9^{2}	s_{18}	s_{18}
$G(/G_4)$	s_6^{3}	s_6^{3}	$s_6^{2}s_3^{2}$	s_6^{3}	s_9^{2}	$s_{12}s_6$	s_6^{3}	s_{18}	s_{18}	s_9^{2}	s_{18}

Available online at www.shd.org.rs/JSCS/

TABLE IV. Continued

USCI	↓G_{12}	↓G_{13}	↓G_{14}	↓G_{15}	↓G_{16}	↓G_{17}	↓G_{18}	↓G_{19}	↓G_{20}	↓G_{21}	↓G_{22}
$G(/G_5)$	s_6^2	s_2^6	s_2^6	s_6^2	s_3^4	s_4^3	s_{12}	s_6^2	s_6^2	s_6^2	s_{12}
$G(/G_6)$	s_6^2	s_6^2	s_6^2	s_6^2	s_3^4	s_{12}	s_{12}	s_6^2	s_6^2	s_6^2	s_{12}
$G(/G_7)$	s_2^6	s_6^2	s_6^2	s_2^6	s_3^4	s_{12}	s_4^3	s_6^2	s_6^2	s_6^2	s_{12}
$G(/G_8)$	s_3^3	$s_6 s_3$	$s_6 s_3$	s_3^3	s_9	$s_6 s_3$	s_3^3	s_9	s_9	s_9	s_9
$G(/G_9)$	s_3^2	s_3^2	s_3^2	s_6	s_3^2	s_3^2	s_6	s_3^2	s_6	s_6	s_6
$G(/G_{10})$	s_3^2	s_6	s_6	s_6	s_3^2	s_6	s_6	s_3^2	s_6	s_6	s_6
$G(/G_{11})$	s_3^2	s_3^2	s_6	s_2^3	s_3^2	s_6	s_2^3	s_6	s_3^2	s_6	s_6
$G(/G_{12})$	s_1^6	s_6	s_6	s_2^3	s_3^2	s_6	s_2^3	s_3^2	s_6	s_6	s_6
$G(/G_{13})$	s_6	$s_2^2 s_1^2$	s_2^3	s_6	s_3^2	$s_4 s_2$	s_6	s_6	s_3^2	s_6	s_6
$G(/G_{14})$	s_6	s_2^3	$s_2^2 s_1^2$	s_3^2	s_3^2	$s_4 s_2$	s_6	s_6	s_6	s_3^2	s_6
$G(/G_{15})$	s_2^3	s_6	s_3^2	s_1^6	s_3^2	s_6	s_2^3	s_6	s_6	s_3^2	s_6
$G(/G_{16})$	s_2^2	s_2^2	s_2^2	s_2^2	s_1^4	s_4	s_4	s_2^2	s_2^2	s_2^2	s_4
$G(/G_{17})$	s_3	$s_1 s_2$	$s_1 s_2$	s_3	s_3	$s_1 s_2$	s_3	s_3	s_3	s_3	s_3
$G(/G_{18})$	s_1^3	s_3	s_3	s_1^3	s_3	s_3	s_1^3	s_3	s_3	s_3	s_3
$G(/G_{19})$	s_1^2	s_2	s_2	s_2	s_1^2	s_2	s_2	s_1^2	s_2	s_2	s_2
$G(/G_{20})$	s_2	s_1^2	s_2	s_2	s_1^2	s_2	s_2	s_2	s_1^2	s_2	s_2
$G(/G_{21})$	s_2	s_2	s_1^2	s_1^2	s_1^2	s_2	s_2	s_2	s_2	s_1^2	s_2
$G(/G_{22})$	s_1	s_1	s_1	s_1	s_1	s_1	s_1	s_1	s_1	s_1	s_1

И З В О Д

ФУЏИТИНО (FUJITA) КОМБИНАТОРНО ПРЕБРОЈАВАЊЕ ЗА НЕРИГИДНУ ГРУПУ
2,4-ДИМЕТИЛБЕНЗЕНА

ALI MOGHANI[1], SOROOR NAGHDI SEDEH[1] и MOHAMMD REZA SOROUHESH[2]

[1]*Department of color physics, Institute for Colorants Paint and Coating (ICPC), Tehran u* [2]*Department of Mathematics, Islamic Azad University, South branch Tehran, Tehran, Iran*

Применом теорије неригидних група показано је да је потпуна неригидна група 2,4-ди-метилбензена нематурирана група и да је изоморфна групи $\mathbf{C}_2$×($\mathbf{C}_3$wr$\mathbf{C}_2$) реда 36, где је $\mathbf{C}_n$ циклична група реда *n*, и где симболи × и wr означавају директни одн. венчасти производ. Показано је да испитивана група има 12 доминантних класа. По први пут су одређене та-

блица марккарактера, таблица свих целобројних карактера, као и таблица јединичних цикличних индекса субдукције (USCI) за све потпуне неригидне групе 2,4-диметилбензена.

REFERENCES

1. S. Fujita, *Bull. Chem. Soc. Jpn.* **71** (1998) 2071
2. S. Fujita, *Bull. Chem. Soc. Jpn.* **71** (1998) 2309
3. S. Fujita, *Bull. Chem. Soc. Jpn.* **71**(1998) 1587
4. F. A. Cotton, *Chemical Application of Group Theory*, Wiley-International, New York, USA, 1971
5. I. Hargittai, H. Hargitta, *Symmetry through the Eyes of a Chemist*, VCH, Weinheim, Germany, 1986
6. S. Fujita, *J. Math. Chem.* **12** (1999) 173
7. S. Fujita, *J. Graph Theory* **18** (1994) 349
8. S. Fujita, *J. Org. Chem.* **67** (2002) 6055
9. S. Fujita, *J. Comput. Chem. Jpn.* (2004) 113
10. S. Fujita, *MATCH Commun. Math. Comput. Chem.* **54** (2005) 251
11. S. Fujita, *MATCH Commun. Math. Comput. Chem.* **55** (2006) 5
12. S. Fujita, *MATCH Commun. Math. Comput. Chem.* **55** (2006) 237
13. S. Fujita, *MATCH Commun. Math. Comput. Chem.* **57** (2007) 5
14. S. Fujita, *Diagrammatical Approach to Molecular Symmetry and Enumeration of Stereoisomers*, University of Kragujevac, Kragujevac, Serbia, 2007
15. S. Fujita, *Theor. Chim. Acta* **91** (1995) 291
16. S. Fujita, *Theor. Chim. Acta* **91** (1995) 315
17. A. Kerber, *MATCH Commun. Math. Comput. Chem.* **46** (2002) 151
18. S. Fujita, *MATCH Commun. Math. Comput. Chem.* **58** (2007) 611
19. S. Fujita, *MATCH Commun. Math. Comput. Chem.* **59** (2008) 509
20. S. Fujita, *MATCH Commun. Math. Comput. Chem.* **61** (2009) 11
21. S. Fujita, *MATCH Commun. Math. Comput. Chem.* **61** (2009) 39
22. S. Fujita, *MATCH Commun. Math. Comput. Chem.* **61** (2009) 71
23. M. R. Darafsheh, A. Darafsheh, *MATCH Commun. Math. Comput. Chem.* **56** (2006) 271
24. A. Moghani, *Bull. Chem. Soc. Jpn.* **82** (2009) 602.
25. H. C. Longuet-Higgins, *Mol. Phys.* **6** (1963) 445
26. Y. G. Smeyers, *Adv. Quantum. Chem.* **24** (1992) 1
27. S. L. Altmann, *Induced Representation in Crystal and Molecules*, Academic Press, London, 1977
28. P. R. Bunker, *Molecular Symmetry in Spectroscopy*, Academic Press, New York, USA, 1979
29. J. S. Lomont, *Applications of Finite Groups*, Academic Press, New York, USA, 1959
30. A. J. Stone, *J. Chem. Phys.* **41** (1964) 1568
31. Y. G. Smeyers, M. Villa, *J. Math. Chem.* **28** (2000) 377
32. K. Balasubramanian, *J. Phys. Chem.* **10** (2004) 5527
33. K. Balasubramanian, *Chem. Phys. Lett.* **391** (2004) 64
34. K. Balasubramanian, *Chem. Phys. Lett.* **398** (2004) 15
35. A. Moghani, S. Naghdi, A. R. Ashrafi, A. Ahmadi, *J. London Math. Soc.* **340** (2007) 630

36. GAP, *Groups, Algorithms and Programming*, Lehrstuhl De für Mathematik, RWTH, Aachen, Germany, http://www.gap-system.org
37. A. Moghani, *J. Serb. Chem. Soc.* **73** (2008) 189
38. M. R Darafsheh, A. Moghani, *Bull. Chem. Soc. Jpn.* **81** (2008) 279
39. M. R. Darafsheh, A. Moghani, S. Naghdi Sedeh, *Acta Chim. Slov*. **55** (2008) 602
40. M. R. Darafsheh, A. Moghani, M. Karami, A. Zaeembashi, S. Naghdi, *Int. J. Chem. Model.* **1** (2009) 435.

Investigation of the kinetics and mechanism of the glycerol chlorination reaction using gas chromatography–mass spectrometry

XIUQUAN LING[1], DINGQIANG LU[1,2]*, JUN WANG[1], MINGXIN LIANG[1], SHUMIN ZHANG[1], WEI REN[1], JIANHUI CHEN[1] and PINGKAI OUYANG[1]

[1]*State Key Laboratory of Materials-Oriented Chemical Engineering, College of Life Science and Pharmaceutical Engineering, Nanjing University of Technology, Nanjing 210009 and* [2]*Jiangsu Provincial Institute of Materia Medica, Nanjing 210009, China*

Abstract: As a primary by-product in biodiesel production, glycerol can be used to prepare an important fine chemical, epichlorohydrin, by the glycerol chlorination reaction. Although this process has been applied in industrial production, unfortunately, less attention has been paid to the analysis and separation of the compounds in the glycerol chlorination products. In this study, a convenient and accurate method to determine the products in glycerol chlorination reaction was established and based on the results the kinetic mechanism of the reaction was investigated. The structure of main products, including 1,3--dichloropropan-2-ol, 2,3-dichloropropan-1-ol, 3-chloro-1,2-propanediol, 2-chloro-1,3-propanediol and glycerol was ascertained by gas chromatography–mass spectrometry and the isomers of the products were distinguished. Apidic acid was considered as the best catalyst because of its excellent catalytic effect and high boiling point. The mechanism of the glycerol chlorination reaction was proposed and a new kinetic model was developed. Kinetic equations of the process in the experimental range were obtained by data fitting and the activation energies of each tandem reaction were 30.7, 41.8, 29.4 and 49.5 kJ mol⁻¹, respectively. This study revealed the process and mechanism of the kinetics and provides the theoretical basis for engineering problems.

Keywords: glycerol; monochloropropanediol; dichloropropanol; chlorination reaction; gas chromatography–mass spectrometry; kinetic model.

INTRODUCTION

Epichlorohydrin is an important fine chemical, which is widely used to prepare organic chemical raw materials such as epoxy resin.[1,2] In China, the production capacity of epichlorohydrin had reached 497 thousand tons until 2008

---

and it is estimated that demand for it will have reached 700 thousand tons in 2012. Currently, the methods to produce epichlorohydrin include the high-temperature chlorination of propylene route and the allyl acetate route,[3,4] which depend on the petroleum industry. Then, with the petroleum energy crisis in recent years and the soar of oil prices, the price of epichlorohydrin on the international market rose. Due to the increase in the production of the biodiesel industry in recent years and the consequential increase in its by-product glycerol (one tenth of the yield of biodiesel), there is an oversupply of glycerol and a slump in its price on the market. The efficient and reasonable utilization of glycerol has become a bottleneck problem for the healthy development of the biodiesel industry chain. Dichloropropanol (DCP), as the raw material of epichlorohydrin production, can be produced by the reaction between glycerol and hydrogen chloride. Thus, the process of preparing epichlorohydrin from glycerol would allow mankind to be less dependent on petroleum and promote the development of the biomass energy industry, which has great economic and social values.

The most important step in the synthesis of DCP from glycerol is the chlorination reaction glycerol.[5,6] This process has been introduced on the industrial scale[7–9] but, unfortunately, less attention has been paid to the analysis and separation of the compounds produced in the reaction. Therefore, there is an urgent need for the development of an accurate method to determine the compositions in this complex reaction system. To date, the primary method for analyzing monochloropropanediol (MCP) and DCP is gas chromatography.[10] Schuhmacher *et al.* and Crews *et al.* determined 1,3-dichloropropan-2-ol (1,3-DCP) by gas chromatography–mass spectrometry (GC–MS).[11,12] Furthermore, Boden *et al.* and Chung *et al.* both reported methods for the simultaneous analysis of 3-chloro-1,2-propanediol (3-MCP) and 1,3-DCP by GC–MS.[13,14] However, the above-mentioned methods not only required the samples to be derivatized before analysis, but also they cannot recognize the isomers present in the reaction system. In addition, the formation of the intermediate MCP complicates the reaction system and causes great difficulties for further research on the dynamics of the reaction. In this study, a GC–MS method that can simultaneously ascertain the composition, including glycerol, 3-MCP, 2-chloro-1,3-propanediol (2-MCP), 1,3-DCP and 2,3-dichloropropan-2-ol (2,3-DCP), in the chlorination reaction system was developed without the necessity of derivatization, which effectively simplified the analysis process and enabled the isomers in products to be distinguished, thus providing a fast and convenient method for further study of the dynamics of the reaction.

Hitherto, there have been only a few reports concerning the kinetics of the glycerol chlorination reaction.[15] Siano *et al.* found that propionic acid was the best catalyst for this reaction, although its boiling point is only slightly higher than that of acetic acid, which is used in the traditional process. They considered that an oxonium group was formed during the glycerol chlorination process and

deduced a dynamic model of the chlorination tandem reactions.[16] However, there were some defects in their hypothesis and the model cannot completely accurately describe the glycerol chlorination process. In this study, the chlorination reaction model has been improved, which reflected the mechanism of the reaction and offered a theoretical basis for the industrial production of epichlorohydrin.

EXPERIMENTAL

Materials and instruments

All chemicals used in the present work, *viz*., glycerol, acetic acid, propanoic acid, malonic acid, succinic acid and apidic acid (all purchased from Ludu, China) were of analytical reagent (A.R.) grade.

Gas chromatographic and mass spectrometric analysis

The GC–MS analyses were performed using a CP 3800-Saturn 2200 gas chromatograph––mass spectrometry instrument (Varian, Middelburg, The Netherlands). The GC analyses were performed using an SP-6890 gas chromatography instrument (Lunan Ruihong, Shandong, China), equipped with a KR-9 capillary column (30 m×0.32 mm×1 μm). The injector and flame ionization detector (FID) temperature were 200 and 280 °C, respectively. The oven temperature was held at 190 °C; N_2 was the carrier gas (1.1 mL min^{-1}). The injected volume was 0.60 μL with the split ratio set at 60:1.

Experimental apparatus

Glycerol chlorination reaction experiments were realized in a self-designed glass apparatus shown in Fig. 1. Glycerol and catalyst were fed into the glass-jacketed reactor, and the external circulation oil bath controller maintained the reaction mixture at the predetermined temperature. Then hydrogen chloride gas, previously dried using a gas dryer, was introduced into the reactor. A porous glass fritter and strong mechanical stirring assured that the gas–liquid interface contacted well. The excess hydrogen chloride gas was fed through a protection bottle and absorbed by alkali liquor in the exit gas absorption bottle. Reaction mixture samples were withdrawn through a valve at the bottom of the reactor for gas chromatographic analysis.
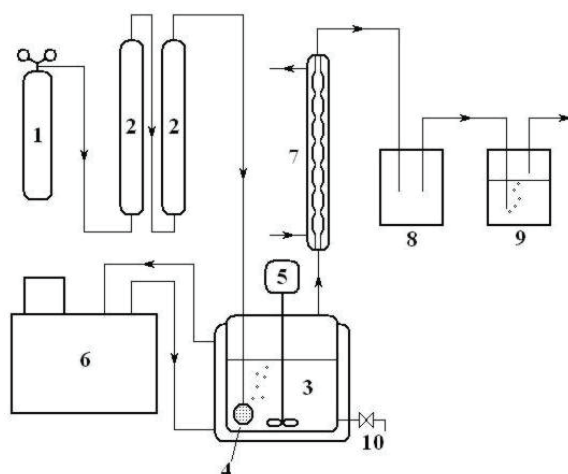
Fig. 1. Schematic diagram of glycerol chlorination reaction apparatus. 1. hydrogen chloride cylinder; 2. gas dryer; 3. reactor; 4. porous fritter; 5. mechanical stirrer; 6. circulation oil bath controller; 7. condenser; 8. protection bottle; 9. exit gas absorber; 10. sampling valve.

RESULTS AND DISCUSSION

The total ion chromatogram of a sample obtained under the optimal chromatographic conditions is shown in Fig. 2. It depicts that there were five components in the glycerol chlorination products and all components in the sample were well separated during 6 min without additional derivatization. These five components were detected with the mass spectrum detector and the mass spectrograms are shown in Fig. 3.
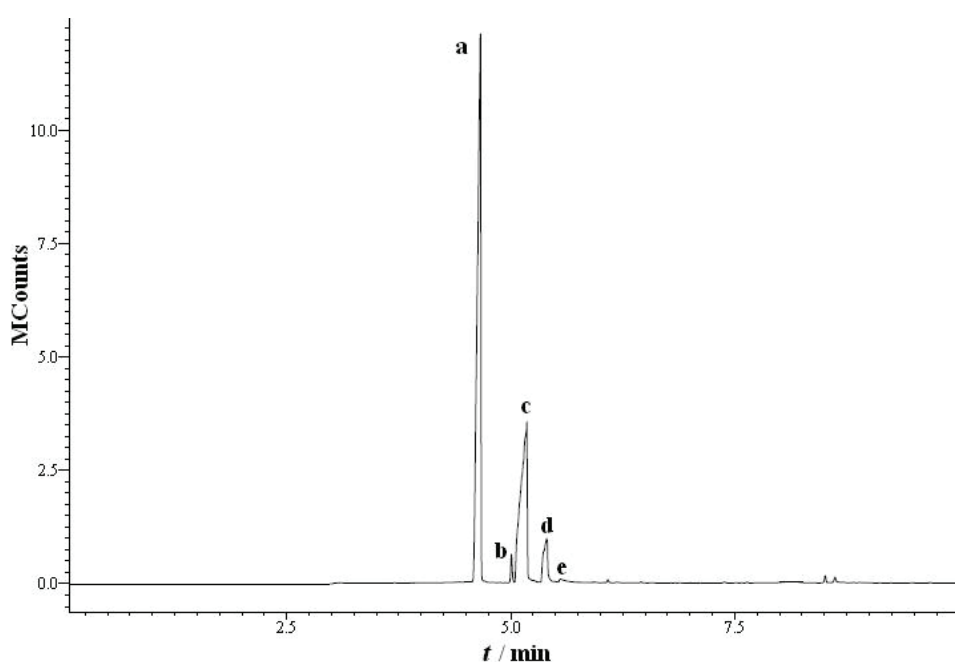
Fig. 2. Total ion chromatogram of the products of glycerol chlorination.

1,3-DCP and 2,3-dichloropropan-1-ol (2,3-DCP) are isomers and, having the same molecular weight, great difficulties are encountered in distinguishing them. Generally, because molecules of alcohols are often fragmented completely under electron impact (EI), the molecular ion peaks of 1,3-DCP and 2,3-DCP can hardly appear in their mass spectrogram. According to the laws of alcohol β-cracking and halide substituent rupture, the molecule of 1,3-DCP may produce a fragment ion with m/z 79 under EI due to the hydroxyl group linking with the β-carbon, while that of 2,3-DCP may produce an m/z 62 fragment peak due to the hydroxyl group linking with the α-carbon. On the other hand, m/z 81 and 64 fragment ion peaks, with one-third of the relative abundance of the m/z 79 and 62 peaks, could appear next to these two peaks, respectively, because of the existence of the isotope ^{37}Cl in the sample. The possible fragmentation pathways of 1,3-DCP and

Available online at www.shd.org.rs/JSCS/

2,3-DCP are shown in Fig. 4. The fragment ion peaks m/z 81 and 79 are both present in the mass spectrogram of component **a** while fragment ion peaks m/z 64 and 62 are present in the spectrogram of component **b**, Fig. 3. Hence, it can be inferred that component **a** in the total ion chromatogram is 1,3-dichloropropan-2-ol and component **b** is 2,3-dichloropropan-1-ol.
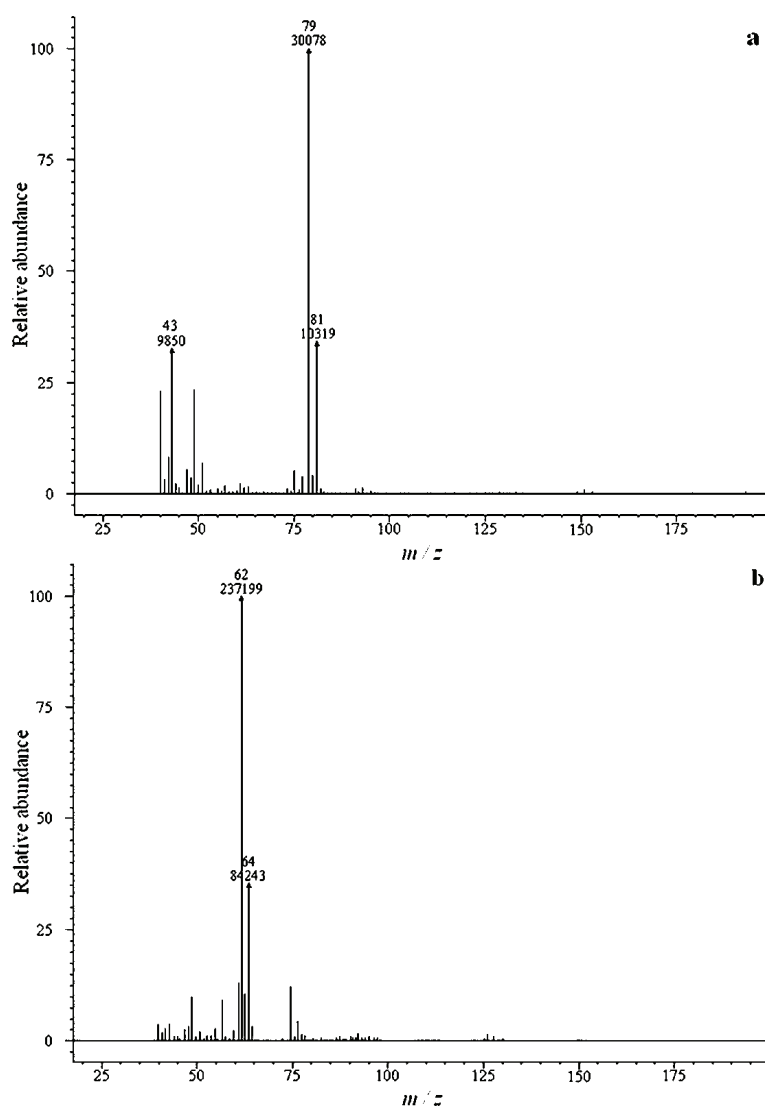
Fig. 3. Mass spectrograms of components **a** and **b**.

LING *et al.*
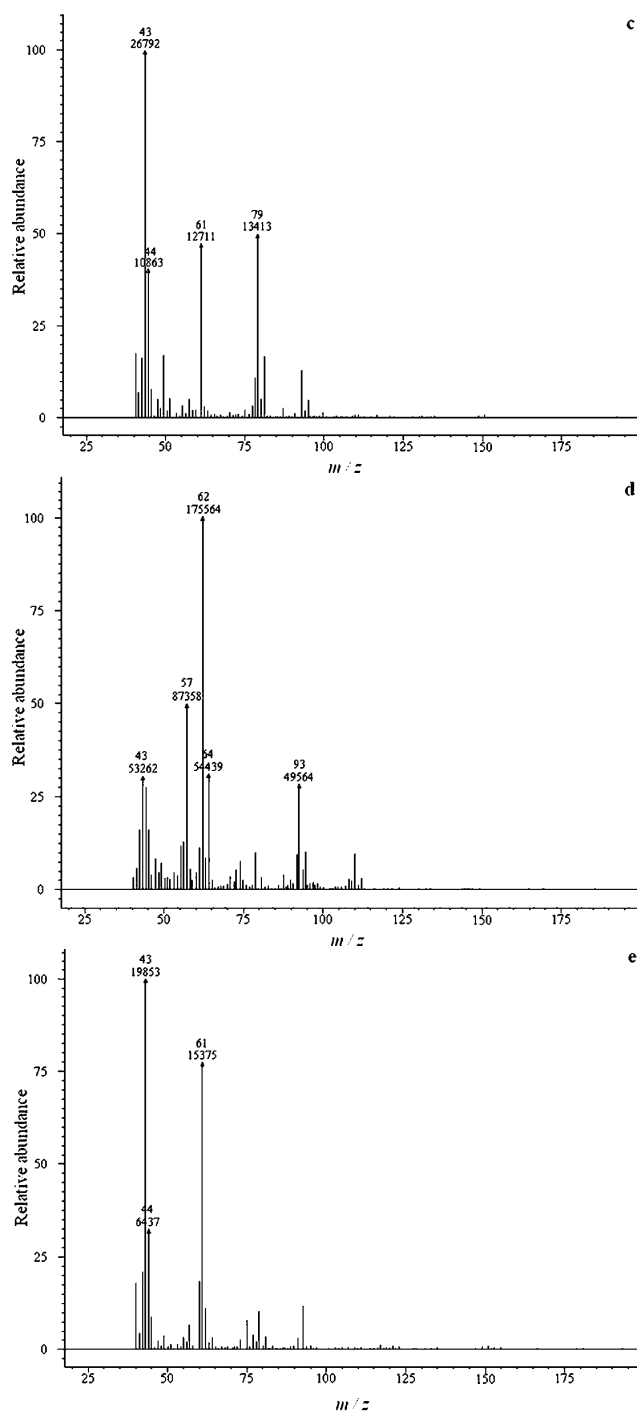
Fig. 3 continued. Mass spectrograms of components **c**, **d** and **e**.
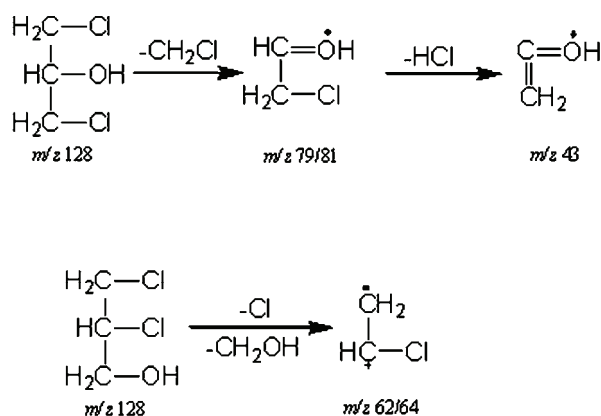
Fig. 4. Fragmentation pathways of 1,3-dichloropropan-2-ol and
2,3-dichloropropan-1-ol under electron impact.

3-MCP and 2-chloro-1,3-propanediol (2-MCP) are also isomers and neither of their molecular ion peaks can appear in the EI mass spectrogram. The molecule of 2-MCP may produce a fragment ion with m/z 62 under EI due to hydroxyl group and chlorine atom linking with their α-carbon and β-carbon respectively, while that of 3-MCP may produce a m/z 79 fragment ion due to hydroxyl group and chlorine atom linking with their α-carbon and γ-carbon, respectively, according to the laws of alcohol β-cracking and halide substituent rupture. In addition, m/z 81 and 64 fragment ion peaks, with one-third of the relative abundance of the m/z 79 and 62 peaks, may appear next to these two peaks, respectively, also because of the existence of the ^{37}Cl isotope in the sample. The possible fragmentation pathways of 3-MCP and 2-MCP are shown in Fig. 5. The fragment ion peaks m/z 79 and 81 are both present in the mass spectrogram of component **c** while the fragment ion peaks m/z 62 and 64 are both present in the mass spectrogram of component **d**. Hence it can be inferred that component **c** in the total ion chromatogram is 3-chloro-1,2-propanediol and component **d** is 2-chloro-1,3-propanediol.

There are three hydroxyl groups in the molecule of glycerol meaning that the molecular ion peak must be absent in its EI mass spectrogram. The molecule of glycerol may produce a fragment ion with m/z 61 under EI according to the law of alcohol β-cracking. The possible fragmentation pathway of glycerol is shown in Fig. 6. These fragment ion peaks are all present in the mass spectrograms of component **e**. Hence, it can be inferred that component **e** in the total ion chromatogram is glycerol.

Tesser *et al.* indicated that there was no relationship between the acidity strength of a catalysts and its catalytic activity,[15] while Phillipe *et al.* proposed that a variety of carboxylic acid could catalyze the chlorination reaction.[17] In the

present study, different kinds of lower carboxylic acids, such as acetic acid, propanoic acid, malonic acid, succinic acid and adipic acid, were utilized as catalysts in the experiments. A comparison of the catalytic effect of a variety of catalysts is depicted in Fig. 7, from which it can be seen that acetic acid, propanoic acid and adipic acid displayed better catalytic effects that the other investigated catalysts. However, the low boiling point of acetic acid and propanoic acid caused severe volatilization loss of these acids, which lowered the rate of the reaction. To overcome these shortcomings, apidic acid was selected as the chlorination catalyst.

Fig. 5. Fragmentation pathways of 3-chloro-1,2-propanediol and 2-chloro-1,3-propanediol under electron impact.

Fig. 6. Fragmentation pathways of glycerol under electron impact.

According to the reaction products glycerol chlorination determined by GC–MS, the net tandem reaction can be schematized in the following manner:

$$\text{(1)}$$

Fig. 7. Comparison of a variety of catalysts on the conversion of dichloropropanol.

The evolution of each component in the reaction product under the optimum condition is depicted in Fig. 8. It can be observed that the concentration of 2-MCP hardly increased when glycerol was still present in the reaction mixture. After a sufficiently long time, the amount of glycerol decreased to a low constant value. Tesser *et al*. considered that conversion of 2-MCP to 2,3-DCP could be neglected, namely reaction path 5 (Eq. (1)) does not occur. Reaction paths 2 and 4 (Eq. (1)) can be considered as being irreversible, due to the low accumulation of 2-MCP and 2,3-DCP throughout the whole reaction process.[15] Moreover, reaction 1 can also be considered as being irreversible because rate of reaction 1 from glycerol to 3-MCP is very high and glycerol can finally be completely converted. According to these hypotheses, the glycerol chlorination reaction model can be modified to the following:

$$
\begin{array}{cccc}
& & \xrightarrow{k_3} & \text{1,3-DCP} \\
& \nearrow^{k_1} \text{3-MCP} \underset{k_5}{\rightleftharpoons} & & (C_4) \\
\text{Gly} & (C_2) & \searrow^{k_4} & \\
(C_1) & & & \text{2,3-DCP} \\
& \searrow_{k_2} \text{2-MCP} & & (C_5) \\
& (C_3) & &
\end{array} \tag{2}
$$
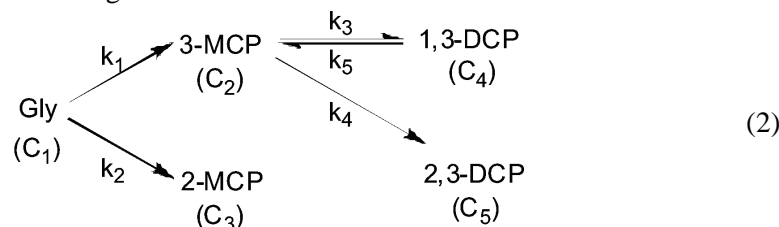
Thus, the kinetic model can be reduced to the following differential equations:

$$\frac{dc_1}{dt} = -k_1c_1 - k_2c_1; \quad \frac{dc_2}{dt} = k_1c_1 - k_3c_2 + k_5c_4 - k_4c_2; \quad \frac{dc_3}{dt} = k_2c_1$$

$$\frac{dc_4}{dt} = k_3c_2 - k_5c_4; \quad \frac{dc_5}{dt} = k_4c_2 \tag{3}$$
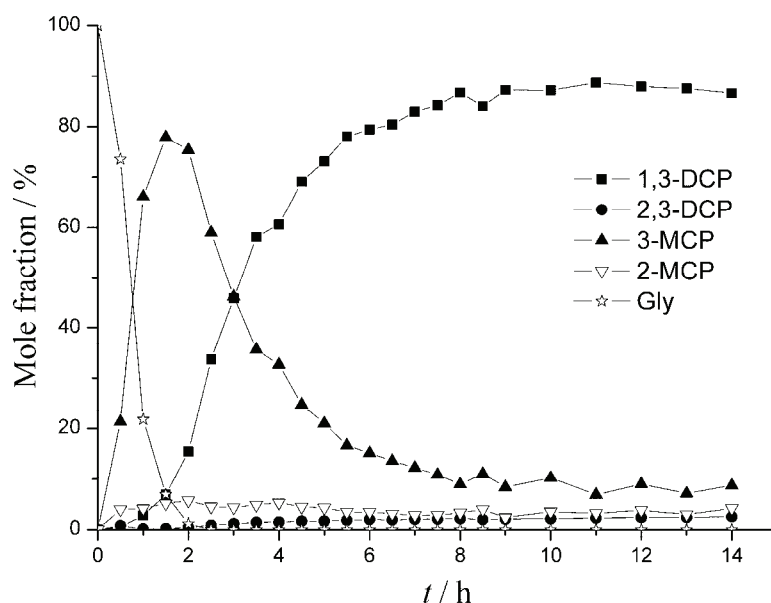
Fig. 8. Evolution of the composition in the glycerol chlorination process under optimum conditions.

The kinetic constants at various temperatures were calculated by non-linear regression in Matlab, based on the kinetic model and the data of the time evolution of the composition, reported in Table I.

TABLE I. Rate constants of the positive reactions at different temperatures

t / °C	$k_1 \times 10^2$ / min^{-1}	$k_2 \times 10^4$ / min^{-1}	$k_3 \times 10^3$ / min^{-1}	$k_4 \times 10^5$ / min^{-1}
90	1.23	3.16	2.42	3.12
100	1.35	4.59	4.18	8.70
110	2.01	6.59	5.39	11.10
120	2.56	9.07	5.03	11.37

Then, according to the Arrhenius equation:

$$\ln k = -\frac{E_a}{RT} + b \tag{4}$$

the slopes, namely the activation energy of the tandem reactions, were determined by plotting –ln k as the ordinate against $1/RT$ as the abscissa. The obtained

values were: $E_a(1) = 30.7$ kJ mol^{-1}, $E_a(2) = 41.8$ kJ mol^{-1}, $E_a(3) = 29.4$ kJ mol^{-1} and $E_a(4) = 49.5$ kJ mol^{-1}. The kinetic constants were then introduced into kinetic equations and the results were in good agreement with experimental data, as shown in Fig. 9, which demonstrates that this kinetic model can predict the chlorination process behavior very well.
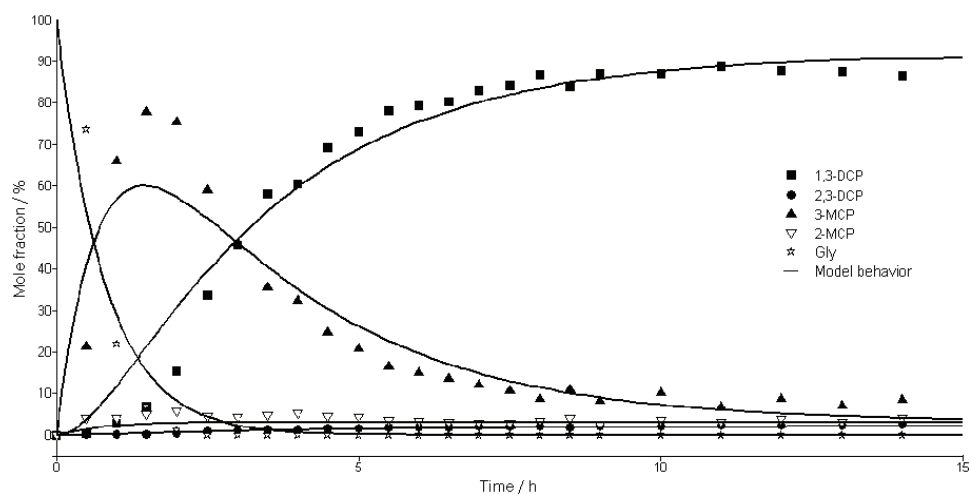
Fig. 9. Comparison between the experimental data and the behavior
predicted by the proposed model.

CONCLUSIONS

A convenient and accurate gas chromatography–mass spectrometry method that can simultaneously determine the composition of glycerol chlorination products was first established. The possibility of distinguishing the isomers of mono-chloropropanediol and dichloropropanol in the reaction products from the mass spectra of the individual products provided the basis for further study of the reaction kinetics and industrial production.

The dynamic behavior of the glycerol chlorination reaction was investigated and a new dynamic model was proposed. According to regression fitting of the experimental data, kinetic equations were obtained and the activation energy of each positive tandem reaction was calculated as follows: $E_a(1) = 30.7$ kJ mol^{-1}, $E_a(2) = 41.8$ kJ mol^{-1}, $E_a(3) = 29.4$ kJ mol^{-1} and $E_a(4) = 49.5$ kJ mol^{-1}. The fitting curves were in good agreement with the experimental data.

И З В О Д

ИСПИТИВАЊЕ КИНЕТИКЕ И МЕХАНИЗМА РЕАКЦИЈЕ ХЛОРОВАЊА ГЛИЦЕРОЛА ГАСНО–МАСЕНОМ СПЕКТРОМЕТРИЈОМ

XIUQUAN LING[1], DINGQIANG LU[1,2], JUN WANG[1], MINGXIN LIANG[1], SHUMIN ZHANG[1], JIANHUI CHEN[1] и PINGKAI OUYANG[1]

[1]*State Key Laboratory of Materials-Oriented Chemical Engineering, College of Life Science and Pharmaceutical Engineering, Nanjing University of Technology, Nanjing 210009 и* [2]*Jiangsu Provincial Institute of Materia Medica, Nanjing 210009, China*

Као примарни споредни производ у производњи биодизела, глицерол се може употребити за синтезу важне супстанце епихлорхидрина, који настаје као интермедијерни производ у процесу хлоровања глицерола. Мада се тај процес користи у индустријским условима, мала пажња је била поклоњена анализи и сепарацији хлорираних производа реакције. У овом раду је испитана кинетика и механизам реакције и описан одговарајући и прецизан метод одређивања производа реакције. Применом гасно–масене спектрометрије утврђено је да производ реакције садржи 1,3-дихлоро 2-пропанол, 2,3-дихлоро 1-пропанол, 3-хлоро-1,2--пропандиол, 2-хлоро-1,3-пропандиол и глицерол. Због високе тачке кључања и добрих каталитичких особина адипинска киселина се показала као најбољи катализатор у овој реакцији. Предпостављен је механизам и развијен је нови кинетички модел ове реакције. Фитовањем експерименталних података добијене су следеће вредности за енергије активације појединачних ступњева: 30,7, 41,8, 29,4 и 49,5 kJ mol^{-1}. Овај рад, разјашњавајући кинетику и механизам процеса, поставља теоријску основу за инжењеризацију овог процеса.

(Примљено 21. новембра 2008, ревидирано 11. јуна 2009)

REFERENCES

1. S. H. Lee, D. R. Park, H. Kim, J. Lee, J. C. Jung, S. Y. Woo, W. S. Song, M. S. Kwon, I. K. Song, *Catal. Commun.* **9** (2008) 1920
2. G. Lewandowski, M. Bartkowiak, E. Milchert, *Oxid. Commun.* **31** (2008) 108
3. B. M. Bell, J. R. Briggs, R. M. Campbell, S. M. Chambers, P. D. Gaarenstroom, J. G. Hippler, B. D. Hook, K. Kearns, J. M. Kenney, W. J. Kruper, D. J. Schreck, C. N. Theriault, C. P. Wolfe, *Clean-Soil Air Water* **36** (2008) 657
4. S. H. Lee, D. R. Park, H. Kim, J. Lee, J. C. Jung, S. Park, K. M. Cho, I. K. Song, *React. Kinet. Catal. Lett.* **94** (2008) 71
5. E. C. Britton, R. L. Heindel, US 2,144,612 (1939)
6. E. C. Britton, H. R. Slagh, US 2,198,600 (1940)
7. D. J. Schreck, W. J. Kruper Jr., R. D. Varjian, M. E. Jones, R. M. Campbell, K. Kearns, B. D. Hook, J. R. Briggs, J. G. Hippler, WO 2006,020,234 (2006)
8. P. Kubicek, P. Sladek, I. Buricova, WO 2005,021,476 (2005)
9. P. Krafft, C. Franck, I. De Andolenko, R. Veyrac, WO 2007,054,505 (2007)
10. J. Gaca, G. Wejnerowska, *Anal. Chim. Acta* **540** (2005) 55
11. R. Schuhmacher, J. Nurmi-Legat, A. Oberhauser, M. Kainz, R. Krska, *Anal. Bioanal. Chem.* **382** (2005) 366
12. C. Crews, G. Le Brun, P. A. Brereton, *Food Addit. Contam.* **19** (2002) 343
13. L. Boden, M. Lundgren, K. E. Stensio, M. Gorzynski, *J. Chromatogr. A* **788** (1997) 195
14. W. C. Chung, K. Y. Hui, S. C. Cheng, *J. Chromatogr. A* **952** (2002) 185
15. R. Tesser, E. Santacesaria, M. Di Serio, G. Di Nuzzi, V. Fiandra, *Ind. Eng. Chem. Res.* **46** (2007) 6456
16. D. Siano, E. Santacesaria, V. Fiandra, R. Tesser, G. Di Nuzzi, M. Di Serio, WO 2006,111,810 (2006)
17. K. Phillipe, G. Patrick, G. Benoit, C. Sara, WO 2005,054,167 (2005).

Available online at www.shd.org.rs/JSCS/

Determination of Cd, Pb and As in sediments of the Sava River by electrothermal atomic absorption spectrometry

SIMONA MURKO[1], RADMILA MILAČIČ[1], MARJAN VEBER[2] and JANEZ ŠČANČAR[1]*

[1]*Department of Environmental Sciences, Jožef Stefan Institute, Jamova 39, 1000 Ljubljana and *[2]*Faculty of Chemistry and Chemical Technology, University of Ljubljana, Aškerčeva 5, 1000 Ljubljana, Slovenia*

Abstract: The applicability of nitric acid, palladium nitrate and a mixture of palladium and magnesium nitrate as matrix modifiers was estimated for the accurate and reproducible determination of cadmium (Cd), lead (Pb) and arsenic (As) in sediments of the Sava River by electrothermal atomic absorption spectrometry, ETAAS. Decomposition of the samples was done in a closed vessel microwave-assisted digestion system using nitric, hydrochloric and hydrofluoric acids, followed by the addition of boric acid to convert the fluorides into soluble complexes. The parameters for the determination of Cd, Pb and As in sediments were optimised for each individual element and for each matrix modifier. In addition, two sediment reference materials were also analysed. In determination of Cd and Pb, nitric acid was found to be the most appropriate matrix modifier. The accurate and reliable determination of Cd and Pb in sediments was possible also in the presence of boric acid. The use of a mixture of palladium and magnesium nitrate efficiently compensated for matrix effects and enabled the accurate and reliable determination of As in the sediments. Quantification of Cd and As was performed by calibration using acid matched standard solutions, while the standard addition method was applied for the quantification of Pb. The repeatability of the analytical procedure for the determination of Cd, Pb and As in sediments was ±5 % for Cd, ±4 % for Pb and ±2 % for As. The *LOD* values of the analytical procedure were found to be 0.05 mg/kg for Cd and 0.25 mg/kg for Pb and As, while the *LOQ* values were 0.16 mg/kg for Cd and 0.83 mg/kg for Pb and As. Finally, Cd, Pb and As were successfully determined in sediments of the Sava River in Slovenia.

Keywords: cadmium; lead; arsenic; sediments; closed vessel microwave assisted digestion; ETAAS.

113

Available online at www.shd.org.rs/JSCS/

INTRODUCTION

Concern over the presence of pollutants, including metals, has resulted in the development of numerous analytical procedures for their selective and sensitive determination in different environmental and biological samples. Sediments have been frequently analysed in order to estimate the extent of pollution and the impact of anthropogenic activities on the environment. They are known to register changes in the environment and the impact due to industrial pollution, hence providing important information about the contamination of rivers, lakes, estuarine waters and other aquatic systems. Using the results of the analysis, temporal and spatial changes in the concentrations of the pollutants in the environment can be estimated.[1,2] For the evaluation of the metal burden in sediments, the total metal concentration is commonly measured.[1,3–5] In routine analysis, decomposition with strong acid solutions, *e.g.*, different mixtures of concentrated inorganic acids, including hydrofluoric acid[1,6–9] or *aqua regia* digestion[1,9–11] was often applied. The concentration of a particular metal determined after aqua regia treatment was considered as the pseudo total concentration.[1] Determination of trace amounts of Cd, Pb and As in environmental samples (sediment, soil, sewage sludge, coal, fly ash, surface and underground water, *etc*.) is of great importance due to their toxicological importance and persistent character in the environment and living organisms.[12] Numerous analytical techniques, *e.g*., flame or electrothermal atomic absorption spectrometry (FAAS or ETAAS), inductively coupled plasma atomic emission spectrometry (ICP–AES), inductively coupled plasma mass spectrometry (ICP–MS), atomic fluorescence spectrometry (AFS), X-ray fluorescence spectrometry (XRF) and neutron activation analysis (NAA) are available for the determination of trace metals.[13] Among them, ETAAS is one of the most frequently employed analytical techniques for the determination of low concentrations of elements present in environmental samples due to its high sensitivity, selectivity, simplicity and low detection limits. However, when trace metal concentrations in environmental samples are determined by ETAAS, high background absorption and interference effects of complex inorganic matrices and high salt contents, which can have distinct effects on the accuracy of an analysis, have to be considered. For a specific sample matrix, measurement parameters should be optimized for each particular element, or for groups of elements that are simultaneously determined, when a multi-element ETAAS system is applied.[14–16] Additionally, a chemical modification technique was used to minimize both the background absorption signals and interference effects.[17,18] The choice of matrix modifier depended not only on the matrix composition, but also on the specific characteristics of a particular element in ETAAS determinations.[16,19–26]. In the analysis of samples with complex matrices, mixed and composite modifiers rather than individual ones are often preferred. As thermal sta-

bilizers, they often permit higher ashing temperatures than their individual components.[27]

A great number of substances have been investigated as matrix modifiers. Palladium nitrate ($Pd(NO_3)_2$) and magnesium nitrate ($Mg(NO_3)_2$) are considered as universal modifiers for ETAAS.[28–33] The most commonly applied matrix modifiers for Cd and Pb analysis by ETAAS were palladium nitrate and palladium––magnesium nitrate.[28,30,32,33–35] Combined matrix modifier consisting of scandium, palladium nitrate and ammonium nitrate was also proposed for Cd and Pb determinations in environmental samples.[36] For As determination by ETAAS, a mixture of palladium and magnesium nitrate was most frequently used.[24,28–30,32] In addition to palladium nitrate and magnesium nitrate-based modifiers, many other compounds have shown modifier properties. Dilute nitric acid was an appropriate matrix modifier for the determination of trace elements in various biological samples[19] Platinum group elements (Pt, Pd, Ir, Rh and Ru) or carbide forming elements (Zr, Nb, Ta, W) may act as permanent modifiers. Alone or in a mixture, they are frequently used for the determination of Cd, Pb and As in environmental samples.[10,12,25,37–39]

To the best of our knowledge, there are no studies in literature concerning the effects of boric acid on the performance of modifiers in the determination of volatile elements, such as Cd, Pb and As, by ETAAS. These elements are frequently determined in sediments after closed-vessel microwave digestion, which requires the use of nitric acid, hydrochloric acid and hydrofluoric acid, followed by the addition of boric acid to convert the fluorides into soluble complexes. In such complex sample matrixes, the use of an appropriate modifier is of critical importance for their reliable determination. The aim of this study was to optimise the measurement parameters and evaluate the applicability of various matrix modifiers for the determination of Cd, Pb and As in sediment samples after closed-vessel microwave assisted digestion followed by ETAAS. The applicability of various matrix modifiers (nitric acid, palladium nitrate and a mixture of palladium and magnesium nitrate) for the determination of the total metal concentrations was examined by analysis of the sediment reference materials CRM 277 and SRM 2704. The optimized analytical procedures were used for the determination of Cd, Pb and As in sediments of the Sava River in Slovenia.

EXPERIMENTAL

Reagents and reference materials

Merck suprapur acids (hydrochloric, nitric and hydrofluoric acid) were used. Boric acid and a stock standard solution of As (1000±2 mg/L in 5 % nitric acid) were purchased from Fluka. A stock standard solution of Cd and Pb (1000±2 mg L^{-1} in 5 % nitric acid), a stock solution of palladium nitrate and magnesium nitrate (10.0±0.2 g L^{-1}) were obtained from Merck. Fresh working standard solutions were prepared by dilution of a particular stock solution with Milli-Q water (Direct-Q 5 Ultrapure water system, Millipore Watertown, MA, USA) and used

in the determination of the total metal concentration. Nitric acid modifier was prepared by dilution of concentrated nitric acid with water 1:3. Palladium nitrate modifier was prepared by dilution of the stock solution with water so that the final concentration of palladium nitrate was 0.2 %. A mixture of palladium and magnesium modifier contained 0.8 mL of 0.2 % palladium nitrate and 0.2 mL of 1 % magnesium nitrate. Two reference materials were used, CRM 277 (trace elements in an estuarine sediment, BCR, Geel, Belgium) and SRM 2704 (Buffalo River sediment, NIST, National Institute of Standards and Technology, USA). All the glassware employed during the analytical procedures was soaked overnight in 10 % (v/v) nitric acid solution, rinsed with Milli-Q water and dried at room temperature.

Instrumentation

Cd, Pb and As were determined by ETAAS on a Hitachi Z-8270 polarized Zeeman atomic absorption spectrophotometer (Tokyo, Japan) equipped with an autosampler. Cd was determined at 228.8 nm, Pb at 283.3 nm and As at 193.7 nm. The spectral bandwidth was 1.30 nm for all analysed elements. The lamp current was 7.5 mA for Cd and Pb and 10 mA for As. 10 μL of sample was introduced into the graphite tube for Cd and Pb determinations and 20 μL for As. 5 μL of modifier was applied into the graphite tube before sample introduction. The wall of pyrolitically coated graphite tubes was used for atomization. The peak areas of the analytical signals were measured.

All samples were digested in a closed-vessel microwave digestion system, CEM MARS 5, CEM Corporation, (Matthews, North Carolina, USA).

Sampling site

The sediments were collected at the sampling sites shown in Fig. 1 along the Sava River in Slovenia. Manual sampling was performed by e use of plastic core liners. The samples of the top layer of the sediment (5 cm) from the shore were collected in polyethylene containers together with surrounding water, transported to the laboratory and stored at 4 °C until analysis., About 3 kg of sample were collected from each location.

Fig. 1. Sampling sites: 1. Mojstrana, 2. Jesenice, 3. Jevnica, 4. Vrhovo,
5. Brežice and 6. Jesenice na Dolenjskem.

In the Slovenian part of the basin, the riverbed is relatively steep and formed from solid rock. Therefore, the samples were taken from the reaches where sediment deposition occurs, usually only a few meters from the riverbank. At the locations Jesenice and Vrhovo, the sediments were sampled just before the hydroelectric dams.

Sample preparation

The sediments were spread on polyethylene foil and divided into four squares. Two diagonal squares were discarded, while other two were mixed and subjected to the same procedure again. The procedure was repeated until approximately 100 g sample remained. The last 100 g of sample was then dried at 40 °C for three days (until constant weight) in the dark, homogenised in an agate mortar and sieved through a 63 µm sieve. Before analysis, the flasks containing the dry sediment samples were shaken virogously for one minute. 0.250±0.001 g of sediment was weighed into a Teflon vessel, 4 mL of nitric acid, 2 mL of hydrofluoric acid and 1 mL of hydrochloric acid were added. Vessels were gently shaken until all the sample was wetted with acid, covered by vessel cups and submitted to closed vessel microwave digestion at the maximal power of 1200 W. The digestion procedure was performed using the following programme, ramp to temperature 30 min (t = 190 °C), hold 60 min (t = 190 °C) and cool 30 min. Subsequently, the Teflon vessels were vented and the vessel caps removed. 12.5 mL of boric acid (4 % w/v) was added to each vessel in order to dissolve the fluorides. The closed--vessel microwave digestion was then applied for a second time using the following programme, ramp to temperature 15 min (t = 190 °C), hold 30 min (t = 190 °C) and cool 30 min. After the digestion, a clear solution was obtained. The contents of the vessels were quantitatively transferred to 30 mL graduated polypropylene flasks and filled to mark with Milli-Q water. These samples were used for the ETAAS determinations. The same digestion procedure, with the exception that no sample was added, was applied to determine blanks. All analyses were realised in duplicate.

Two parallel aliquots of 1 g of the sediment samples were dried to constant weight at 60 °C in order to determine their moisture content. The results of the concentrations of Cd, Pb and As are expressed on the basis of the dry mass.

The ETAAS determinations were realised under clean room conditions (class 10000).

RESULTS AND DISCUSSION

Optimisation of the ashing temperature in electrothermal temperature programme for determination of Cd, Pb and As in sediment samples by ETAAS

For accurate and reliable determinations of the total concentrations of Cd, Pb and As by ETAAS in digested environmental samples, the experimental parameters should be optimised for each particular element and specific sample matrix. In the present work, each stage of the electrothermal temperature programme was optimised with and without modifier with special attention given to the ashing temperature. The efficiencies of three different matrix modifiers, *i.e.*, nitric acid, palladium nitrate, and a mixture of palladium and magnesium nitrate, were compared. In the optimization procedure, the highest ashing temperature was experimentally determined. For this purpose, the intensities (peak area) of the analytical atomic absorption signals and the background absorbance signals of working standard solutions containing 2.5 ng mL^{-1} of Cd and 40 ng mL^{-1} of Pb and As

were measured. Aqueous standard solutions were prepared as well as standard solutions in a mixture of acids by applying the sample digestion procedure described above under Sample preparation. The aqueous standard solutions contained 0.5 % (v/v) nitric acid to maintain the analytes in solution. The optimization was commenced without modifier, the addition of modifier followed in the following order: nitric acid, palladium nitrate and the mixture of palladium and magnesium nitrate. To exclude the influence of one modifier on another, the graphite tube was changed after application of a particular modifier. The absorbance signals (peak area) for Cd, Pb and As were measured three times for each parameter under the electrothermal temperature programmes presented in Table I.

TABLE I. Measurement parameters (electrothermal temperature programme) for the determination of Cd, Pb and As in sediments by ETAAS with Zeeman background correction; wavelength, Cd: 228.8 nm; Pb: 283.3 nm; As: 193.7 nm; spectral bandwidth, 1.30 nm; lamp current, 7.5 mA for Cd and Pb, 10 mA for As; sample volume, 10 μL for Cd and Pb, 20 μL for As; modifier volume: 5 μL (before sample introduction)

Stage No.	Metal	Temp. start, °C	Temp. end, °C	Time ramp, s	Time hold, s	Gas flow, mL min^{-1}
1			Dry			
	–	50	90	10	5	200
2			Dry			
	–	90	100	10	5	200
3			Dry			
	–	100	140	10	5	200
3[a]		140	200	20	0	200
4			Ash			
	Cd	140	b	10	15	100
	Pb	140	b	10	15	100
	As	200	b	10	20	100
5			Atomization			
	Cd	1500	1500	0	4	0
	Pb	2000	2000	0	4	0
	As	2500	2500	0	4	0
6			Clean			
	Cd	1800	1800	0	5	200
	Pb	2200	2200	0	5	200
	As	2600	2600	0	5	200
7			Cool			
	–	–	–	0	5	200

[a]Only for As; [b]optimal temperature of the appropriate matrix modifier

Special attention was devoted to the optimisation of the ashing temperature. Hence, for each element, the influence of the ashing temperature on the absorption signal was studied over a wide temperature range. The results of the opti-

misation of the ashing temperatures for Cd, Pb and As are presented in Figs. 2–4, respectively.
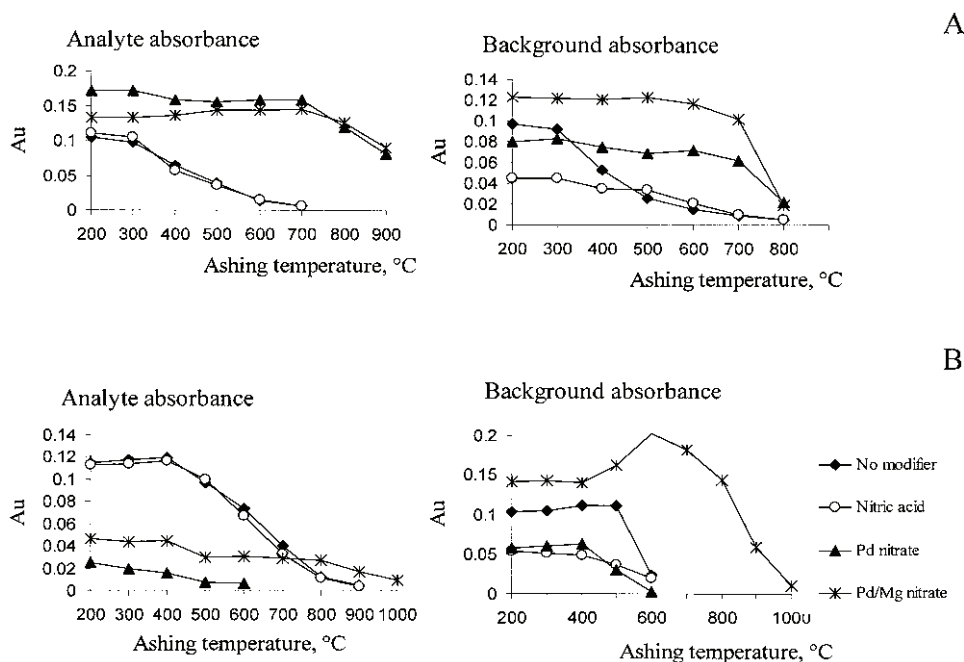
Fig. 2. Optimization of the ashing temperature for Cd in standards (2.5 ng mL^{-1}) prepared in water (A) and in acids used for digestion of the sediments (B). Analyte and background absorbance represent peak area signals expressed in arbitrary units

Data from Fig. 2A and 3A indicate almost the same response of the analytic absorbance signals for Cd and for Pb standards prepared in water if no modifier or nitric acid was used, while the background absorbances were lower when nitric acid was applied. The loss of free Cd and Pb atoms occurred at temperatures higher than 300 and 400 °C, respectively. Palladium nitrate and the mixture of palladium and magnesium nitrate allowed the temperature to be increased up to 700 °C without loss of free Cd atoms and up to 1200 °C without loss of free Pb atoms.

Data from Fig. 2B and 3B further indicate nearly the same response of the analytic absorbance signals for Cd and Pb standards prepared in the acids used for digestion if no modifier or nitric acid was used. Again, the background absorbance was lower when nitric acid was applied. The loss of free Cd atoms occurred at a temperature higher than 400 °C and of free Pb atoms at temperature higher than 300 °C. The addition of palladium nitrate or the mixture of palladium and magnesium nitrate resulted in a substantial losses of free Cd and Pb atoms. The intensity of this effect increased with increasing ashing temperature. It was

experimentally proven that these interferences arose from boric acid, which was applied in the closed vessel microwave digestion of the samples. Nitric acid that efficiently transformed the matrix components to nitrates enabled retention of the Cd and Pb atoms within the graphite tube up to temperatures of 400 °C and 300 °C, respectively, also in the presence of boric acid. Since nitric acid also minimized the background absorption signals, accurate and repeatable measurements of Cd and Pb concentrations in the acid mixture were possible.
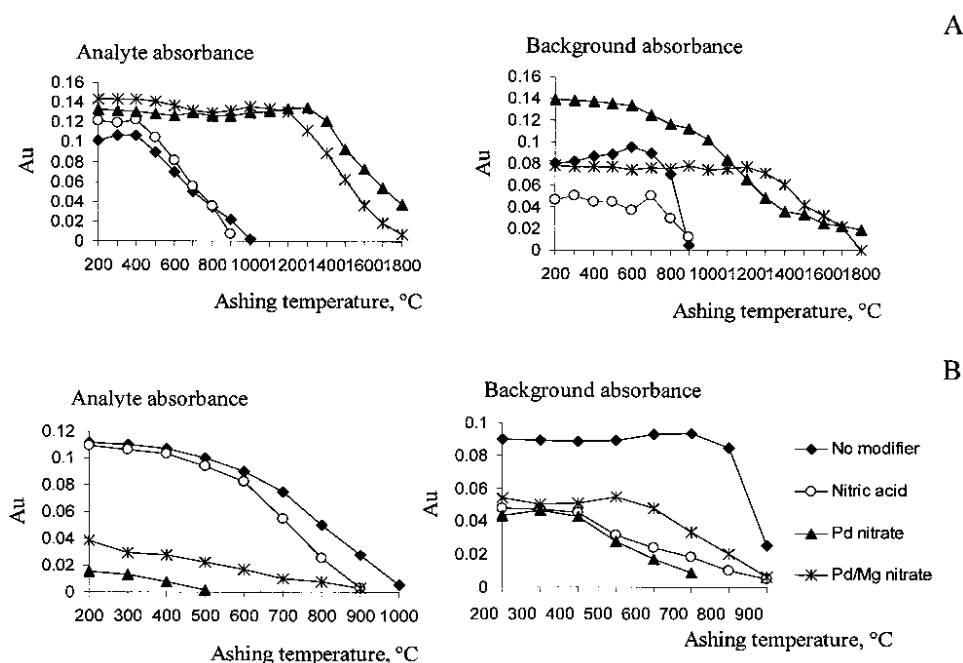
Fig. 3. Optimization of the ashing temperature for Pb in standards (40 ng mL^{-1}) prepared in water (A) and in acids used for digestion of the sediments (B). Analyte and background absorbances represent peak area signals expressed in arbitrary units.

Data from Fig. 4A showed low absorbances for the As standards prepared in water if no modifier was used. This effect is related to the high volatility of As at temperatures as low as 200 or 400 °C.[40] To prevent losses of analyte prior to the atomization step, modifiers based on palladium nitrate or mixtures of palladium and magnesium nitrate are generally recommended.[40] Data from Fig. 4A further indicate that for As standards prepared in water, the use of palladium nitrate and the mixture of palladium and magnesium nitrate enabled the rising of the ashing temperature to be increased up to 1400 °C, while the background absorbance was appreciably lower when a mixture of palladium and magnesium nitrate was applied.
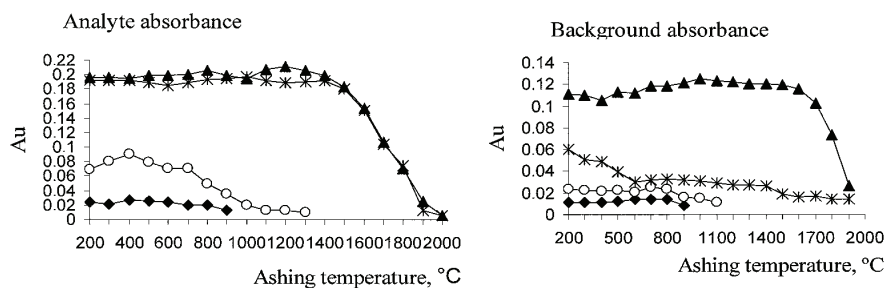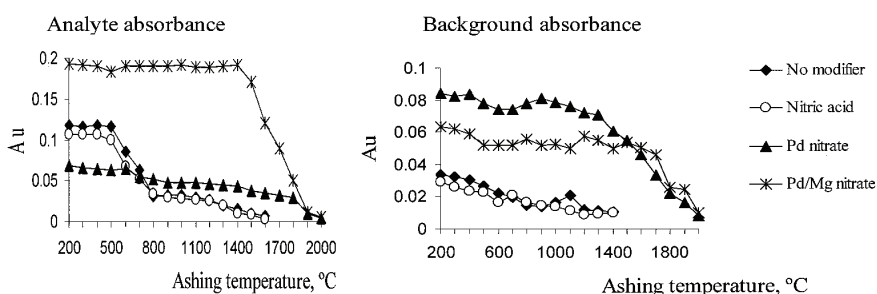
Fig. 4. Optimization of the ashing temperature for As in standards (40 ng mL^{-1}) prepared in water (A) and in acids used for digestion of the sediments (B). Analyte and background absorbances represent peak area signals expressed in arbitrary units.

Data from Fig. 4B indicate that for the As standards prepared in the acids used for digestion, the responses of analytical absorbance signals were low when no modifier, or nitric acid and palladium nitrate modifier were used. The employment of the mixture of palladium and magnesium nitrate modifier efficiently stabilised the free As atoms even in the presence of boric acid up to a temperature of 1400 °C. In addition, the background absorbance was low enough to enable compensation by the Zeeman correction.

Although Cd, Pb and As are all volatile elements, the obtained experimental data demonstrated that there is no universal modifier for all three elements, when they are analysed in the presence of boric acid, making the simultaneous multi-element determination of Cd, Pb and As by ETAAS impossible.

To examine the performances of the modifiers in the determination of Cd, Pb and As in sediments by ETAAS, sediment reference materials were further analysed after closed-vessel microwave assisted digestion.

Analysis of sediment reference materials and comparison of the performances of various matrix modifiers

In order to check the accuracy and precision in the determination of Cd, Pb and As in sediments, two reference materials, CRM 277 and SRM 2704, with dif-

ferent concentration ranges of the investigated elements and different sample matrices were analysed. The concentrations of Cd, Pb and As were determined by ETAAS using the optimised electrothermal temperature programme. The samples were digested according to the procedure described above under sample preparation. Three modifiers were used: nitric acid, palladium nitrate and the mixture of palladium and magnesium nitrate. The optimal ashing temperatures based on findings from Figs. 2 to 4 were applied for each element and each matrix modifier. Standards prepared in the acids used for digestion and the standard addition method was used for calibration. Analysis of the reference materials were realised in six parallel determinations. Each sample was measured three times and the average value was calculated. The results of the determination of Cd, Pb and As in the reference materials CRM 277 and SRM 2704 are presented in Table II. The results that agree the best with the certified values are given in bold type. From these data, the optimal modifier and the optimal mode of calibration for an individual element is also evident.

Table II. Concentrations (average of six parallel samples ± standard deviation) of Cd, Pb and As (mg kg^{-1}) in certified reference materials CRM 277 and SRM 2704. The calibration was performed by a working curve using acid-matched standards (A) and by the use of the standard addition method (B). Temperature (t / °C) represents the optimal ashing temperature for Cd and Pb, while t^a / °C is the optimal ashing temperature for As

Element/ /sample	Nitric acid $t = 300$ °C A / mg kg^{-1}	Pd nitrate $t = 300$ °C $t^a = 400$ °C A / mg kg^{-1}	Pd/Mg nitrate $t = 400$ °C $t^a = 700$ °C A / mg kg^{-1}	Nitric acid $t = 300$ °C B / mg kg^{-1}	Pd nitrate $t = 300$ °C $t^a = 400$ °C B / mg kg^{-1}	Pd/Mg nitrate $t = 400$ °C $t^a = 700$ °C B / mg kg^{-1}	Certified value
Cd CRM 277	11.6 ± 0.2	13.0 ± 0.6	10.8 ± 0.3	16.2 ± 0.2	11.8 ± 0.8	14.0 ± 0.3	11.9 ± 0.4
SRM 2704	3.60 ± 0.17	3.58 ± 0.21	2.38 ± 0.38	5.47 ± 0.17	3.74 ± 0.15	4.18 ± 0.51	3.45 ± 0.22
Pb CRM 277	119 ± 4	179 ± 4	159 ± 4	145 ± 2	143 ± 1	145 ± 2	146 ± 3
SRM 2704	137 ± 6	211 ± 11	154 ± 1	166 ± 6	150 ± 9	146 ± 7	161 ± 17
As CRM 277	29.8 ± 2.9	26.5 ± 3.6	48.5 ± 0.4	60.5 ± 5.6	47.8 ± 4.0	49.1 ± 1.3	47.3 ± 1.6
SRM 2704	14.9 ± 1.2	29.9 ± 2.8	23.7 ± 0.3	11.5 ± 0.6	46.2 ± 7.8	37.4 ± 1.9	23.4 ± 0.8

Data from Figs. 2 and 3, and Table II, indicate that nitric acid is an appropriate modifier for the determination of both Cd and Pb in sediment samples after application of the optimal ashing temperature. Furthermore, the data from Table II indicate good agreement between the determined and certified values of the Cd concentrations in the reference materials when acid-matched standard solutions were used for calibration. The application of other modifiers or the standard addition method gave worse or unsatisfactory recoveries for Cd in the analysed reference sediment materials. It is also evident from the data presented in Table II that good agreement between the determined and certified values were obtained for the Pb concentrations in the reference materials when the standard addition

method was applied in the calibration procedure. The employment of other modifiers or acid matched standard solutions gave worse or unsatisfactory recoveries for Pb in the analysed reference sediment materials.

Data from Fig. 4 and Table II indicate that on application of the optimal ashing temperature, a mixture of palladium and magnesium nitrate is an appropriate modifier for the determination of As in sediment samples. Data from Table II further indicate good agreement between the determined and certified values of the As concentrations in the reference materials when acid-matched standard solutions were applied in the calibration procedure. Other modifiers or the use of the standard addition method did not efficiently compensate the matrix effects and, consequently, the agreement between the determined and certified As values was poor.

Based on the present investigation of the performances of nitric acid, palladium nitrate and the mixture of palladium and magnesium nitrate modifiers, and analysis of reference sediment materials after closed-vessel microwave assisted digestion of the samples, it was experimentally demonstrated that the optimal conditions for ETAAS determination of Cd and Pb in sediment samples are when nitric acid at an ashing temperature of 300 °C was applied as the matrix modifier. Accurate and reliable results were obtained for Cd when acid-matched standard solutions were employed for calibration, while for Pb, the standard addition method should be applied in the calibration procedure. For accurate and reliable determination of As in sediments, the optimal modifier is a mixture of palladium and magnesium nitrate at an ashing temperature of 700 °C and the application of acid-matched standard solutions in the calibration procedure.

Linearity, repeatability, limit of detection and limit of quantification

It was experimentally proven that the linearity of the ETAAS determinations ranged from 0.5 to 5 ng mL^{-1} for Cd and from 5 to 50 ng mL^{-1} for Pb and As. The correlation coefficients were better than 0.998 for the three determined elements.

The repeatability of the analytical procedure for the determination of Cd, Pb and As in sediments by ETAAS under optimal conditions was checked by the analysis of six parallel samples of the reference sediment materials CRM 277 and SRM 2704. The results indicated that the repeatability of measurement was ± 5 % for Cd, ± 4 % for Pb and ± 2 % for As.

The limits of detection of the analytical procedure calculated on a 3 *s* basis (the value of three times the standard deviation of the blank) were found to be 0.05 mg kg^{-1} for Cd and 0.25 mg kg^{-1} for Pb and As, while the limits of quantification calculated on a 10 *s* basis (a value of ten times the standard deviation of the blank) were 0.16 mg kg^{-1} for Cd and 0.83 mg kg^{-1} for Pb and As.

Analysis of sediment samples of the Sava River

The optimised analytical procedure for the determination of Cd, Pb and As by ETAAS was applied in the analysis of Sava River sediments. The results of the analysis of the Sava River sediments are presented in Fig. 5. To estimate the environmental status of the sediments of the Sava River, the EPA sediment quality guideline was followed.[41] This guideline proposes the maximal concentrations of chemical compounds that maintain healthy aquatic life associated with bed sediments. The TEL values (threshold effects level) in the EPA guideline refer to the range of concentrations below which adverse toxic effects are not to be expected or are only occasionally observed.[41]
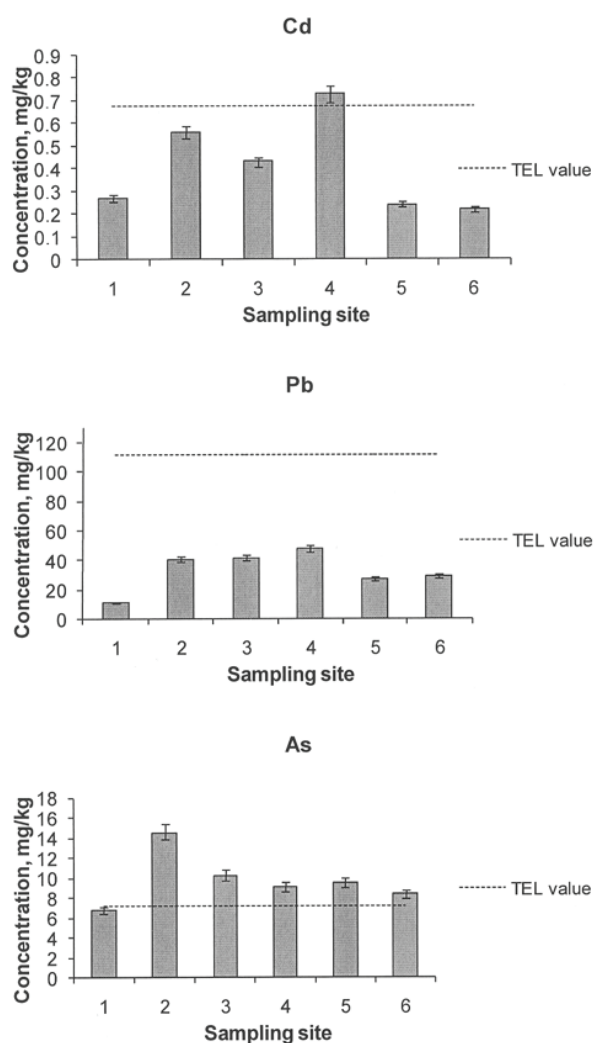
Fig. 5. Concentrations of Cd, Pb and As (mg kg^{-1}) in sediments of the Sava River determined by ETAAS. The results represent the average of two parallel samples. In each bar, the two concentrations that characterize the mean value are indicated.

Data of Fig. 5 indicate that the concentrations of Cd in the sediments of the Sava River were low and ranged between 0.22 and 0.73 mg kg^{-1}. The highest Cd concentration that slightly exceeded the TEL value (0.676 mg kg^{-1})[41] was found in the accumulation basin of the hydroelectric power plant Vrhovo (sampling site 4). The cadmium concentrations in the sediments of the Slovenian part of the Sava River are comparable to previously reported data[42] and to the majority of concentrations determined in River Po (0.4 to 1.4 mg kg^{-1})[43] and are lower than most of the Cd concentrations determined in the sediments of the Danube River (around 2 up to 25 mg Cd kg^{-1})[44] and the Seine River (1 to 2 mg Cd kg^{-1}).[45] Cadmium concentrations are also much lower than those determined at mining area sites (2 to 130 mg Cd kg^{-1}),[2] (around 0.7 up to 7.3 mg Cd kg^{-1})[46] and (2 to 9 mg d kg^{-1})[47]).

Furthermore, the results presented in Fig. 5 indicate that the concentrations of Pb in the sediments of the Sava River ranged between 11 and 48 mg kg^{-1}, which are below the TEL value (112 mg kg^{-1}).[41] The highest Pb concentrations were found in the accumulation basins of the hydroelectric power plants at Jesenice (sampling site 2) and Vrhovo (sampling site 4), as well as at Jevnica (sampling site 3). The lead concentrations in the Slovenian part of the Sava River are in general comparable to previously reported data (around 40 up to 60 mg Pb kg^{-1})[48] and to concentrations of Pb in River Po (40 to 70 mg Pb kg^{-1})[45] and in the Danube River (30 to 100 mg Pb kg^{-1})[44] and are much lower than those reported for mining areas (100 to 9000 mg Pb kg^{-1})[2] and (500 to 5000 mg Pb kg^{-1}).[47]

From the data of Fig. 5, it can be also seen that the concentrations of As in the Slovenian part of the Sava River sediments range from 6.8 to 14.6 mg As kg^{-1}. These As concentrations in general slightly exceed the TEL value (7.24 mg kg^{-1})[41] Since the As concentrations are also close to the TEL value at the sampling site Mojstrana, an unpolluted area near the origin of the Sava River, the concentrations of As in the investigated sediments are most probably characterized by the natural background value of As. The arsenic concentrations in the sediments from the Slovenian part of the Sava River are in general comparable to those of its tributary Savinja and the Rivers Voglajna and Hudinja (around 16 mg As kg^{-1})[46] and are in general lower than those reported for the Danube River (9.0 to 68.9 mg As kg^{-1}).[45]

CONCLUSIONS

The parameters for the determination of Cd, Pb and As in sediments after closed-vessel microwave assisted digestion by ETAAS with Zeeman background correction were optimised. For the decomposition of the samples, a mixture of nitric, hydrochloric and hydrofluoric acids was applied, followed by the addition of boric acid to dissolve the insoluble fluorides. To compensate the matrix effects, the applicability of nitric acid, palladium nitrate and a mixture of palladium

Available online at www.shd.org.rs/JSCS/

and magnesium nitrate modifiers were evaluated for accurate and reproducible determination of Cd, Pb and As in sediments. Nitric acid, which was applied for the first time in the analysis of sample matrixes, that contained boric acid, was found to be the most efficient matrix modifier for the determination of Cd and Pb in sediment samples. By chemical transformation of the matrix components to nitrates with consequential reduction of the background signal, accurate and reliable determinations of Cd and Pb were achieved at an ashing temperature of 300 °C. For the determination of As, the optimal modifier was found to be a mixture of palladium and magnesium nitrate. It allowed the efficient compensation of matrix effects, prevented the loss of analyte at an ashing temperature of 700 °C, and enabled the accurate and reliable determination of As in sediments. For the quantification of Cd and As, the best results were obtained when acid-matched standard solutions were employed in the calibration procedure, while for the quantification of Pb, the standard addition method should be applied.

The optimised analytical procedures were successfully applied in the determination of Cd, Pb and As in sediments of the Sava River in Slovenia. The results indicated that the concentrations of Cd, Pb and As were in general lower than those reported for other moderately polluted rivers in Europe.

ИЗВОД

ОДРЕЂИВАЊЕ Cd, Pb И As ИЗ НАСЛАГА РЕКЕ САВЕ ЕЛЕКТРОТЕРМИЧКОМ АТОМСКОМ АПСОРПЦИОНОМ СПЕКТРОМЕТРИЈОМ

SIMONA MURKO[1], RADMILA MILAČIČ[1], MARJAN VEBER[2] и JANEZ ŠČANČAR[1]

[1]Department of Environmental Sciences, Jožef Stefan Institute, Jamova 39, 1000 Ljubljana и [2]Faculty of Chemistry and Chemical Technology, University of Ljubljana, Aškerčeva 5, 1000 Ljubljana, Slovenia

Применљивост азоте киселине, паладијум-нитрата и смеше паладијум- и магнезијум-нитрата као модификатора матрице оцењена је у случају поузданог и репродуктивног одређивања кадмијума, олова и арсена из наслага реке Саве електротермичком атомском апсорпционом спектрометријом, ETAAS. Узорци су разграђени у затвореном микроталасном дигестору помоћу азоте, хлороводоничне и флуороводоничне киселине, уз накнадно додавање борне киселине, чиме су флуориди преведени у растворне комплексе. Параметри одређивања Cd, Pb и As у наслагама оптимизовани су за сваки елемент и сваки модификатор матрице понаособ. Такође су анализирана два референтна материјала наслага. Азотна киселина се показала као најпогоднији модификатор матрице за одређивање Cd и Pb. Тачно и поуздано одређивање Cd и Pb из наслага било је могуће и у присуству борне киселине. Утицај матрице је успешно компензован употребом смеше паладијум- и магнезијум-нитрата, што је омогућило тачно и поуздано одређивање As из наслага. Квантитативно одређивање Cd и As урађено је помоћу калибрације стандардим растворима за киселу средину, док је за квантитативно одређивање Pb примењена стандардна метода адиције. Репродуктивност аналитичке процедуре за одређивање Cd, Pb и As из наслага износила је ±5, ±4 и ±2 %, редом. *LOD* вредности аналитичке процедуре износиле су 0,05 mg/kg за Cd и 0,25 mg/kg за Pb и As, док

Available online at www.shd.org.rs/JSCS/

су *LOQ* вредности износиле 0,16 mg/kg за Cd и 0,83 mg/kg за Pb и As. На крају, Cd, Pb и As су успешно одређени из наслага реке Саве дуж тока кроз Словенију.

(Примљено 12. јануара, ревидирано 11. јуна 2009)

REFERENCES

1. J. Ščančar, R. Milačič, M. Horvat, *Water Air Soil Pollut.* **118** (2000) 87
2. P. Svete, R. Milačič, B. Pihlar, *J. Environ. Monit.* **3** (2001) 586
3. M. Ravanelli, O. Tubertini, S. Valcher, W. Martinotti, *Water Air Soil Pollut.* **99** (1997) 697
4. P. Avila-Perez, U. M. Balcazar, G. Zarazua-Ortega, I. Barcelo-Quintal, C. Diaz- Delgado, *Sci. Total Environ.* **234** (1999) 185
5. K. Chen, J. J. Jiao, *Environ. Pollut.* **151** (2008) 576
6. V. Sandroni, C. M. M. Smith, *Anal. Chim. Acta* **468** (2002) 335
7. C. Brunori, I. Ipolyi, L. Macaluso, R. Morabito, *Anal. Chim. Acta* **510** (2004) 101
8. J. Dai, J. Song, X. Li, H. Yuan, N. Li, G. Zheng, *Environ. Pollut.* **145** (2007) 656
9. ISO 11466 *International standard, Soil quality – extraction of trace elements soluble in aqua regia*, 03-01 (1995)
10. J. B. B. da Silva, M. M. M. da Silva, A. J. Curtius, B. Welz, *J. Anal. At. Spectrom.* **14** (1999) 1737
11. J. Sastre, A. Sahuquillo, M. Vidal, M. G. Rauret, *Anal. Chim. Acta* **462** (2002) 59
12. E. C. Lima, R. V. Barbosa, J. L. Brasil, A. H. D. P. Santos, *J. Anal. At. Spectrom.* **17** (2002) 1523
13. O. T. Butler, J. M. Cook, C. F. Harrington, S. J. Hill, J. Rieuwerts, D. L. Miles, *J. Anal. At. Spectrom.* **23** (2008) 249
14. M. Berglund, W. Frech, D. C. Baxter, B. Radziuk, *Spectrochim. Acta Part B* **48** (1993) 1381
15. P. R. M. Correia, C. S. Nomura, P. V. Oliveira, *Anal. Sci.* **19** (2003) 1519
16. J. P. Pancras, J. M. Ondov, R. Zeisler, *Anal. Chim. Acta* **538** (2005) 303
17. D. L. Tsalev, V. I. Slaveykova, P. B. Mandjukov, *Spectrochim. Acta Rev.* **13** (1990) 225
18. Z. M. Ni, Z. Rao, M. Li, *Anal. Chim. Acta* **334** (1996) 177
19. J. Ščančar, R. Milačič. I. Falnoga, M. Čemažar, P. Bukovec, *J. Pharm. Biomed. Anal.* **22** (2000) 993
20. A. V. Filgueiras, I. Lavilla, C. Bendicho, *Anal. Chim. Acta* **466** (2002) 303
21. O. Acar, *Anal. Chim. Acta* **526** (2004) 103
22. A. B. Volynsky, *Spectrochim. Acta B* **59** (2004) 1799
23. L. Husakova, J. Šramkova, T. Černohorsky, M. Barinova, *Talanta* **72** (2007) 1400
24. P. Bermejo-Barrera, M. C. Barciela-Alonso, J. Moreda-Piñeiro, C. González-Sixto, A. Bermejo-Barrera, *Spectrochim. Acta B* **51** (1996) 1235
25. E. C. Lima, J. L. Brasil, A. H. D. P. Santos, *Anal. Chim. Acta* **484** (2003) 233
26. J. A. Nobrega, J. Rust, C. P. Calloway, B. T. Jones, *Spectrochim. Acta Part B* **59** (2004) 1337
27. O. Acar, Z. Kiliç, A. R. Türker, *Anal. Chim. Acta* **382** (1999) 329
28. G. Schlemmer, B. Welz, *Spectrochim. Acta B* **41** (1986) 1157
29. B. Welz, G. Schlemmer, J. R. Mudakavi, *J. Anal. At. Spectrom.* **3** (1988) 93
30. B. Welz, G. Schlemmer, J. R. Mudakavi, *J. Anal. At. Spectrom.* **7** (1992) 1257
31. V. A. Granadillo, J. A. Navarro, R. A. Romeo, *J. Anal. At. Spectrom.* **8** (1993) 615
32. X. Q. Shan, B. Wen, *J. Anal. At. Spectrom.* **10** (1995) 791
33. J. Y. Cabon, A. Ke Bihan, *Spectrochim. Acta B* **51** (1996) 1245

34. M. C. Barciela-Alonso, P. Pazos-Capeáns, M. E. Regueira-Miguens, A. Bermejo-Barrera, P. Bermejo-Barrera, *Anal. Chim. Acta* **524** (2004) 115
35. M. B. O. Giacomelli, M. C. Lima, S. Volnei, R. M. de Carvalho Jr., J. B. B. da Silva, P. B. Barrera, *Spectrochim. Acta B* **57** (2002) 2151
36. O. Acar, *Talanta* **65** (2005) 672
37. E. C. Lima, F. Barbosa Jr., F. J. Krug, *Anal. Chim. Acta* **409** (2000) 267
38. F. Barbosa, Jr., E. C. Lima, F. J. Krug, *Analyst* **125** (2000) 2079
39. M. L. Munoz, A. J. Aller, *J. Anal. At. Spectrom.* **21** (2006) 329
40. M. V. Reboucas, S. L. C. Ferreira, B. Neto de Barros, *Talanta* **67** (2005) 195
41. EPA, *An overview of sediment quality in the United States. Report describes qualitatively the nature and extent of contaminated sediments*, 1999, 04-25-1999 http://www.epa.gov/waterscience/library/sediment/overview.pdf (accessed June, 2005)
42. S. Franciskovic-Bilinski, *Fresenius Environ. Bull.* **17** (2008) 188
43. D. Vignati, M. Pardos, J. Diserens, G. Ugazio, R. Thomas, J. Dominik, *Water Res.* **37** (2003) 2847
44. P. Woitke, J. Wellmitz, D. Helm, P. Kube, P. Lepom, P. Litheraty *Chemosphere* **51** (2003) 633
45. M. Meybeck, L. Lestel, P. Bonté, R. Moilleron, J.-L. Colin, O. Rousselot, D Hervé, C. de Pontèves, C. Grosbois, D. R. Thevénot, *Sci. Total Environ.* **375** (2007) 204
46. S. Franciskovic-Bilinski, H. Bilinski, D. Tibljaš, D. Hanžel, *Fresenius Environ. Bull.* **15** (2006) 220
47. J. C. Santos Bermejo, R. Beltrán, J. L. Gómez Ariza, *Environ. Internat*. **29** (2003) 69
48. V. Orescanin, S. Lulić, G. Pavlović, L. Mikelić, *Environ. Geol.* **46** (2004) 605.

The effect of the application of halotolerant microorganisms on the efficiency of a pilot-scale constructed wetland for saline wastewater treatment

MILANA KARAJIĆ[1]*, ALEŠ LAPANJE[2], JAKA RAZINGER[2], ALEXIS ZRIMEC[2] and DANIJEL VRHOVŠEK[1]

[1]LIMNOS Company for Applied Ecology, Podlimbarskega 31, 1000 Ljubljana and [2]Institute of Physical Biology, Toplarniška 19, 1000 Ljubljana, Slovenia

Abstract: In order to find the optimal design characteristics of constructed wetlands for saline wastewater treatment, halotolerant microorganisms, isolated from the water of the Sečovlje salterns, were inoculated into the media of a pilot-scale constructed wetland (CW). The purpose of this study was to examine the influence of different salinities on the efficiency of halotolerant microorganisms for the removal of pollutants in order to evaluate the possibility of their employment for saline wastewater treatment. The efficiency of ammonium removal (34.1 %) was the highest with 0 % NaCl in wastewater and slightly lower (31.8 %) when 2 g/dm^3 saccharose was added to aerated 1.5 % NaCl wastewater. The highest removal efficiency of chemical oxygen demand (COD) in the pilot-scale subsurface flow (SSF) CW was 83.6 % when saccharose (2 g/dm^3) was added to aerated 1.5 % NaCl wastewater. It was found that removal efficiency of the pilot-scale constructed wetland with inoculated halotolerant microorganisms showed a higher sensitivity to aeration and the presence of saccharose than to variation of the salinity of the wastewater. It can be concluded that halotolerant microorganisms, isolated from the Sečovlje salterns, are not sensitive to the changes in salinity and are, therefore, an alternative in the treatment of saline wastewater with a constructed wetland. However, with aeration their efficiency could be further improved.

Keywords: constructed wetlands; saline wastewater; halotolerant microorganisms.

INTRODUCTION

Seawater infiltration,[1] road deicing,[2,3] and landfill leachates,[4,5] as well as the chemical, petroleum, textile, leather and agro-food industries,[6] generate large amounts of saline wastewater. Consequently, pollution removal in hypersaline

---

129

wastewater is likely to represent up to 5 % of the global wastewater treatment requirement.[7] The discharge of such wastewater affects aquatic life, water pot ability and agriculture. Thus, legislation is becoming more stringent and the treatment of saline wastewater, both for organic matter and salt removal, is nowadays compulsory in many countries. Saline effluents are conventionally treated through physico-chemical means, as biological treatment is strongly inhibited by salts. However, as the costs of physico-chemical treatments are particularly high, alternative systems for the treatment of organic matter from saline wastewater are nowadays increasingly the focus of research.[6] One of the alternative systems is constructed wetlands (CW). The use of this system is becoming very popular in many countries[8] but its application for saline wastewater treatment has not been studied extensively. Lin *et al.*[9] found that salinity played an important role in the growth of microorganisms, resulting in a switch of the microbial population when studying the effects of salinity on the degradation of atrazine in a subsurface flow (SSF) constructed wetland (CW). They found that increasing salinity depressed the activity of the microorganisms and, therefore, caused a poor degradation efficiency of the CW. Studies by Nitisoravut and Klomjek[10] also reported that the effect of salinity on biological oxygen demand (BOD) removal appeared to approach an exponential phase. The same restraining effect showed that salinity inhibited the metabolism of microorganisms in the wetland environment, which may be critical for the proper functioning and maintenance of the system.[9]

In order to maximize the efficiency CW treatment of saline wastewater and keep its area to a minimum, it is necessary to find the optimal CW design characteristics. One of the most important characteristics is the microorganisms, but usually they are sensitive to salinity. Several studies, conducted with conventional cultures of bacteria indicated that the following four common difficulties exist when treating saline and hypersaline wastes with organisms derived from freshwater and soil ecosystems:[11] limited extent of adaptations,[12–14] sensitivity to changes in ionic strength,[15,16] reduced degradation kinetics and high effluent suspended solids concentrations.[17] Several studies have shown[18–23] that utilization of salt-tolerant microorganisms in biological treatment could be a reasonable approach for the treatment of high salinity wastewater.[24] Although the number of studies dealing with the biological treatment of saline wastewater is increasing rapidly, not much is known regarding the application of halotolerant microorganisms in CW.

The aim of this study was to examine the efficiency of halotolerant microorganisms in correlation with wastewater salinity using a pilot-scale SSF CW. The high concentration of nutrients and organic matter in the salt ponds of the Sečovlje salterns, the high concentration of salt and its oscillation during rainstorms, designate the Sečovlje salterns as very interesting for the isolation of halotolerant microorganisms and their application in the media of constructed

wetland for saline wastewater treatment. With this in mind, a pilot-scale SSF CW was designed, constructed and operated with halotolerant microorganisms, isolated from water of the Sečovlje salterns, inoculated in the media. Plants were not included in the pilot-scale SSF CW since the aim was to investigate the efficiency of halotolerant microorganisms in a sand/gravel/peat environment of varying salinity. It is known from the literature that plants accelerate the growth of microorganisms, especially in the area of the root environment,[25–28] but the employed halotolerant microorganisms were isolated from the water of the Sečovlje salterns and naturally they were not attached to the roots of plants. Changes in salinity also often occur in real CW and the aim was to investigate the efficiency of halotolerant microorganisms, isolated from the Sečovlje salterns, during Salinity shocks in the pilot-scale SSF CW.

EXPERIMENTAL

A pilot-scale SSF CW was constructed from three rectangular plastic tanks, each with the dimensions: length 0.77 m, width 0.16 m and depth 0.58 m, which were separated by 0.20–0.25 m long empty compartments on both sides (Fig. 1). The total length of the pilot-scale SSF CW was 2.99 m. Between the three soil-filled compartments, two perforated compartment walls were placed across the flow of the water. There was only water in these four narrow empty compartments. In every soil-filled compartment, there was a perforated pipe reaching to the bottom. The pipe ended with part of a plastic bottle from which a small plastic tube led to a glass bottle with a solution of barium hydroxide to catch carbon dioxide, as a measure of the microbial activity in the soil.[29–31] A perforated rubber pipe connected to an aquarium air pump, which was switched on only during the aeration treatment, was laid at the bottom of the pilot-scale SSF CW. The hydraulic retention time was determined by adding 0.1 % NaCl to the influent and the conductivity of the effluent was measured.[32]

The medium of the pilot-scale SSF CW was prepared as a mixture of sand (limestone) and peat. The sand was prepared from particles of different sizes: 1–4 mm (30 %; 0.12 m^3), 4–8 mm (60 %; 0.24 m^3) and 8–16 mm (10 %; 0.04 m^3). The chemical composition of the sand was: $CaCO_3$, 30.56 %; $MgCO_3$, 21.8 %; SO_3, 0.09 %; MnO_2, 0.02 %; TiO_2, trace; Fe_2O_3, 0.00 %; Al_2O_3, 0.00 % and SiO_2, 0.08 %. Peat, with the following characteristics: pH 3.5–4.0; organic matter, 35 % and total nitrogen, 0.4 %, was added to make up 10 % of the total volume. The final pH value of the medium mixture was 7.4.

The employed halotolerant microorganisms were isolated[33] from the active solar Sečovlje salterns in the autumn of 2005. The halotolerant microorganisms were cultivated for three months in synthetic wastewater (artificial wastewater (ART) medium)[34] and the optical density (*OD*) was measured at 600 nm to monitor their growth. The microorganisms were then stored at –20 °C. Before inoculation into the pilot-scale SSF CW, they were reactivated in the synthetic wastewater for one week. The reactivated culture (300 cm^3) was added to the first 115 dm^3 of the synthetic wastewater that was added into the pilot-scale SSF CW. The synthetic wastewater used throughout the study was composed of 130 mg/dm^3 yeast extract, 130 mg/dm^3 casein peptone, 130 mg/dm^3 meat extract, 317 mg/dm^3 CH_3COONH_4, 40 mg/dm^3 NH_4Cl, 24 mg/dm^3 K_2HPO_4, 8 mg/dm^3 KH_2PO_4, 100 mg/dm^3 $CaCO_3$, 100 mg/dm^3 $MgCO_3$, 40 mg/dm^3 NaCl and 5 mg/dm^3 $FeSO_4 \cdot 7H_2O$. The volume of the wastewater in the pilot-scale SSF CW was 115 dm^3. The salinity of the synthetic wastewater was changed from no added NaCl to 1.5 % NaCl and to 3 % NaCl. When the measurements were realized with and

without the aeration and with added saccharose in a concentration of 2 g/dm^3, as a source of organic carbon in the synthetic wastewater of pilot-scale SSF CW, the salt concentration in the synthetic wastewater was 1.5 % NaCl. When the synthetic wastewater contained 0 % and 3 % NaCl, the pilot-scale SSF CW was not aerated and no saccharose was added. Synthetic wastewater with 1.5 % NaCl was added to pilot-scale SSF CW together with halotolerant microorganisms and this salinity was maintained for two months with the wastewater being replaced weekly with fresh synthetic wastewater, without aeration. After this initial two-month period, the conditions in the pilot-scale SSF CW (salinity, aeration, and saccharose) were changed biweekly. In addition, the wastewater was replaced with fresh wastewater once a week. First, synthetic wastewater with 1.5 % NaCl was aerated for two weeks. Then synthetic wastewater with 3 % NaCl circulated for two weeks and after that, 1.5 % NaCl wastewater without aeration was circulated for a further two weeks. It was then replaced with 0 % NaCl synthetic wastewater for one week and finally with 1.5 % NaCl synthetic wastewater, which was aerated and contained 2 g/dm^3 saccharose, for two weeks. When changing the synthetic wastewater in the pilot-scale SSF CW, fresh synthetic wastewater was pumped into the first compartment at a flow of 1.7×10^{-6} m^3/s, while simultaneously, the old synthetic wastewater flowed out from the fourth/last compartment through the valve. Water was pumped into the pilot-scale SSF CW with an aquarium pump (Hydor Seltz L20 II). The same inflow and outflow were set with an aquarium pump and valves. After all of the fresh synthetic wastewater had been pumped into the pilot-scale SSF CW, the system was set to pump the water from the last compartment to the first one at a flow of 1.7×10^{-6} m^3/s, using an aquarium pump.
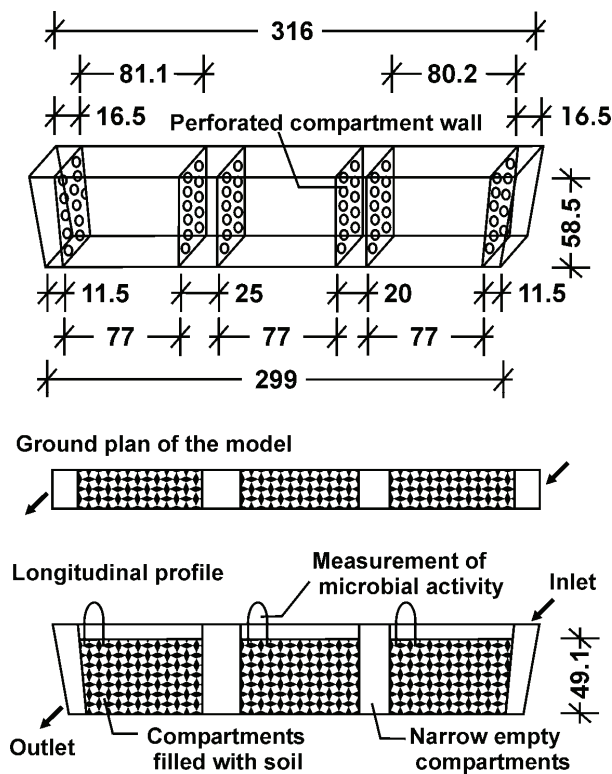
Fig. 1. Pilot-scale SSF CW with dimensions (cm).

Effluents from all four compartments of the pilot-scale SSF CW were analyzed daily for the first fifteen days after inoculation and subsequently less frequently. Samples of the treated synthetic wastewater were then taken on the first, third and seventh day after adding fresh synthetic wastewater. Water samples were taken from each water compartment. The efficiency of the pilot-scale SSF CW was assessed based on the difference between the ammonium, phosphate and *COD* concentrations at the influent and the effluent.[32] The concentrations of ammonium, phosphate and *COD* were measured using a LF2400 Windaus photometer, Germany. To determine the ammonium, phosphate and COD concentrations, the Windaus "Ready mixed cuvette test kit", Cat. No. 3773900, "Aquanal test kit", Cat. No. 3745100, and "CSB-Fertigkuvetten Type 1500", Cat. No. 804691826, were used, respectively. The pH value, the oxygen and carbon dioxide concentrations and the redox potential were also measured. The redox potential, pH and oxygen concentration were measured in all four water compartments with a WTW Sonde Multi 350i/SET, Wissenschaftlich, Germany, every second day. The COD value was measured in the first and last compartment. All the mention parameters were measured according to APHA.[35]

The carbon dioxide concentration in the soil[29–31] and the ETS activity (electro transport system activity)[36] were measured in order to determine the microbial activity. The measurements of the ETS activity and CO_2 concentration were realized using an Ocean Optics USB2000 spectrometer, USA. The ETS activity and carbon dioxide concentration in the soil were measured in all three compartments every second day of the experiments.

RESULTS

The pH in pilot-scale SSF CW was around 8.3, varying from 7.7 to 8.5 without aeration; therefore it was optimal for nitrification and slightly higher than optimal for denitrifiers.[37] In the case where the wastewater contained 2 g/dm^3 saccharose, the pH varied from 6.4 to 8.1, thus being optimal also for denitrifiers. The concentration of oxygen in the pilot-scale SSF CW was mostly lower than 0.4 mg/dm^3, except during the first days of the cycle when fresh synthetic wastewater was added. The oxygen concentrations without aeration were less than 1.5 mg/dm^3, but with aeration and without saccharose it increased. The redox potential was around –90 to –60 mV, which means anaerobic conditions existed in the pilot-scale SSF CW. With aeration, the redox potential increased to +20 mV, however the conditions were still anoxic.

After the second week of inoculation, an increase of the ETS activity in 1.5 % NaCl without aeration was noticed and it remained between 2×10^{-9} and 4×10^{-9} dm^3O_2 g^{-1} h^{-1}. The ETS activity, as a measure of the respiration capacity of the microbial community, increased only in aerated 1.5 % NaCl wastewater with 2 g/dm^3 of added saccharose. The ETS activity was the lowest with 0 % NaCl without aeration and the highest with 3 % NaCl.

During the first two weeks of the inoculation period with 1.5 % NaCl, the concentrations of carbon dioxide in the water and soil were lower than later. The carbon dioxide concentrations in the water and soil were similar in all concentrations of salt (0, 1.5 and 3 % NaCl). With 2 g/dm^3 of saccharose in the aerated

wastewater, the concentrations of carbon dioxide were the highest during the first day of measurements in the water and in the soil and then decreased.

For all salinity conditions (0, 1.5 and 3 % NaCl), the most significant reduction of the ammonium concentration was registered after seven days. The best removal efficiency was observed in wastewater in the absence of NaCl (Table I). In 1.5 % NaCl wastewater, the removal efficiency was reduced with or without aeration in comparison to that of wastewater in absence of NaCl. However the combination of aeration and saccharose significantly increased the removal efficiency to the same level as that of wastewater in the absence of NaCl. Under high salinity conditions (3 % NaCl), the ammonium removal efficiency was equivalent to the one in wastewater containing 1.5 % NaCl.

After inoculation, the phosphate removal efficiency was around 50 % in the wastewater with 1.5 % NaCl without aeration. Changes in salinity (reduction to 0 % or increase to 3 % NaCl) led to a reduced removal efficiency, especially in the case of the lower NaCl concentration (Table I). Aeration alone and in combination with saccharose addition, also had a negative impact on the phosphate removal efficiency.

The concentration of COD decreased most on the last (seventh) day of every cycle. The final concentrations of COD on the last day for all salt concentrations (0, 1.5 and 3 % NaCl) were approximately the same (Table I), leading to the conclusion that salinity did not affect the removal efficiency of COD. Aeration increased the COD removal efficiency and when saccharose was added to aerated wastewater, the concentration of COD first increased, however the greatest reduction of COD was also achieved under these conditions.

DISCUSSION

Reddy and Patrick[38] pointed out that losses of ammonium through volatilization from flooded soils and sediments are insignificant if the pH value is below 7.5 and very often the losses are not serious if the pH is below 8.0. According to pH, high losses of ammonium through volatization are not to be expected in the pilot-scale SSF CW. In the study of Baere *et al.*,[39] the pH dropped significantly after each shock treatment with a high concentration of NaCl. Also in the presented experiment, the lowest pH was registered with 3 % NaCl.

Carbon dioxide is a product of microbial metabolism and the obtained results confirmed earlier suggestions that saccharose as an energy source and aeration would stimulate the growth of the halotolerant microorganisms, which were isolated from the Sečovlje salterns, thus increasing the amount of produced carbon dioxide. This increase probably caused the drop in pH under these conditions. However, since the carbon dioxide concentration decreased on a third day, the amount of added saccharose was obviously enough only for about three days of intensive metabolism. After the third day the pH also started to rise and on the seventh day it was at the same level as for the other conditions.

TABLE I. Removal efficiencies over time (%); S.D. = standard deviation; aer. = aeration; d1 = first day of circulating wastewater; d3 = third day of circulating wastewater; d7 = seventh day of circulating wastewater; Min. = minimum removal efficiency; Max. = maximum removal efficiency

Quantity	1.5 % NaCl without aer.			1.5 % NaCl with aer.			1.5 % NaCl with aer. + saccharose[a]			0 % NaCl without aer.			3 % NaCl without aer.		
	d1	d3	d7	d1	d3	d7	d1	d3	d7	d1	d3	d7	d1	d3	d7
NH_4-N															
Mean	14.4	13.3	17.0	6.8	14.8	17.0	15.9	26.1	31.8	18.2	15.9	34.1	6.8	7.9	15.9
S.D.	17.7	13.5	16.4	8.7	14.5	16.4	6.4	3.2	4.9	12.9	4.5	4.5	12.6	10.2	12.6
Min.	0	0	0	0	0	0	9.1	18.2	27.3	9.1	9.1	27.3	0	0	0
Max.	99.7	45.4	45.4	18.2	36.4	45.4	27.3	27.3	36.4	36.4	18.2	36.4	36.4	37.3	27.3
COD															
Mean	30.4	29.1	44.3	54.2	54.2	70.6	42.1	58.0	83.6	14.0	50.6	64.4	22.0	41.9	52.1
S.D.	12.7	12.7	16	15.9	15.9	1.1	23.4	28.7	3.6	12.6	15.5	11.2	17.1	23.4	14.5
Min.	7.9	7.9	20.9	42.9	42.9	70.6	16.0	15.1	81.1	5.1	39.7	56.5	7.1	19.0	40.7
Max.	50.2	55.7	68.2	65.5	65.5	70.6	61.3	75.5	88.7	22.9	61.6	72.3	42.9	65.4	72.3
PO_4															
Mean	30.8	55.1	54.3	28.6	28.6	25.0	0	28.6	25	0	-57.1	0	26.8	23.2	12.5
S.D.	49.0	36.7	30.2	20.2	10.8	16.6	0	10.8	16.6	0	26.1	0	9.1	7.4	16.1
Min.	-128.6	-14.3	0	0	14.3	0	0	14.3	0	0	-85.7	0	14.3	14.3	0
Max.	92.9	92.9	92.9	42.9	42.9	42.9	0	42.9	42.9	0	-28.6	0	42.9	28.6	42.9

[a] c (saccharose) = 2 g/dm³

Obviously, the available oxygen was quickly consumed by the microorganisms and after the first day there was a lack of oxygen, making the conditions in the pilot-scale SSF CW similar to those in wetlands.[40] Salinity, however, did not influence the oxygen concentrations, which were very low for all the studied salinities. The low concentrations of oxygen resulted in the redox potential being independent of salinity and hence the registered variations were the same in different cycles and for different salinities. Conversely, the redox potential changed under conditions of aeration, when the amount of oxygen was increased and consequently the redox potential also. However, even when the pilot-scale SSF CW was aerated and the redox potential had positive values, the conditions were still anoxic (< 100 mV). This means that the pilot-scale SSF CW should be more aerated, with more air pumps in each compartment to achieve oxic conditions in order to increase the efficiencies of the removal of pollutants. The presence of plants usually enhances the aeration of CW but based on the results obtained in this study additional aeration is proposed. When 2 g/dm^3 saccharose was added to the synthetic wastewater, oxygen was consumed during degradation processes and also aeration could not import enough oxygen to the pilot-scale SSF CW.

As the ETS activity is a measure of microbial activity, it could be concluded that the halotolerant microorganisms were adapted and inoculated into the system after two weeks under the employed conditions (1.5 % NaCl). Also, the increased production of carbon dioxide in the first two weeks and the stable production after the second week of inoculation confirm that the halotolerant microorganisms had adapted to the conditions in the pilot-scale SSF CW after the second week and were successfully inoculated. From the results of the ETS activity at 3 % salinity, it could be concluded that the halotolerant microorganisms isolated from the Sečovlje salterns and inoculated into the pilot-scale SSF CW were neither affected by 3 % salinity nor by a drop of salinity, since the ETS activity at 0 % NaCl was similar to that with 1.5 % NaCl. The increase in the ETS activity with aerated 1.5 % NaCl wastewater containing saccharose means that the number of microorganisms increased due to the aeration and the presence of the additional energy. Lin *et al.*[9] reported that salinity impacted the growth of bacteria resulting in a switch of the microbial community in a pilot-scale SSF CW that was inoculated with a conventional culture of bacteria. However, in the present case, the ETS activity was not reduced by 3 % salinity, hence the conclusion could be that the same microorganisms were active at 1.5 % and 3 % NaCl, thus they were insensitive to the sudden increase in salinity.

Generally, anaerobic conditions in a pilot-scale SSF CW cause low removal of ammonium because the oxidation of ammonia to nitrite and then of nitrite to nitrate (nitrification process) occurs under aerobic conditions by autotrophic bacteria. Contrary to Dahl *et al.*,[41] who found inhibition of the nitrifiers in the case of a rapid increase in the chloride concentration with conventional microorga-

nisms, the results obtained in this study indicate that the removal of ammonium ions was not influenced by increased salt concentrations in the case of the inoculated halotolerant microorganisms. These results are in accordance with Kargi and Dincer,[18] who found that the adverse effects of high salt concentrations were significantly alleviated by the use of salt-tolerant microorganisms. Vymazal[42] concluded that the ability of a horizontal flow CW to nitrify ammonia is very limited because anaerobic conditions usually exist. This is in accordance with the present results where, at the same salinity, high removal of ammonium did not occur even with aeration of the pilot-scale SSF CW because the conditions were still anoxic. To aerate the system of SSF CW, different aeration systems for the introduction of oxygen were suggested, such as frequent water level fluctuation (tidal-flow),[43–45] passive air pumps (vertical-flow)[46] or direct mechanical aeration of the water in the gravel bed (horizontal-flow),[47–49] which was improved by Nivala *et al.*[50] The lower concentration of ammonium found in the experiment with saccharose were also in accordance with the study of Vymazal,[42] who reported that some degradation processes require energy (typically derived from an organic carbon source) to proceed, and others release energy, which can be used by organisms for growth and survival. This suggests that the added saccharose stimulated the growth of the microbial community and also the nitrification process because saccharose acts as a source of energy.

The higher concentration of phosphate with 0 % NaCl indicates that phosphate was washed out with 0 % saline wastewater. This is in accordance with the study of Bulc,[5] in which it was found that all the phosphorus was washed out during precipitation.

As was found by Akratos and Tsihrintzis,[8] the organic removal efficiencies were significantly higher than those for nitrogen and phosphorus removal. This is the case in most wetland systems and it is probably the consequence of nitrogen and phosphorus removal requiring longer hydraulic retention times.

When comparing different salt concentrations, the mean values for COD removal showed the best efficiency with 0 % NaCl (64.4 %) followed by 3 % salinity (52.1 %) and 1.5 % salinity (44.3 %), indicating that the used microorganisms were not affected by salinity and could therefore improve the saline wastewater treatment process in CW. In the case of 1.5 % NaCl in the wastewater, it was noticed that higher removal efficiencies were achieved with aeration compared to non-aerated wastewater. This means that aeration improves organic matter decomposition processes and that they were hindered by lack of oxygen. The removal efficiencies of COD in the pilot-scale SSF CW with 1.5 % NaCl wastewater were the highest with aeration and 2 g/dm^3 saccharose addition, but the final COD concentration was same as without added saccharose, which therefore did not help in lowering the final COD concentration but did help in increasing the ammonium removal efficiency. The removal efficiencies of the pilot-scale

SSF CW with inoculated halotolerant microorganisms did not depend on variations of the salinity but did depend much more on aeration and the presence of saccharose. Additionally, the experiment indicated that the inoculated halotolerant microorganisms in the pilot-scale SSF CW were tolerant to salinity variations.

The found removal efficiencies of ammonium and COD confirmed the study of Garcia *et al.*[51] that the removal efficiency of an SSF CW is rather low for COD and ammonia, usually < 70 % and < 30 %, respectively. They indicated that the efficiencies were more dependent on aeration and the presence of sugar as an organic carbon source. This was also confirmed by the variation of the percent removal of ammonium and COD with time. The process of aeration of the pilot-scale SSF CW did not improve the removal efficiency for ammonium, but improved the COD removal efficiency by 26 %, when experiments with the same salinity (1.5% NaCl), with or without aeration, were compared. This confirms the results of Scholz,[52] who claimed that the ammonium removal efficiency is more dependent on the aerobic conditions than COD removal. A higher removal efficiency was found with aeration of the pilot-scale SSF CW, but not as much as expected. This could be explained by the low redox potential in the pilot-scale SSF CW, meaning that the aeration was not adequate.

The fact that ETS and reduction of COD were the highest in the presence of saccharose and aeration shows that saccharose and aeration stimulated the growth and metabolism of the halotolerant microorganisms. These results are in accordance with the study of Burchell *et al.*,[53] in which it was found that the addition of organic matter to the soils used for an in-stream CW significantly increased biomass growth when compared to the addition of inorganic matter. The same final concentrations of COD for all conditions are a consequence of the added saccharose and aeration, which stimulated the growth of the microbes and metabolism by using the organic matter as a source of energy. Since the COD concentrations were similar at all conditions with varying salinity, the COD removal efficiency was not influenced by salinity changes.

The relatively high values of the standard deviation of the removal efficiencies (Table I) for ammonium and phosphate are the consequence of high variations of the removal efficiency during the operation period. Akratos and Tsihrintzis[8] explained that variations occur because the bacteria for nitrogen are less efficient at low temperatures. Similarly, the water temperature was not constant in the pilot-scale CW employed in the present study. It changed from 14 to 26 °C. The negative values of the phosphate removal efficiencies and lack of oxygen in the pilot-scale CW confirmed that phosphate is mainly removed by adsorption on the porous media[32] and that reducing conditions (*i.e.*, lack of oxygen) can lead to solubilization of minerals and release of dissolved phosphorus.[32,54] The COD removal efficiencies were relatively stable during the entire operation under all

conditions. This can be seen from the relatively low standard deviation values of the removal efficiencies for COD, compared to standard deviation of ammonium and phosphate. Similarly, the study by Akratos and Tsihrintzis[8] found that the removal efficiencies for COD were stable, while ammonium and phosphate removal efficiencies were not observed in their pilot-scale CWs.

CONCLUSIONS

Salinity changes in the studied pilot-scale SSF CW did not have a strong influence on the removal efficiency of pollutants, mainly because the processes were affected by a lack of oxygen and energy.

According to the increase in the carbon dioxide concentration and ETS activity, the microorganisms required about two weeks to establish a stable population.

Salinity affects the process of ammonium removal, which was more effecttive in the absence of salinity. However, in saline wastewater, the NaCl concentration had no impact on the removal efficiencies. The process of ammonium removal in the pilot-scale SSF CW was affected by the available energy, which could be seen from the increase in the removal efficiency when saccharose was added. According to the literature, the process is strongly dependant on the available oxygen, but since the pilot-scale SSF CW was not aerated sufficiently with the employed aeration system, the removal efficiencies for ammonium were low.

A higher concentration of phosphate was detected with 0 % NaCl in wastewater. This indicates that phosphate was washed out under these conditions.

Aeration and saccharose addition increased the COD removal efficiency but the final COD concentrations were the same, therefore the additional source of energy is not as important in this case as for ammonium removal. The COD removal efficiency was affected by lack of oxygen but salinity did not have an influence.

The results obtained from the pilot-scale SSF CW show that the use of halotolerant microorganisms can improve the efficiency of saline wastewater treatment. Special attention should be paid to the aerobic/anaerobic conditions because anaerobic conditions strongly hinder COD removal regardless of salinity. In addition, ammonium removal is not sensitive to changes in salinity but care should be taken about aeration and also about providing the energy required for ammonium removal. Plants and their rhizosphere are players in the aeration of ecosystems and therefore provide better conditions for aerobic microorganisms. Thus, the use of plants, preferably halotolerant varieties in association with halotolerant microorganisms could improve removal efficiencies in the treatment of wastewater. However, the obtained results show that aeration alone is not sufficient and that parameters other than aeration (*e.g.*, sugar addition) should be in-

cluded in the design of SSF CWs with halotolerant microorganisms to improve saline wastewater treatment.

И З В О Д

УТИЦАЈ ПРИМЕНЕ ХАЛОТОЛЕРАНТНИХ МИКРООРГАНИЗАМА НА ЕФИКАСНОСТ ЕКСПЕРИМЕНТАЛНОГ СИСТЕМА ПОЉА ЗА БИОЛОШКО ПРЕЧИШЋАВАЊЕ СЛАНЕ ОДПАДНЕ ВОДЕ

MILANA KARAJIĆ[1], ALEŠ LAPANJE[2], JAKA RAZINGER[2], ALEXIS ZRIMEC[2] и DANIJEL VRHOVŠEK[1]

[1]LIMNOS Company for Applied Ecology, Podlimbarskega 31, 1000 Ljubljana u
[2]Institute of Physical Biology, Toplarniška 19, 1000 Ljubljna, Slovenia

У циљу проналажења оптималних карактеристика система поља за биолошко пречишћавање слане одпадне воде, халотолерантни микроорганизми, изоловани из воде солане Сечовље, били су инокулирни у медијум експерименталног система поља за биолошко пречишћавање. Циљ рада био је да се испита утицај различитог салинитета на ефикасност пречишћавања слане одпадне воде са халотолерантним микроорганизмима, са намером да се оцене могућности примене халотолерантних микроорганизама за пречишћавање слане одпадне воде. Ефикасност одстрањивања амонијум јона (34,1 %) била је највећа са 0 % NaCl у одпадној води и мало нижа (31,8 %) када је 2 g/dm^3 сахарозе било додато у озрачену одпадну воду са 1,5 % NaCl. Највећа ефикасност смањења хемијске потрошње кисеоника (КПК) у експерименталном систему поља за биолошко пречишћавање са подповршинским током износила је 83,6 % када је сахароза (2 g/dm^3) била додата у озрачену одпадну воду са 1,5 % NaCl. Ефикасност експерименталног система поља за биолошко пречишћавање са инокулираним халотолерантним микроорганизмима показује већу осетљивост на озрачивање и присуство сахарозе, него на варијацију салинитета одпадне воде. Може се закључити да халотолерантни микроорганизми, изоловани из солане Сечовље, нису осетљиви на промене салинитета и због тога су алтернатива у третману слане одпадне воде системом поља за биолошко пречишћавање. Њихова ефикасност може бити унапређена озрачивањем.

(Примљено 8. јуна, ревидирано 8. новембра 2009)

REFERENCES

1. B. F. Jones, A. Vengosh, E. Rosenthal, Y. Yechieli, in *Seawater Intrusion in Coastal Aquifers-Concepts, Methods and Practices,* J. Bear, A. H. D. Cheng, S. Sorek, D. Ouazar, I. Herrera, Eds., Kluwer, Dordrecht, 1999, p. 51
2. T. Bulc, D. Vrhovšek, *Wastewater treatment of highway run-off in a constructed wetland*, in *Voda in ceste, Strokovno posvetovanje*, Slovensko društvo za hidravlične raziskave, DRC, Novo Mesto, Slovenija, 1996, p. 73 (in Slovenian)
3. A. Lundmark, *Predicting environmental impact of deicing salt – a modelling approach*, Dept. of Land and Water Resources Engineering, KTH, 2003, http://www.lwr.kth.se/ /Forskningsprojekt/predmodell_vagsalt/Predicting%20envrionmental%20impacts%20 of%20deicing%20salt.pdf (06. 06. 2008)
4. M. Zupančič-Justin, *Tracking of the pollutants during rehabilitation of a municipal landfill site using leachate pre-treatment and recirculation*, Doctoral dissertation, University of Ljubljana, Biotechnical Faculty, Ljubljana, Slovenia, 2006, p. 83
5. T. Bulc, *Ecol. Eng.* **26** (2006) 365
6. O. Lefebvre, R. Moletta, *Water Res.* **40** (2006) 3671

7. O. Lefebvre, N. Vasudevan, K. Thanasekaran, R. Moletta, J. Godon, *Extremophiles.* **10** (2006) 505
8. C. S. Akratos, V. A. Tsihrintzis, *Ecol. Eng.* **29** (2007) 173
9. T. Lin, Y. Wen, L. Jiang, J. Li, S. Yang, Q. Zhou, *Chemosphere* **72** (2008) 122
10. S. Nitisoravut, P. Klomjek, *Water Res.* **39** (2005) 4413
11. C. R. Woolard, R. L. Irvine, *Water Sci. Technol.* **31** (1995) 41
12. R. Y. Tokuz, W. W. Eckenfelder, in *Proceedings of 33rd Purdue Industrial Waste Conference*, (1978), Lewis Publishers, Chelsea, 1978, p. 200
13. J. M. Wong, in *Proceedings of the 46th Annual Purdue Industrial Waste Conference*, (1992), Lewis Publishers, Chelsea, 1992
14. M. R. Hockenbury, D. Burstein, E. S. Jamro, in *Proceedings of the 32nd Industrial Waste Conference*, (1978), Purdue University, Lewis Publishers; Chelsea, 1978
15. D. F. Kincannon, A. F. Gaudy, *Biotechnol. Bioeng.* **10** (1968) 483
16. G.W. Lawton, C.V. Egger, *Sewage Ind. Wastes* **29** (1957) 1228
17. F. J. Ludzack, D. K. Noran, *J. Water Pollut. Control Fed.* **37** (1965) 1404
18. F. Kargi, A. R. Dincer, *Bioprocess. Eng.* **15** (1996) 51
19. F. Kargi, A. Uygur, *Environ. Technol.* **17** (1996) 325
20. G. T. Tellez, N. Nirmalakhandan, J. L. Gardea-Torresdey, *Water Res.* **29** (1995) 1711
21. C. Hinteregger, F. Streichsbier, *Biotechnol. Lett.* **19** (1997) 1099
22. A. R. Dincer, F. Kargi, *Environ. Technol.* **20** (1999) 1147
23. L. Yang, C. T. Lai, W. K. Shieh, *Water Res.* **34** (2000) 3303
24. P. Dan, *PhD Thesi*s, Asian Institute of Technology, School of Environment, Resources and Development, Bangkok, 2001, p. 27
25. W. Armstrong, *Water-logged soils*, in *Environment and plant ecology,* J. R. Etherington, Ed., John Wiley, Chichester, 1982, p. 290
26. I. A. Mendelsson, M. T. Postek, *Am. J. Botany* **69** (1982) 904
27. R. H. Kadlec, R. L. Knight, J. Vymazal, H. Brix, P. Cooper, R. Haberl, *Constructed Wetlands for Pollution Control: Processes, Performance, Design and Operation*, Scientific and Technical Report No. 8, International Water Association, London, 2000, p. 10
28. N. F. Gray, *Biology of Wastewater Treatment*, 2nd Ed., Vol. 4, Imperial College Press, London, UK, 2004, p. 641
29. A. O. Hanstveit, *Chemosphere* **25** (1992) 605
30. E. Heath, *PhD Thesis*, University of Ljubljana, Faculty of Chemistry and Chemical Technology, Ljubljana, Slovenia, 1998, p. 57 (in Slovenian)
31. M. Zupančič, *MSc Thesis*, University of Ljubljana, Biotechnical Faculty, Ljubljana, Slovenia, 2001, p.49
32. R. Kadlec, R. Knight, *Treatment Wetlands*, CRC Press, Boca Raton, FL, 1996, p. 29
33. M. Koprivnikar, Diploma work, University of Ljubljana, Biotechnical Faculty, Ljubljana, Slovenia, 2008, p.42
34. T. Kosjek, E. Heath, B. Kompare, *Anal. Bioanal. Chem.* **387** (2007) 1379
35. APHA, AWWA, WPCF, *Standard Methods for Examination of Water and Wastewater*, 17th ed., Washington DC, 1990, p. 10
36. J. T. Trevors, *Water Res.* **18** (1984) 581
37. E. A. Paul, F. E. Clark, *Soil microbiology and biochemistry,* Academic Press, San Diego, CA, 1996, p. 340
38. K. R. Reddy, W. H. Patrick, *Crit. Rev. Environ. Control* **13** (1984) 273

39. D. L. A. Baere, M. Devocht, P. Van Assche, *Water Res.* **18** (1984) 543
40. B. Moss, *Ecology of Fresh Waters*, Blackwell Science, Oxford, 1998, p. 3
41. C. Dahl, C. Sund, G. H. Kristensen, L. Vredenbregt, *Water Sci. Technol.* **36** (1997) 345
42. J. Vymazal, *Sci. Total Environ.* **380** (2007) 48
43. D. C. Austin, E. Lohan, E. Verson, *Nitrification and denitrification in a tidal vertical flow wetland pilot, in Proceedings of Water Environment Federation Technical Conference*, (2003), Los Angeles, CA, 2003
44. L. L. Behrends, F. J. Sikora, H. S. Coonrod, E. Bailey, C. McDonald, in *Proceedings of WEFTEC'96 the 69th annual conference and exposition of the water environment federation*, (1996), Dallas, TX, 1996, p. 251
45. K. E. Zoeller, M. E. Byers, US Patent 5897777 (1999)
46. M. Green, E. Friedler, I. Safrai, *Water Res.* **32** (1998) 3513
47. J. A. Dufay, US Patent 6159371 (2000)
48. D. A. Flowers, US Patent 6447682 B1 (2002)
49. S. D. Wallace, US Patent 6200469 B1 (2001)
50. J. Nivala, M. B. Hoos, C. Cross, S. Wallace, G. Parkin, *Sci. Total Environ.* **380** (2007) 19
51. J. Garcia, P. Aguirre, J. Barragan, R. Mujeriego, V. Matamoros, J. P. Bayona, *Ecol. Eng.* **25** (2005) 405
52. M. Scholz, J. Xu, *Ecol. Eng.* **18** (2002) 385
53. M. R. Burchell, R. W. Saggs, C. R. Lee, S. Broome, G. M. Chescheir, J. Osborne, *J. Environ. Qual.* **36** (2007) 194
54. S. C. Reed, R. W. Crites, J. E. Middlebrooks, *Natural Systems for Waste Management and Treatment*, McGraw Hill, New York, USA, 1995, p. 20.

2009 List of referees

Editorial Board of the Journal is grateful to the following referees for reviewing the manuscripts during 2009:

Samir Abdelgaleil, *Faculty of Agriculture, Alexandria University El-Shatby, Alexandria, Egypt*

Mohammad Abdollahi, *Faculty of Pharmacy and Pharmaceutical Sciences Rescarch Centre, Tehran University of Medical Sciences, Tehran, Iran*

Ornella Abollino, *Dipartimento di Chimica Analitica, Università di Torino, Italia*

Biljana Abramović, *Department of Chemistry, Faculty of Science, University of Novi Sad, Serbia*

Hazem Abu Shawish, *Faculty of Science, Al-Aqsa University, Gaza, Palestine*

Yaser Abu-Lebdeh, *Department of Chemistry, University of Montreal, Montreal, Canada*

Alan Aitken, *School of Chemistry, University of St. Andrews, St Andrews, Scotland, UK*

Mara Aleksić, *Faculty of Pharmacy, University of Belgrade, Serbia*

Rade Aleksić, *Faculty of Technology and Metallurgy, University of Belgrade, Serbia*

Ahmet Alim, *Public Health Laboratory, Sivas Directorate of Health, Sivas, Turkey*

Ivana Aljančić, *Institute of Chemistry, Technology and Metallurgy, University of Belgrade, Serbia*

Rossano Amadelli, *Universita' Degli Studi di Ferrara, Ferrara, Italy*

Katarina Anđelković, *Faculty of Chemistry, University of Belgrade, Serbia*

Carlos S. Andreo, *CEFOBI, Universidad Nacional de Rosario, Rosario. Argentina*

Vesna Antić, *Faculty of Agriculture, University of Belgrade, Zemun, Serbia*

Sankarlingam Arunachalam, *School of Chemistry, Bharathidasan University, Tamil Nadu, India*

Teodor Ast, *Faculty of Technology and Metallurgy, University of Belgrade, Serbia*

Noor Aziah Aziz, *School of Industrial Technology, Universiti Sains Malaysia, Penang, Malaysia*

Ksenija Babić-Samardžija, *Baker Petrolite, Commercial Development Group, Texas, USA*

Petr Babula, *ÚPL VFU, Brno, Czechoslovakia*

Morteza Bahram, *Bu-Ali Sina University, Hamadan, Iran*

Alexandru T. Balaban, *Texas A&M University at Galveston, USA*
Slavica Bačić, *Vinča Institute of Nuclear Sciences, Belgrade, Serbia*
Rada Baošić, *Faculty of Chemistry, University of Belgrade, Serbia*
Jiří Barek, *Faculty of Science, Charles University in Prague, Prague, Czech Republic*
Gilles Barnathan, *Université de Nantes ISOMer, Nantes, France*
Ramon Bataller, *Centro de Investigación Biomédica Esther Koplowitz, Barcelona, Spain*
Ines Batinić-Haberle, *Department of Radiation Oncology-Cancer Biology, Duke University Medical Center, Durham, USA*
Hasan Baydar, *Faculty of Agriculture, University of Suleyman Demirel, Isparta, Turkey*
Alexandra Bazes, *Université Européenne de Bretagne, Université de Bretagne-Sud, Lorient Cedex, France*
Irina Petrovna Beletskaya, *Organoelement Chemistry Laboratory, Moscow State University, Russia*
Sheshanath Bhosale, *School of Chemistry, Monash University, Clayton, Australia*
Hakan Bilhan, *Faculty of Dentistry, Istanbul University, Istanbul, Turkey*
Ivica Blažević, *Faculty of Chemistry and Technology, University of Split, Croatia*
Duško Blegojević, *Institute for Biological Research "S. Stanković", Faculty of Biology, University of Belgrade, Serbia*
Darinka Bogdanović, *Faculty of Agriculture, University of Novi Sad, Serbia*
Tomislav Bolanča, *Faculty of Chemical Engineering and Technology, University of Zagreb, Croatia*
Goran Bošković, *Faculty of Technology, University of Novi Sad, Serbia*
Snežana Bošković, *Vinča Institute of Nuclear Sciences, Belgrade, Serbia*
Biljana Božin, *Faculty of Medicine, Department of Pharmacy, University of Novi Sad, Serbia*
Samuel Braverman, *Department of Chemistry, Bar-Ilan University, Ramat Gan, Israel*
Ilija Brčeski, *Faculty of Chemistry, University of Belgrade, Serbia*
Enric Brillas, *LCTEM, Facultat de Quimica, Universitat de Barcelona, Spain*
Gustavo Brunetto, *Universidade Federal de São João Del Rei Campus Dom Bosco, São João Del Rei, Brasil*
Chenxin Cai, *College of Chemistry and Environmental Science, Nanjing Normal University, Nanjing, P.R. China*
Milorad Cakić, *Faculty of Technology, University of Niš, Leskovac, Serbia*
Valerija Češljević, *Department of Chemistry, Faculty of Science, University of Novi Sad, Serbia*
Nicos Chaniotakis, *Department of Analytical Chemistry, University of Crete*

André B. Charette, *Department of Chemistry, Université de Montréal, Montréal, Canada*

Sung Chul Yoon, *Environmental Biotechnology National Core Research Center, Gyeongsang National University, Jinju, Korea*

Paolo Colombo, *Istituto di Biomedicina ed Immunologia Molecolare Alberto Monroy, Consiglio Nazionale delle Ricerche, Palermo, Italy*

Bernie Creaven, *ITT Dublin, Institute of Technology Tallaght, Dublin, Ireland*

Željko Čupić, *Institute of Chemistry, Technology and Metallurgy, University of Belgrade, Serbia*

Olga Cvetković, *Institute of Chemistry, Technology and Metallurgy, University of Belgrade, Serbia*

Zorica Cvijović, *Faculty of Technology and Metallurgy, University of Belgrade, Serbia*

Nikola Cvjetičanin, *Faculty of Physical Chemistry, University of Belgrade, Serbia*

Carla Da Porto, *Dipartimento di Scienze degli Alimenti, Università di Udine, Udine, Italy*

Dragoljub Dakić, *Vinča Institute of Nuclear Sciences, Belgrade, Serbia*

Aleksandra Daković, *Institute For Technology of Nuclear and Other Raw Materials, Belgrade, Serbia*

Ljiljana Damjanović, *Faculty of Physical Chemistry, University of Belgrade, Serbia*

Ljljana Damjanović, *Faculty of Physical Chemistry, University of Belgrade, Serbia*

Shiladitya DasSarma, *University of Maryland, College Park USA*

Roche de Guzman, *Department of Biomedical Engineering, Wayne State University, Detroit, MI, USA*

Aleksandar Dekanski, *Institute of Chemistry, Technology and Metallurgy, University of Belgrade, Serbia*

Hanyuan Deng, *Hunan Normal University, Changsha, P.R. China*

Francesco Di Quarto, *Dipartimento di Ingegneria Chimica, dei Processi e dei Materiali, Università di Palermo, Italia*

Ljiljana Dimitrijević, *Torlak Institute of Immunology and Virology, Beograd, Serbia*

Radovan Dimitrijević, *Faculty of Mining and Geology, University of Belgrade, Serbia*

Aleksandar Dimitrov, *Faculty of Technology and Metallurgy, University "St. Cyril & Methodius", Skopje, Republic of Macedonia*

Svetlana Đogo, *Faculty of Pharmacy, University of Belgrade, Serbia*

Hans Dolhaine, *Henkel R. D., Dsuesseldorf, Germany*

Vera Dondur, *Faculty of Physical Chemistry, University of Belgrade, Serbia*

Bojan Đorđević, *Faculty of Technology and Metallurgy, University of Belgrade, Serbia*

Ljiljana Došen-Mićović, *Faculty of Chemistry, University of Belgrade, Serbia*

Branko Dunjić, *Faculty of Technology and Metallurgy, University of Belgrade, Serbia*

Miloš Đuran, *Faculty of Science, University of Kragujevac, Kragujevac, Serbia*

Predrag Đurđević, *Faculty of Chemistry, University of Kragujevac, Kragujevac, Serbia*

Jean-Luc Duroux, *Institut GEIST, Faculté de Pharmacie, 2, Limoges Cedex, France*

Srđan Pejanović, *Faculty of Technology and Metallurgy, University of Belgrade, Serbia*

Mostafa El-Sheekh, *Botany Department, Faculty of Science, Tanta University, Egypt*

Slavica Erić, *Institute of Pharmaceutical Chemistry, Faculty of Pharmacy, University of Belgrade, Serbia*

Ernesto Estrada, *University of Strathclyde, Glasgow, Scotland, UK*

Hao Fang, *Shandong University, Jinan, P.R. China*

Wieslava Ferenc, *University of Maria-Sklodowska Curie, Lublin, Poland*

Zorana Ferjančić, *Faculty of Chemistry, University of Belgrade, Serbia*

Brigida Fernandez de Simon, *Centro de Investigación Forestal (CIFOR-INIA), Madrid, Spain*

Ana Cristina Figueiredo, *Universidade de Lisboa, Faculdade de Ciências de Lisboa, Lisboa, Portugal*

Jovanka Filipović, *Faculty of Technology and Metallurgy, University of Belgrade, Serbia*

Shinsaku Fujita, *Department of Chemistry, Kyoto Institute of Technology, Matsugasaki, Kyoto, Japan*

Boris Furtula, *Faculty of Science, University of Kragujevac, Kragujevac, Serbia*

Thomas Gamse, *Graz University of Technology, Graz, Austria*

Jasmina Glamočlija, *Institute for Biological Research "S. Stanković", Faculty of Biology, University of Belgrade, Serbia*

Velizar Gochev, *Biological Faculty, University of Plovdiv, Plovdiv, Bulgaria*

Dejan Gođevac, *Institute of Chemistry, Technology and Metallurgy, University of Belgrade, Serbia*

Gordana Gojgić-Cvijović, *Institute of Chemistry, Technology and Metallurgy, University of Belgrade, Serbia*

Snežana Gojković, *Faculty of Technology and Metallurgy, University of Belgrade, Serbia*

Manferd Gossen, *Zentrum für Molekulare Biologie (ZMBH), Universität Heidelberg, Heidelberg, Germany*

Željko Grbavčić, *Faculty of Technology and Metallurgy, University of Belgrade, Serbia*

Branimir Grgur, *Faculty of Technology and Metallurgy, University of Belgrade, Serbia*

Hyoung Jin Choi, *Department of Polymer Science and Engineering, Inha University, Korea*

Dragan Jocić, *University of Twente, the Netherlands*

Milan Joksović, *Faculty of Science, University of Kragujevac, Kragujevac, Serbia*

John Arthur Joule, *Chemistry Department, University of Manchester, Manchester, UK*

Petar Jovančić, *Faculty of Technology and Metallurgy, University of Belgrade, Serbia*

Branimir Jovančićević, *Faculty of Chemistry, University of Belgrade, Serbia*

Bratislav Jovanović, *Faculty of Technology and Metallurgy, University of Belgrade, Serbia*

Ljiljana Jovanović, *Department of Chemistry, Faculty of Science, University of Novi Sad, Serbia*

Milan Jovanović, *Vinča Institute of Nuclear Sciences, Belgrade, Serbia*

Vladislava Jovanović, *Institute of Chemistry, Technology and Metallurgy, University of Belgrade, Serbia*

Vesna Jović, *Institute of Chemistry, Technology and Metallurgy, University of Belgrade, Serbia*

Ivan Juranić, *Faculty of Chemistry, University of Belgrade, Serbia*

Goran Kaluđerović, *Department of Chemistry, Institute Martin Luter, Halle, Saale, Germany*

Mohammad-Ali Kamyabi, *Department of Chemistry, Zanjan University, Zanjan, Islamic Republic of Iran*

Zorica Kačarević, *Vinča Institute of Nuclear Sciences, Belgrade, Serbia*

Halit Kantekin, *Faculty of Arts and Sciences, Karadeniz Technical University, Trabzon, Turkey*

Janusz Kapusniak, *Institute of Chemistry and Environmental Protection, Jan Dlugosz University in Częstochowa, Częstochowa, POLAND*

Ljiljana Karanović, *Faculty of Mining and Geology, University of Belgrade, Serbia*

Ioannis Karapanagiotis, *ORMYLIA Art Diagnosis Center, Sacred Convent of the Annunciation, Ormylia, Greece*

Fikret Karci, *Faculty of Science-Arts, Pamukkale University, Kınıklı-Denizli, Turkey*

Regina Karousou, *School of Biology, Aristotle University of Thessaloniki, Thessaloniki, Greece*

Arvind M. Kayastha, *School of Biotechnology, Banaras Hindu University, Varanasi, India*

Adalbert Kerber, *University of Bayreuth, Bayreuth, Germany*

Slavko Kevrešan, *Faculty of Technology, University of Novi Sad, Serbia*

Mirjana Kijevčanin, *Faculty of Technology and Metallurgy, University of Belgrade, Serbia*

Anđelija Malenović, *Institute of Pharmaceutical Chemistry, Faculty of Pharmacy, University of Belgrade, Serbia*

Gopal Rao Mallavarapu, *Central Institute of Medicinal and Aromatic Plants, Resource Centre, Bangalore, India*

Emilia Mancini, *Department of Pharmaceutical Science, University of Salerno, Fisciano, Italia*

Zoran Mandić, *Faculty of Chemical Engineering and Technology, University of Zagreb, Croatia*

Ljuba Mandić, *Faculty of Chemistry, University of Belgrade, Serbia*

Dragan Manojlović, *Faculty of Chemistry, University of Belgrade, Serbia*

Jasmina Marković, *Faculty of Physical Chemistry, University of Belgrade, Serbia*

Rade Marković, *Faculty of Chemistry, University of Belgrade, Serbia*

Svetlana Marković, *Faculty of Science, University of Kragujevac, Kragujevac, Serbia*

Ana Martin Castro, *Organic Chemistry Department, University of Madrid, Spain*

Constantin Marutoiu, *Babes-Bolyai University, Cluj Napoca, Romania*

Khalid Masood, *Center for Scientific Review, National Institutes of Health, Bethesda, USA*

Gordana Matić, *Institute for Biological Research "S. Stanković", Faculty of Biology, University of Belgrade, Serbia*

Branko Matović, *Vinča Institute of Nuclear Sciences, Belgrade, Serbia*

Hitoshi Matsuki, *Institute of Technology and Science, The University of Tokushima, Tokushima, Japan*

Naohide Matsumoto, *Faculty of Chemistry, Kumamoto, Japan*

Jacqui McRae, *Faculty of Life and Social Sciences, Swinburne University of Technology, Hawthorn, Australia*

Gonzalo J. Mena Rejón, *Facultad de Química, Universidad Autónoma de Yucatán, Mérida, Yucatán, México*

Durali Mendil**, *Faculty of Science and Arts, Gaziosmanpasa University, Tokat, Turkey*

Slavko Mentus, *Faculty of Physical Chemistry, University of Belgrade, Serbia*

Ljljlana Mićović, *Faculty of Chemistry, University of Belgrade, Serbia*

Nevena Mihailović, *Institute for the Application of Nuclear Energy - INEP, Beograd-Zemun, Serbia*

Dušan Mijin, *Faculty of Technology and Metallurgy, University of Belgrade, Serbia*

Marian Mikołajczyk, *Department of Heteroorganic chemistry, Polish Academy of Sciences, Łódź, Poland*

Jelena Miladinović, *Faculty of Technology and Metallurgy, University of Belgrade, Serbia*

Duane D. Miller, *College of Pharmacy, Medicinal Chemistry Faculty, Memphis, TN, USA*

Feyyaz Onur, *Faculty of Pharmacy, Ankara University, Turkey*
Dušanka Opsenica, *Faculty of Chemistry, University of Belgrade, Serbia*
Dejan Opsenica, *Institute of Chemistry, Technology and Metallurgy, University of Belgrade, Serbia*
Aleksandar Orlović, *Faculty of Technology and Metallurgy, University of Belgrade, Serbia*
Hakan Ozer, *Faculty of Agriculture, Ataturk University, Erzurum, Turkey*
Vladimir Panić, *Institute of Chemistry, Technology and Metallurgy, University of Belgrade, Serbia*
Chong Rae Park, *Carbon Nanomaterials Design Laboratory, Seoul National University, Seoul, Republic of Korea*
Francesca Paradisi, *UCD School of Chemistry and Chemical Biology, Belfield, Ireland*
Miomir Pavlović, *Institute of Chemistry, Technology and Metallurgy, University of Belgrade, Serbia*
Hasmukh Chandra Patel, *Sardar Patel University, Vallabh Vidhyanagar, Gujarat, India*
José Luis Pérez Pavón, *Facultad de Ciencias Qumicas, Universidad de Salamanca, Spain*
Alessandro Pedretti, *Instituto di Chemica Farmaceutica e Tossicologica Pietro Pratesi, Universita degli Studi di Milano, Italy*
Miljenko Perić, *Faculty of Physical Chemistry, University of Belgrade, Serbia*
Živomir Petronijević, *Faculty of Technology, University of Niš, Leskovac, Serbia*
Srđan Petrović, *Faculty of Technology and Metallurgy, University of Belgrade, Serbia*
Petar Pfendt, *Faculty of Chemistry, University of Belgrade, Serbia*
Branka Pilić, *Faculty of Technology, University of Novi Sad, Serbia*
Sanja Podunavac-Kuzmanović, *Faculty of Technology, University of Novi Sad, Serbia*
Lionello Pogliani, *Dipartimento di Chimica, Universitá della Calabria, Rende, Italy*
Slovenko Polanc, *Faculty of Chemistry and Chemical Technology, University of Ljubljana, Ljubljana, Slovenia*
Dejan Poleti, *Faculty of Technology and Metallurgy, University of Belgrade, Serbia*
Aleksandar Popović, *Faculty of Chemistry, University of Belgrade, Serbia*
Gordana Popović, *Faculty of Pharmacy, University of Belgrade, Serbia*
Dragan Povrenović, *Faculty of Technology and Metallurgy, University of Belgrade, Serbia*
Velimir Popsavin, *Department of Chemistry, Faculty of Science, University of Novi Sad, Serbia*

Peter Segla, *Department of Inorganic Chemistry, Slovak Technical University, Bratislava, Slovak Republic*

Joseph Selvin, *Department of Microbiology, Bharathidasan University, Tiruchirappalli, India*

Slobodan Šerbanović, *Faculty of Technology and Metallurgy, University of Belgrade, Serbia*

Abbas Shafiee, *Faculty of Pharmacy, Pharmaceutical Science Research Center, Tehran University of Medical Science, Tehran, Iran*

Prawez Alam Shaheed, *Bhagat Singh College, Punjab, India*

Branisalav Simonović, *Institute of General and Physical Chemistry, Belgrade, Serbia*

Dušan Sladić, *Faculty of Chemistry, University of Belgrade, Serbia*

Wendy-Anne Smith, *Division of Molecular Biotechnology, Telethon Institute for Child Health Research, Subiaco, Western Australia*

Brigitte Söhling, *Institute fur Biotechnologie, Martin-Luther Universitat Halle, Halle, Germany*

Bogdan Šolaja, *Faculty of Chemistry, University of Belgrade, Serbia*

Effat Souri, *Faculty of Pharmacy and Pharmaceutical Sciences Research Center, University of Tehran, Tehran, Iran*

Selma Spirtović-Halilović, *Faculty of Pharmacy, University of Sarajevo, Bosnia and Herzegovina*

Vojislav I. Srdanov, *Department of Chemistry, University of California at Santa Barbara, CA, USA*

Zbigniew Sroka, *Department of Pharmacognosy, Wrocław Medical University, Wrocław, Poland*

Janusz Stafiej, *Institute of Physical Chemistry, Polish Academy of Sciences, Warsaw, Poland*

Trajče Stafilov, *The Institute of Chemistry, University of Skopje, Republic of Macedonia*

Stancho Stanchev, *Department of Organic Chemistry, Faculty of Pharmacy, Sofia, Bulgaria*

Dragomir Stanisavljev, *Faculty of Physical Chemistry, University of Belgrade, Serbia*

Radmila Stikić, *Faculty of Agriculture, University of Belgrade, Zemun, Serbia*

Đorđe Stojaković, *Faculty of Chemistry, University of Belgrade, Serbia*

Ksenija Stojanović, *Faculty of Chemistry, University of Belgrade, Serbia*

Gordana Stojanović, *Faculty of Natural Sciences and Mathematics, University of Niš, Serbia*

Maria E Street, *Department of Pediatrics, University Hospital, Parma, Italia*

Roongnapa Suedee, *Faculty of Pharmaceutical Sciences, Prince of Songkla University, Hatyai, Thailand*

Angela Vogts, *ICBM, Carl von Ossietzky University of Oldenburg, Oldenburg, Germany*

Tatjana Volkov-Husović, *Faculty of Technology and Metallurgy, University of Belgrade, Serbia*

Bojana Voncina, *Faculty of Mechanical Engineering, University of Maribor, Maribor, Slovenia*

Leonid G. Voskressensky, *Organic Chemistry Department of Russian Peoples' Friendship University, Moscow, Russia*

Miroslav Vrvić, *Faculty of Chemistry, University of Belgrade, Serbia*

Gordana Vučković, *Faculty of Chemistry, University of Belgrade, Serbia*

Biserka Vujičić, *Faculty of Technology, University of Novi Sad, Serbia*

Rastko D. Vukićević, *Faculty of Science, University of Kragujevac, Kragujevac, Serbia*

Karel Vytras, *University of Pardubice, Czech Republic*

Guido L.B. Wiesenberg, *Department for Agroecosystem Research, University of Bayreuth, Germany*

Yi-Ming Xie, *College of Materials Science and Engineering, Huaqiao University, Quanzhou, Fujian, P. R. China*

Toshihiro Yamase, *Tokyo Institute of Technology, Nagatsuta, Midoriku, Yokohama, Japan*

Xuegeng Yang, *Leibniz Institute for Solid State and Materials Research, Dresden, Germany*

Qi-Zhuang Ye, *Indiana University School of Medicine, Indianapolis, USA*

George Zachariadis, *Department of Chemistry, Aristotle University of Thessaloniki, Greece*

Snežana Zarić, *Faculty of Chemistry, University of Belgrade, Serbia*

Davorka Završnik, *Faculty of Pharmacy, University of Sarajevo, Bosnia and Herzegovina*

Mira Zečević, *Faculty of Pharmacy, University of Belgrade, Serbia*

Jianming Zhang, *Max Planck Institute for Polymer Research, Mainz, Germany*

Xinhuai Zhao, *Key Lab of Dairy Science, Northeast Agricultural University, Harbin, P. R. China*

Mayalen Zubia, *Université de Bretagne Occidentale, Technopôle Brest-Iroise, Plouzané, France*